U-PB DETRITAL ZIRCON GEOCHRONOLOGY OF THE LATE PALEOCENE EARLY EOCENE WILCOX GROUP, EAST-CENTRAL TEXAS

A Thesis

by

PRESTON JAMES WAHL

Submitted to the Office of Graduate and Professional Studies of
Texas A&M University
in partial fulfillment of the requirements for the degree of

MASTER OF SCIENCE

Chair of Committee,	Thomas E. Yancey
Co-Chair of Committee,	Mike Pope
Committee Members,	Brent V. Miller
	Walter Ayers
Head of Department,	Rick Giardino

August 2015

Major Subject: Geology

ABSTRACT

Sediment delivery to Texas and the northwestern Gulf of Mexico during the Early Paleogene represents an initial cycle of tectonic-influenced deposition that corresponds with the timing of late Laramide uplift. Sediments shed from Laramide uplifts to east-central Texas and the northwestern Gulf of Mexico during this time are preserved in strata of the Wilcox Group and lower Claiborne Group. U-Pb dating of detrital zircons from closely spaced stratigraphic units within these groups and the underlying Midway Group by laser ablation inductively coupled plasma mass spectrometry (LA-ICP-MS) reveals the relative arrival time of late Laramide-age detrital zircons to east-central Texas and distinct detrital zircon age assemblages. Comparison of zircon age assemblages from this study with data from potential source regions and additional Wilcox and Claiborne Group samples along the Texas and Louisiana Gulf Coastal Plain provides insight into paleodrainage during the Early Paleogene.

The relative arrival time of late Laramide-age detrital zircons to east-central Texas corresponds with deposition of the Hooper Formation of the Wilcox Group, although the presence of these detrital zircons fluctuates within younger samples. Comparison of composite detrital zircon age spectra from sediment source regions and from locations along the Texas and Louisiana Gulf Coastal Plain shows that source regions contain unique distributions of ages, with age components that are similar to Gulf Coastal Plain data. Detrital zircon age data may support relatively similar sediment sources or a similar paleodrainage area for the majority of observed ages within the Midway Group, Wilcox

Group, and Carrizo Formation in east-central Texas. Louisiana Wilcox Group and east-central Texas (Tehuacana Member through Carrizo Formation) data are similar and contrast with data of the south Texas Wilcox Group. This may support similar paleodrainage for Louisiana and east-central Texas and a different paleodrainage to the south Texas area. Data may also support the introduction of a new sediment source or a greater contribution of detrital zircons from an already existing source by the time of Queen City Formation (lower Claiborne Group) deposition in east-central Texas. Comparison of Louisiana Claiborne Group data with east-central Texas Queen City Formation data indicates that this source was also available during deposition of younger Claiborne Group strata in Louisiana.

DEDICATION

This thesis is dedicated to my parents, Dwayne and Sharon Wahl, and my brothers, Billy and Michael. Sharon, thank you for seeing the geologist in me at an early age and never giving up on me. Thank you for all the music lessons and trips to the bookstore, for teaching me to play chess, and for letting me dig through rock piles outside the grocery store in Bismarck. Dwayne, thank you for passing on to me a work ethic that knows no end, and for teaching me that dedication and passion for your work truly pays off.

ACKNOWLEDGEMENTS

TABLE OF CONTENTS

LIST OF FIGURES

FIGURE   Page

LIST OF TABLES

CHAPTER I

INTRODUCTION

Sediment delivery to Texas and the northwestern Gulf of Mexico during the Early Paleogene is characterized by a substantial increase in clastic sediment volume during the Late Paleocene, followed by an overall decline in sediment delivery until the Late Eocene (Galloway and Williams 1991; Galloway et al. 2011). This phase of sediment delivery represents the first Paleogene cycle of tectonic-influenced deposition (Winker 1982) and corresponds with the timing of late Laramide uplift within the North American continental interior (Cather and Chapin 1990; Lawton 2008). A second phase of sediment delivery resulted from regional uplift in the Western Cordillera during the Late Eocene to Oligocene (Galloway 1977; Mix et al. 2011; Chamberlain 2012; Fan et al. 2014a). Extended sediment deposition on the margins of the Gulf of Mexico resulted in an overall transition from open marine shelf settings during the Early Paleocene to non-marine settings by the Oligocene, modulated by variations in sediment supply, subsidence, and eustatic sea level (Yancey and Davidoff 1991; Davidoff and Yancey 1993a). Sediments shed from Laramide uplifts to Texas and the northwestern Gulf of Mexico during the Paleocene and Early Eocene are preserved in strata of the Wilcox Group and lower Claiborne Group (Winker 1982; Galloway and Williams 1991; Crabaugh 2001). Wilcox Group strata are mostly Late Paleocene in age and include the first and greatest pulse of clastic sediment delivered to the region. Shelf-margin outbuilding was accompanied by sediment accumulation in large fluvial and deltaic depositional systems (Edwards 1981; Fisher and McGowen 1967; Ayers and Lewis 1985; Galloway et al. 2000). Submarine canyons that formed during the development of these depositional systems were conduits for sediment delivery to the northwestern deep water Gulf of Mexico (Hoyt 1959; Galloway and others 1991).

Wilcox Group and Claiborne Group strata are an important economic resource in the Texas Gulf Coastal Plain and northwestern Gulf of Mexico. East-central Texas reportedly contains approximately 29 percent (16,980 million tons) of total Texas Wilcox Group

lignite coal reserves (Kaiser et al. 1980). Sheet sands and amalgamated and leveed channel systems of the deep water Wilcox Group contain large amounts of hydrocarbons, making it an important play in the northwestern Gulf of Mexico (Meyer et al. 2005). Wilcox Group and Claiborne Group strata are also important aquifers (Thorkildsen and Price 1991).

The presence of these resources continues to result in scientific reports addressing the geological aspects of these units, including sedimentary provenance. Identification of the source of sediments to the Late Paleocene Wilcox Group clastic wedge in Texas began with reports suggesting derivation from Laramide uplifts to the west and the continental interior (Storm 1945; Murray 1955). This interpretation was based on nearly equal amounts of volcanic and metamorphic rock lithoclasts in Wilcox sandstones (Harris 1962; Loucks et al. 1984) and remains a popular interpretation (Winker 1982; Galloway 1989; Galloway et al. 2000; Galloway 2005). An alternative provenance interpretation based on the abundance of kyanite and staurolite in the heavy-mineral fraction of the Calvert Bluff, Carrizo, and Reklaw Formations in Texas suggests an Ouachita-Appalachian and Grenville source (Todd and Folk 1957), although a southern Laramide source also was supported in a similar study (Brewton 1970). A shift in source areas to a silicic volcanic source during the Middle to Late Eocene was suggested based on an increased abundance of euhedral detrital zircons in sediments (Callender and Folk 1958). This corresponds with a time of great silicic volcanism in western North America (Loucks et al. 1984; Galloway et al. 2000; Heintz et al. 2015).

U-Pb detrital zircon geochronology of samples from the Calvert Bluff and Carrizo Formations in east-central Texas contain abundant Laramide-age (75-53 Ma) detrital zircons (Hutto et al. 2009). The emphasis of this study is to determine the relative arrival time of late Laramide-age sediments to the region. U-Pb detrital zircon geochronology of closely spaced stratigraphic horizons within strata of the Midway group, Wilcox Group, and lower Claiborne Group in east-central Texas has potential to identify distinct zircon age assemblages and provide insight into the provenance of sedimentary deposits and

the timing of changes in sedimentary sources. Sandstone samples were obtained from the Middle Paleocene Tehuacana Member at the top of the Kincaid Formation of the Midway Group to the Queen City Formation of the lower part of the Claiborne Group (Figure 1). Samples from the Calvert Bluff Formation at Big Brown Mine and the Carrizo Formation are from Hutto et al. (2009), and were analyzed previously at the University of Arizona LaserChron Center. Samples from each stratigraphic level were obtained from outcropping sections between the Trinity River and Colorado River, an area located within the Houston Embayment structural basin (Figure 2). Samples were obtained from both from fluvial channel deposits and sheet sands deposited in shallow marine settings (Gardner 1935; Beckman and Turner 1945; Ayers and Lewis 1985; Yancey et al. 2010). Further details for each analyzed sample are provided in Appendix F.

Similar, but less focused studies of detrital zircon geochronology of Early Paleogene sediments include areas in Texas (Mackey et al. 2012; Blum and Pecha 2014), in Louisiana (Craddock and Kylander-Clark 2013; Blum and Pecha 2014), and northeastern Mexico (Lawton et al. 2009). Comparable studies were completed in Utah (Dickinson et al. 2012), and the Laramide intermontane basins (Fan et al. 2011; May et al. 2013). U-Pb geochronology applied to older strata that are relevant to this study include parts of the Colorado Plateau (Dickinson and Gehrels 2008a, 2008b), Appalachian foreland basins (Eriksson et al. 2004; Park et al. 2010) and additional areas within the continental interior and farther west. These studies provide insight into sedimentary source areas, from which detrital zircons may have been derived as primary or recycled sediments, and aids in interpretation of sedimentary provenance and paleodrainage for sediment transported to the Houston Embayment during the Early Paleogene.
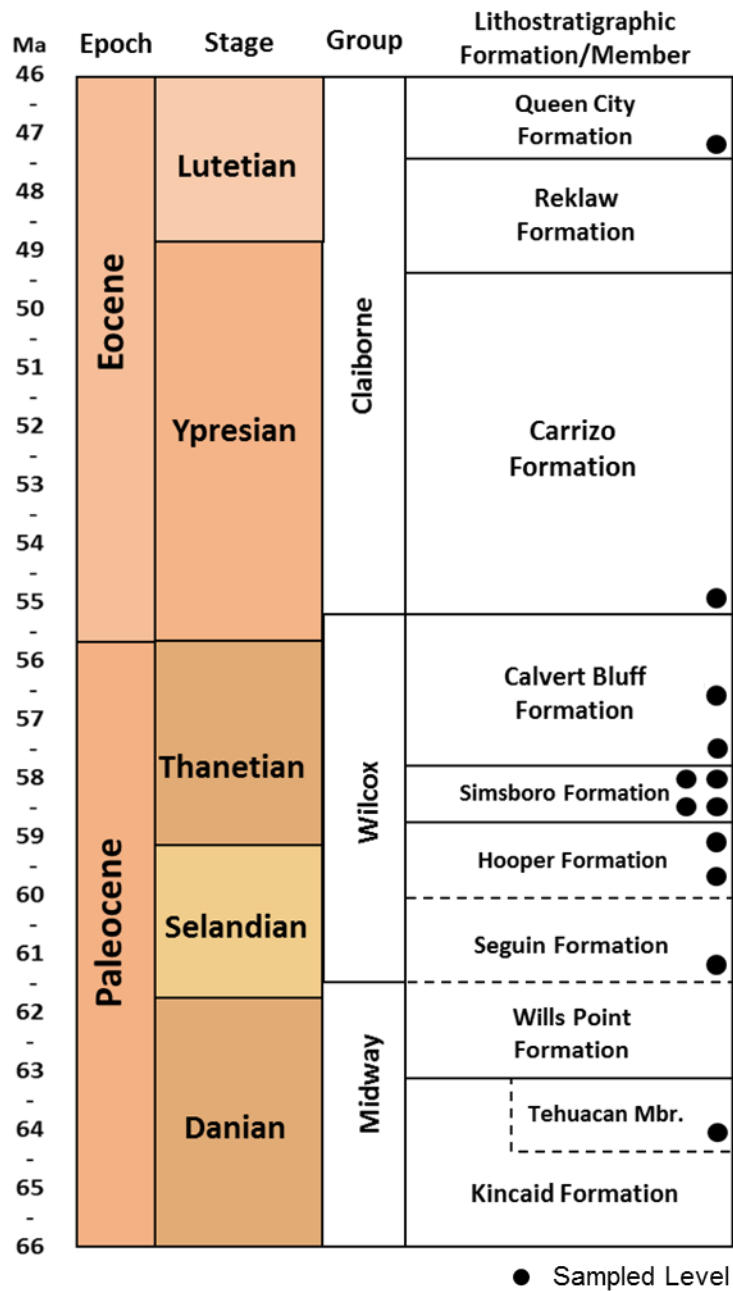
Figure 1. Generalized stratigraphic column for east-central Texas showing stratigraphic levels of sampling. Middle Calvert Bluff and lower Carrizo Formation samples are from Hutto et al. (2009). Timescale from Gradstein et al. (2012) and references therein.
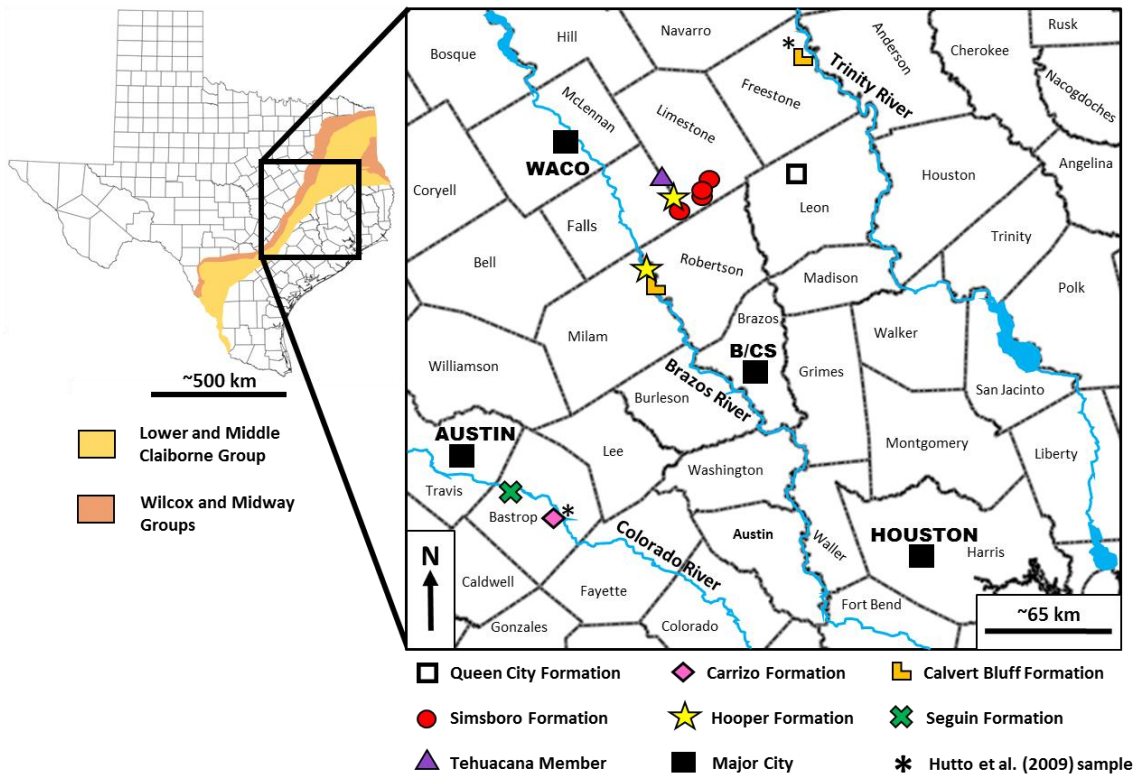
Figure 2. Location of samples collected between the Trinity and Colorado Rivers in east-central Texas. B/CS (Bryan/College Station).

CHAPTER II

GEOLOGIC BACKGROUND

The Gulf of Mexico passive margin records a complex history of sediment deposition since its inception during the Middle Jurassic to Early Cretaceous (160-140 Ma). Initial development of the Gulf of Mexico was associated with separation of the Yucatan Peninsula block from the North American Plate (Salvador 1987). Gulf of Mexico geologic history, including structural development and episodes of deposition was presented in Galloway (2000), which was complimented by a study addressing Gulf of Mexico development during the Cenozoic (Galloway et al. 2011). Development of Paleogene sediment dispersal systems extending east and south to the Gulf of Mexico from areas in the continental interior and westward was established by Late Cretaceous withdrawal of the Western Interior Seaway (Elder and Kirkland 1994). Deposition of Wilcox Group and lower Claiborne Group sediments occurred on the northwestern Gulf of Mexico margin from the Late Paleocene to Early Eocene, and corresponds with timing of Late Laramide orogenesis (Coney 1976; Lawton 2008) and continued development of the Western Cordillera (DeCelles 2004). The Laramide Orogeny (ca. 80-55 Ma) (English and Johnston 2004) commonly is considered to have resulted from regional NE-SW compressional forces and crustal shortening related to flat-slab subduction of the Farallon Plate beneath the North American Plate (Dickinson and Snyder 1978; DeCelles 2004), although other models exist (English and Johnston 2004). This resulted in an area east of the Sevier fold and thrust belt characterized by intermontane basins (Chapin and Cather 1983; Dickinson et al. 1988) and associated asymmetric basement cored uplifts that characterize Laramide-style deformation (Dickinson and Snyder 1978; Lawton 2008). Laramide intermontane basins were at or near sea level during the Early Eocene (Fan et al. 2011). Recent studies focusing on the timing of increased elevation and relief in the central Rocky Mountains support the idea that present elevation of the entire central Rockies and adjacent parts of the Great Plains was reached concurrently during the Late Eocene (Fan et al. 2014a), and that basin floors attained much of their elevation during the Early Eocene to Early Oligocene (Fan et al. 2014b).

Although Laramide tectonism is largely considered a primary influence on sediment delivery to the northwestern Gulf of Mexico during the Early Paleogene, climate, runoff rates, basin area, and river basin elevation of the region where headwaters are sourced also are important factors (Milliman and Syvitski 1992). Climate along the Texas Gulf Coast during Late Paleocene to Early Eocene time ranged from subtropical to tropical (Galloway et al. 2011). The span of upper Midway Group through lower Claiborne Group deposition in east-central Texas coincides with a trend of slow temperature rise during the Late Paleocene, and gradual cooling into the Miocene. This trend includes a major climatic event known as the Paleocene Eocene Thermal Maximum, which is characterized by an abrupt temperature increase of 4-5 °C in high latitude locations and deep ocean waters that lasted less than 10^4 years (Kennett and Stott 1991; Zachos et al. 1993). Climate in Laramide foreland areas increased from 12°C to 19°C in the Late Paleocene and remained at approximately 20 °C in the Early Eocene, while rainfall values ranged from 130-150 cm/yr to 80-140 cm/yr, respectively (Wilf 2000).

Paleocene and Eocene stratigraphic nomenclature Texas has historically been sub-divided into major transgressive and regressive successions bound by major breaks in lithology (Sellards et al. 1932; Stenzel 1938; Hargis 1986). In east-central Texas, Early Paleogene lithostratigraphic units are the Midway, Wilcox, and Claiborne Groups. The following descriptions address the general lithostratigraphy of the east-central Texas area. More detailed information regarding lithostratigraphic description of units is available in associated references. The Paleocene section of the Midway Group generally consists of abundant shale with minor sandstone beds, and comprises the Kincaid Formation, that includes the Tehuacana Member, and the Wills Point Formation (Gardner 1935). These formations were deposited in an open marine setting represented by two overall shallowing upward successions below the Wilcox Group (Kellough 1959). The Wilcox Group contains abundant sandstone and shale, and has extensive lignite deposits. The Wilcox Group includes the Seguin Formation at its lowermost boundary, which underlies the Hooper, Simsboro, and the Calvert Bluff Formations (Sellards et al. 1932; Stenzel 1938). Wilcox Group depositional settings range from shallow marine, estuarine, fluvial-deltaic, and coastal plain settings (Sellards et al. 1932; Stenzel 1938;

7

Davidoff and Yancey 1991; Ayers and Lewis 1985). The overlying Early Eocene Claiborne Group generally consists of interbedded sandstone and shale, and comprises the Carrizo, Reklaw, and Queen City Formations from base to top (Sellards et al. 1932; Eargle 1968). These units were deposited in shallow marine, shoreface, coastal plain, and interdeltaic embayment and constructive deltaic settings (Sellards et al. 1932; Stenzel 1938; Guevara and Garcia 1972; Yancey et al. 2010).

Early Paleogene sequence stratigraphic development along the northwestern Gulf of Mexico margin are addressed in Galloway and Williams (1991) and Davidoff and Yancey (1993a,b). Galloway and Williams (1991) subdivided Paleogene strata in the northwestern Gulf of Mexico into successions of clastic sediment bound by marine maximum flooding surfaces (genetic sequences), a method which was further utilized in Xue and Galloway (1993, 1995) and Galloway et al. (2000). Crabaugh and Elsik (2000) and Crabaugh (2001) identified four major 3rd-order depositional sequences of clastic sediment load delivered to the Texas Wilcox Group, and suggest that major transgressions bounding Wilcox Group Strata correspond with times of minimal to no deformation in the Sevier-Laramide region. The depositional sequence model described in Vail et al. (1987) was applied to subsurface units in east-central Texas to determine eustatic cyclity in Paleocene and Eocene sediments, and comparatively demonstrated that the lithostratigraphic approach defining most of the stratigraphic formations in east-central Texas produces time-transgressive units (Yancey and Davidoff 1991; Davidoff and Yancey 1993a,b). Further information regarding stratigraphy, depositional systems, and depositional geometries that correspond with Early Paleogene upper Midway Group to lower Claiborne Group strata in this area is available in various publications (Fisher 1964; Fisher and McGowen 1967; Guevara and Garcia 1972; Berg 1979; Ayers and Lewis 1985; Yancey and Davidoff 1991; Galloway 2000; Dickey and Yancey 2010; Galloway et al. 2011; Yancey et al. 2012). Relative thicknesses associated with the depositional systems for upper Midway Group through lower Claiborne Group strata between the Colorado River and Trinity River are shown in Figure 3. Average unit thicknesses were obtained from Geologic Atlas of Texas maps produced by the Bureau of Economic Geology, or from literature addressing Midway Group, Wilcox Group, and

Claiborne Group formation and member thicknesses in the subsurface and/or outcrop (Sellards et al. 1932; Gardner 1935; Stenzel 1938; Bammel 1979; Ayers et al. 1986).
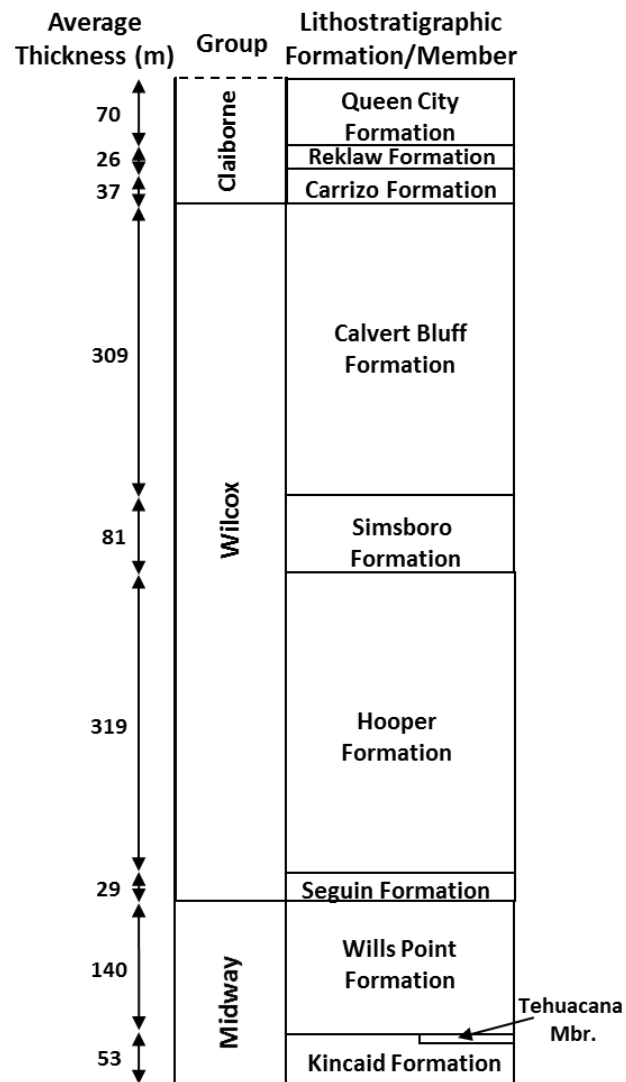
Figure 3. Stylized average thickness column for lithostratigraphic units in east-central Texas between the Trinity and Colorado Rivers. Thicknesses averaged from outcrop and well log data were obtained from Bastrop, Lee, Burleson, Milam, Robertson, Limestone, Freestone, and Leon Counties.

CHAPTER III

METHODS

Sample preparation and analysis were conducted in the Department of Geology and Geophysics at Texas A&M University. From each sampling horizon, sandstone samples were fully disaggregated using a hammer or a round glass jar. Samples were then elutriated in order to isolate the densest mineral fraction, and sieved using a Fisher Scientific standard testing sieve to obtain grains 63 to 300 μm in size. An HCL solution was applied to samples that contained calcium carbonate cement in order to assist with disaggregation. Fully disaggregated samples of 63 to 300 μm diameter grains were sorted into evenly represented aliquots using a Carpco microsplitter. Detrital zircon grains and other heavy minerals from individual aliquots were further concentrated using Methylene Iodide (MEI) heavy liquids separation (ρ=3.32 g/cm^3), which separates greater density minerals (zircon: 4.6-4.8 g/cm^3) from the major population of grains (predominantly quartz). By identifying specific optical properties with a Olympus SZ61 Zoom Stereo microscope, individual detrital zircon grains were physically separated from other heavy minerals. Details on the morphology of zircon are available in Corfu et al. (2003).

Once separated, detrital zircons were mounted on a strip of double-sided adhesive tape attached to a 2x2 inch glass plate. Two samples, with a minimum of 300 detrital zircon grains per sample were mounted on adhesive tape for each glass plate, in addition to an assortment of zircon standards and glass standards with known ages or reference values. The number of standards mounted depended on their size and the number of analyzed detrital zircon grains. Although obtaining ~100 or more useable analyses is a common goal, this number varies between studies and depends on the analysis method (Lawton et al. 2009; Craddock and Kylander-Clark 2013, Mackey et al. 2012). Usefulness of data and useable analyses refers to U-Pb isotopic data for a respective grain that are less than 10% discordant. With respect to the source component in a population of grains, an analysis of 117 detrital zircon grains identifies the entire 5% source component at a 95%

confidence interval (Vermeesch 2004). For this study, the number of useable analyses obtained for respective samples varied between 94 and 140.

Figure 4 shows the general arrangement of sample detrital zircons, zircon standards, and glass standards for this study. Zircon standards used include Peixe (1099 Ma) (Dickinson and Gehrels 2003), 91500 (1062.4 Ma) (Wiedenbeck et al. 1995), and FC-1 (564 Ma) (Paces and Miller 1993). Glass standards used were National Institute of Standards and Technology (NIST) 610 and 612. 91500 and Peixe were used as either primary or secondary standards for respective samples depending on the limited availability of Peixe. FC1 was used only as a secondary standard. NIST 610 and 610 glass standards were used for instrumental tuning before any analyses were performed. Primary zircon standards were used to calculate fractionation factors, which were applied to detrital zircon sample and secondary zircon standard data to correct for any instrumental variations during analyses. Fractionation factors were determined by dividing the known isotopic ratios of primary zircon standards by the average value of all non-erroneous calculated data of that respective standard on a given day. Secondary zircon standards were used to determine the relative reproducibility and precision of detrital zircon sample data. Since the ages of secondary zircon standards are known, comparing fractionation factor corrected ages with the known age of secondary standards indicated the reliability of analyzed detrital zircon sample data. These details are discussed in the following section.

A one-inch cylindrical plastic container was mounted to each adhesive tape covered glass plate containing samples and standards. A combination of Struers Epofix Hardener and Epofix Resin liquids were poured into the cylindrical container to coat each sample and standard, and left to harden for 12 hours. Air bubbles trapped next to mounted grains while epoxy was poured were manually removed from the mixture of hardener and resin. Once hardened, pucks were heated between 80-100 ˚C for 12 hours in a Cole Parmer Laboratory Oven, which reduced the risk of grains becoming dislodged during polishing. A Sherline Lathe was used to remove excess epoxy so the final height of each puck
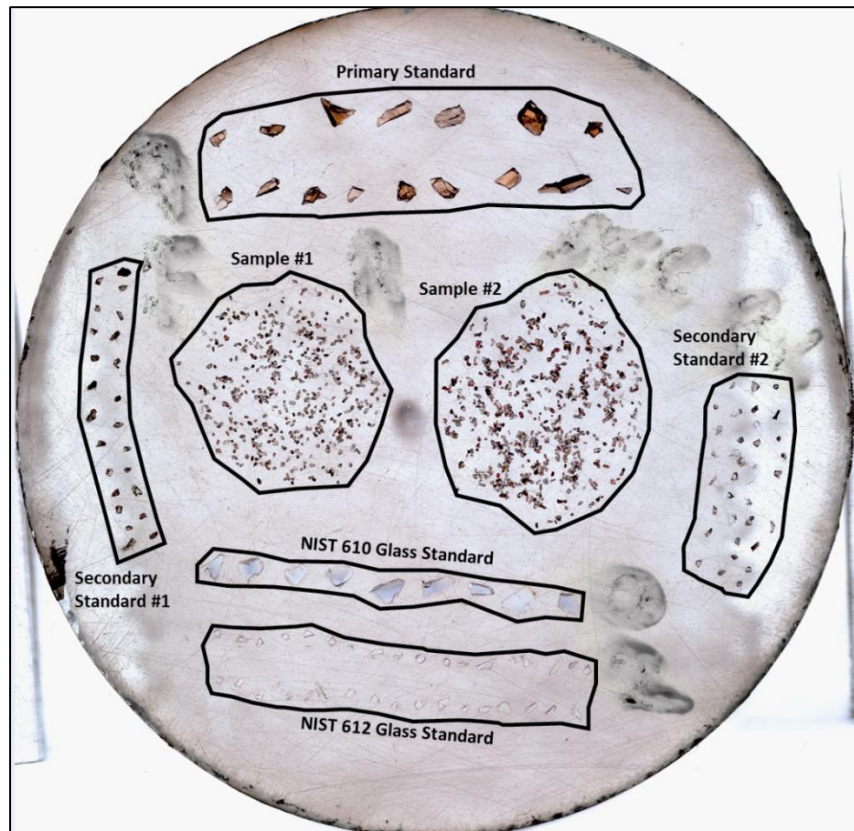
Figure 4. Arrangement of detrital zircon samples, primary standards, secondary standards, and NIST glass standards in an epoxy puck. The epoxy puck is the gray to semi-opaque colored area. Epoxy puck diameter is approximately 1 inch.

was approximately 0.5 cm. The surface of each puck was ground using a standard 1000-μm and 600-μm sandpaper film to expose the approximate center of each detrital zircon grain and the surface of associated zircon standards and glass standards. When selecting pairs of samples for each puck, similar grain sizes were chosen to expose grains from both samples to the same degree during grinding. Exposed grains were then polished with 6.0, 1.0, and 0.25 μm Struers MD-Dac diamond polishing cloths. Each polishing cloth was mounted on a Struers LaboForce-1 polishing machine and used in conjunction with Struers DP-Lubricant and Suspension applied to each cloth (6.0, 1.0 and 0.25-μm). Polishing cloths were thoroughly cleaned and pucks were placed in a Branson B200 ultrasonic cleaner to ensure that diamond residue from the cloths and any grains

that were dislodged during polishing did not contaminate other samples. Puck surfaces were polished to an ultra-smooth condition before being carbon coated using a LADD vacuum evaporator in preparation for electron microscopy imaging.

Cathodoluminescence (CL) and backscatter electron (BSE) imaging of the pucks was done using a four-spectrometer Cameca SX50 electron microprobe under the direction of Dr. Ray Guillemette. CL imaging provides insight into the internal structure and zonation of zircon grains (Smith and Stenstrom 1965), aiding in identification and analysis of zircon cores, and avoidance of inclusions, recycled cores, metamorphic rims, or metamict grains. The BSE image relates to the composition (mean atomic number) of the imaged mineral (Paterson et al. 1989). This allowed for differentiation between zircon and non-zircon before laser ablation inductively coupled plasma mass spectrometry (LA-ICP-MS) was utilized. Non-zircons identified by BSE were removed from the images, and a composite image for each sample was made by overlaying CL images on an optical image of identical samples (Figure 5). These composite images provided a reference detrital zircon grain map for positioning of the laser spot with respect to the arrangement of grains during LA-ICP-MS. Detrital zircons within these grain map images are numbered and correspond with external shape parameters measured during image processing (Appendix D).

LA-ICP-MS was performed in the Texas A&M University Radiogenic Isotope Geochemistry Laboratory. A previous study of LA-ICP-MS and TIMS (Thermal Ionization Mass Spectrometry) U-Pb zircon ages for similar sample populations reported that LA-ICP-MS was able to produce data within 2-4% (two sigma) uncertainty (Chang et al. 2006), although limitations of the LA-ICP-MS method are included in various publications (Feng et al. 1993; Fryer et al. 1993; Chang et al. 2006). The LA-ICP-MS procedure and methods for data reduction and evaluation were modeled after those developed by the Radiogenic Isotope and Geochronology Laboratory(RIGL) at Washington State University (WSU) and the Arizona LaserChron Center (Gehrels et. al 2006). High resolution LA-ICP-MS was performed using an Element XR single collector mass
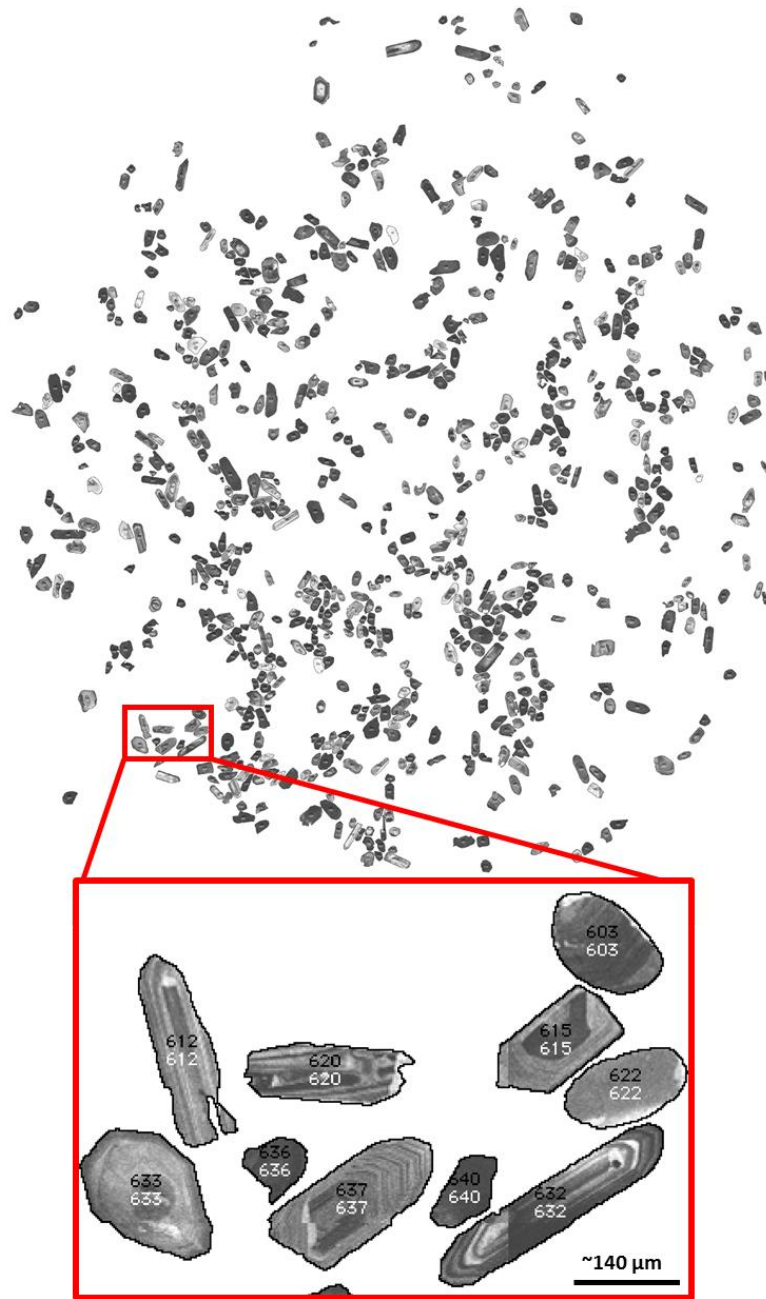
Figure 5. Detrital zircon grain map example. Grain map is a mosaic of CL images overlain onto the outline of identical optical images.

spectrometer and Analyte Exite Excimer laser ablation system by Photon-Machines Inc. Programs used during analyses included Element 3.0 and Chromium 2.1 software. A laser spot size of 29.6 μm was used during analyses. The laser ablation system was powered by an ATLex 300si laser and operated with a wavelength of 193 nm and pulses less than 4.0 nanoseconds in duration. Fluence was set at ~40% (2.2-2.4 J/cm2), and grain ablation took place at a 10 Hz laser repetition rate. He (0.8 L/min) and Ar (0.9-1.1 L/min) gas carried particles of vaporized sample to the ICP detector (measured in counts per second).

The order of grain ablation and data collection began with the necessary number of NIST 610 or 612 analyses required until the ICP instrument was properly tuned to maximize U and Th signals while minimizing the ThO signal. Approximately 5-6 samples of FC-1 or Peixe were then analyzed. Isotopic data from the 5-6 samples were uploaded into WSU RIGL reduction and fractionation Excel spreadsheets to determine fractionation and %1σ standard deviation values that indicate whether or not the laser is functioning properly. Uploaded data include $^{207}Pb/^{235}U$, $^{206}Pb/^{238}U$, and $^{207}Pb/^{206}Pb$ ratios with associated 1σ absolute error values. Data analysis then proceeded for each sample in the following order: analysis of four primary zircon standards (Peixe or 91500), eight grains (from sample "X"), two secondary zircon standards (FC-1), eight additional grains (sample "X"), two secondary zircon standards (Peixe or 91500), and four primary zircon standards (Peixe or 91500). If Peixe was used as a primary zircon standard for a certain sample, 91500 was used as a secondary zircon standard (and vice versa). This order of 28 analyses was termed one group. Grouping of grains was repeated until 160 sample grains had been analyzed for each sample. Data acquisition for one grain lasts approximately 90 seconds and is termed a sequence. This includes approximately 32 seconds of sample time, followed by a brief laser warm-up time (~5 seconds), then approximately 40 seconds of grain ablation with 300 total sweeps. The sequence is repeated after the laser spot is repositioned above the next selected grain.

Isotopic data for primary zircon standards were uploaded into WSU RIGL Excel spreadsheets designed for data processing. Processed primary zircon standard data were then uploaded into similar Excel templates to determine fractionation factors. Calculated fractionation factors and data for detrital zircon samples and secondary zircon standards were then uploaded into a separate Excel spreadsheet for data processing. Fractionation factors calculated from primary zircon standards of an individual group "correct" the detrital zircon and secondary zircon standard data corresponding with that respective group. Processing of detrital zircon samples, primary zircon standards, and secondary zircon standards included removing outlying data not representative of zircon cores that indicate an initial crystallization age. Detrital zircon sample, primary zircon standard, and secondary zircon standard $^{207}Pb/^{235}U$, $^{206}Pb/^{238}U$, $^{207}Pb/^{206}Pb$ ages were each determined using Equations 1-3 (Faure and Mensing 2005).The value for $^{235}U/^{238}U$ is a constant on Earth (1/137.88), and the symbol "i" refers to the initial value of respective isotopic ratios. Decay constants for ^{235}U ($\lambda2$) and ^{238}U ($\lambda1$) are 9.8485 x10^-10 and 1.55125 x10^-10, respectively (Steiger and Jager 1977). Corrected isotopic and age data were compiled and percent discordance between $^{207}Pb/^{235}$ and $^{206}Pb/^{238}U$ ages was determined. Processed detrital zircon and secondary zircon standard data were filtered to obtain only detrital zircon samples and secondary zircon standards with isotopic ratios and ages that are less than 10% discordant (Equations 3-4). The final ages, isotopic ratios, and associated 1σ absolute error values were selected from Pb^{206}/U^{238} or Pb^{207}/Pb^{206} data based on a commonly used arbitrary 600 Ma cutoff age. Pb^{206}/U^{238} values were used if ages were younger than 600 Ma. Isoplot 3.0 software (Ludwig 2003) was used to create probability density plots, histograms, Concordia plots (Appendix E) (Ahrens 1955; Wetherill 1956, 1963), and to determine the youngest detrital zircon age for each respective sample. Detrital zircon age data were analyzed statistically using the Kolmogorov-Smirnov (K-S) test, which determines the probability that two zircon populations are not from the same source population (Berry 2001). More specifically, the K-S test compares the maximum probability difference between two Cumulative Distribution Functions. The criterion for analysis considers whether or not a probability value (P) for two selected populations is less than 0.05, which indicates that there is a 2σ (95%) confidence level that the two populations are statistically dissimilar.

Equation 1. $(^{206}\text{Pb}/^{204}\text{Pb}) = (^{206}\text{Pb}/^{204}\text{Pb})\text{i} + \dfrac{(^{238}\text{U})}{(^{204}\text{U})}(e^{\lambda 1t} - 1)$

Equation 2. $(^{207}\text{Pb}/^{204}\text{Pb}) = (^{207}\text{Pb}/^{204}\text{Pb})\text{i} + \dfrac{(^{235}\text{U})}{(^{204}\text{U})}(e^{\lambda 2t} - 1)$

Equation 3. $\dfrac{(^{207}\text{Pb}/^{204}\text{Pb}) - (^{207}\text{Pb}/^{204}\text{Pb})\text{i}}{(^{206}\text{Pb}/^{204}\text{Pb})\ (^{206}\text{Pb}/^{204}\text{Pb})\text{i}} = \dfrac{(^{235}U)}{(^{238}U)}\dfrac{(e^{\lambda 2t} - 1)}{(e^{\lambda 1t} - 1)}$

Equation 4. $\% \ discordancy = \dfrac{(^{207}\text{Pb}/^{235}\text{U}) - (^{206}\text{Pb}/^{238}\text{U})}{(^{207}\text{Pb}/^{235}\text{U})}$

DETRITAL ZIRCON GEOCHRONOLOGY

Fractionation and Secondary Zircon Standards

Fractionation factors of primary zircon standards and ages of secondary zircon standards were plotted with respect to the day of analysis (Figure 6). This allowed visual identification of scatter or drift of fractionation factors and ages, and gave an indication of how well daily fractionation correction was working. Areas where secondary zircon standard datapoints are absent represent days when that zircon standard was used as a primary standard to determine fractionation.
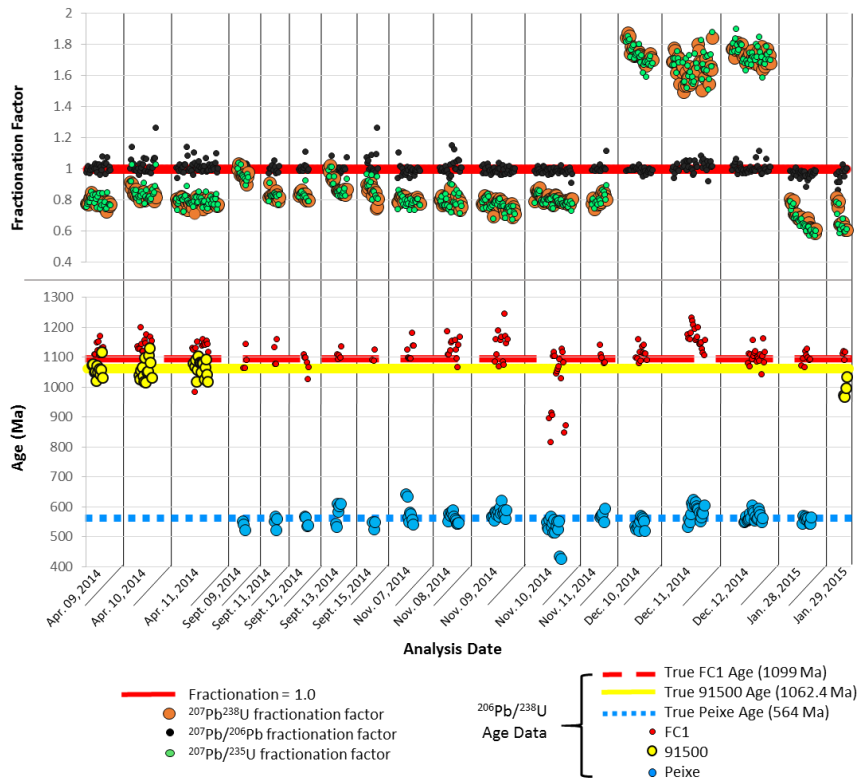
Figure 6. Fractionation factor and secondary zircon standard ^{206}Pb/^{238}U ages. Values are plotted with respect to analysis date.

Average age, standard deviation, and relative standard deviation of FC1, Peixe, and 91500 zircon standards for all analyses are shown in Table 1. Despite significant changes in fractionation factor for primary standards, the overall relative standard deviation of secondary zircon standard ages ranges from 3.23-5.28%, which is an acceptable range and supports the reproducibility of actual sample ages to a similar range of uncertainty.

Table 1. Calculated standard deviation (Std. Dev.), average age, and relative standard deviation (Rel. St. Dev.) values for secondary standards with respect to analysis date. Blank sections represent standards that were used as primary standards on respective days. Known ages of standards are noted in parentheses.

Analysis Date	Std. Dev. (Ma)			Average Age (Ma)			Rel. St. Dev. (%)		
	FC1	Peixe	91500	FC1 (1099 Ma)	Peixe (564 Ma)	91500 (1062.4 Ma)	FC1	Peixe	91500
4/9/2014	21.17		24.50	1130.1019		1059.3934	1.87		2.31
4/10/2014	26.05		34.75	1141.9420		1058.6736	2.28		3.28
4/11/2014	44.85		26.99	1114.6355		1065.8574	4.02		2.53
9/9/2014	37.71	15.16		1089.0707	537.8362		3.46	2.82	
9/11/2014	41.27	20.09		1111.3199	549.0839		3.71	3.66	
9/12/2014	30.22	16.40		1079.2995	551.5736		2.80	2.97	
9/13/2014	17.24	33.91		1107.8010	580.1655		1.56	5.85	
9/15/2014	20.04	14.12		1099.7840	540.0916		1.82	2.61	
11/7/2014	30.30	38.50		1120.1383	580.2737		2.70	6.64	
11/8/2014	33.49	16.25		1131.2547	563.4012		2.96	2.88	
11/9/2014	52.14	15.50		1139.1725	578.9916		4.58	2.68	
11/10/2014	106.06	40.41		1013.5339	525.5641		10.46	7.69	
11/11/2014	24.65	14.90		1100.5993	571.2565		2.24	2.61	
12/10/2014	24.00	18.00		1111.0079	541.8334		2.16	3.32	
12/11/2014	33.90	25.37		1165.5060	584.4067		2.91	4.34	
12/12/2014	27.54	15.79		1101.4686	567.5332		2.50	2.78	
11/28/2015	19.72	10.53		1095.8046	556.5776		1.80	1.89	
11/29/2015	13.48		30.61	1108.7001		993.5998	1.22		3.08
Overall Values									
	Std. Dev. (Ma)			Average Age (Ma)			Rel. St. Dev. (%)		
	FC1	Peixe	91500	FC1 (1099 Ma)	Peixe (564 Ma)	91500 (1062.4 Ma)	FC1	Peixe	91500
	58.39	29.69	34.07	1110.8857	562.1662	1055.7015	5.26	5.28	3.23

Average percent reproducibility of each zircon standard ranges from 2.80-3.06%. The reproducibility of detrital zircon sample data is addressed by comparing fraction factors for $^{207}Pb/^{206}Pb$, $^{207}Pb/^{235}U$, and $^{206}Pb/^{238}U$ with secondary standard ages. $^{207}Pb/^{206}Pb$ fractionation factors average 0.99. Fractionation factors for $^{206}Pb/^{238}U$ and $^{207}Pb/^{235}U$ are

almost identical to one another and are the most variable. Average fractionation factors for $^{206}Pb/^{238}U$ and $^{207}Pb/^{235}U$ from 04/09/2014 to 08/10/2014 were 0.81, while average fractionation factor was 1.7 between 12/10/2014 and 12/12/2014, and 0.66 on 01/28/2015 and 01/29/2015. The substantial increase in average fractionation factor from 0.81 to 1.7 may be due to daily instrumental variations, variations in plasma, or air infiltration into the stage of the LA-ICP-MS instrument. Variations in secondary zircon standard ages do not directly correspond with changes in fractionation factor between these three averages, nor do secondary zircon standard ages directly correspond with scatter or drift of fractionation on individual days. This is apparent when comparing fractionation with more pronounced scatter or drift of ages on 09/11/2014, 11/11/2014, and 12/11/2014. Slight drift of fractionation is apparent on multiple analysis days, but is acceptable if the level of reproducibility of secondary zircon standards is still within 3-5%. The best observed case where fractionation drift corresponds with secondary zircon standard ages is on 01/29/2015 with a slight drift of 91500 values, but relative standard deviation of 91500 is approximately 3% on that day.

Relative standard deviation values of 10.46% and 7.69% for FC1 and Peixe analyzed on 11/10/2014 are due to eight outlying values. Standard deviation of secondary zircon standard ages for the same day are 106.06 Ma and 40.41 Ma for FC1 and Peixe, respectively. These 8 outlying values correspond with 29 detrital zircon ages from the Calvert Bluff Formation (Black Shoals) sample, including 3 ages younger than 57 Ma. Relative standard deviation of FC1 and Peixe that correspond with the remaining ages of this sample are acceptable, with overall values of 2.96% and 3.19%, respectively. This level of uncertainty for the 29 detrital zircon ages is taken into consideration when making interpretations, especially for those that may correspond with Laramide-age zircon arrival. Two additional cases are present, where relative standard deviation of Peixe is 6.64% and 5.85% on 11/7/2014 and 9/13/2014. Other secondary standards on these two days, however, are less than 3% relative standard deviation. Outlying values like those most apparent on 11/10/2014, 11/7/2014, and 9/13/2014 are attributed to poor analytical procedure.

East-Central Texas Data

Detrital zircon geochronology data are presented for 12 Paleocene and Early Eocene stratigraphic horizons. These data show the distribution of detrital zircon ages within Midway Group through Claiborne Group strata in east-central Texas. Figure 7 shows normalized probability density plots and associated histogram for these 12 samples. All normalized probability density plots for data original to this report are ordered with respect to stratigraphic level. Figure 8 shows filled normalized probability density plots on a color-coded 2012 Geologic Time Scale (GTS 2012) from Gradstein et al. (2012). A 300 Ma and younger subset of the detrital zircon dataset is presented in Figures 9-10. Labels included on the right-hand side of probability density plots correspond to the formation or member that was sampled and/or the respective sampling location identifier if multiple samples were collected from one formation at different locations. Sample labels are as follows: Teh (Tehuacana Member), Se-E (Seguin Formation, Elysium), H-PC (Hooper Formation, Polecat Creek), H-DR (Hooper Formation, Dennison Ranch), Si-B (Basal Simsboro Formation, Rt. 14 roadcut), Si-LP (Simsboro Fm., Luminant Pit), Si-TQ (Simsboro Fm., Thornton Quarry), Si-KM (Simsboro Formation, Kosse Mine), CB-BS (Calvert Bluff Formation, Black Shoals), CB-BBM (Calvert Bluff Formation, Big Brown Mine), CZ (Carrizo Formation), and QC (Queen City Formation). Details regarding location and stratigraphic sampling of the above mentioned samples are available in Appendix G. The proportion of grains that correspond with color-coded geologic time intervals indicated in Figure 8 and Figure 10 are presented in Table 2.

The detrital zircon age spectrum for the entire population of ages (n=1297) ranges from Archean to Cenozoic, with the oldest and youngest ages being 3217 Ma and 52.5 Ma, respectively. Data for measured youngest detrital zircon ages are included in Appendix C with probability density plots and associated histograms for each sample. Youngest detrital zircon ages calculated for each sample except CB-BS are older than or within error of the relative depositional age at a 95% confidence level. The CB-BS sample has youngest detrital zircon age calculated at 52.5 +1.9/-2.3 Ma. However, the youngest distribution of ages for CB-BS corresponds with secondary zircon standards analyzed on

11/10/2014 that have a 10.46-7.69% relative standard deviation (Table 1), which raises concerns regarding the reliability of corresponding detrital zircon ages.

Because of the dissimilar distribution of data in sample QC compared with other samples, a composite probability density plot and associated histogram of detrital zircon age assemblages excluding QC is presented in Figure 11, with data for sample QC plotted above the composite plot for qualitative comparison. A composite probability density plot with associated histograms for all ages younger than 300 Ma is shown in Figure 12. Probability density curve peaks, pronounced deviations from a normal distribution (shoulders), and intervening sections between these features (valleys) in Figures 11-12 represent the composite of data from multiple samples, and may not exactly match features present in individual samples. Peaks, shoulders, and valleys for ages younger than 300 Ma highlight the variability in age peaks observed in Figures 9-10 and in later figures.
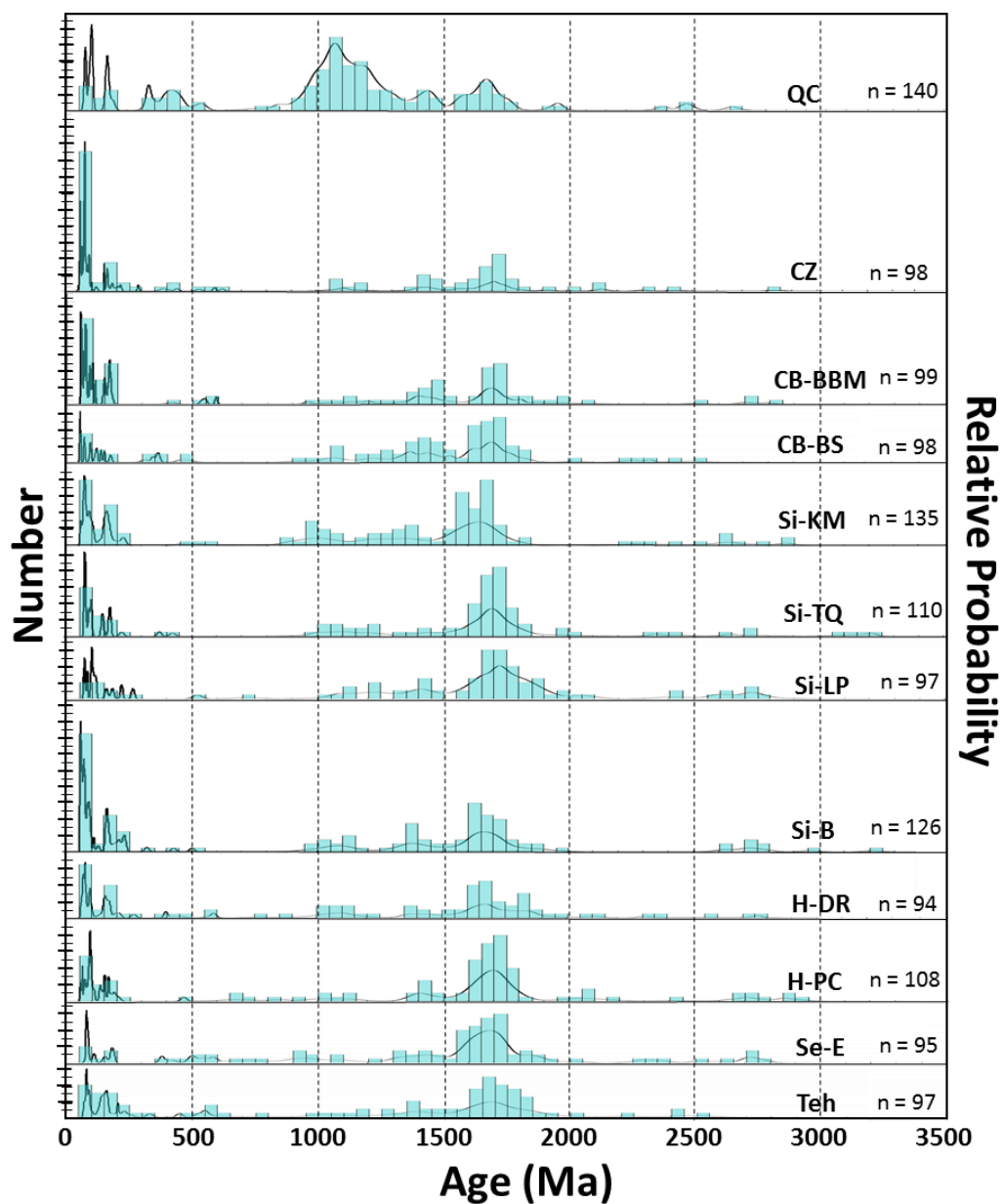
Figure 7. Normalized probability density plots and associated histograms for east-central Texas detrital zircon samples. See text for abbreviation details. Bin widths are 50 Ma. Symbol n indicates number of grains in a respective sample.

23
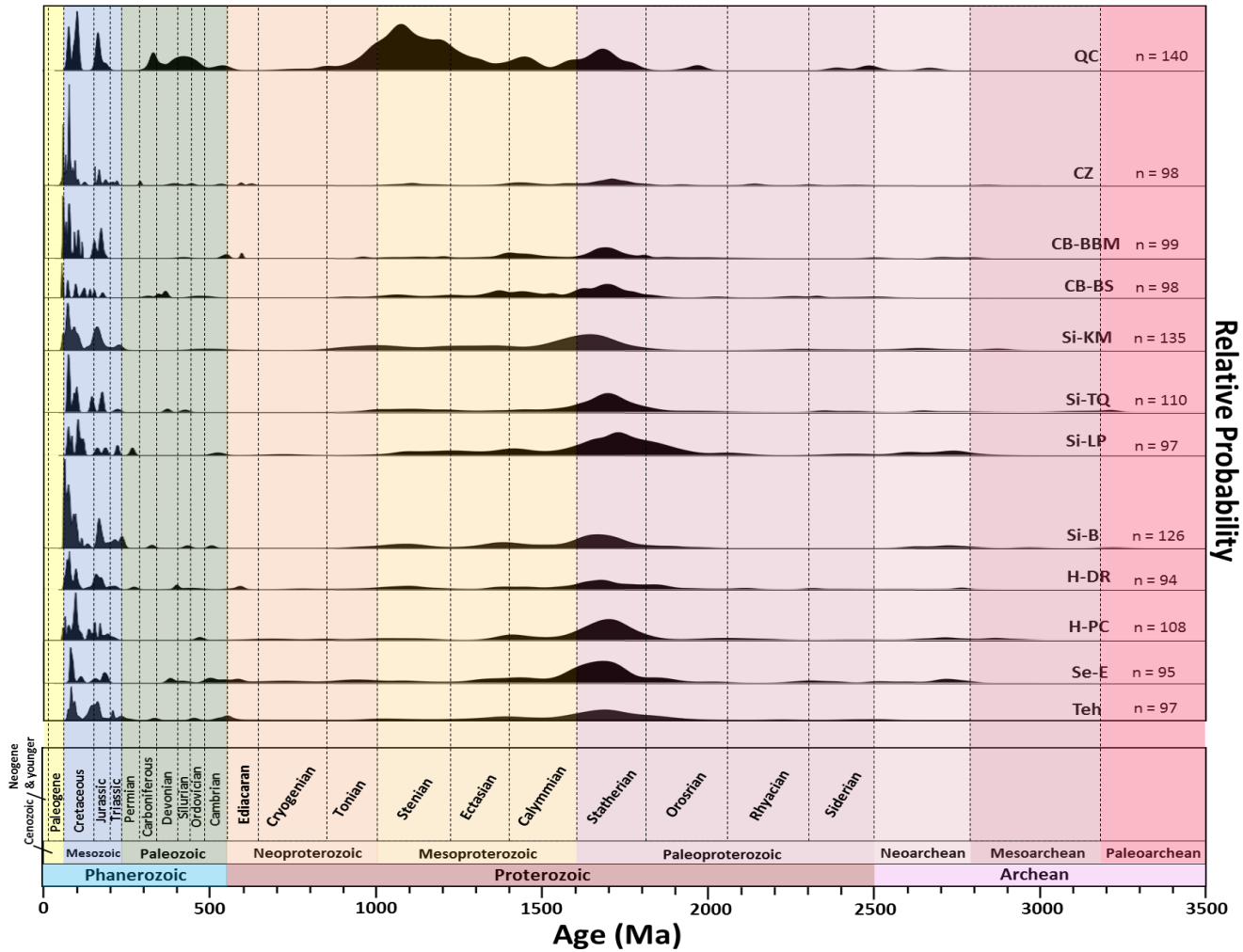
Figure 8. GTS (2012) timescale overlain on normalized probability density plots for east-central Texas detrital zircon samples. Geologic Time Scale (GTS 2012) from Gradstein et al. (2012).
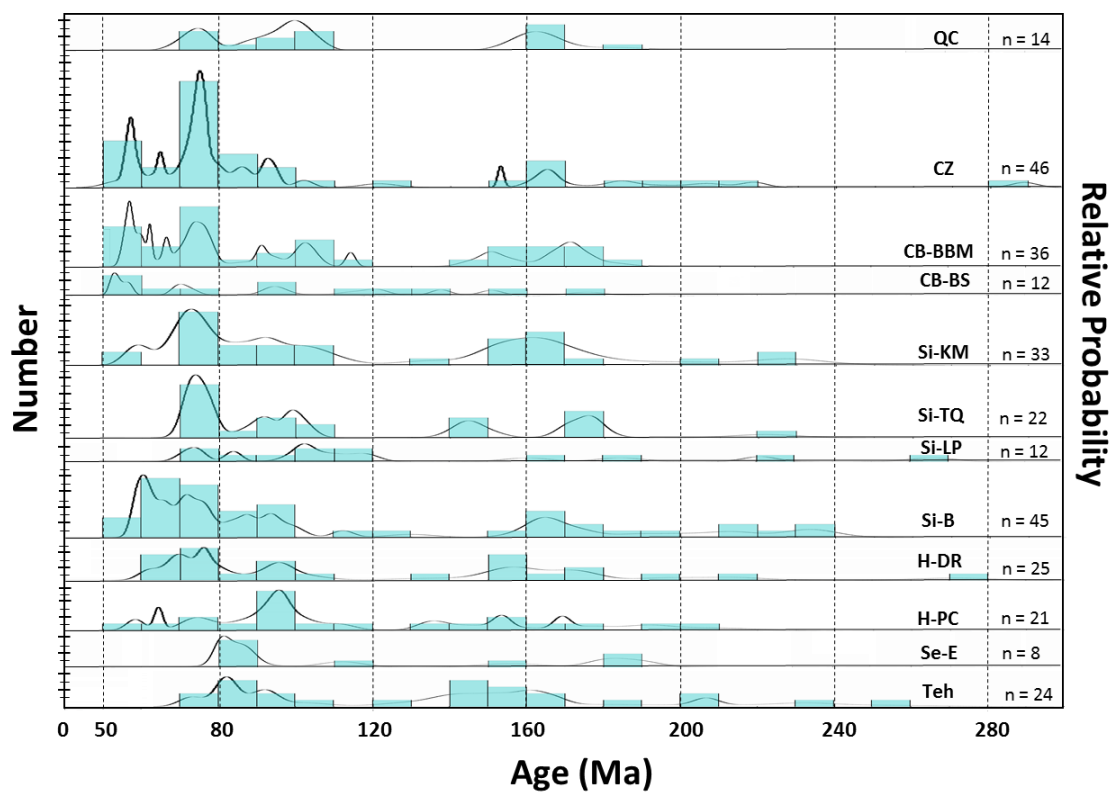
Figure 9. Normalized probability density plots and associated histograms for east-central Texas detrital zircon samples with ages younger than 300 Ma. Bin width is 10 Ma.
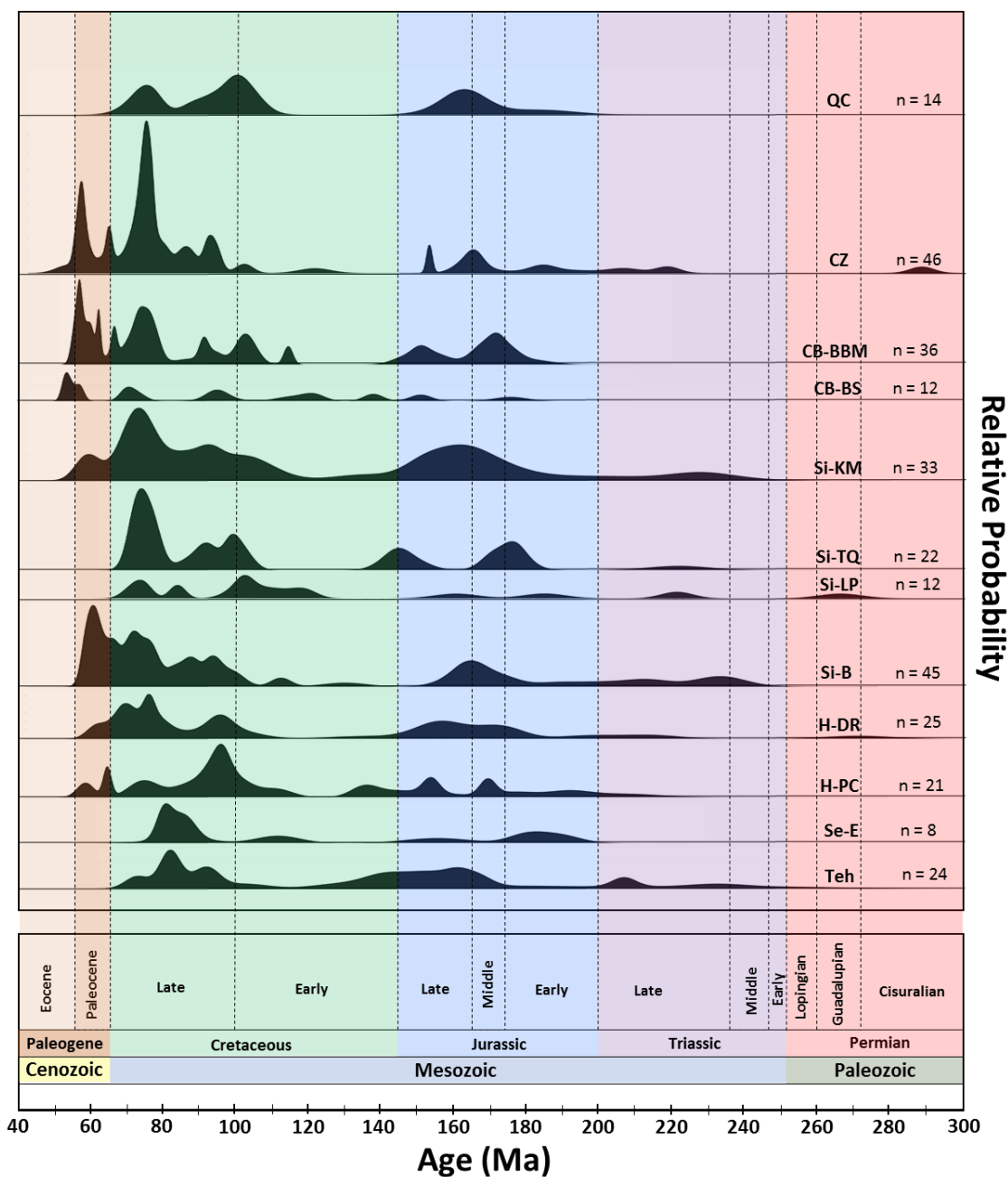
Figure 10. GTS (2012) timescale overlain on normalized probability density plots for east-central Texas detrital zircon samples with ages younger than 300 Ma.

Table 2. Number of grains and percent proportion with respect to GTS (2012). Total grain count is 1297 for east-central Texas samples.

Time Unit	Age Range (Ma)	# of Grains	Proportion (%)	Time Unit	Age Range (Ma)	# of Grains	Proportion (%)
Epoch				**Era**			
Eocene	34-56	8	0.62	Cenozoic	0-66	38	2.93
Paleocene	56-66	30	2.31	Mesozoic	66-252	258	19.89
Late Cretaceous	66-100	133	10.25	Paleozoic	252-541	47	3.62
Early Cretaceous	100-145	33	2.54	Neoproterozoic	541-1000	59	4.55
Late Jurassic	145-164	36	2.78	Mesoproterozoic	1000-1600	354	27.29
Middle Jurassic	164-174	21	1.62	Paleoproterozoic	1600-2500	484	37.32
Early Jurassic	174-201	19	1.46	Neoarchean	2500-2800	44	3.39
Late Triassic	201-237	16	1.23	Mesoarchean	2800-3200	11	0.85
Middle Triassic	237-247	0	0.00	Paleoarchean	3200-3600	2	0.15
Early Triassic	247-252	1	0.08				
				Eon			
Period				Phanerozoic	0-541	343	26.45
Paleogene	23-66	38	2.93	Proterozoic	541-2500	897	69.16
Cretaceous	66-145	165	12.72	Archean	>2500	57	4.39
Jurassic	145-201	76	5.86				
Triassic	201-252	17	1.31				
Permian	252-299	3	0.23				
Carboniferous	299-359	8	0.62				
Devonian	359-419	14	1.08				
Silurian	419-444	6	0.46				
Ordovician	444-485	6	0.46				
Cambrian	485-541	10	0.77				
Ediacaran	541-635	14	1.08				
Cryogenian	635-850	13	1.00				
Tonian	850-1000	32	2.47				
Stenian	1000-1200	126	9.71				
Ectasian	1200-1400	91	7.02				
Calymmian	1400-1600	137	10.56				
Statherian	1600-1800	378	29.14				
Orosrian	1800-2050	69	5.32				
Rhyacian	2050-2300	16	1.23				
Siderian	2300-2500	21	1.62				
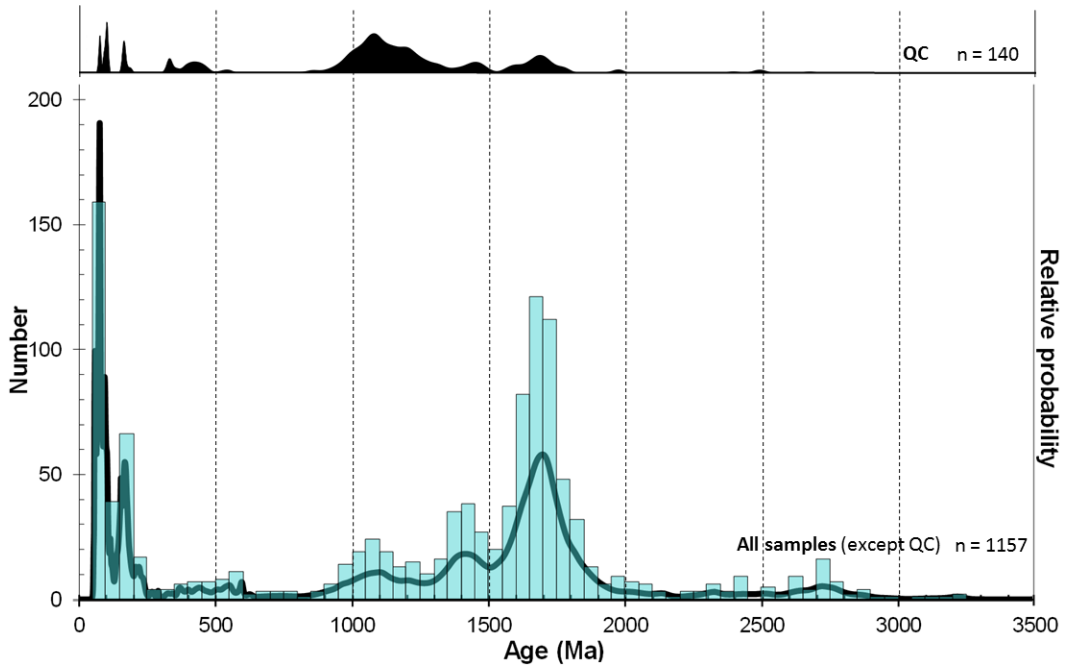
Figure 11. Normalized composite probability density plot for QC detrital zircon ages, positioned above a similar style plot and associated histogram for east-central Texas (Teh-CZ) samples. Bin width is 50 Ma.
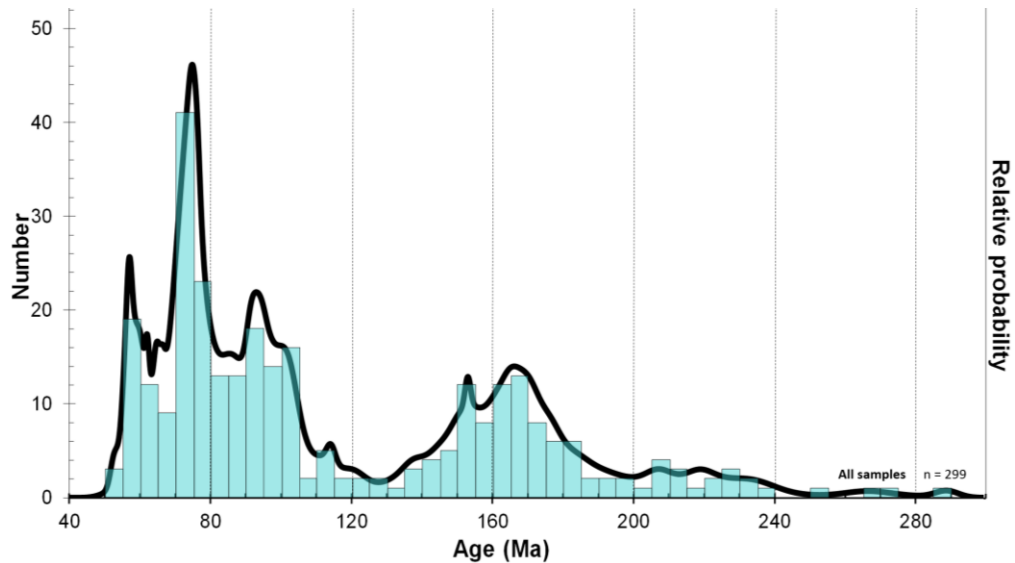
Figure 12. Composite probability density plot for east-central Texas samples with ages younger than 300 Ma. Bin width is 5 Ma.

East-Central Texas Results and Discussion

Qualitative observation of probability density curve peaks, shoulders, and valleys aided in identification of eight detrital zircon age groups. Age intervals with few and/or scattered ages that correspond with poorly developed probability curve peaks are also compiled into groups (Groups A and E), as absence of ages within certain time intervals can also be useful for determination of sediment source. A qualitative approach to group division similar to the one mentioned was done for Wilcox Group detrital zircons in south Texas (Mackey et al. 2012), whereas a more quantitative approach was applied for equivalent strata in Louisiana (Craddock and Kylander-Clark 2013). Age distributions (groups) outlined in these two reports are similar to one another and to this report only in general. The distributions of detrital zircon ages within groups identified here is first shown in Figures 13-14, and the relative proportion of grains with respect to each group are included in Appendix H. These include Groups A (3217-1970 Ma), B (1958-1530 Ma), C (1518-1303 Ma), D (1293-843 Ma), E (799-676 Ma), F (652-265 Ma), G (251-134 Ma), and H (130-52 Ma). Age values listed for these groups correspond with measured detrital zircon ages instead of relative time. For simplicity, beginning with Group A for all probability density plots, the lower boundary of each group corresponds with the youngest value of that group (e.g. 1970, 1530, etc.). Group H contains pronounced multi-modal age distributions that can be further sub-divided into subgroups using Figure 12, while also considering the distribution of data in individual samples (Figures 9-10). However, only Subgroup HL includes ages that closely correspond with late Laramide ages, which makes it a major topic of discussion in later sections. Peaks or shoulders of composite probability density plots were considered robust if the number of corresponding grains with overlapping ages is greater than or equal to 15. This restriction emphasizes the most pronounced probability density peaks and shoulders while excluding those related to underrepresented and scattered grains. Age peaks or shoulders are considered robust for individual probability density plots if the number of corresponding grains with overlapping ages is three or greater, although features with the minimum required number are interpreted with caution. The second method is similar to that used in Craddock and Kylander-Clark (2013), which was adapted from Gehrels (2012). Selecting the minimum cutoff for robust composite probability density peak at 15 grains emphasizes age labels

in every group except Group E, which contains only 9 total grains and represents less than 1% of all grains.
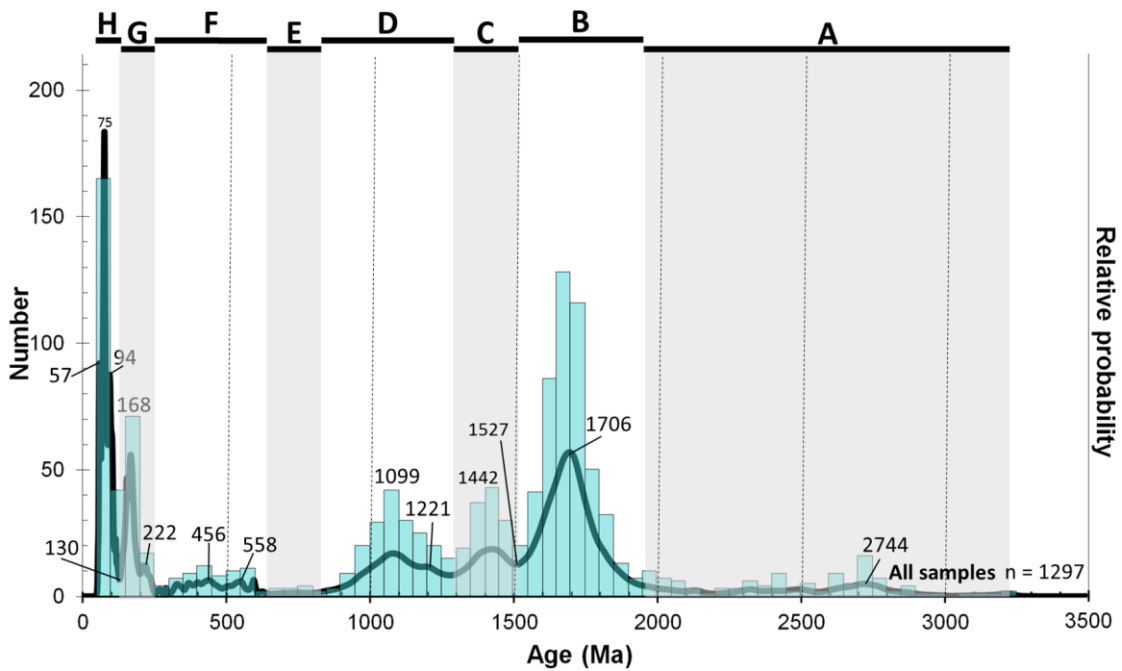
Figure 13. Composite probability density plot with age groups and age labels for detrital zircon ages in east-central Texas. Identified groups are indicated. Bin width is 50 Ma. Robust grains are a minimum of n=15. Full age-range composite probability density plots exclude certain robust age labels that are more easily viewed in Figure 15.

Group A includes Paleoarchean to Paleoproterozoic detrital zircon ages that constitute a robust composite age peak at 2744 Ma, but Group A ages are more scattered in individual samples when compared with Groups B-D (Figure 14). Group A robust age peaks and shoulders are entirely absent in samples younger than the Simsboro Formation. However, CB-BBM and QC both contain Group A peaks defined by up to two overlapping ages, which may indicate that this observation is a result of the filter used for determining robustness. Group B contains a well-developed Paleoproterozoic to Mesoproterozoic composite age distribution with an age peak at 1706 Ma, and contains nearly 38% of
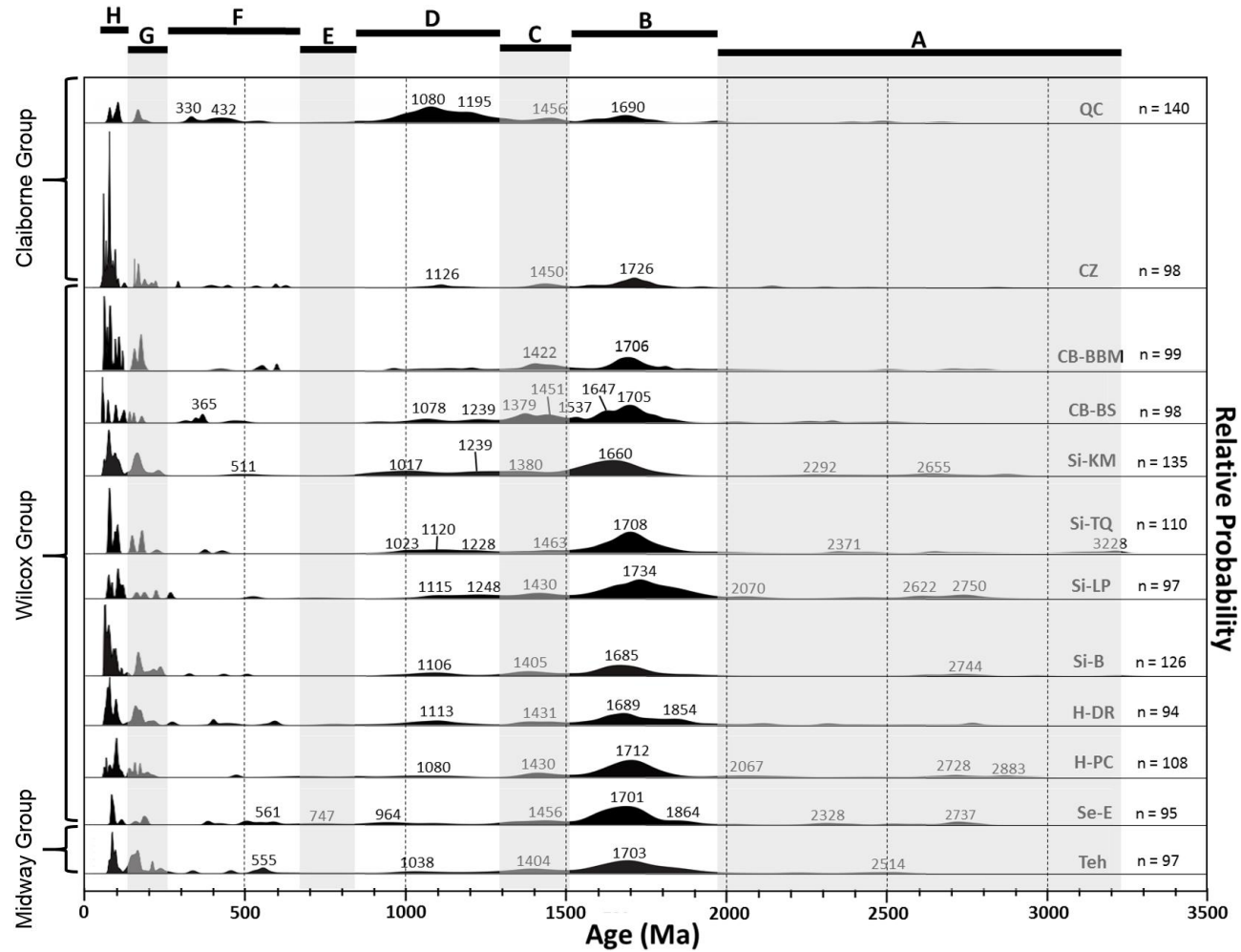
Figure 14. Normalized probability density plots for each sample with age groups and age labels. Labeled probability density curve shoulders and peaks are represented by three or more overlapping ages. Age peaks for grains younger than 300 Ma are included in Figure 16.

all ages. The proportion of Group B within individual samples varies from approximately 29-53% in samples Teh-CZ, in contrast with almost 16% in sample QC. Conversely, Group D contains Mesoproterozoic and Neoproterozoic ages that are dominant in sample QC (51%) compared with an average of 10% in older samples. Robust Group D ages in individual samples are similar to the composite age peaks at 1099 Ma and 1221 Ma, but sample QC ages comprise 36% of the entire group. Sample QC also contains the majority of Group F ages (22%). With the exception of sample QC, Groups D and F also contain a relatively scattered distribution of ages.

Figures 15-16 show the distribution of detrital zircon ages in east-central Texas samples for ages younger than 300 Ma that correspond with Groups G-H. Group G contains Triassic through Early Cretaceous ages and comprises nearly 8% of all grains. Robust composite age peaks for this group occur at 153 Ma and 168 Ma. The age distributions for robust Group G age peaks and shoulders in individual samples are either bimodal and correspond with either robust composite age peaks, or are unimodal with an intermediate age. A minimal number of ages occur between Groups G and H (ca. 150-105 Ma). This paucity of data is highlighted by a valley at 130 Ma in Figure 15 that is also apparent within individual samples (Figure 16). Group H ages are Early Cretaceous to Early Eocene, comprise nearly 15% of all ages, and can be separated into multiple subgroups based on qualitative interpretations of peaks and valleys (Figures 15-16). Robust composite age peaks are defined at 94 Ma, 75 Ma, and 57 Ma, and robust shoulders include ages at 101 Ma and 86 Ma. Robust age peaks or shoulders within individual samples correspond closely with the 75 Ma, 94 Ma, and 101 Ma composite age peaks. Only samples Se-E and CB-BS do not contain robust age peaks or shoulders between 90-105 Ma, and a near equivalent of the Group H 75 Ma composite age peak is robust to within +/- 1 Ma for individual samples except for Teh, Se-E, Si-LP, and CB-BS. However, only sample Se-E does not contain a non-robust age peak that corresponds with the 90-105 Ma interval and 75 Ma composite age peak. Subgroup HL contains Paleocene and very Early Eocene ages that comprise 18% of Group H. These ages first appear in sample H-PC, and are absent in older (Teh, Se-E) and a minority of younger (Si-LP, Si-TQ, QC)

samples. Robust Subgroup HL age peaks within Figure 16 are restricted to samples Si-B, CB-BS, CB-BBM, and CZ.
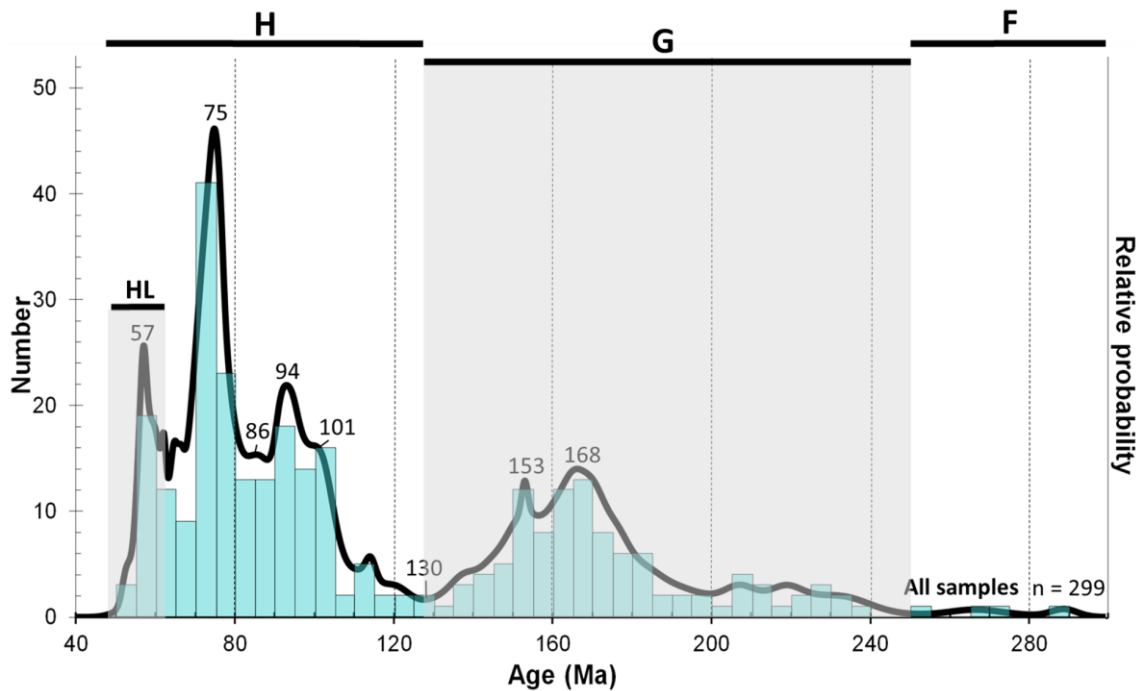
Figure 15. Composite probability density plot with associated histograms, age groups, and age labels for all samples in east-central Texas with ages younger than 300 Ma. Bin width is 5 Ma. Robust peaks and shoulders correspond with a minimum of n = 15.

The distribution of ages within east-central Texas samples shows a relative similarity between the Tehuacana Member of the Midway Group (Teh), the Wilcox Group (Se-E to CB-BBM), and the Carrizo Formation (CZ) of the lower Claiborne Group. This similarity suggests that these samples may have had similar sediment sources, or a similar paleodrainage area for the majority of detrital zircon ages present. The presence of younger zircons in younger Wilcox Group samples is compatible with derivation from the same source area if that source is a site of continuing igneous activity. Additionally, the pronounced distribution ages within Group D (1293-843 Ma) of the Queen City Formation
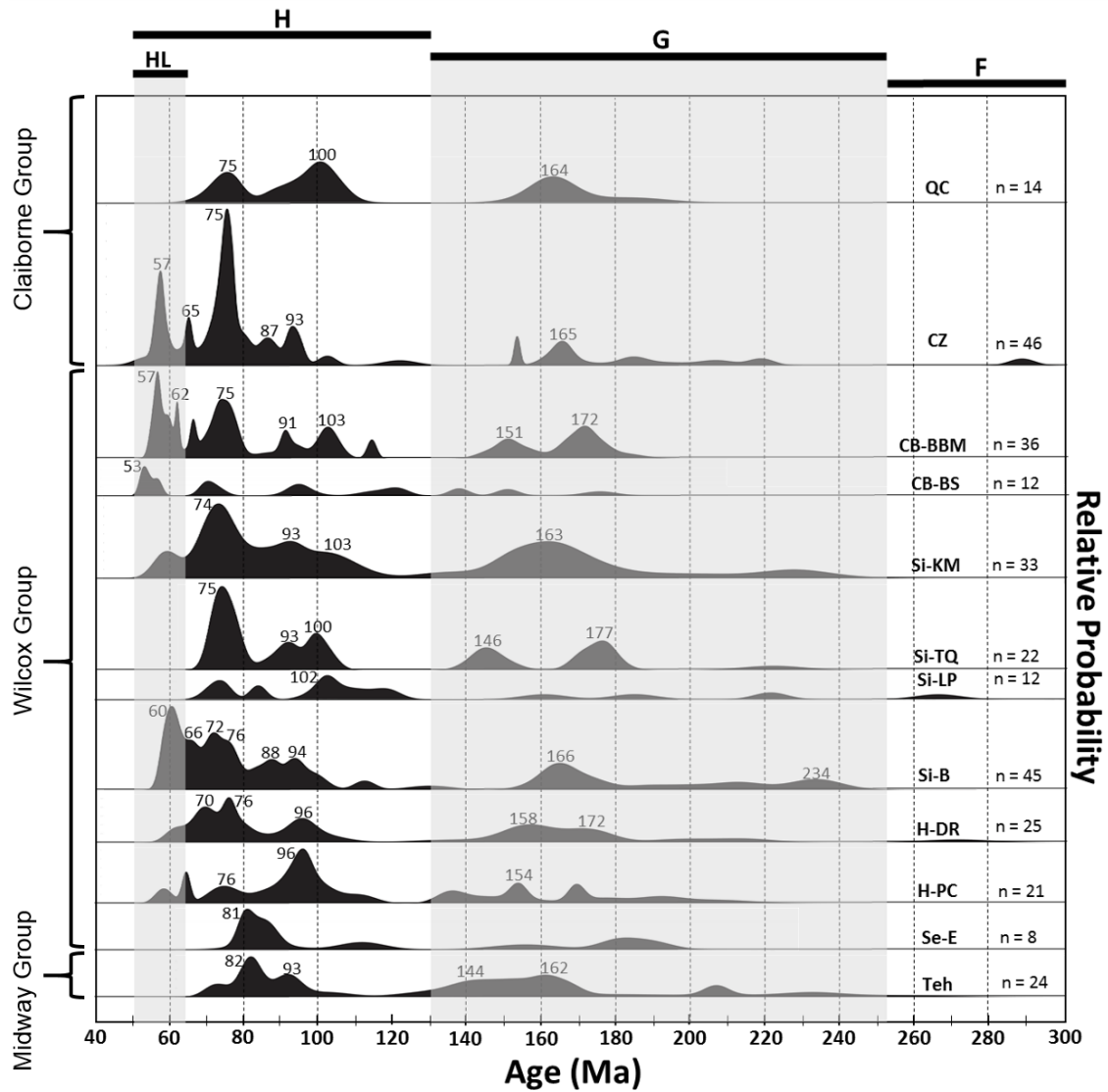
Figure 16. Normalized probability density plots for each sample with age groups and age labels for ages younger than 300 Ma. Robust peaks and shoulders correspond with a minimum of n = 3.

(QC) is distinctly different compared with older samples, and may suggest contribution from a new sediment source and/or a greater amount of detrital zircons from a previously existing source during deposition of the Queen City Formation. This does not discount continued sediment contribution from other previously existing sources, although

recycling of previously deposited sediments in east-central Texas is a possibility for these samples.

Presence of Subgroup HL ages first identified within the Hooper Forrmation (H-PC) of the Wilcox Group identifies the relative arrival time of late Laramide-age detrital zircons to east-central Texas. However, fluctuation of these ages in younger samples is apparent, especially within the Simsboro Formation, where Si-LP and Si-TQ lack late Laramide-age detrital zircon ages. The observable inconsistency in late Laramide ages in Subgroup HL, as well as ages in other groups may be contributed to a number of factors that introduce a natural bias or a bias related to sample preparation and measurement (Sircombe et al. 2001; Cawood et al. 2003; Fedo et al. 2003; Vermeesch 2004; Moecher and Samson 2006; Hay and Dempster 2009; Slama and Kosler 2012). Some of these include the type of relief in source areas and its change in time (Cawood et al. 2003) and the number of analyzed detrital zircon ages for each sample (Vermeesch 2004). The observed differences between Mesozoic and younger ages between samples could also simply be due to less associated analytical uncertainty.

Kolmogorov-Smirnov Test

Detrital zircon age data from east-central Texas were analyzed using the K-S statistical test to address potential dissimilarity between samples. K-S test results for samples containing all ages suggest similarity between the Tehuacana Member and all Wilcox Group samples except Si-LP (Table 3). The Midway Group, Wilcox Group, and Carrizo Formation samples show a 55% internal consistency. Samples Se-E, H-PC, and Si-TQ are the only samples that show similarity with Si-LP, making it the most dissimilar Wilcox Group sample. The Queen City Formation is the most dissimilar of all samples, with no probability values greater than 0.001. When considering detrital zircon age distributions, the Carrizo Formation qualitatively corresponds more closely with older samples (Teh-CB-BBM) compared with the only other Claiborne Group Formation (QC). However, the Carrizo Formation is the second most dissimilar of all samples, being consistent with only Si-B and CB-BBM.

Table 3. K-S test probability (P) values for all samples using error in the Cumulative Distribution Function. Values correspond to individual samples. Yellow/bolded values correspond to P values greater than 0.05 that are not statistically dissimilar.

	Teh	Se-E	H-PC	H-DR	Si-B	Si-LP	Si-TQ	Si-KM	CB-BS	CB-BBM	CZ	QC
Teh		0.111	0.268	0.996	0.205	0.032	0.491	0.629	0.273	0.138	0.002	0.000
Se-E	0.111		0.574	0.068	0.000	0.189	0.477	0.028	0.382	0.000	0.000	0.000
P-PC	0.268	0.574		0.142	0.008	0.381	0.999	0.004	0.214	0.004	0.000	0.000
H-DR	0.996	0.068	0.142		0.639	0.005	0.349	0.647	0.111	0.350	0.024	0.001
Si-B	0.205	0.000	0.008	0.639		0.000	0.024	0.256	0.005	0.976	0.156	0.000
Si-LP	0.032	0.189	0.381	0.005	0.000		0.240	0.000	0.006	0.000	0.000	0.000
Si-TQ	0.491	0.477	0.999	0.349	0.024	0.240		0.009	0.365	0.011	0.000	0.000
Si-KM	0.629	0.028	0.004	0.647	0.256	0.000	0.009		0.184	0.158	0.001	0.001
CB-BS	0.273	0.382	0.214	0.111	0.005	0.006	0.365	0.184		0.005	0.000	0.000
CB-BBM	0.138	0.000	0.004	0.350	0.976	0.000	0.011	0.158	0.005		0.441	0.000
CZ	0.002	0.000	0.000	0.024	0.156	0.000	0.000	0.001	0.000	0.441		0.000
QC	0.000	0.000	0.000	0.001	0.000	0.000	0.000	0.001	0.000	0.000	0.000	

A greater degree of statistical dissimilarity occurs between samples when young age peaks were within range of the stratigraphic depositional age (Laskowski et al. 2013). Additionally, removal of these ages leads to a much greater degree of internal consistency between samples (some cases up to 98%). Seven of the 12 youngest detrital zircon ages calculated for each sample of this report are within error of the relative depositional age, which supported completion of an additional K-S test. When Paleocene and Eocene grains are removed from the dataset for this study, the results are only slightly different (Table 4). This may suggest that the primary ages controlling whether or not samples are statistically dissimilar during K-S testing are not Paleocene or Eocene. Further K-S testing was done where ages younger than 300 Ma were removed that are potentially representative of igneous or metamorphic activity within the Western Cordillera (Tobisch et al. 1986; Busby-Spera 1988; Barth et al. 1997; Dunne et al. 1998; Ducea, 2001 Saleeby et al. 2008; Gehrels et al. 2009; Miller et al. 2009; LaMaskin 2012). This was done to determine how discrepancy within this age interval influenced K-S test results, and to determine the similarity between samples with respect to older detrital zircons. K-S test results for this scenario are substantially different (Table 5). Test results indicate that the distribution of grains that primarily influences similarity or dissimilarity of samples corresponds with zircons with ages between 66-300 Ma. The Midway Group, Wilcox Group, and Carrizo Formation show 89% internal consistency once ages older

than 300 Ma were removed, compared to just 55% when all ages are considered. A minor number of Wilcox Group samples are still statistically dissimilar, including CB-BS (with H-PC, Si-LP), Si-KM (with H-PC, Si-LP, Si-TQ), and Si-LP (with Si-B). Similar to Table 4, sample QC is still entirely dissimilar from all other samples.

Table 4. K-S test probability (P) values using error in the Cumulative Distribution Function for samples excluding Paleocene and Eocene ages

	Teh	Se-E	H-PC	H-DR	Si-B	Si-LP	Si-TQ	Si-KM	CB-BS	CB-BBM	CZ	QC
Teh		0.112	0.200	1.000	0.914	0.032	0.491	0.679	0.129	0.681	0.058	0.000
Se-E	0.112		0.756	0.120	0.010	0.189	0.471	0.035	0.552	0.013	0.000	0.000
H-PC	0.200	0.756		0.143	0.032	0.432	0.981	0.003	0.241	0.017	0.001	0.000
HP-DR	1.000	0.120	0.143		0.988	0.010	0.474	0.615	0.082	0.854	0.123	0.000
Si-B	0.914	0.010	0.032	0.988		0.003	0.112	0.791	0.023	0.990	0.193	0.000
Si-LP	0.032	0.189	0.432	0.010	0.003		0.239	0.000	0.009	0.004	0.000	0.000
Si-TQ	0.491	0.471	0.981	0.474	0.112	0.239		0.012	0.496	0.059	0.002	0.000
Si-KM	0.679	0.035	0.003	0.615	0.791	0.000	0.012		0.124	0.643	0.009	0.000
CB-BS	0.129	0.552	0.241	0.082	0.023	0.009	0.496	0.124		0.027	0.000	0.000
CB-BBM	0.681	0.013	0.017	0.854	0.990	0.004	0.059	0.643	0.027		0.425	0.001
CZ	0.058	0.000	0.001	0.123	0.193	0.000	0.002	0.009	0.000	0.425		0.000
QC	0.000	0.000	0.000	0.000	0.000	0.000	0.000	0.000	0.000	0.001	0.000	

Table 5. K-S test probability (P) values using error in the Cumulative Distribution Function for samples excluding ages 300 Ma and younger.

	Teh	Se-E	H-PC	H-DR	Si-B	Si-LP	Si-TQ	Si-KM	CB-BS	CB-BBM	CZ	QC
Teh		1.000	0.444	0.993	0.770	0.164	0.682	0.432	0.818	1.000	1.000	0.000
Se-E	1.000		0.531	1.000	0.796	0.086	0.553	0.322	0.563	0.963	0.997	0.000
H-PC	0.444	0.531		0.365	0.243	0.559	0.999	0.003	0.029	0.206	0.334	0.000
HP-DR	0.993	1.000	0.365		0.986	0.216	0.648	0.411	0.524	0.926	0.989	0.000
Si-B	0.770	0.796	0.243	0.986		0.038	0.363	0.720	0.702	1.000	0.934	0.000
Si-LP	0.164	0.086	0.559	0.216	0.038		0.395	0.000	0.003	0.084	0.149	0.000
Si-TQ	0.682	0.553	0.999	0.648	0.363	0.395		0.007	0.063	0.344	0.520	0.000
Si-KM	0.432	0.322	0.003	0.411	0.720	0.000	0.007		0.979	0.361	0.385	0.000
CB-BS	0.818	0.563	0.029	0.524	0.702	0.003	0.063	0.979		0.866	0.873	0.000
CB-BBM	1.000	0.963	0.206	0.926	1.000	0.084	0.344	0.361	0.866		0.995	0.000
CZ	1.000	0.997	0.334	0.989	0.934	0.149	0.520	0.385	0.873	0.995		0.000
QC	0.000	0.000	0.000	0.000	0.000	0.000	0.000	0.000	0.000	0.000	0.000	

K-S test results may suggest that ages younger than 300 Ma are a primary influence on dissimilarity between samples. Additionally, results may support the suggestions made for similarity between the Midway Group, Wilcox Group, and Carrizo Formation, and uniqueness of the Queen City Formation (Figures 14, 16). However, interpretations made from K-S test results may be biased when considering the sensitivity of the test to various factors, including the number of analyses per sample, the proportion and presence of ages, and analytical uncertainty. Further details on K-S test sensitivity are available in a manual designed by the Arizona LaserChron Center at the University of Arizona (www.geo.arizona.edu/alc). A plot of absolute error vs. measured age for all data from this study shows contrast between the level of analytical uncertainty in older and younger ages (Figure 17). This is attributed to $^{206}Pb/^{238}U$ and $^{207}Pb/^{206}Pb$ ages that were used for ages younger and older than an approximately ca. 600 Ma cutoff, respectively. Because this distinct difference in uncertainty in younger ages corresponds with ages the K-S test considers influential on sample dissimilarity, it is likely that K-S test results are an artifact of the test itself. Furthermore, slight differences in the number of analyses per sample and the proportion and presence of ages are also likely biasing K-S test results. These stated sensitivities bring into question the reliability and suitability of the K-S test for this type of study, which has been addressed previously in Vermeesch (2013).
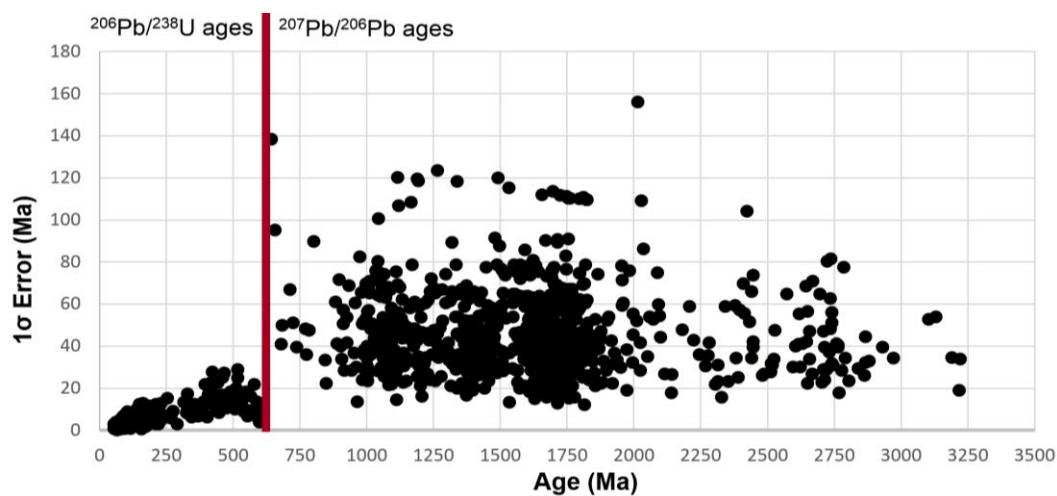
Figure 17. One-sigma absolute error vs. age for all detrital zircon ages within 10% discordance. Red line indicates the boundary between isotopic ages used in this study.

CHAPTER V

SOURCE REGIONS AND GULF COASTAL PLAIN LOCATIONS

Detrital zircon ages from east-central Texas correspond with timing of major igneous and metamorphic events in North America (Whitmeyer and Karlstrom 2007; Craddock and Kylander-Clark 2013 and references therein). Ages of much of the detrital zircons deposited along the Gulf Coast correspond with components of source terranes related to assembly of the Laurentian shield (Yavapai Province (1.8-1.72 Ga), the Mazatzal Province (1.72-1.60 Ga), the Granite-Rhyolite Province (1.55-1.35 Ga)), Grenville orogenic terrane (1.30-0.95 Ga), and the Cordilleran Arc (<0.25 Ga); (Figure 18). Identifying the source of detrital zircons based on comparison of measured ages with ages of known basement terranes is complicated by the possibility of sediment recycling, where grains may be eroded, transported, and deposited in a site nearby or far removed from the original source (Eriksson et al. 2004; Dickinson et al. 2009). Determining provenance is further complicated by the possibility of changes in paleodrainage in areas proximal to basement sources and basins containing recycled sediments.
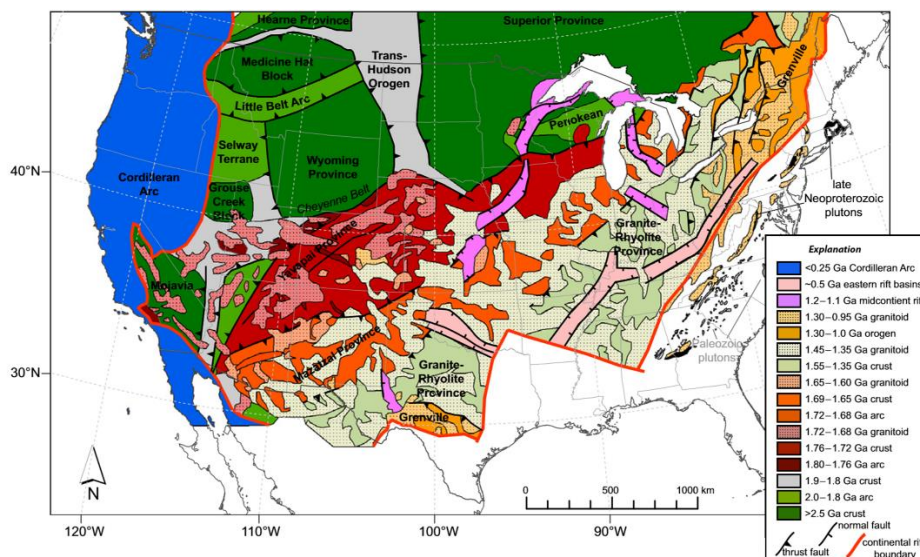
Figure 18. North American basement terranes. From Craddock and Kylander-Clark (2013) and references therein.

To address potential paleodrainage implications, comparison was made with compiled detrital zircon data from western and northern Cordillera areas and from Paleogene samples within the Texas and Louisiana Gulf Coastal Plain. Paleogeographic maps with inferred paleodrainage during Late Paleocene and Early Eocene time from Galloway et al. (2011) are shown in Figure 19, although other paleodrainage maps are available (e.g. Mackey et al. 2012; Craddock and Kylander-Clark 2013). Probability density plots of detrital zircon age compilations include Upper Cretaceous (Sevier foreland basin) and Paleogene (Laramide intramontane basins) strata for the Rocky Mountain region (from Craddock and Kylander-Clark, 2013), including the southern Rocky Mountain region of New Mexico, Utah, and Arizona (Dickinson and Gehrels 2008b), and the northern Rocky Mountain region of Wyoming (Fan et al. 2011; May et al. 2013), and northwestern Montana (Fuentes et al. 2011). Compiled detrital zircon composite age spectra from the McCoy/Bisbee Paleobasin and northern Mexico are included in this report for a southwestern source region (Doebbert 2013), and data were not available for the eastern Rocky Mountain area (Colorado Front Ranges). Texas and Louisiana Gulf Coastal Plain comparison samples included detrital zircon age spectra from the South Texas Wilcox Group (Mackey et al. 2012) and the Louisiana Wilcox Group and Claiborne Group (Craddock and Kylander-Clark 2013). The location of samples corresponding to regional sources and Gulf Coastal Plain samples are shown in Figure 20, while corresponding probability density plots are shown in Figures 21-22. Robust peaks for certain samples were determined from Craddock and Kylander-Clark (2013), and observable differences between robust ages presented in this and previous studies may be attributed to differences in labeling methodology rather than data. For this reason, the overall assemblage of detrital zircon ages was considered more reliable when making observations and interpretations.

Several important similarities and differences appear in composite detrital zircon age assemblages of the northern Rocky Mountain, southern Rocky Mountain, and southwestern source regions. The distribution of Precambrian and Paleozoic ages and presence of robust age peaks are generally similar between source regions for Groups A
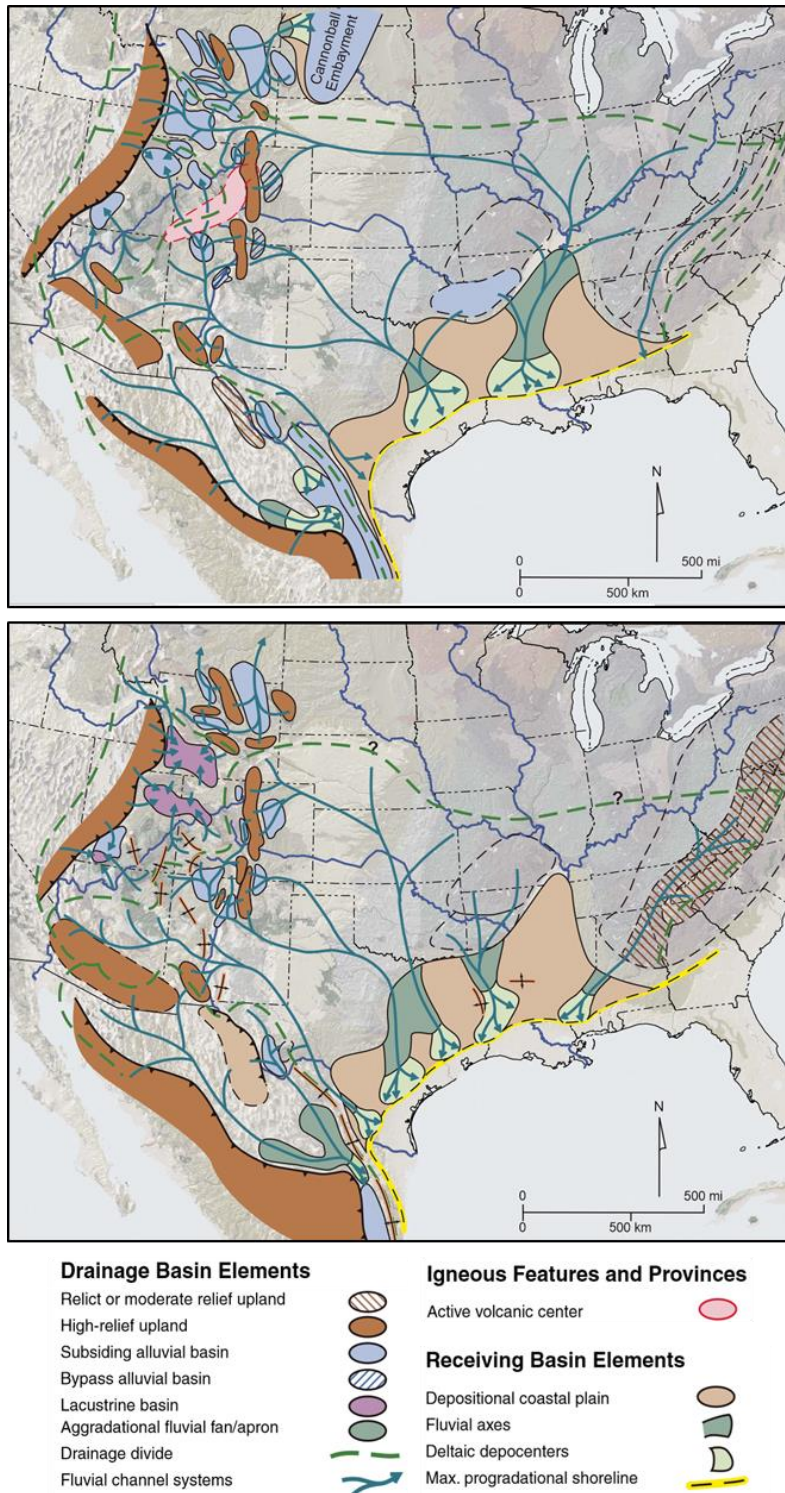
Figure 19. Paleogeographic reconstructions with inferred paleodrainage pathways during the Late Paleocene (top) and Early Eocene (bottom). Dark blue lines indicate major modern rivers. From Galloway et al. (2011) and references therein.

through F, although the northern Rocky Mountain region lacks a robust Group C age peak (Figures 21-22). The distribution of Group G Triassic-Jurassic ages and the presence of robust age peaks for the southern Rocky Mountain region and southwestern region are similar. Data for both of these regions contrast with Triassic-Jurassic data for the northern Rocky Mountain region, although not all areas within this region are underrepresented with respect to these ages (Fan et al. 2011) and the disproportionate amount of Cretaceous ages may cause other age components to appear less pronounced. Pronounced Early Jurassic ages of Group G at ca. 130 Ma appear to be unique to the southwestern region. There is a more pronounced age distribution (ca. 105–90 Ma) for Group H in the northern Rocky Mountain region, but these ages and similar robust age peaks occur in the other source regions. Latest Cretaceous ages and robust 78 Ma and 72 Ma age peaks occur in the southwestern region and northern Rocky Mountain region, respectively, and no equivalent ages occur in the southern Rocky Mountain region. Subgroup HL (64-52 Ma) contains no developed age distributions or age peaks for any of these source regions, apart from a minor component of the southwestern region. Minimal to no ages for the southwestern and southern Rocky Mountain source regions is expected because Paleogene data were underrepresented or absent, but this is not the case for the northern Rocky Mountain region, which discounts this region as a source of late Laramide-age detrital zircons.

Like the source regions, Texas and Louisiana Gulf Coastal Plain samples contain a relatively similar distribution of Precambrian and Paleozoic ages and presence of robust age peaks for Groups A through F, although the Louisiana Wilcox group lacks a robust Group C age peak. Only the east-central Texas samples contain robust Group F and A age peaks, and only Louisiana samples lack robust Group G age peaks, although these observations may be attributed to differences in robustness between studies. Triassic-Jurassic ages appear relatively similar for each location, with the Louisiana Wilcox Group and east-central Texas (Teh-CZ) showing closest similarity. Although robust Mesozoic age peaks do not occur in the Louisiana Wilcox Group, overall similarities in age distributions make these samples compatible. The minor presence of grains between ca. 150-105 Ma within east-central Texas (Teh-CZ) corresponds with Louisiana Wilcox
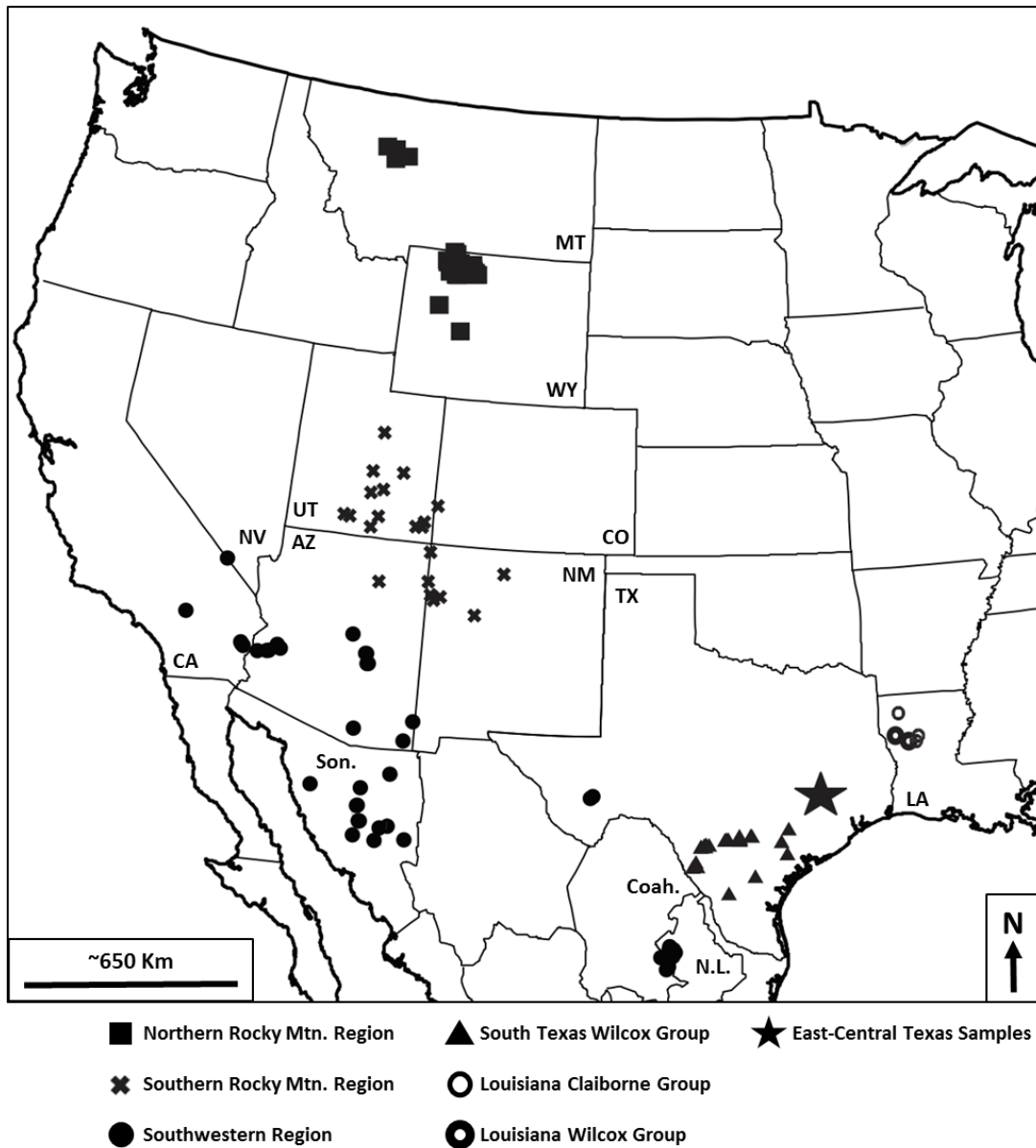
Figure 20. Locations of compiled studies for source regions and Texas and Louisiana Gulf Coastal Plain locations. Southwestern regional plots compiled by Doebbert (2013) from: Barth et al. (2004), Davis et al. (2010), Dickinson and Gehrels (2008a), Dickinson and Gehrels (2009), Dickinson et al. (2009), Gleason et al. (2007), Lawton et al. (2009), Mauel et al. (2011), Poole et al. (2008), Spencer et al. (2011), and Stewart et al. (2001). MT (Montana), WY (Wyoming), CO (Colorado), TX (Texas), NM (New Mexico), LA (Louisiana), AZ (Arizona), CA (California), NV (Nevada), UT (Utah), Coah. (Coauhila), N.L. (Nuevo Leon).
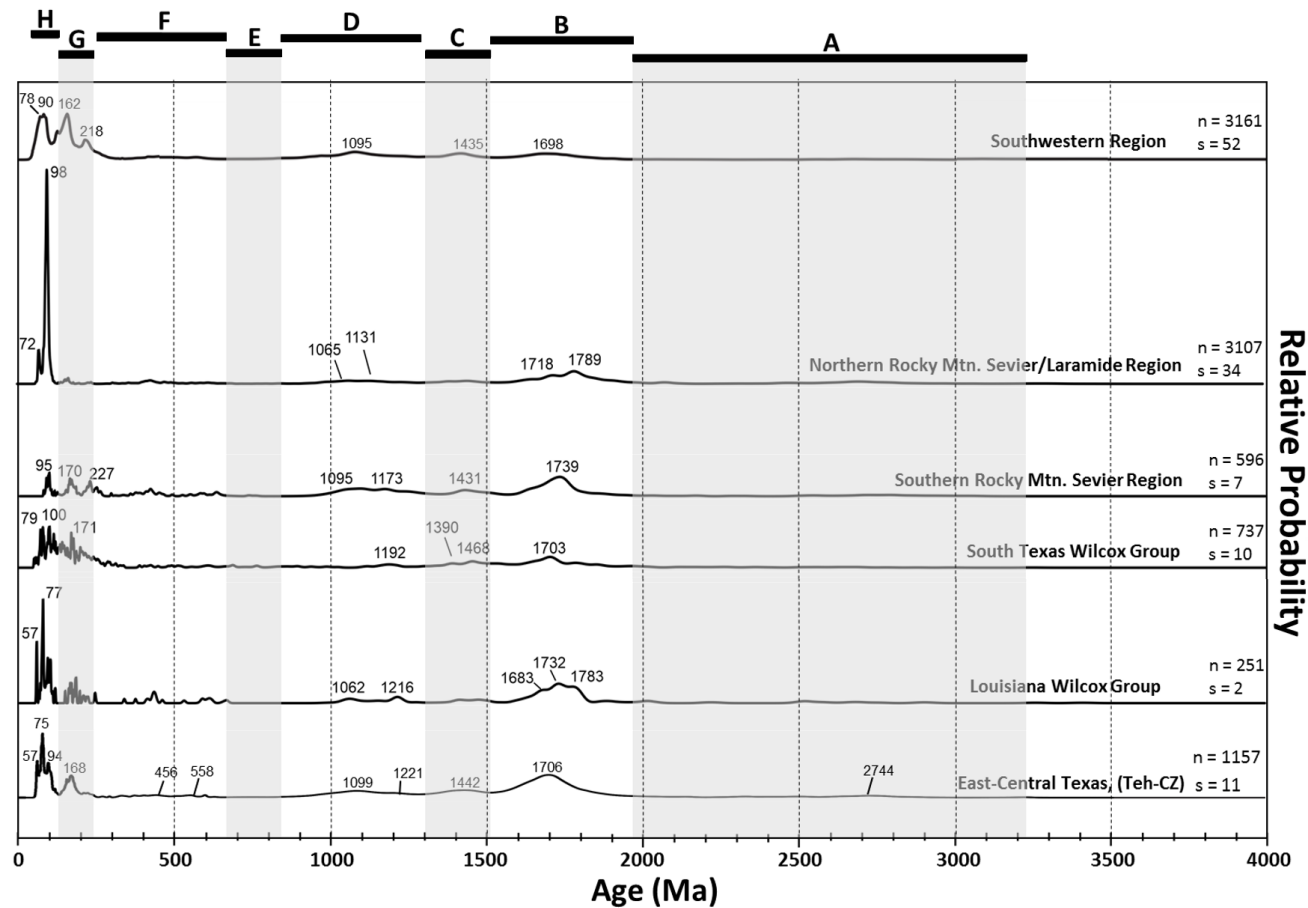
Figure 21. Normalized probability density plots of detrital zircon age spectra compilations for source regions and Texas and Louisiana Gulf Coastal Plain locations. See text for sample details. Symbol n indicates number of grains; s indicates number of samples. Robust age labels for samples here are defined in text. Robust age peaks for Louisiana, south Texas, and the Rocky Mountain regions are from Craddock and Kylander-Clark (2013).
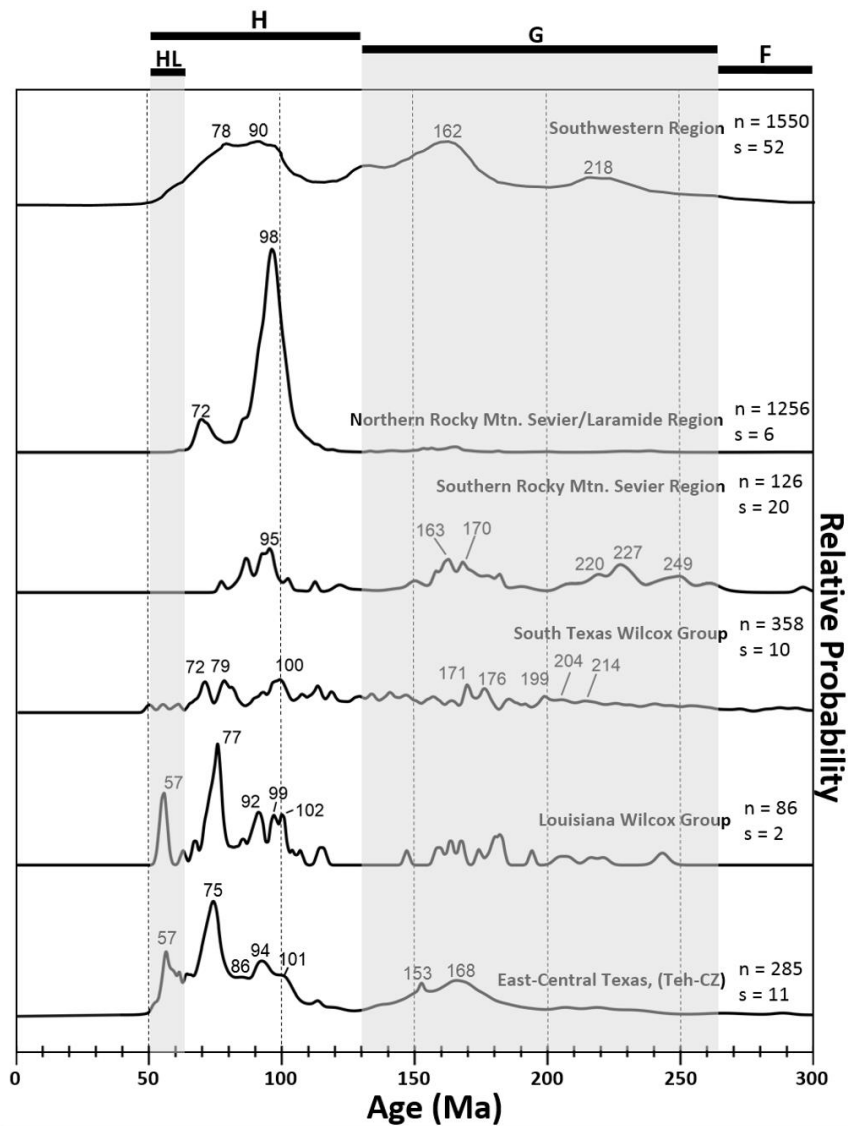
Figure 22. Normalized probability density plots of detrital zircon age spectra compilations for source regions and Texas and Louisiana Gulf Coastal Plain locations for ages younger than 300 Ma.

Group samples, but not with the south Texas Wilcox Group. East-central Texas, south Texas, and Louisiana samples contain corresponding Cretaceous ages within Group H at ca. 105-90 Ma and ca. 77-72 Ma, with generally similar robust age peaks and shoulders. Similar to Triassic and Jurassic ages of Group G, the distribution of ages in Group H for the Louisiana Wilcox Group and east-central Texas (Teh-CZ) are very similar.

Finally, Subgroup HL ages and a robust 57 Ma age peak occur in east-central Texas (Teh-CZ) and the Louisiana Wilcox Group, but these ages are generally absent in the south Texas Wilcox Group.

East-central Texas (Teh-CZ) data are compatible with age components from each of the source regions when considering only the presence of ages. The distribution of most Middle Proterozoic and older ages and robust age peaks of Groups A through F for this location and each source region are similar, apart from absence of a robust Group C age peak in the northern Rocky Mountain region. The distribution of Triassic-Jurassic ages in east-central Texas (Teh-CZ) corresponds more closely with the southern Rocky Mountain and southwestern regions. Because of the extent of sample locations for the southwestern region (Figure 20), it is possible that not every location represented by the composite dataset contains a similar distribution of ages. This is the case for ca. 150-105 Ma ages, which are primarily represented in parts of northern Mexico (Lawton et al. 2009; Mauel et al. 2011). The distribution of Late Cretaceous Group H ages between ca. 105-90 Ma for each sample is relatively similar, while the distribution of Late Cretaceous ages are more similar to the northern Rocky Mountain and southwestern regions. Interpreted northern and eastern drainage from the northern Rocky Mountain region towards the Cannonball Embayment at this time (Cherven and Jacobs 1985; Galloway et al. 2011) may discount this source region as a contributor of sediments to the Gulf of Mexico. It is possible that source regions not presented here were contributors of detrital zircons to the Gulf of Mexico, which is likely the case for the Rocky Mountain Front in Colorado and parts of New Mexico. However, based on the available information and data comparisons, it is suggested that detrital zircons were contributed from parts of the southwestern and the southern Rocky Mountain source regions. Qualitative similarity between detrital zircon age assemblages in the Louisiana Wilcox Group and east-central Texas (Teh-CZ) (Figures 21-22) may support the same relationships for the Louisiana Wilcox Group, as well as the idea that this location had similar sediment sources, or a similar paleodrainage area for the majority of observed detrital zircon ages.

The distribution of south Texas Wilcox Group ages appears to be relatively similar to each source region for Groups A through F, but is most similar to the southwestern and southern Rocky Mountain source regions based on Triassic-Jurassic and Late Cretaceous ages. The northern Rocky Mountains region is generally discounted for this location based on an unlikely paleodrainage pathway (Figure 19) and literature support (Cherven and Jacobs 1985). Presence of more pronounced ca. 150-105 Ma ages only in south Texas and the southwestern source region support a drainage connection, and may suggest differences in paleodrainage between the two Texas locations. Interpreted paleodrainage constraints for Gulf Coastal Plain locations are shown in Figure 23. The sediment source suggested for the ca. 150-105 Ma ages in the south Texas Wilcox Group is the Peninsular Range Batholith and Alisitos Arc of southern California and the Baja Peninsula (Lawton et al. 2009; Mackey et al. 2012). If these detrital zircon ages were also sourced to east-central Texas and Louisiana, then there would likely be a pronounced distribution of ca. 150-105 Ma ages in these locations. Absence of pronounced Subgroup HL ages and a robust ca. 57 Ma age peak in the south Texas Wilcox Group further supports unique overall paleodrainage for this location, as only one northernmost sample within the upper Wilcox Group (Carrizo Formation) in south Texas contains late Laramide-age detrital zircons (Mackey et al. 2012).

Comparison of Queen City Formation, Louisiana Claiborne Group, and older data in east-central Texas and Louisiana also shows important similarities and differences (Figures 24-25). Detrital zircon data indicate a relative similarity between ages of the Queen City Formation and Louisiana Claiborne Group with respect to Groups A through G. Differences in Group H (130-52 Ma) and younger ages may be attributed to the number of grains analyzed per sample, as well as contributions from silicic volcanic ash deposits from the Sierra Madre Occidental for ages younger than ca. 45 Ma (McDowell 2007). Both samples show a more pronounced distribution of Group D (1293-843 Ma) ages in contrast with the Louisiana Wilcox Group and east-central Texas (Teh-CZ) data (Figures 14, 24). The distribution of ages for both of these samples is similar to components of the southwestern and southern Rocky Mountain regions, apart from much more pronounced number of Group D ages. These comparisons may support partial derivation from these

47

source regions. Comparison between samples in Figures 24-25 may support similar suggestions for the Louisiana Wilcox Group with those that were made for the Queen City
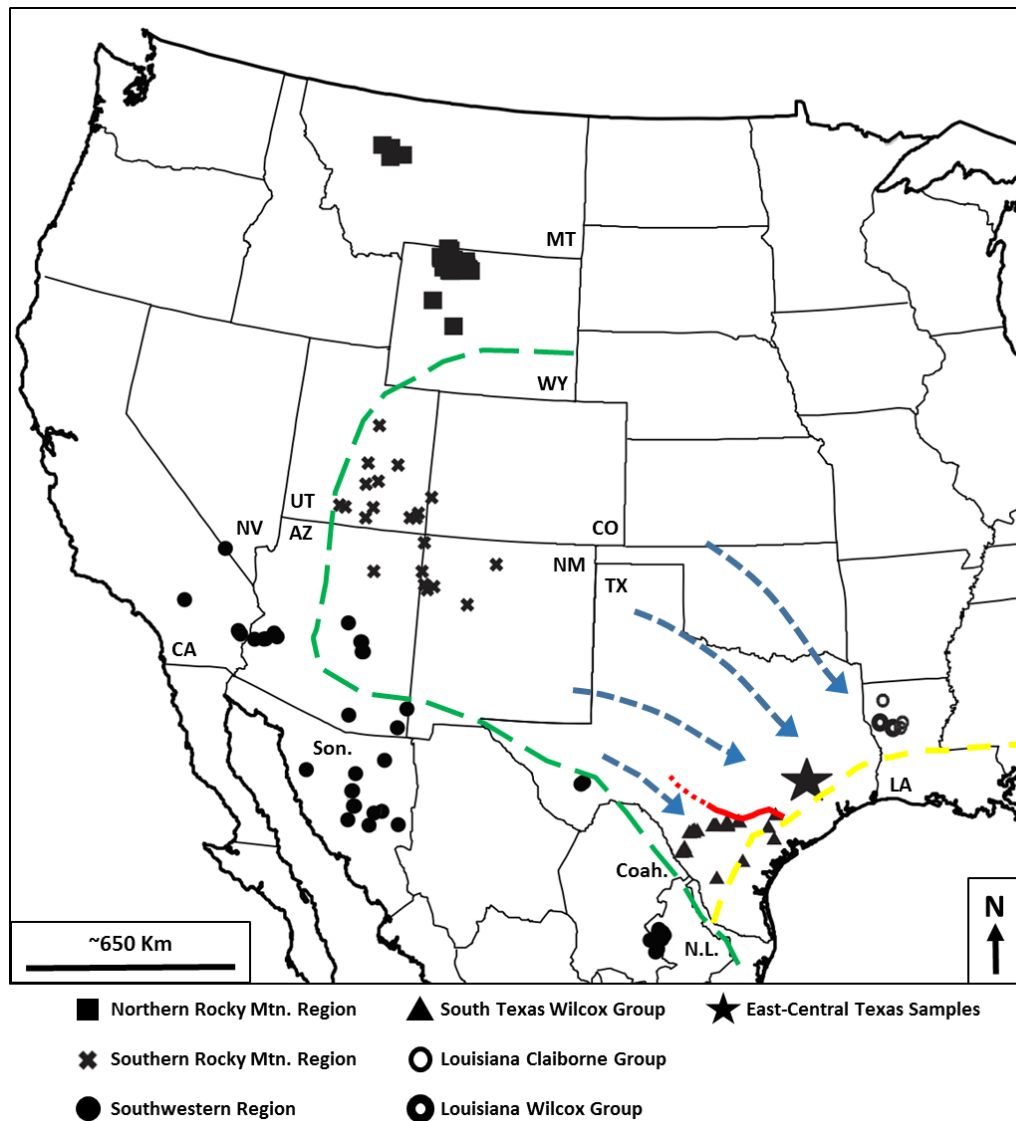
Figure 23. Late Paleocene-Early Eocene paleodrainage constraints for Texas and Louisiana Gulf Coastal Plain locations. Drainage corresponds with the south Texas Wilcox Group, east-central Texas (Teh-CZ), and Louisiana Wilcox Group. Red line indicates paleodrainage divide between Gulf Coastal Plain locations. Western paleodrainage divide (green dashes) and maximum progradation of the shoreline (yellow dashes) are after Galloway et al. (2011). Blue dashes indicate generalized fluvial pathways.

Formation in east-central Texas, in that the same new or more pronounced sediment source (Group D: 1293-843 Ma) first identified in the Queen City Formation was also available during deposition of these units. Louisiana Claiborne Group data are from the Sparta, Cook Mountain, and Cockfield Formations. These formations are younger than the Queen City Formation, which means that the Queen City Formation is the oldest identified stratigraphic level that contains a more pronounced distribution of Group D ages. Furthermore, K-S test results from Craddock and Kylander-Clark (2013) show that no Louisiana Claiborne Group samples are statistically similar to Louisiana Wilcox Group samples (Craddock and Kylander-Clark 2013). This may support the contrast between these samples (Figure 24) observed in Group D and is consistent with K-S test results for the Queen City Formation (Tables 3-5), although K-S test results are still questionable when considering bias due to sensitivity.

Detrital zircon geochronology applied to Wilcox Group strata reported 62–54 Ma grains from Mississippi embayment to south-central Texas (Blum and Pecha 2014). These ages are equivalent to late Laramide-age detrital zircons of Subgroup HL. None of the source regions that include Early Paleogene data contain a robust age peak within Subgroup HL corresponding with Louisiana Wilcox Group and east-central Texas (Teh-CZ) samples, and these ages do not occur in any eastern source. Since the majority of data used for source region comparison includes Mesozoic strata, it is possible that this age component was not identified in the source region data because Early Paleogene data were underrepresented. This is not likely for the northern Rocky Mountain region because each sample contains Early Paleogene data, but is possible for the entire southern Rocky Mountains region and much of the southwestern region. It is also possible that these zircons were derived from an area not represented in this report. Potential source(s) of late Laramide-age detrital zircons (Figure 26) include the Santa Rita lineament in southern New Mexico (Chapin et al. 1978; 2004; Wilks and Chapin 1997) and the Colorado Mineral Belt in the Colorado Plateau area (Cunningham et al. 1994; Chapin et al. 2004; Chapin 2012). These two sources are considered more likely based on their close proximity to Laramide uplifts and no indication of paleodrainage divides between
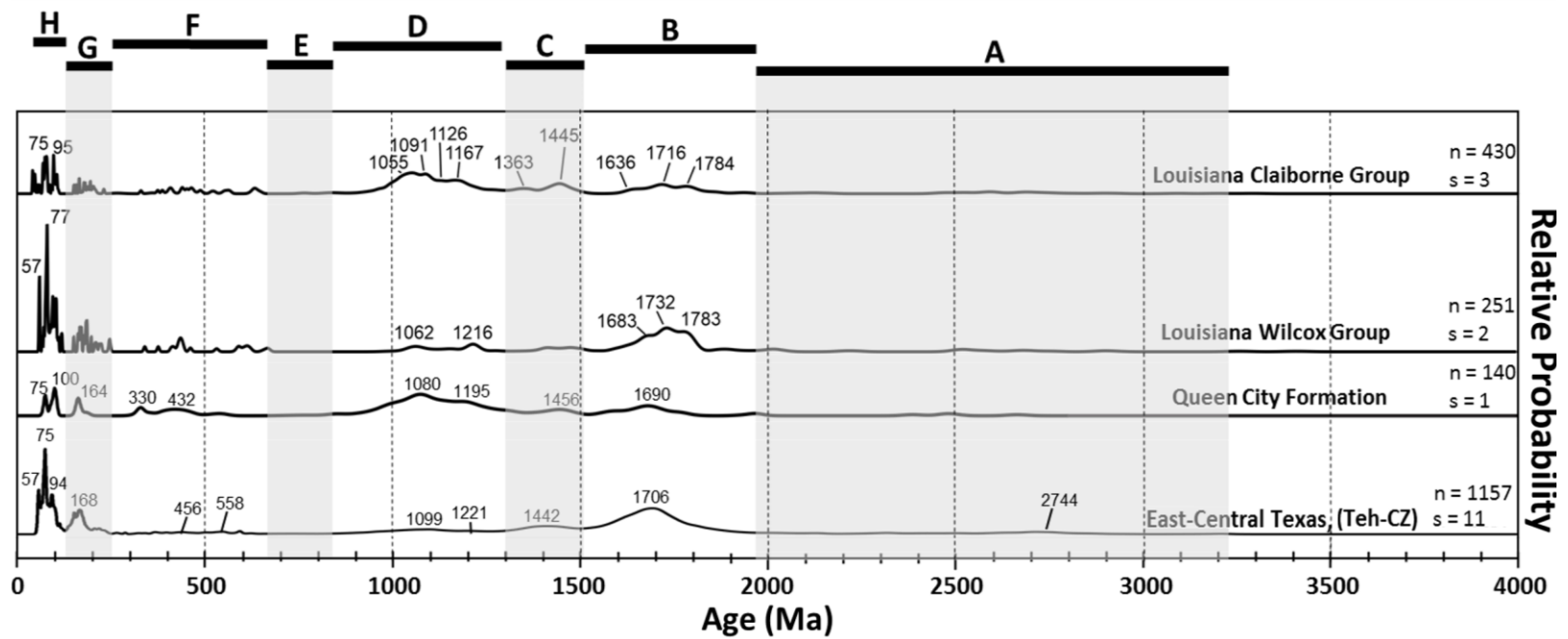
Figure 24. Normalized probability density plots of detrital zircon age spectra compilations for east-central Texas and Louisiana. Data show similarities and differences between primarily Wilcox Group and Claiborne Group samples.
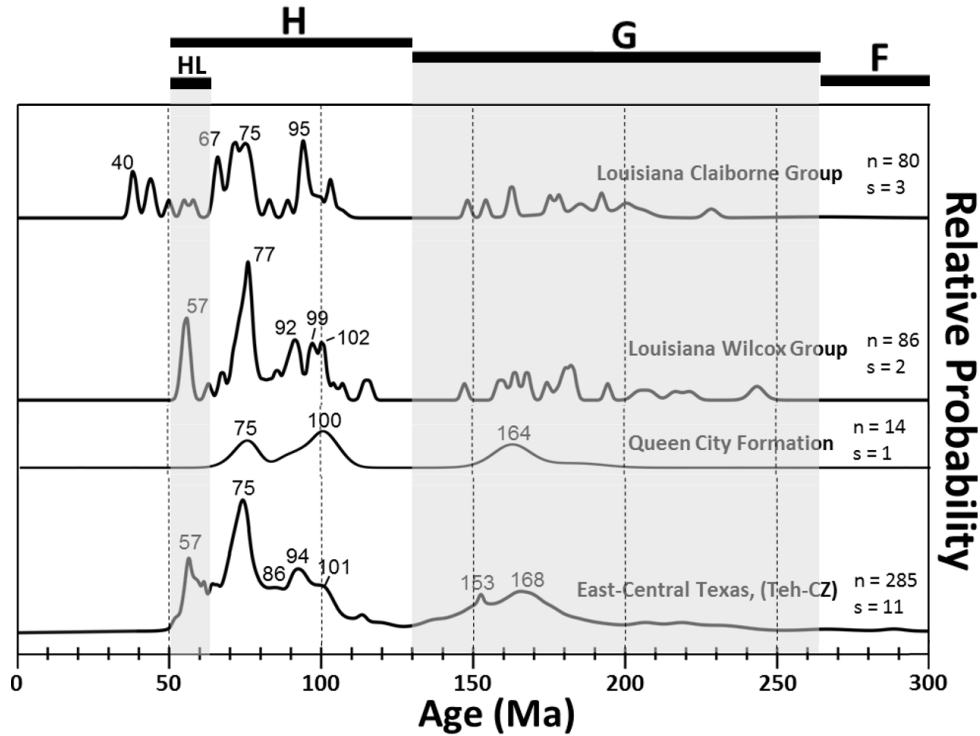
Figure 25. Normalized probability density plots of detrital zircon age spectra compilations for east-central Texas and Louisiana for ages younger than 300 Ma.

them and the Gulf of Mexico (Figure 19). Although data are not available for the north-central Rocky Mountain Front, the Colorado Mineral Belt could also be providing these detrital zircons to the Louisiana Wilcox Group and east-central Texas samples from this location. The Coast Mountains Batholith in northwestern North America (DeCelles et al. 2009), the Idaho Batholith (Gaschnig et al. 2010), and parts of southwestern Arizona (Shafiqullah et al. 1980 and references therein) and northern Mexico (Damon et al. 1983a, 1983b; McDowell and Mauger 1994; McDowell et al. 2001) are not considered potential sources based primarily on interpreted paleogeographic restrictions on fluvial drainage pathways (Figure 19) (Davis et al. 2010; Galloway et al. 2011; Blakey 2013). K-Ar and Ar-Ar ages (61-54 Ma) determined from igneous intrusive rocks in the Santa Rita lineament in southern New Mexico are presented in (Chapin et al. 2004) with respect to data from the New Mexico Geochronological Database (Wilks and Chapin 1997). This feature is a northeast trending structural and magmatic zone similar to the Colorado

Mineral Belt that spans from Hidalgo County to Sierra County (Chapin et al. 1978). The Colorado Mineral Belt is a composite of three main age groups of igneous intrusive rocks, one of which contains Late Cretaceous through Middle Eocene ages (ca. 75–43 Ma) (Cunningham et al. 1994; Chapin 2012). This feature trends northeast from the Four Corners area within the Ute Mountains to an area in the Front Range near Boulder, Colorado and is considered to be the only Laramide magmatic belt present between southern Idaho and the Santa Rita Lineament in southern New Mexico (Chapin et al. 2004).
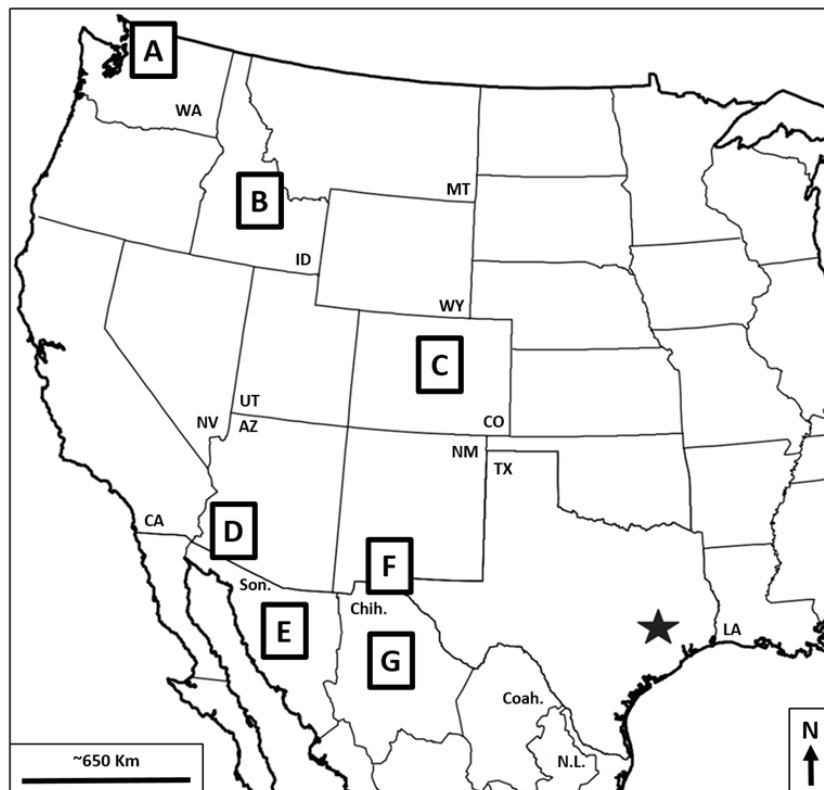
A: Coast Mountains Batholith of Washington State

B: Idaho Batholith

C: Colorado Mineral Belt

D: Southwestern Arizona

E: Locations within Sonora, Mexico

F: Santa Rita Lineament

G: Locations within Chihuahua, Mexico

Figure 26. General location of potential sources of late Laramide-age detrital zircons.

CHAPTER VI

CONCLUSIONS

U-Pb detrital zircon geochronology of closely spaced stratigraphic levels within the Midway, Wilcox, and Claiborne Group in east-central Texas identifies the relative arrival time of late Laramide-age detrital zircons to the region. First observation of late Laramide-age detrital zircons is within the Hooper Formation (H-PC) of the Wilcox Group, although the presence of these ages fluctuates between younger samples. These ages are also present in Wilcox Group data in Louisiana, but are generally absent in the Wilcox Group of south Texas. Potential contributors of Late Laramide-age detrital zircons to the Louisiana Wilcox Group and east-central Texas Wilcox Group samples may include the Colorado Mineral Belt and the Santa Rita Lineament in southern New Mexico, which appear as more likely candidates based on close proximity to Laramide uplifts and previous paleodrainage interpretations.

Detrital zircon age spectra of individual samples in east-central Texas supports similar sediment sources, or a similar paleodrainage area for the majority of Midway Group, Wilcox Group, and Carrizo Formation detrital zircon ages. Close comparison of east-central Texas (Teh-CZ) and Louisiana Wilcox Group detrital zircon ages supports similar conclusions for Louisiana data, whereas differences in south Texas Wilcox Group ages supports a unique paleodrainage for this location. Further comparison between Gulf Coastal Plain samples may support the introduction of a new sediment source and/or a greater contribution of detrital zircons from a previously existing source during deposition of the east-central Texas Queen City Formation. This new or more pronounced source also appears to have been available during deposition of younger Claiborne Group strata in Louisiana. The distribution of ages for Gulf Coastal Plain samples is similar to components of the southwestern and southern Rocky Mountain regions, apart from much more pronounced number of Group D ages within the Louisiana Wilcox Group and Queen City Formation. The above suggestions for east-central Texas and Louisiana data are generally supported by K-S test results, although biased results because of sensitivity to

analytical uncertainty and other factors questions the suitability of this test for geochronologic study.

Recommendations for Future Study

Recommendations for future study include a comparison of existing datasets with regional data from Mesozoic through Paleogene strata in the Rocky Mountain Front in Colorado, and from similar age strata in New Mexico. Additionally, sampling of Carrizo Formation and younger Claiborne Group strata along the Gulf Coast may identify the relative arrival time and the regional extent of the more pronounced Group D (1293-843 Ma) detrital zircon ages that were identified within the Queen City Formation in east-central Texas and in Louisiana Claiborne Group samples.

Results for Gulf Coastal Plain location data presented in this study have implications on deepwater petroleum systems. Because the Wilcox Group is a target for hydrocarbon production in the deepwater Gulf of Mexico, results from this study may be valuable when considering spatial changes in reservoir characteristics. Differing sediment sources and paleodrainage along the northwestern Gulf of Mexico may relate to respective down-dip reservoir quality. Additionally, the introduction of a new sediment source or greater contribution of detrital zircons from an already existing source to the Claiborne Group in Louisiana and east-central Texas may also be recognizable in equivalent deepwater deposits.

REFERENCES CITED

Ahrens, L. 1955. "Implications of the Rhodesia Age Pattern." *Geochimica et Cosmochimica Acta* 8: 1-15.

Ayers, W.B., Jr., and A. H. Lewis. 1985. "The Wilcox Group and Carrizo Sand (Paleogene) in East-Central Texas: Depositional Systems and Deep-Basin Lignite." The University of Texas at Austin, *Bureau of Economic Geology Special Publication*. 19 p. 30 plates.

Ayers, W., A. Lewis, and G. Collins. 1986. "Resistivity, Lignite, and Lithofacies Mapping of the Wilcox Group, East-Central Texas." in Kaiser, W. et al. (eds), Geology and Groundwater Hydrology of Deep Basin Lignite in the Wilcox Group of East Texas, University of Texas at Austin, *Bureau of Economic Geology Special Publication* 4: 31-50.

Bammel, B. 1979. "Stratigraphy of the Simsboro Formation, East-Central Texas." Department of Geology, Baylor University, *Baylor Geological Studies Bulletin* 37: 1-40.

Barnes, V.E. 1970. "Waco Sheet." The University of Texas at Austin, Bureau of Economic Geology. Geologic Atlas of Texas. scale 1:250,000. 1 sheet.

Barnes, V.E.. 1974. "Austin Sheet." The University of Texas at Austin, Bureau of Economic Geology. Geologic Atlas of Texas. scale 1:250,000. 1 sheet.

Barth, Andrew P., Joseph L. Wooden, Carl E. Jacobson, and Kelly Probst. 2004. "U-Pb Geochronology and Geochemistry of the McCoy Mountains Formation, Southeastern California: A Cretaceous Retroarc Foreland Basin." *Geological Society of America Bulletin* 116 (1-2): 142–53. doi:10.1130/B25288.1.

Barth, A.P., J. L. Wooden, K. A. Howard, and J. L. Richards. 2008. "Late Jurassic Plutonism in the Southwest U.S. Cordillera." in Wright, J.E., and Shervais, J.W., (eds.). Ophiolites, Arcs and Batholiths: A Tribute to Cliff Hopson: *Geological Society of America Special Paper* 438: 379–396. doi: 10.1130/2008.2438(13).

Beckman, M. W., and F. E. Turner. 1943. "Stratigraphy and Age of Seguin Formation of Central Texas." *AAPG Bulletin* 27: 608–621. doi: 10.1306/3D9335B4-16B1-11D7-8645000102C1865D.

Berg, R. 1979. "Stratigraphy of the Claiborne Group." in Kersey, D., and Stanton, R., (eds.). Lower Tertiary of the Brazos River Valley. Guidebook of the Houston Geological Society. 7 p.

Berry, R.F., G.A. Jenner, S. Meffre, and M. N. Tubrett. 2001. "A North American Provenance for Neoproterozoic to Cambrian Sandstones in Tasmania?" *Earth and Planetary Science Letters* 192: 207-222.

Blakey, Ron. "North American Key Time-Slice Paleogeographic Maps: Paleocene (62-58 Ma)." Last modified 2013. NAU Geology. http://cpgeosystems.com/.

Blum, Michael, and Mark Pecha. 2014. "Mid-Cretaceous to Paleocene North American Drainage Reorganization from Detrital Zircons." *Geology* 42 (7): 607–10. doi:10.1130/G35513.1.

Brewton, J. L. 1970. "Heavy Mineral Distribution in the Carrizo Formation (Eocene), East Texas." Master's Thesis, Univeristy of Texas at Austin.

Busby-Spera, C. J. 1988. "Speculative Tectonic Model for the Early Mesozoic Arc of the Southwest Cordilleran United States." *Geology* 16: 1121-1125.

Cather, S. M., and C. Chapin. 1990. "Paleogeographic and Paleotectonic Setting of Laramide Sedimentary Basins in the Central Rocky Mountain Region, Alternative Interpretation and Reply." *Geological Society of America Bulletin* 100: 1023-1039.

Cawood, P.A., A. A. Nemchin, M. Freeman, K. Sircombe. 2003. "Linking Source and Sedimentary Basin: Detrital Zircon Record of Sediment Flux along a Modern River System and Implications for Provenance Studies." *Earth and Planetary Science Letters* 210: 259-268.

Chamberlain, P., C., H. T. Mix, A. Mulch, M. T. Hren, M. L. Kent-Corson, S. J. Davis, T. W. Horton, and S. A. Graham. 2012. "The Cenozoic Climatic and Topographic Evolution of the Western North American Cordillera." *American Journal of Science* 312: 213–262. doi: 10.2475/02.2012.05.

Chang, Zhaoshan, Jeffery D. Vervoort, William C. McClelland, and Charles Knaack. 2006. "U-Pb Dating of Zircon by LA-ICP-MS." Geochemistry, Geophysics, Geosystems 7 (5): 1-14. doi:10.1029/2005GC001100.

Chapin, C. E. 2012. "Origin of the Colorado Mineral Belt." *Geosphere* 8 (1): 28–43. doi:10.1130/GES00694.1.

Chapin, C. E., R. M. Chamberlin, G. R. Osburn, D. W. White, and A. R. Sanford. 1978. "Exploration Framework of the Socorro Geothermal Area, New Mexico." in Chapin, C. E., and Elston, W. E. (eds.), Field Guide to Selected Cauldrons and Mining Districts of the Datil-Mogollon Volcanic Field, New Mexico. *New Mexico Geological Society Special Publication* 7: 115–129.

Chapin, C. E., Maureen Wilks, and W. C. McIntosh. 2004. "Space-Time Patterns of Late Cretaceous to Present Magmatism in New Mexico—Comparison with Andean Volcanism and Potential for Future Volcanism." *New Mexico Bureau of Geology & Mineral Resources Bulletin* 160: 13–40.

Chevren, V.B., and A. F. Jacobs. 1985. "Evolution of Paleogene Depositional Systems, Williston Basin." in Flores, R.M., and Kaplan, S.S., (eds.). Cenozoic Paleogeography of the West-Central United States. Rocky Mountain Paleogeography Symposium 3. Rocky Mountain Section. Society for Sedimentary Geology. p. 127–170.

Crabaugh, J. P. 2001. "Nature and Growth of Nonmarine-to-Marine Clastic Wedges: Examples from the Upper Cretaceous Iles Formation, Western Interior (Colorado) and the Lower Paleogene Wilcox Group of the Gulf of Mexico Basin (Texas)." Ph.D. Dissertation, University of Wyoming.

Crabaugh, J. P., and Elsik, W. C. 2000. "Calibration of the Texas Wilcox Group to the Revised Cenozoic Time Scale: Recognition of Four, Third-Order Clastic Wedges (2.7-3.3 m.y. in Duration)." *South Texas Geological Society Bulletin* 41: 10-17.

Craddock, William H., and Andrew R. C. Kylander-Clark. 2013. "U-Pb Ages of Detrital Zircons from the Tertiary Mississippi River Delta in Central Louisiana: Insights into Sediment Provenance." *Geosphere* 9 (6): 1832–1851. doi:10.1130/GES00917.1.

Coney, P. J. 1976. Plate Tectonics and the Laramide Orogeny." in Woodward, L. A. and Northrop, S. A. (eds.), Tectonics and Mineral Resources of Southwestern North America, New *Mexico Geological Society Special Publication* 6: 5–10.

Corfu, F., J. M. Hanchar, P. Hoskin, P. Kinny. 2003. "Atlas of Zircon Textures." *Reviews in Mineralogy and Geochemistry* 53: 469-500.

Cunningham, Charles G., Charles W. Naeser, Richard F. Marvin, Robert G. Luedke, and Alan R. Wallace. 1994. "Ages of Selected Intrusive Rocks and Associated Ore Deposits in the Colorado Mineral Belt." *U.S. Geological Survey Bulletin* 2109: 1–37.

Damon, P.E., M. Shafiqullah, and K. F. Clark. 1983a. "Geochronology of the Porphyry Copper Deposits and Related Mineralization of Mexico." *Canadian Journal of Earth Sciences* 20: 1052–1071.

Damon, P.E., M. Shafiqullah, J. Roldan-Quintana, and J. J. Cocheme 1983b. "El Batolito Laramide (90–40 M.A.) de Sonora." Memoria, XV Convencion Nacional, Asociacio´n de Ingenieros de Minas, Metalurgistas y Geo´logos de Me´xico, A.C., p. 65–95

Davidoff, Andrew, and Yancey, Thomas E. 1993a. "Relating Sequence Stratigraphy to Lithostratigraphy in Siliciclastic Dominated Shelf Settings, Paleogene, Central-

East Texas." *Gulf Coast Association of Geological Societies Transactions* 43: 97-107.

Davidoff, Andrew, and Thomas E. Yanccy. 1993b. "Eustatic Cyclicity in the Paleocene and Eocene: Data from the Brazos River Valley, Texas." *Tectonophysics* 222 (3-4): 371–95. doi:10.1016/0040-1951(93)90360-V.

Davis, Steven J., William R. Dickinson, George E. Gehrels, Jon E. Spencer, Timothy F. Lawton, and Alan R. Carroll. 2010. "The Paleogene California River: Evidence of Mojave-Uinta Paleodrainage from U-Pb Ages of Detrital Zircons." *Geology* 38 (10): 931–34. doi:10.1130/G31250.1.

DeCelles, Peter G. 2004. "American Journal of Science Late Jurassic to Eocene Evolution of the Cordilleran Thrust Belt and Foreland Basin System, Western U.S.A." *American Journal of Science* 304 (February): 105–168. doi:10.2475/ajs.304.2.105.

DeCelles, Peter G., Mihai N. Ducea, Paul Kapp, and George Zandt. 2009. "Cyclicity in Cordilleran Orogenic Systems." *Nature Geoscience* 2 (4): 251–257. doi:10.1038/ngeo469.

Dickey, R. L., and T. E. Yancey. 2010. "Palynological Age Control Sediments Bracketing the Paleocene-Eocene Boundary, Bastrop, Texas." *Gulf Coast Association of Geological Societies Transactions* 60: 717–724.

Dickinson, William R., and George E. Gehrels. 2003. "U-Pb Ages of Detrital Zircons from Permian and Jurassic Eolian Sandstones of the Colorado Plateau, USA: Paleogeographic Implications." *Sedimentary Geology* 163: 29–66.

Dickinson, William R., and George E. Gehrels. 2008a. "U-Pb Ages of Detrital Zircons in Relation to Paleogeography: Triassic Paleodrainage Networks and Sediment Dispersal Across Southwest Laurentia." *Journal of Sedimentary Research* 78: 745-764.

Dickinson, William R., and George E. Gehrels. 2008b. "Sediment Delivery to the Cordilleran Foreland Basin: Insights from U-Pb Ages of Detrital Zircons in Upper Jurassic and Cretaceous Strata of the Colorado Plateau." *American Journal of Science* 308 (10): 1041–82. doi:10.2475/10.2008.01.

Dickinson, William R., and George E. Gehrels. 2009. "U-Pb Ages of Detrital Zircons in Jurassic Eolian and Associated Sandstones of the Colorado Plateau: Evidence for Transcontinental Dispersal and Intraregional Recycling of Sediment." *Geological Society of America Bulletin* 121 (3-4): 408–33. doi:10.1130/B26406.1.

Dickinson, William R., Margaret A. Klute, Michael J. Hayes, Susanne U. Janecke, Erik R. Lundin, Mary A. Mckittrick, and Mark D. Olivares. 1988. "Paleogeographic and Paleotectonic Setting of Laramide Sedimentary Basins in the Central Rocky Mountain Region." *Geological Society of America Bulletin* 100 (7): 1023–39. doi:10.1130/0016-7606(1988)100<1023:PAPSOL>2.3.CO;2.

Dickinson, William R., Timothy F. Lawton, and George E. Gehrels. 2009. "Recycling Detrital Zircons: A Case Study from the Cretaceous Bisbee Group of Southern Arizona." *Geology* 37 (6): 503–506. doi:10.1130/G25646A.1.

Dickinson, William R., Timothy F. Lawton, Mark Pecha, Steven J. Davis, George E. Gehrels, and Richard A. Young. 2012. "Provenance of the Paleogene Colton Formation (Uinta Basin) and Cretaceous-Paleogene Provenance Evolution in the Utah Foreland: Evidence from U-Pb Ages of Detrital Zircons, Paleocurrent Trends, and Sandstone Petrofacies." *Geosphere* 8 (4): 854–880. doi:10.1130/GES00763.1.

Dickinson, William R., and Walter S. Snyder. 1978. "Plate tectonics of the Laramide Orogeny." in: Western United States. *Geological Society of America Memoir* 151: 355-366.

Doebbert, Amalia. 2013. "Applications of Detrital Zircon Geochronology and Isotope Geochemistry in Provenance Study." PhD Dissertation, University of Wisconsin, Madison.

Ducea, M. 2001. The California Arc: Thick Granitic Batholiths, Eclogitic Residues, Lithospheric-Scale Thrusting, and Magmatic Flare-Ups." *GSA Today* 11: 4– 10. doi: 10.1130/1052-5173(2001)011<0004:TCATGB >2.0.CO;2.

Dunne, C.G., T. P. Garvey, M. Osborne, D. Schneidereit, A. E. Fritsche, and J. D. Walker. 1998. "Geology of the Inyo Mountains Volcanic Complex: Implications for Jurassic Paleogeography of the Sierran Magmatic Arc in Eastern California." *Geological Society of America Bulletin* 110: 1376–1397. doi: 10.1130/0016-7606(1998)110<1376:GOTIMV >2.3.CO;2.

Eargle, H. 1968. "Nomenclature of Formations of Claiborne Group, Middle Eocene Coastal Plain of Texas." *Geological Survey Bulletin* 1251-D: 1-25.

Edwards, M., B.1981. "Upper Wilcox Rosita Delta System of South Texas: Growth-Faulted Shelf-Edge Deltas." *AAPG Bulletin* 65: 54-73. doi: 10.1306/2F91976F-16CE-11D7-8645000102C1865D.

English, Joseph M., and Stephen T. Johnston. 2004. "The Laramide Orogeny: What Were the Driving Forces?" *International Geology Review* 46 (9): 833–38. doi:10.2747/0020-6814.46.9.833.

Elder, W.P., and J. L. Kirkland. 1994. "Cretaceous Paleogeography of the Southern Western Interior Region." in Caputo, M.V., Peterson, J.A., and Franczyk, K.J., (eds.). Mesozoic System of the Rocky Mountain Region, USA: Rocky Mountain Section SEPM (Society for Sedimentary Geology). Denver. p. 415–440.

Eriksson, K. A.; Campbell, I. H.; Palin, J. M.; Allen, C. M.; and Bock, B. 2004. "Evidence for Multiple Recycling in Neoproterozoic through Pennsylvanian Sedimentary Rocks of the Central Appalachian Basin." *Journal of Geology* 112: 261–276.

Fan, M., P. G. DeCelles, G. E. Gehrels, D. L. Dettman, J. Quade, and S. L. Peyton. 2011. "Sedimentology, Detrital Zircon Geochronology, and Stable Isotope Geochemistry of the Lower Eocene Strata in the Wind River Basin, Central Wyoming." *Geological Society of America Bulletin* 123 (5-6): 979–96. doi:10.1130/B30235.1.

Fan, Majie, Paul Heller, Sarah D. Allen, and Brian G. Hough. 2014a. "Middle Cenozoic Uplift and Concomitant Drying in the Central Rocky Mountains and Adjacent Great Plains." *Geology* 42 (6): 547–50. doi:10.1130/G35444.1.

Fan, Majie, Brian G. Hough, and Benjamin H. Passey. 2014b. "Middle to Late Cenozoic Cooling and High Topography in the Central Rocky Mountains: Constraints from Clumped Isotope Geochemistry." *Earth and Planetary Science Letters* 408: 35–47. doi:10.1016/j.epsl.2014.09.050.

Faure, G., and T. M. Mensing. 2005. "Isotopes: Principles and Applications." Hoboken, NJ. John Wiley & Sons, 897 p.

Fedo, C.M., K. N. Sircombe, R. H. Rainbird. 2003. "Detrital Zircon Analysis of the Sedimentary Record." In: Hanchar, J.M., Hoskin, P. (Eds.), Zircon: Experiments, Isotopes, and Trace Element Investigations. *Mineralogical Society of America, Reviews in Mineralogy 53 (10): 277-303.*

Feng, R., N. Machado, and J. Ludden. 1993. "Lead Geochronology of Zircon by Laser Probe–Inductively Coupled Plasma Mass Spectrometry (LP–ICPMS)." *Geochimica Cosmochimica Acta* 57: 3479–3486.

Fisher, W.L. 1964. "Sedimentary Pattern in Eocene Cyclic Deposits, Northern Gulf Coast Region." *Kansas Geological Survey Bulletin* 169: 151-170.

Fisher, W., and J. McGowen. 1967. "Depositional Systems in the Wilcox Group of Texas and Their Relationship to Occurrence of Oil and Gas." reprinted from: *Gulf Coast Association of Geological Societies Transactions* 17: 105-124.

Fryer, B.J., S.E. Jackson, and H.P. Longerich. 1993. "The Application of Laser Ablation Microprobe–Inductively Coupled Plasma Mass Spectrometry (LAM–ICPMS) to In Situ (U–Pb) Geochronology." *Chemical Geology* 109: 1–8.

Fuentes, Facundo, Peter G. DeCelles, Kurt N. Constenius, and George E. Gehrels. 2011. "Evolution of the Cordilleran Foreland Basin System in Northwestern Montana, U.S.A." *Geological Society of America Bulletin* 123 (3-4): 507–33. doi:10.1130/B30204.1.

Galloway, W. E. 1977. "Catahoula Formation of the Texas Coastal Plain: Depositional Systems, Composition, Structural Development, Ground-Water Flow History, and Uranium Distribution." Report of investigations of the Bureau of Economic Geology. The University of Texas at Austin. no. 87. 59 p.

Galloway, W. 1989. "Genetic Stratigraphic Sequences in Basin Analysis: II. Application to Northwest Gulf of Mexico Cenozoic Basin." *AAPG Bulletin* 73: 143–154.

Galloway, W. E. 2009. "Gulf of Mexico Basin Depositional Record of Cenozoic North American Drainage Basin Evolution." *Fluvial Sedimentology* 7: 409–423. doi:10.1002/9781444304350.ch22.

Galloway, W. E., W. F. Dingus, and R. E. Paige. 1991. "Seismic and Depositional Facies of Paleocene-Eocene Wilcox Group Submarine Canyon Fills, Northwest Gulf Coast, U.S.A." Chapter 13: Seismic Facies and Sedimentary Processes of Submarine Fans and Turbidite Systems. *New York, Springer-Verlag.* p. 247–271.

Galloway, W., P. Ganey-Curry, X. Li, and R. Buffer. 2000. "Cenozoic Depositional History of the Gulf of Mexico Basin." *AAPG Bulletin* 84 (11): 1743-1774.

Galloway, William E, and Thomas A. Williams. 1991. "Sediment Accumulation Rates in Time and Space : Paleogene Genetic Stratigraphie Sequences of the

Northwestern Gulf of Mexico Basin." *Geology* 19: 986–989. doi:10.1130/0091-7613(1991)019<0986.

Galloway, W. E., T. L. Whiteaker, and P. Ganey-Curry. 2011. "History of Cenozoic North American Drainage Basin Evolution, Sediment Yield, and Accumulation in the Gulf of Mexico Basin." *Geosphere* 7 (4): 938–973. doi:10.1130/GES00647.1.

Gardner, J., 1935. "The Midway Group of Texas." *University of Texas Bulletin* 3301: 403 p.

Gaschnig, Richard M., Jeffrey D. Vervoort, Reed S. Lewis, and William C. McClelland. 2010. "Migrating Magmatism in the Northern US Cordillera: In Situ U-Pb Geochronology of the Idaho Batholith." *Contributions to Mineralogy and Petrology* 159 (6): 863–83. doi:10.1007/s00410-009-0459-5.

Gehrels, G. 2012. "Detrital Zircon U-Pb Geochronology: Current Methods and New Opportunities." in Busby, C., and Azor, A., (eds.), Tectonics of Sedimentary Basins: Recent Advances. Chichester, UK. *Blackwell Publishing Ltd.* p. 47–62.

Gehrels, G., et al. 2009. "U-Th-Pb Geochronology of the Coast Mountains Batholith in North-Coastal British Columbia: Constraints on Age and Tectonic Evolution." *Geological Society of America Bulletin* 121: 1341-1361.

Gehrels, G., V. Valencia and A. Pullen. 2006. "Detrital Zircon Geochronology by Laser-Ablation Multicollector ICPMS at the Arizona LaserChron Center." *The Paleontological Society Papers* (12): 67-76.

Gleason, J. D., G. E. Gehrels, W. R. Dickinson, P. J. Patchett, and D. A. Kring. 2007. "Laurentian Sources for Detrital Zircon Grains in Turbidite and Deltaic Sandstones of the Pennsylvanian Haymond Formation, Marathon Assemblage, West Texas, U.S.A." *Journal of Sedimentary Research* 77 (11): 888–900. doi:10.2110/jsr.2007.084.

Gradstein, F., J. Ogg, M. Schmitz, and G. Ogg. 2012. "The Geologic Timescale." *Elsevier* 1-2: 1-1129.

Guevara, Edgar, and Roberto Garcia. 1972. "Depositional Systems and Oil-Gas Reservoirs in the Queen City Formation (Eocene), Texas." *Gulf Coast Association of Geological Societies* 22: 1-22.

Hay, D., and T. Dempster, T. 2009. "Zircon Alteration, Formation, and Preservation in Sandstones." *Sedimentology* 56: 2175-2191. doi: 10.111/j.1365-3091.2009.01075.x.

Hargis, Richard N. 1996. "Major Transgressive Shales of the Wilcox Northern Portion of South Texas." *Gulf Coast Association of Geological Societies Transactions* 46: 465–67.

Harris, R. 1962. "Petrology of the Eocene Sabinetown-Carrizo Contact, Bastrop County, Texas." *Journal of Sedimentary Petrology* 2 (2): 263-283.

Heintz, Mindi L., Thomas E. Yancey, Brent V. Miller, and Matthew T. Heizler. 2014. "Tephrochronology and Geochemistry of Eocene and Oligocene Volcanic Ashes

of East and Central Texas." *Geological Society of America Bulletin* 10: 1–11. doi:10.1130/B31146.1.

Henry, C.D., and J. M. Basciano. 1979. "Environmental Geology of the Wilcox Group Lignite Belt, East Texas." The University of Texas at Austin, *Bureau of Economic Geology, Report of Investigations* no. 98, 10 p.

Hoyt, William V. 1959. "Erosional Channel in the Middle Wilcox near Yoakum, Lavaca County, Texas." *Gulf Coast Association of Geological Societies Transactions* 9: 41-50.

Hutto, Andrew P., Thomas E. Yancey, and Brent V. Miller. 2009. "Provenance of Paleocene–Eocene Wilcox Group Sediments in Texas: The Evidence from Detrital Zircons." *Gulf Coast Association of Geological Societies Transactions* 59: 357–362.

Kaiser, W.R., W. B. Ayers, and L. W. La Brie, 1980. "Lignite Resources in Texas." The University of Texas at Austin, *Bureau of Economic Geology, Report of Investigations* no. 104, 52 p.

Kellough, Gene R. 1959. "Biostratigraphic and Paleoecologic Study of Midway Foraminifera along Tehuacana Creek, Limestone County, Texas." *Gulf Coast Association of Geological Societies Transactions* 9: 147-160.

Kennett, J. P., and L. D. Stott. 1991. "Abrupt Deep-Sea Warming, Palaeoceanographic Changes and Benthic Extinctions at the End of the Palaeocene." *Nature* 353 (6341): 225–229. doi:10.1038/353225a0.

LaMaskin, Todd. A. 2012. "Detrital Zircon Facies of Cordilleran Terranes in Western North America." *GSA Today* 22(3), doi:10.1130/GSATG142A.1.

Laskowski, Andrew K., Peter G. Decelles, and George E. Gehrels. 2013. "Detrital Zircon Geochronology of Cordilleran Retroarc Foreland Basin Strata, Western North America." *Tectonics* 32 (5): 1027–48. doi:10.1002/tect.20065.

Lawton, Timothy F. 2008. "Laramide Sedimentary Basins," in Miall, A. (ed.) The Sedimentary Basins of the United States and Canada. Amsterdam, The Netherlands, *Elsevier* 5: 429-450.

Lawton, Timothy F., Ira A. Bradford, Francisco J. Vega, George E. Gehrels, and Jeffrey M. Amato. 2009. "Provenance of Upper Cretaceous-Paleogene Sandstones in the Foreland Basin System of the Sierra Madre Oriental, Northeastern Mexico, and Its Bearing on Fluvial Dispersal Systems of the Mexican Laramide Province." *Geological Society of America Bulletin* 121 (5-6): 820–36. doi:10.1130/B26450.1.

Loucks, R. G., M. M. Dodge, and W. E. Galloway. 1984. "Regional Controls on Diagenesis and Reservoir Quality in Lower Tertiary Sandstones along the Texas Gulf Coast." in D. A. McDonald and R. C. Surdam, (eds.), Clastic Diagenesis. *AAPG Memoir* 37: 15–45.

Ludwig, K.J. 2003. "Isoplot 3.00." *Berkeley Geochronology Center Special Publication* no. 4, 70 p.

Mackey, G., B. Horton, and K. Milliken. 2012. "Provenance of the Paleocene-Eocene Wilcox Group, Western Gulf of Mexico Basin, Evidence for Integrated Drainage

of the Southern Laramide Rocky Mountains and Cordilleran Arc." *Geological Society of America Bulletin* 124: 1,007-1,024.

Mauel, D. J., T. F. Lawton, C. Gonzalez-Leon, A. Iriondo, and J. M. Amato. 2011. "Stratigraphy and Age of Upper Jurassic Strata in North-Central Sonora, Mexico: Southwestern Laurentian Record of Crustal Extension and Tectonic Transition." *Geosphere* 7 (2): 390–414. doi:10.1130/GES00600.1.

May, Steven R., Gary G. Gray, Lori L. Summa, Norman R. Stewart, George E. Gehrels, and Mark E. Pecha. 2013. "Detrital Zircon Geochronology from the Bighorn Basin, Wyoming, USA: Implications for Tectonostratigraphic Evolution and Paleogeography." *Geological Society of America Bulletin* 125 (9-10): 1403–1422. doi:10.1130/b30824.1.

McCarley, Ann Boggs. 1981. "Metamorphic Terrane Favored over Rocky Mountains as Source of Claiborne Group, Eocene, Texas Coastal Plain." *Journal of Sedimentary Research* 51 (4): 1267–76. doi:10.1306/212F7E82-2B24-11D7-8648000102C1865D.

McDowell, F.W. 2007. "Geologic Transect across the Northern Sierra Madre Occidental Volcanic Field, Chihuahua and Sonora, Mexico." Geological Society of America Digital Map and Chart Series 6, 70 p. doi: 10.1130/2007.DMCH006

McDowell, F.W., and R. W. Mauger. 1994. "K-Ar and U-Pb Zircon Chronology of Late Cretaceous and Tertiary Magmatism in Central Chihuahua State, Mexico." *Geological Society of America Bulletin* 106: 118–132. doi:10.1130/00167606(1994) 106<0118:KAAUPZ>2.3. CO;2.

McDowell, F. W., J. Roldan-Quintana, and J. Connelly. 2001. "Duration of Late Cretaceous-Early Tertiary Magmatism in East-Central Sonora, Mexico." *Geological Society of America Bulletin* 113 (4): 521-531.

Meyer, Dave, Larry Zarra, David Rains, Bob Meltz, and Tom Hall. 2005. "Emergence of the Lower Tertiary Wilcox Trend in the Deepwater Gulf of Mexico." *World Oil 226* (5): 72–77.

Miller, R.B., S. R. Paterson, and J. P. Matzel. 2009. "Plutonism at Different Crustal Levels: Insights from the ~5–40 km (Paleodepth) North Cascades Crustal Section, Washington." in Miller, R.B., and Snoke, A.W., (eds.), Crustal Cross Sections from the Western North American Cordillera and Elsewhere: Implications for Tectonic and Petrologic Processes. *Geological Society of America Special Paper* 456: 125–149. doi: 10.1130 /2009.2456(05).

Milliman, John D., and James P. M. Syvitski. 1992. "Geomorphic/Tectonic Control of Sediment Discharge to the Ocean: The Importance of Small Mountainous Rivers." *The Journal of Geology* 100 (5): 525–44. doi:10.1086/629606.

Mix, Hari T., Andreas Mulch, Malinda L. Kent-Corson, and C. Page Chamberlain. 2011. "Cenozoic Migration of Topography in the North American Cordillera." *Geology* 39 (1): 87–90. doi:10.1130/G31450.1.

Moecher, D., and S. Samson. "Differential Zircon Fertility of Source Terranes and Natural Bias in the Detrital Zircon Record: Implications for Sedimentary Provenance Analysis." *Earth and Planetary Science Letters* 247: 252-266.

Murray, Grover E. 1955. "Midway Stage, Sabine Stage, and Wilcox Group." *AAPG Bulletin* 39 (5): 671–696. *doi:10.1306/5CEAE1C6-16BB-11D7-645000102C1865D.*

Paces, J.B., and J. D. Miller. 1993. "Precise U-Pb Ages of Duluth Complex and Related Mafic Intrusions, Northeastern Minnesota: Geochronological Insights to Physical, Petrogenetic, Paleomagnetic, and Tectonomagmatic Process Associated with the 1.1 Ga Midcontinent Rift System. *Journal of Geophysical Research* 98:13,997-14,013.

Park, Hyunmee, David L. Barbeau Jr., Alan Rickenbaker, Denise Bachmann-Krug, and George E. Gehrels. 2010. "Application of Foreland Basin Detrital-Zircon Geochronology to the Reconstruction of the Southern and Central Appalachian Orogen." *The Journal of Geology* 118 (1): 23–44. doi:10.1086/648400.

Paterson, B. A. 1989. "Zoning in Granitoid Accessory Minerals as Revealed by Backscattered Electron Imagery." *Mineralogical Magazine* 53 (369): 55–61. doi:10.1180/minmag .1989.053.369.05.

Paterson, S. R., D. Okaya, V. Memeti, R. Economos, and R. B. Miller. 2011. "Magma Addition and Flux Calculations of Incrementally Constructed Magma Chambers in Continental Margin Arcs: Combined Field, Geochronologic, and Thermal Modeling Studies." *Geosphere* 7 (6): 1439–68. doi:10.1130/GES00696.1.

Poole, F. G., George E. Gehrels, and John H. Stewart. 2008. "Significance of Detrital Zircons in Upper Devonian Ocean-Basin Strata of the Sonora Allochthon and Lower Permian Synorogenic Strata of the Mina Mexico Foredeep, Central Sonora, Mexico." in Blodgett, R. B., and Stanley, G. D., Jr., (eds.). The Terrane Puzzle:

New Perspectives from Paleontology and Stratigraphy from the North American Cordillera. *Geological Society of America Special Paper* 442: 121-131.

Saleeby, J.B., M. N. Ducea, C. J. Busby, E. S. Nadin, P. H. Wetmore. 2008. "Chronology of Pluton Emplacement and Regional Deformation in the Southern Sierra Nevada Batholith, California." in Wright, J.E., and Shervais, J.W., (eds.). Ophiolites, Arcs and Batholiths: A Tribute to Cliff Hopson. *Geological Society of America Special Paper* 438 397–427. doi: 10.1130/2008 .2438(14).

Salvador, Amos. 1987. "Late Triassic – Jurassic Paleogeography and Origin of Gulf of Mexico Basin." *AAPG Bulletin* 71: 419 – 451.

Sellards, E. H., W. S. Adkins and F. B. Plummer. 1932. "The Geology of Texas, Volume 1, Stratigraphy." *University of Texas Bulletin* 3232: 819 p.

Shafiqullah, M., P. E. Damon, D. J. Lynch, S. J. Reynolds, and R. N. Raymond. 1980. "K-Ar Geochronology and Geologic History of Southwestern Arizona and Adjacent Areas." in Jenney, J.P., and Stone, C., (eds.). Studies in Western Arizona. *Arizona Geological Society Digest* 12: 201-260.

Sircombe, Keith, Wouter Bleeker, and Richard Stern. 2001. "Detrital Zircon Geochronology and Grain-Size Analysis of a ~2800 Ma Mesoarchean Proto-Cratonic Cover Succession, Slave Province, Canada." *Earth and Planetary Science Letters* 189 (3-4): 207-220. doi: 10.1016/S0012-821X(01)00363-6.

Slama, Jiri, and Jan Kosler. 2012. "Effects of Sampling and Mineral Separation on Accuracy of Detrital Zircon Studies." *Geochemistry, Geophysics, Geosystems* 13: 1-17. doi: 10.1029/2012GC004106.

Smith, J.V. and R. C. Stenstrom. 1965. "Electron-Excited Luminescence as a Petrologic Tool." *Journal of Geology* 73: 627-635.

Spencer, Christopher J., Anthony R. Prave, Peter A. Cawood, and Nick M. W. Roberts. 2014. "Detrital Zircon Geochronology of the Grenville/Llano Foreland and Basal Sauk Sequence in West Texas, USA." *Geological Society of America Bulletin* 126 (7-8): 1117–28. doi:10.1130/B30884.1.

Steiger, R., and E. Jaeger. 1977. "Subcommission on Geochronology: Convention on the Use of Decay Constants in Geo- and Cosmochronology." *Earth and Planetary Science Letters* 36: 359-362.

Stenzel, H. B.. 1938. "The Geology of Leon County, Texas." *Texas University Publication* 3818, 295 p.

Stewart, John H., George E. Gehrels, Andrew P. Barth, Paul K. Link, Nicholas Christie-Blikc, and Chester T. Wrucke. 2001. "Detrital Zircon Provenance of Mesoproterozoic to Cambrian Arenites in the Western United States and Northwestern Mexico." *Geological Society of America Bulletin* 113: 1343-1356.

Storm, L. 1945. "Resume of Facts and Opinions on Sedimentation in Gulf Coast Region of Texas and Louisiana," *AAPG Bulletin* 29 (9): 1304-1335.

Thorkildsen, David, and Robert D. Price. 1991. "Ground-Water Resources of the Carrizo-Wilcox Aquifer in the Central Texas Region." *Texas Water Development Board Report* 332: 1-46.

Tobisch, Othmar T., Jason Saleeby, and Richard S. Fiske. 1986. "Structural History of Continental Volcanic Arc Rocks, Eastern Sierra Nevada, California: A Case for Extensional Tectonics." *Tectonics* 5: 65–94. doi: 10.1029/TC005i001p00065.

Todd, Thomas, and Robert Folk. 1957. "Basal Claiborne of Texas, Record of Appalachian Tectonism During Eocene." AAPG Bulletin 41 (11) 2,545-2,566.

Vermeesch, Pieter. 2004. "How Many Grains are Needed for a Provenance Study?" *Earth and Planetary Science Letters* 224: 441–451.

Vermeesch, Pieter. 2013. "Multi-Sample Comparison of Detrital Age Distributions." *Chemical Geology* 341:140-146.

Wetherill, George. 1956. "Discordant Uranium-Lead Ages." *American Geophysical Union Transactions* 37: 320-326.

Wetherill, George. 1963. "Discordant Uranium-Lead Ages, Pt. 2; Discordant Ages Resulting from Diffusion of Lead and Uranium." *Journal of Geophysical Research* 68: 2957-2965.

Whitmeyer, Steven J, and Karl E Karlstrom. 2007. "Tectonic Model for the Proterozoic Growth of North America." *Geosphere* 3 (4): 220–259. doi:10.1130/GES00055.1.

Wiedenbeck, M., P. Alle, F. Corfu, W. Griffin, M. Meier, F. Oberli, A. Von Quadt, J. Roddick, and W. Spiegel. 1995. "Three Natural Zircon Standards for U-Th-Pb, Lu-Hf, Trace Element and REE Analyses." *Geostandards Newsletter* 19: 1–23.

Wilf, Peter. 2000. "Late Paleocene-Early Eocene Climate Changes in Southwestern Wyoming: Paleobotanical Analysis." *Geological Society of America Bulletin* 112 (2): 292–307. doi:10.1130/0016-7606(2000)112<292:LPECCI>2.0.CO;2.

Wilks, Maureen, and Charles E. Chapin. 1997. "The New Mexico Geochronological Database." New Mexico Bureau of Mines and Mineral Resources, Digital Database Series, Database DDS–DB1.

Winker, Charles. 1982. "Cenozoic Shelf Margins, Northwestern Gulf of Mexico." *Gulf Coast Association of Geological Societies Transactions* 32: 428–448.

Xue, Lianqing, and William E. Galloway. 1993. "Sequence Stratigraphic and Depositional Framework of the Paleocene Lower Wilcox Strata, Northwest Gulf of Mexico Basin." *Gulf Coast Association of Geological Societies Transactions* 43: 453–464.

Xue, Lianqing, and William E. Galloway. 1995. "High-Resolution Depositional Framework of the Paleocene Middle Wilcox Strata, Texas Coastal Plain: *American Association of Petroleum Geologists Bulletin* 79: 205–230, doi: 10.1306/8D2B14F8-171E-11D7-8645000102C1865D.

Yancey, Thomas E., and Andrew J. Davidoff. 1991. "Paleogene Sequence Stratigraphy and Lithostratigraphy in the Brazos River Valley, Texas. GCAGS fieldtrip Guidebook, 41st Ann. Meeting, 112 p.

Yancey, Thomas E, Andrew Dunham, and Kevin Durney. 2012. "Paleocene-Eocene Marine Transgression in the Upper Calvert Bluff Formation, Wilcox Group, Bastrop County, Texas." *Gulf Coast Association of Geological Societies Transactions* 62: 491–503.

Yancey, Thomas E., Thomas F. Hull, and Regina L. Dickey. 2010. "Depositional Environments of Sediments near the Paleocene-Eocene Boundary, Bastrop, Texas." *Gulf Coast Association of Geological Societies Transactions* 60: 679–691.

Zachos, James C., Kyger C. Lohmann, James C. Walker, and Sherwood W. Wise. 1993. "Abrupt Climate Change and Transient Climates during the Paleogene: A Marine Perspective." *The Journal of Geology* 101 (2): 191–213. doi:10.1086/648216.

APPENDIX A

DETRITAL ZIRCON ISOTOPIC RATIOS AND APPARENT AGES

Table A-1. Detrital zircon data table for sample Teh. Sample analyzed by LA-ICP-MS on 4-10-2014, 4-11-2014, and 1-29-2015. Age data are in Ma.

	Isotopic Ratios						Apparent Ages					
Sample Name	$^{207}Pb/^{235}U$	1σ abs. err.	$^{206}Pb/^{238}U$	1σ abs. err.	$^{207}Pb/^{206}Pb$	1σ abs. err.	$^{207}Pb/^{235}U$	1σ abs. err.	$^{206}Pb/^{238}U$	1σ abs. err.	$^{207}Pb/^{206}Pb$	1σ abs. err.
<10 % Discordant Samples												
TH_7	0.094	0.006	0.013	0.000	0.005	0.003	90.83	5.32	82.39	2.55	0.00	-98.99
TH_26	0.230	0.009	0.033	0.001	0.051	0.002	209.79	7.35	206.84	3.18	243.08	74.78
TH_29	4.334	0.151	0.299	0.005	0.105	0.003	1699.79	28.38	1688.13	26.98	1714.32	48.58
TH_30	4.271	0.176	0.301	0.008	0.103	0.003	1687.80	33.26	1694.82	41.82	1679.21	49.72
TH_31	1.847	0.074	0.178	0.003	0.075	0.002	1062.53	26.05	1058.64	18.97	1070.51	63.35
TH_33	4.368	0.168	0.295	0.007	0.107	0.003	1706.37	31.24	1665.46	35.02	1757.11	49.34
TH_34	3.114	0.115	0.247	0.005	0.091	0.003	1436.06	28.06	1422.53	27.24	1456.29	51.77
TH_35	0.081	0.005	0.013	0.000	0.045	0.003	78.74	5.04	82.66	2.95	0.00	109.46
TH_36	4.374	0.201	0.295	0.010	0.108	0.003	1707.36	37.33	1665.26	50.10	1759.54	51.78
TH_38	0.164	0.008	0.022	0.001	0.054	0.002	153.86	6.79	140.11	5.20	370.85	66.31
TH_39	3.057	0.126	0.223	0.007	0.099	0.002	1421.88	31.11	1299.28	39.34	1610.28	39.59
TH_43	2.749	0.098	0.230	0.006	0.087	0.002	1341.88	26.10	1336.23	30.20	1350.60	44.91
TH_47	0.183	0.006	0.025	0.001	0.052	0.001	170.22	5.44	161.43	3.29	293.88	63.45
TH_48	3.690	0.113	0.273	0.005	0.098	0.002	1569.13	24.18	1554.84	26.53	1588.13	39.86
TH_52	3.380	0.171	0.260	0.006	0.094	0.004	1499.73	38.86	1491.88	31.92	1509.24	75.83
TH_53	3.232	0.187	0.236	0.008	0.099	0.004	1464.75	43.97	1366.15	43.52	1609.18	78.95
TH_56	0.971	0.061	0.107	0.005	0.066	0.003	688.73	31.08	654.84	26.68	799.26	89.87
TH_57	4.134	0.218	0.297	0.008	0.101	0.004	1661.02	42.30	1675.45	41.06	1641.23	75.67
TH_58	3.847	0.198	0.282	0.007	0.099	0.004	1602.73	40.59	1601.13	36.08	1603.24	75.29
TH_60	0.079	0.005	0.011	0.000	0.051	0.003	77.30	4.90	72.60	3.00	224.00	118.00
TH_62	3.859	0.154	0.283	0.007	0.099	0.003	1605.25	31.69	1604.63	35.91	1605.62	51.36
TH_63	2.842	0.118	0.236	0.006	0.087	0.003	1366.72	30.74	1368.35	31.50	1363.72	59.14
TH_67	0.269	0.014	0.037	0.001	0.053	0.002	242.27	10.88	232.32	7.92	339.29	84.27
TH_68	4.696	0.232	0.292	0.011	0.117	0.004	1766.52	40.61	1652.72	54.35	1903.41	54.06
TH_70	3.847	0.161	0.281	0.008	0.099	0.003	1602.73	33.22	1595.93	39.76	1611.22	51.79
TH_71	3.915	0.153	0.283	0.007	0.100	0.003	1616.83	31.10	1607.08	33.97	1629.09	51.26
TH_72	4.634	0.160	0.309	0.007	0.109	0.003	1755.49	28.39	1735.73	34.53	1779.04	41.38
TH_76	5.348	0.225	0.339	0.011	0.114	0.003	1876.51	35.31	1883.63	51.78	1868.56	44.83
TH_77	4.629	0.155	0.315	0.007	0.107	0.002	1754.55	27.53	1764.49	32.36	1742.67	41.92
TH_78	2.868	0.138	0.233	0.009	0.089	0.003	1373.47	35.51	1350.06	46.13	1409.99	52.92
TH_79	5.157	0.170	0.331	0.007	0.113	0.003	1845.55	27.70	1842.09	32.63	1849.39	41.30
TH_82	8.519	0.328	0.443	0.012	0.140	0.004	2287.95	34.40	2363.47	53.37	2221.11	43.31
TH_83	3.015	0.110	0.244	0.006	0.090	0.002	1411.47	27.38	1405.99	31.55	1419.68	44.85
TH_84	0.738	0.025	0.089	0.002	0.060	0.002	561.03	14.23	552.32	9.66	596.76	53.77
TH_87	2.550	0.100	0.221	0.006	0.084	0.002	1286.48	28.34	1289.32	30.94	1281.97	52.35
TH_89	0.174	0.009	0.024	0.001	0.052	0.002	163.23	7.94	155.76	5.71	273.20	89.56
TH_91	0.180	0.013	0.024	0.002	0.055	0.002	168.09	11.29	151.39	9.62	410.40	77.62
TH_92	0.414	0.020	0.053	0.002	0.057	0.002	351.77	13.95	333.13	10.91	476.99	72.61
TH_93	10.115	0.345	0.462	0.009	0.159	0.004	2445.38	31.04	2447.13	39.91	2444.12	42.34
TH_94	3.748	0.156	0.276	0.008	0.099	0.003	1581.59	32.76	1570.11	41.83	1597.15	48.49
TH_95	4.274	0.116	0.299	0.005	0.104	0.002	1688.38	22.06	1685.58	24.75	1692.05	36.48
TH_96	5.111	0.206	0.331	0.011	0.112	0.003	1837.99	33.62	1843.12	52.80	1832.36	40.96
TH_97	0.754	0.026	0.085	0.002	0.064	0.002	570.60	15.10	527.96	12.97	744.58	49.88

Table A-1 Continued

Sample Name	Isotopic Ratios						Apparent Ages					
	$^{207}Pb/^{235}U$	1σ abs. err.	$^{206}Pb/^{238}U$	1σ abs. err.	$^{207}Pb/^{206}Pb$	1σ abs. err.	$^{207}Pb/^{235}U$	1σ abs. err.	$^{206}Pb/^{238}U$	1σ abs. err.	$^{207}Pb/^{206}Pb$	1σ abs. err.
<10 % Discordant Samples												
TH_98	2.995	0.104	0.235	0.006	0.092	0.002	1406.43	26.06	1362.10	31.32	1474.44	44.18
TH_100	10.979	0.338	0.478	0.010	0.167	0.003	2521.36	28.24	2519.14	45.56	2523.31	34.05
TH_101	3.286	0.104	0.232	0.005	0.103	0.002	1477.68	24.23	1343.69	27.52	1675.93	38.10
TH_103	0.872	0.079	0.104	0.008	0.061	0.004	636.62	42.16	635.45	44.10	640.99	138.75
TH_106	4.880	0.143	0.322	0.006	0.110	0.002	1798.81	24.39	1797.96	30.27	1799.98	38.09
TH_107	0.103	0.005	0.014	0.001	0.052	0.002	99.62	4.94	91.32	3.69	303.57	83.74
TH_108	0.755	0.029	0.091	0.003	0.060	0.001	571.02	16.73	561.58	16.49	609.27	51.41
TH_109	4.375	0.142	0.302	0.008	0.105	0.002	1707.70	26.46	1703.12	37.31	1713.74	35.78
TH_110	1.817	0.059	0.178	0.004	0.074	0.002	1051.58	20.92	1058.49	23.31	1037.72	42.65
TH_111	0.171	0.018	0.023	0.002	0.054	0.004	159.86	15.49	146.28	12.73	366.54	153.93
TH_112	0.104	0.005	0.014	0.000	0.052	0.002	100.27	4.32	92.69	3.03	284.97	79.45
TH_115	0.093	0.004	0.013	0.000	0.053	0.001	89.94	3.41	81.37	2.44	324.31	62.01
TH_118	4.349	0.134	0.302	0.007	0.105	0.002	1702.76	25.20	1699.18	35.01	1707.59	34.03
TH_120	2.895	0.075	0.238	0.004	0.088	0.002	1380.54	19.40	1374.21	21.70	1390.47	33.90
TH_122	0.581	0.021	0.073	0.002	0.058	0.002	465.18	13.43	451.63	10.99	532.77	61.32
TH_125	1.676	0.046	0.169	0.003	0.072	0.001	999.41	17.37	1004.18	17.72	989.11	38.47
TH_127	3.829	0.124	0.274	0.007	0.101	0.002	1598.96	25.68	1560.31	33.49	1650.42	39.18
TH_130	4.057	0.165	0.290	0.010	0.102	0.002	1645.78	32.57	1639.40	50.90	1654.06	34.40
Teh_1	0.088	0.011	0.014	0.001	0.046	0.007	85.24	10.14	88.57	6.04	0.00	302.33
Teh_2	0.310	0.026	0.040	0.003	0.056	0.004	274.39	20.08	251.07	15.52	470.07	136.67
Teh_3	0.143	0.012	0.020	0.001	0.052	0.003	135.95	10.47	128.20	7.65	265.06	142.25
Teh_5	4.403	0.362	0.302	0.018	0.105	0.007	1712.94	65.88	1701.29	89.78	1720.35	111.98
Teh_8	2.494	0.208	0.218	0.013	0.083	0.005	1270.22	58.83	1271.44	70.07	1260.86	123.62
Teh_10	2.653	0.219	0.223	0.014	0.086	0.005	1315.46	59.05	1298.50	70.82	1335.99	118.39
Teh_12	4.840	0.396	0.319	0.019	0.110	0.007	1791.86	66.58	1785.81	92.77	1792.11	110.36
Teh_13	4.700	0.385	0.316	0.019	0.107	0.007	1767.33	66.37	1770.26	92.51	1757.03	110.68
Teh_14	2.193	0.180	0.199	0.012	0.080	0.005	1178.77	55.55	1168.29	64.00	1190.70	119.01
Teh_15	4.790	0.395	0.311	0.019	0.111	0.007	1783.18	67.02	1747.36	92.81	1818.59	109.82
Teh_16	6.247	0.522	0.362	0.022	0.125	0.008	2011.03	70.63	1990.70	105.55	2025.36	109.19
Teh_17	4.783	0.392	0.322	0.019	0.107	0.007	1781.98	66.53	1800.76	93.78	1753.23	110.71
Teh_18	1.925	0.157	0.181	0.011	0.077	0.005	1089.94	53.17	1074.97	58.95	1112.52	120.58
Teh_19	0.241	0.020	0.033	0.002	0.053	0.004	218.90	16.40	208.94	12.49	319.00	146.38
Teh_20	4.491	0.371	0.304	0.019	0.107	0.007	1729.28	66.35	1711.31	91.07	1744.25	111.40
Teh_21	0.209	0.018	0.028	0.002	0.053	0.004	192.76	15.17	180.72	11.42	334.43	151.60
Teh_22	0.169	0.015	0.023	0.001	0.052	0.004	158.16	13.16	148.03	9.44	304.21	169.32
Teh_23	4.070	0.343	0.289	0.018	0.102	0.006	1648.26	66.41	1638.22	91.45	1654.16	112.37
Teh_24	0.084	0.010	0.012	0.001	0.049	0.007	81.79	9.76	78.62	5.71	166.80	301.14
Teh_25	4.264	0.350	0.276	0.017	0.111	0.007	1686.49	65.42	1573.63	83.95	1823.07	109.95
Teh_26	0.172	0.014	0.023	0.001	0.054	0.004	160.98	12.31	146.47	8.78	371.71	141.33
Teh_27	0.114	0.010	0.016	0.001	0.051	0.004	109.63	8.88	102.99	6.23	247.78	157.67
Teh_29	9.816	0.818	0.453	0.028	0.157	0.010	2417.67	74.01	2406.43	123.07	2420.81	104.31
Teh_30	0.171	0.016	0.024	0.002	0.051	0.005	159.91	13.95	154.67	9.75	229.53	195.62
Teh_31	3.705	0.306	0.258	0.016	0.104	0.007	1572.36	64.00	1477.21	79.41	1695.65	113.91
Teh_32	2.156	0.177	0.196	0.012	0.080	0.005	1166.99	55.35	1151.44	63.12	1188.58	119.83
Teh_33	3.014	0.259	0.229	0.015	0.095	0.006	1411.19	63.41	1329.63	78.49	1529.55	115.53
Teh_35	4.510	0.375	0.295	0.018	0.110	0.007	1732.84	66.77	1666.12	89.80	1807.59	111.13

Table A-1 Continued

Sample Name	Isotopic Ratios						Apparent Ages					
	$^{207}Pb/^{235}U$	1σ abs. err.	$^{206}Pb/^{238}U$	1σ abs. err.	$^{207}Pb/^{206}Pb$	1σ abs. err.	$^{207}Pb/^{235}U$	1σ abs. err.	$^{206}Pb/^{238}U$	1σ abs. err.	$^{207}Pb/^{206}Pb$	1σ abs. err.
<10 % Discordant Samples												
Teh_37	4.198	0.122	0.298	0.006	0.102	0.003	1673.72	23.46	1682.83	28.98	1661.70	45.27
Teh_38	4.393	0.127	0.303	0.006	0.105	0.003	1710.96	23.58	1705.51	29.00	1717.04	45.17
Teh_39	4.396	0.130	0.303	0.006	0.105	0.003	1711.52	24.16	1707.17	30.48	1716.24	45.59
Teh_40	4.775	0.141	0.335	0.007	0.103	0.003	1780.45	24.49	1863.36	32.42	1683.99	46.59
Teh_41	2.906	0.087	0.242	0.005	0.087	0.002	1383.53	22.24	1397.17	25.65	1361.90	48.61
Teh_42	0.825	0.027	0.101	0.002	0.059	0.002	611.08	15.14	619.49	12.71	579.29	70.60
Teh_44	0.178	0.006	0.026	0.001	0.049	0.002	166.42	5.11	167.11	3.50	155.74	78.04
Teh_45	4.520	0.149	0.317	0.008	0.103	0.003	1734.73	27.01	1777.11	38.11	1683.40	48.32
>10% Discordant Samples												
TH_42	0.098	0.004	0.013	0.000	0.053	0.002	94.49	4.11	84.70	2.32	349.06	88.62
TH_46	3.181	0.136	0.223	0.008	0.103	0.003	1452.62	32.58	1300.12	39.81	1683.12	45.49
TH_128	3.203	0.105	0.224	0.006	0.104	0.002	1457.99	25.10	1304.51	30.48	1689.48	35.52
TH_90	0.082	0.005	0.011	0.000	0.053	0.002	80.39	4.33	71.74	2.99	345.88	86.93
Teh_36	0.177	0.006	0.023	0.001	0.056	0.002	165.39	5.20	146.63	3.26	442.37	74.09
TH_75	2.198	0.094	0.171	0.006	0.093	0.002	1180.41	29.28	1019.10	30.31	1489.41	48.23
TH_121	2.972	0.103	0.206	0.006	0.105	0.002	1400.61	26.04	1206.08	29.75	1710.69	39.62
TH_129	0.182	0.009	0.022	0.001	0.059	0.001	170.16	7.62	142.81	6.00	569.92	52.90
TH_99	5.165	0.178	0.269	0.007	0.139	0.004	1846.94	28.83	1537.70	33.07	2215.80	43.04
TH_123	0.229	0.009	0.027	0.001	0.061	0.002	209.47	7.23	173.80	5.16	632.58	52.93
TH_114	0.113	0.006	0.014	0.001	0.060	0.002	108.43	5.28	86.80	3.65	614.78	69.09
TH_102	3.676	0.163	0.215	0.008	0.124	0.004	1566.09	34.81	1252.75	40.01	2018.75	50.96
TH_28	0.085	0.006	0.010	0.001	0.060	0.002	83.27	5.30	65.97	3.64	613.00	76.54
TH_64	0.225	0.017	0.025	0.001	0.064	0.003	205.69	13.99	161.93	9.38	741.85	110.19
TH_113	0.790	0.054	0.075	0.004	0.077	0.003	591.29	29.95	463.34	26.08	1119.19	77.66
TH_116	0.195	0.015	0.022	0.002	0.064	0.003	181.17	12.73	141.94	9.64	729.98	84.73
Teh_28	2.738	0.226	0.176	0.011	0.112	0.007	1338.84	59.58	1046.45	58.73	1836.16	109.73
TH_126	0.724	0.024	0.069	0.002	0.076	0.002	553.25	14.20	428.46	10.10	1106.93	47.32
TH_88	2.161	0.215	0.150	0.014	0.104	0.003	1168.53	66.68	901.50	78.99	1704.19	47.85
TH_117	5.254	0.242	0.249	0.010	0.153	0.003	1861.50	38.56	1434.66	52.37	2378.88	34.48
TH_73	0.116	0.005	0.013	0.000	0.065	0.002	111.78	4.92	83.61	2.70	763.06	71.40
TH_28	0.110	0.005	0.012	0.000	0.068	0.002	105.59	4.96	75.24	2.72	859.75	68.55
TH_81	0.403	0.023	0.039	0.002	0.076	0.003	343.53	16.64	244.33	9.98	1084.09	85.02
TH_44	0.261	0.016	0.026	0.001	0.072	0.003	235.73	12.49	166.47	7.64	998.29	81.73
Teh_7	1.217	0.107	0.086	0.006	0.103	0.006	808.46	47.78	529.25	34.94	1675.00	112.33
TH_50	0.163	0.010	0.015	0.001	0.081	0.003	153.63	8.57	93.34	3.67	1225.37	82.13
TH_74	0.126	0.012	0.011	0.001	0.082	0.003	120.25	10.42	70.93	6.03	1255.24	64.18
Teh_34	0.540	0.045	0.039	0.002	0.099	0.006	438.29	29.04	248.43	14.79	1610.48	115.09
TH_80	0.301	0.014	0.023	0.001	0.095	0.004	267.33	10.53	146.42	4.13	1529.70	67.91
Teh_6	0.434	0.038	0.031	0.002	0.101	0.007	366.07	26.57	197.20	13.21	1642.02	114.99
TH_49	0.113	0.020	0.009	0.002	0.090	0.005	108.68	18.33	58.50	9.90	1421.14	109.82
TH_85	0.131	0.005	0.010	0.000	0.093	0.003	125.32	4.67	65.57	1.56	1491.82	58.57
Teh_9	0.706	0.078	0.043	0.004	0.119	0.012	542.63	45.49	270.16	21.89	1945.28	168.34
TH_104	1.171	0.046	0.062	0.002	0.138	0.003	787.22	21.34	385.07	11.95	2202.43	39.25
TH_66	0.184	0.010	0.012	0.000	0.112	0.005	171.31	8.20	76.08	2.47	1836.15	77.71
TH_55	0.175	0.013	0.011	0.000	0.118	0.008	163.77	11.25	68.93	2.96	1925.99	116.75
TH_86	0.419	0.014	0.023	0.000	0.130	0.003	355.65	10.24	148.99	2.96	2099.54	43.57
Teh_4	0.491	0.041	0.027	0.002	0.133	0.009	405.43	27.40	169.28	10.25	2141.54	107.67
TH_51	0.174	0.012	0.010	0.000	0.123	0.007	163.30	10.22	66.08	2.86	1996.18	93.74

Table A-1 Continued

Sample Name	207Pb/235U	1σ abs. err.	206Pb/238U	1σ abs. err.	207Pb/206Pb	1σ abs. err.	207Pb/235U	1σ abs. err.	206Pb/238U	1σ abs. err.	207Pb/206Pb	1σ abs. err.
			Isotopic Ratios						Apparent Ages			
						>10% Discordant Samples						
TH_40	0.221	0.016	0.013	0.001	0.127	0.009	202.70	13.26	80.71	3.27	2059.25	121.22
TH_45	0.284	0.021	0.013	0.001	0.153	0.010	253.61	16.80	86.09	4.38	2380.15	107.27
Teh_11	0.386	0.042	0.017	0.001	0.159	0.018	331.10	30.35	111.70	7.93	2449.12	177.01
TH_69	0.418	0.035	0.017	0.001	0.176	0.011	354.51	25.01	110.30	7.16	2611.48	100.01
Teh_43	6.650	0.255	0.104	0.003	0.464	0.016	2065.95	33.35	637.25	17.14	4130.70	51.21
TH_124	0.471	0.019	0.018	0.001	0.188	0.005	391.70	12.80	115.98	3.55	2725.41	42.98
TH_32	0.360	0.021	0.013	0.001	0.196	0.009	312.07	15.46	85.11	3.30	2796.21	75.45
TH_32	0.394	0.021	0.014	0.000	0.202	0.010	337.43	15.32	90.55	2.52	2843.29	78.07
TH_59	0.390	0.023	0.014	0.000	0.206	0.010	334.61	16.34	87.93	2.68	2873.95	77.31
TH_105	0.192	0.008	0.007	0.000	0.203	0.007	178.26	7.10	43.95	1.43	2854.43	51.26
TH_61	0.611	0.035	0.018	0.001	0.240	0.010	483.98	21.65	118.01	4.84	3117.82	64.05
TH_54	0.741	0.049	0.018	0.001	0.299	0.018	563.19	28.28	114.76	4.00	3465.57	90.87
TH_25	0.347	0.026	0.010	0.001	0.264	0.014	302.44	19.66	61.13	3.61	3271.30	80.00
TH_18	0.075	0.080	0.002	0.002	0.028	0.054	73.14	73.25	11.01	11.86	0.00	1230.96
TH_65	-0.135	-0.133	-0.002	-0.002	0.418	0.024	-146.87	-169.88	-15.07	-14.90	3976.08	83.58
TH_119	-0.420	-0.152	-0.007	-0.003	0.422	0.023	-552.53	-308.60	-46.66	-16.69	3989.73	78.77
TH_25	-0.542	-0.172	-0.010	-0.003	0.410	0.024	-793.39	-478.98	-62.10	-19.75	3947.10	84.64
TH_27	-0.424	-0.541	-0.006	-0.008	0.475	0.026	-559.56	-2849.27	-41.80	-54.47	4166.68	78.50
TH_37	-0.716	-0.219	-0.014	-0.004	0.381	0.025	-1278.42	-1503.34	-88.55	-26.64	3834.26	97.29

Table A-2. Detrital zircon data table for sample Se-E. Sample analyzed by LA-ICP-MS on 4-9-2014 and 4-10-2014. Age data are in Ma.

Sample Name	207Pb/235U	1σ abs. err.	206Pb/238U	1σ abs. err.	207Pb/206Pb	1σ abs. err.	207Pb/235U	1σ abs. err.	206Pb/238U	1σ abs. err.	207Pb/206Pb	1σ abs. err.
			Isotopic Ratios						Apparent Ages			
						<10 % Discordant Samples						
ES_2	4.485	0.142	0.308	0.008	0.106	0.002	1728.16	25.97	1730.19	38.06	1725.75	32.47
ES_4	0.199	0.008	0.030	0.001	0.048	0.002	184.63	7.02	189.55	5.60	122.22	75.05
ES_5	4.541	0.160	0.310	0.009	0.106	0.002	1738.55	28.87	1739.00	44.69	1738.06	32.85
ES_8	0.952	0.033	0.108	0.003	0.064	0.001	678.93	17.11	662.64	18.02	733.39	39.67
ES_9	0.916	0.031	0.102	0.003	0.065	0.002	660.07	16.53	625.37	15.44	780.55	47.84
ES_10	14.462	0.456	0.541	0.014	0.194	0.003	2780.53	29.54	2786.69	56.38	2776.11	28.92
ES_11	0.183	0.012	0.024	0.001	0.054	0.002	170.86	10.32	155.90	8.87	383.48	82.41
ES_12	4.328	0.191	0.299	0.012	0.105	0.002	1698.79	35.71	1685.38	58.52	1715.42	33.44
ES_14	0.627	0.023	0.080	0.002	0.057	0.001	494.29	14.09	499.10	13.77	472.58	47.64
ES_15	0.789	0.027	0.095	0.002	0.060	0.001	590.81	15.06	586.55	13.94	607.69	49.21
ES_16	4.549	0.164	0.311	0.009	0.106	0.002	1740.05	29.58	1743.96	45.59	1735.76	33.55
ES_19	3.768	0.124	0.278	0.007	0.098	0.002	1585.94	26.00	1578.97	36.51	1595.62	33.37

Table A-2 Continued

Sample Name		Isotopic Ratios							Apparent Ages			
	$^{207}Pb/^{235}U$	1σ abs. err.	$^{206}Pb/^{238}U$	1σ abs. err.	$^{207}Pb/^{206}Pb$	1σ abs. err.	$^{207}Pb/^{235}U$	1σ abs. err.	$^{206}Pb/^{238}U$	1σ abs. err.	$^{207}Pb/^{206}Pb$	1σ abs. err.
					<10 % Discordant Samples							
ES_23	4.068	0.131	0.292	0.007	0.101	0.002	1647.83	25.85	1652.61	36.18	1642.15	34.62
ES_24	0.095	0.004	0.013	0.000	0.053	0.002	91.73	4.16	82.92	2.72	327.87	86.06
ES_25	2.107	0.096	0.190	0.007	0.080	0.003	1151.07	30.81	1123.73	36.44	1203.36	60.18
ES_29	4.194	0.143	0.298	0.007	0.102	0.002	1672.87	27.51	1681.05	36.69	1663.16	38.65
ES_30	3.617	0.159	0.260	0.010	0.101	0.002	1553.20	34.42	1488.80	48.88	1642.45	40.34
ES_31	4.628	0.179	0.315	0.009	0.107	0.003	1754.38	31.86	1764.84	45.74	1742.47	43.08
ES_32	4.175	0.157	0.307	0.009	0.099	0.002	1669.22	30.32	1724.79	42.82	1600.57	43.09
ES_33	5.213	0.158	0.333	0.006	0.114	0.002	1854.78	25.43	1853.12	30.74	1857.16	38.59
ES_35	4.307	0.142	0.301	0.007	0.104	0.002	1694.62	26.89	1697.54	33.15	1691.54	42.42
ES_36	3.107	0.112	0.247	0.007	0.091	0.002	1434.42	27.25	1421.37	34.94	1454.38	39.57
ES_37	4.301	0.175	0.297	0.010	0.105	0.002	1693.57	32.89	1676.10	48.53	1715.79	39.14
ES_39	8.716	0.305	0.429	0.012	0.147	0.003	2308.77	31.42	2303.24	55.73	2313.73	31.33
ES_40	4.164	0.133	0.299	0.008	0.101	0.002	1666.92	25.91	1687.68	37.77	1640.94	33.10
ES_41	14.132	0.507	0.546	0.016	0.188	0.003	2758.60	33.46	2809.47	68.01	2721.65	29.41
ES_42	2.806	0.093	0.233	0.006	0.087	0.002	1357.04	24.56	1349.67	32.32	1368.73	35.71
ES_43	1.881	0.066	0.190	0.006	0.072	0.001	1074.37	23.03	1118.69	29.86	985.57	36.43
ES_44	3.147	0.146	0.224	0.009	0.102	0.002	1444.23	35.18	1301.61	49.05	1661.01	32.78
ES_46	3.906	0.113	0.283	0.006	0.100	0.002	1614.89	23.22	1607.82	30.86	1624.19	33.29
ES_47	1.396	0.051	0.145	0.004	0.070	0.001	887.12	21.42	872.60	24.33	923.58	41.97
ES_48	13.332	0.381	0.519	0.011	0.186	0.003	2703.44	26.64	2696.79	46.58	2708.48	29.22
ES_49	3.871	0.114	0.285	0.006	0.098	0.002	1607.56	23.56	1617.15	31.78	1595.10	33.74
ES_50	4.044	0.153	0.291	0.008	0.101	0.002	1643.01	30.34	1645.26	40.24	1639.43	44.48
ES_53	3.284	0.127	0.257	0.007	0.093	0.002	1477.36	29.64	1471.99	36.24	1484.37	49.90
ES_54	6.768	0.259	0.340	0.010	0.144	0.004	2081.57	33.25	1886.16	45.74	2280.22	42.06
ES_55	4.568	0.165	0.313	0.008	0.106	0.003	1743.47	29.73	1754.22	39.11	1729.89	44.20
ES_56	3.952	0.171	0.286	0.010	0.100	0.002	1624.38	34.55	1622.51	49.50	1626.10	45.32
ES_58	4.385	0.271	0.271	0.015	0.117	0.003	1709.48	49.89	1548.15	76.35	1912.58	42.65
ES_60	10.543	0.422	0.438	0.013	0.175	0.004	2483.71	36.50	2341.02	59.84	2601.95	40.28
ES_62	0.835	0.030	0.102	0.003	0.060	0.001	616.48	16.57	624.12	16.25	587.50	48.68
ES_63	0.530	0.031	0.067	0.003	0.058	0.001	432.12	20.06	416.32	20.83	516.24	54.10
ES_66	3.149	0.156	0.237	0.010	0.096	0.002	1444.67	37.36	1371.97	52.34	1552.49	46.41
ES_67	3.978	0.263	0.289	0.018	0.100	0.002	1629.76	52.25	1636.48	87.99	1620.25	43.66
ES_68	0.195	0.007	0.028	0.001	0.050	0.001	181.18	6.23	180.51	4.98	188.93	58.13
ES_69	13.621	0.541	0.524	0.017	0.188	0.004	2723.73	36.87	2717.71	70.05	2727.45	37.39
ES_72	4.357	0.246	0.304	0.015	0.104	0.002	1704.13	45.51	1713.15	75.87	1692.22	43.51
ES_73	1.418	0.060	0.147	0.005	0.070	0.002	896.73	24.70	885.56	27.26	923.43	53.91
ES_74	3.071	0.140	0.247	0.010	0.090	0.002	1425.37	34.27	1423.83	50.80	1427.69	36.00
ES_75	5.392	0.163	0.340	0.007	0.115	0.002	1883.55	25.56	1884.99	34.46	1881.98	33.23
ES_76	5.092	0.156	0.328	0.007	0.113	0.002	1834.78	25.66	1826.80	34.65	1843.87	32.99
ES_77	3.236	0.177	0.231	0.011	0.102	0.002	1465.74	41.49	1338.09	59.93	1655.90	36.24
ES_78	0.124	0.008	0.018	0.001	0.051	0.002	118.52	7.24	112.01	6.01	251.33	86.51
ES_79	3.730	0.217	0.275	0.015	0.098	0.002	1577.76	45.55	1564.63	74.11	1595.39	37.06
ES_81	0.096	0.011	0.013	0.001	0.052	0.005	92.63	10.18	85.49	7.08	280.36	203.59
ES_82	4.297	0.143	0.301	0.008	0.104	0.002	1692.87	26.98	1694.46	39.86	1690.49	31.51
ES_84	3.031	0.130	0.260	0.010	0.085	0.001	1415.55	32.11	1488.86	50.31	1306.48	33.49
ES_86	3.657	0.196	0.260	0.013	0.102	0.002	1562.05	41.85	1488.95	65.84	1661.92	33.04
ES_87	3.988	0.233	0.262	0.014	0.110	0.002	1631.70	46.36	1499.29	73.06	1806.45	32.91
ES_88	2.731	0.094	0.231	0.007	0.086	0.001	1337.05	25.17	1340.12	34.17	1331.71	32.40

Table A-2 Continued

Sample Name	Isotopic Ratios						Apparent Ages					
	$^{207}Pb/^{235}U$	1σ abs. err.	$^{206}Pb/^{238}U$	1σ abs. err.	$^{207}Pb/^{206}Pb$	1σ abs. err.	$^{207}Pb/^{235}U$	1σ abs. err.	$^{206}Pb/^{238}U$	1σ abs. err.	$^{207}Pb/^{206}Pb$	1σ abs. err.
<10 % Discordant Samples												
ES_89	0.735	0.030	0.089	0.003	0.060	0.002	559.24	17.40	547.55	17.05	606.63	53.16
ES_90	0.911	0.031	0.106	0.003	0.062	0.001	657.79	16.56	652.12	16.99	676.81	40.97
ES_92	0.097	0.005	0.014	0.000	0.052	0.002	94.26	4.44	87.14	2.68	278.31	93.33
ES_93	4.357	0.155	0.303	0.008	0.104	0.002	1704.19	29.04	1706.83	37.55	1700.89	40.60
ES_96	3.875	0.145	0.285	0.008	0.099	0.002	1608.40	29.68	1615.70	38.82	1598.81	41.52
ES_100	6.328	0.240	0.369	0.010	0.124	0.003	2022.41	32.73	2023.62	47.26	2021.11	41.84
ES_101	1.497	0.061	0.156	0.004	0.069	0.002	929.21	24.39	936.47	24.47	911.96	57.57
ES_103	1.947	0.070	0.187	0.005	0.076	0.002	1097.30	23.85	1103.74	25.78	1084.49	44.36
ES_104	9.057	0.485	0.429	0.021	0.153	0.003	2343.82	47.79	2302.25	93.29	2380.40	34.53
ES_105	5.015	0.171	0.339	0.008	0.107	0.002	1821.79	28.55	1883.75	40.13	1751.88	38.89
ES_107	4.518	0.139	0.310	0.006	0.106	0.002	1734.36	25.29	1740.59	31.15	1727.07	36.82
ES_109	2.871	0.088	0.236	0.005	0.088	0.002	1374.33	22.88	1367.11	25.03	1385.79	38.49
ES_110	5.149	0.175	0.332	0.008	0.112	0.002	1844.23	28.48	1850.08	38.43	1837.86	39.49
ES_111	0.091	0.004	0.013	0.000	0.053	0.002	88.82	3.71	80.39	1.94	322.13	87.64
ES_112	4.290	0.133	0.300	0.006	0.104	0.002	1691.50	25.17	1693.58	30.72	1689.15	37.05
ES_113	0.468	0.018	0.061	0.002	0.056	0.002	389.78	12.37	380.97	9.31	442.63	64.55
ES_114	3.102	0.104	0.248	0.006	0.091	0.002	1433.23	25.39	1427.27	30.30	1442.32	40.19
ES_115	1.777	0.064	0.170	0.004	0.076	0.002	1036.97	23.10	1012.87	23.84	1088.35	47.72
ES_116	3.412	0.166	0.241	0.011	0.103	0.002	1507.26	37.48	1390.00	55.42	1676.39	33.73
ES_117	4.485	0.129	0.304	0.006	0.107	0.002	1728.17	23.60	1710.44	29.71	1749.92	34.19
ES_119	4.148	0.121	0.291	0.006	0.103	0.002	1663.77	23.65	1645.89	30.76	1686.63	32.47
ES_120	10.042	0.294	0.439	0.009	0.166	0.003	2438.61	26.72	2347.54	40.74	2515.67	31.11
ES_122	4.413	0.120	0.305	0.006	0.105	0.002	1714.69	22.26	1718.40	27.27	1710.38	32.59
ES_123	3.969	0.117	0.271	0.006	0.106	0.002	1627.82	23.71	1543.92	29.23	1738.23	33.36
ES_124	4.322	0.138	0.302	0.007	0.104	0.002	1697.57	25.93	1701.56	36.62	1692.87	33.20
ES_125	0.653	0.031	0.082	0.003	0.058	0.002	510.07	19.12	508.86	20.06	515.75	56.63
ES_126	3.992	0.115	0.288	0.006	0.101	0.002	1632.60	23.18	1631.51	27.92	1634.22	36.22
ES_127	3.272	0.203	0.242	0.014	0.098	0.002	1474.31	47.23	1395.34	73.74	1590.12	36.08
ES_129	2.668	0.156	0.213	0.007	0.091	0.004	1319.75	42.28	1243.70	37.39	1444.33	77.70
ES_132	1.515	0.085	0.154	0.004	0.071	0.003	936.63	33.58	921.86	24.46	970.29	82.82
ES_133	3.775	0.209	0.278	0.008	0.099	0.004	1587.45	43.59	1580.09	39.07	1596.10	75.74
ES_135	4.324	0.258	0.325	0.012	0.096	0.004	1697.96	48.02	1813.86	55.93	1556.59	75.61
ES_136	2.657	0.151	0.224	0.007	0.086	0.004	1316.70	41.03	1305.31	35.46	1334.13	78.92
ES_137	4.089	0.241	0.316	0.011	0.094	0.004	1652.13	46.93	1772.38	52.52	1501.26	76.72
ES_138	4.788	0.278	0.316	0.010	0.110	0.005	1782.79	47.56	1772.60	49.54	1793.64	74.75
>10% Discordant Samples												
ES_57	9.374	0.682	0.392	0.026	0.173	0.004	2375.28	64.61	2133.64	121.06	2589.00	40.54
ES_51	1.951	0.077	0.165	0.005	0.086	0.002	1098.89	26.22	983.15	26.88	1335.12	48.41
ES_85	0.132	0.005	0.018	0.001	0.054	0.001	125.65	4.70	112.36	3.41	384.51	57.88
ES_18	0.087	0.004	0.012	0.000	0.054	0.002	84.89	4.02	75.65	2.76	353.93	82.89
ES_131	1.465	#DIV/0!	0.133	0.003	0.080	#DIV/0!	915.92	#DIV/0!	804.12	19.86	1194.71	#DIV/0!
ES_128	5.534	0.378	0.396	0.019	0.101	0.004	1905.90	57.12	2149.31	87.05	1649.25	76.24

Sample Name	Isotopic Ratios						Apparent Ages					
	$^{207}Pb/^{235}U$	1σ abs. err.	$^{206}Pb/^{238}U$	1σ abs. err.	$^{207}Pb/^{206}Pb$	1σ abs. err.	$^{207}Pb/^{235}U$	1σ abs. err.	$^{206}Pb/^{238}U$	1σ abs. err.	$^{207}Pb/^{206}Pb$	1σ abs. err.
					>10% Discordant Samples							
ES_121	0.086	0.004	0.011	0.000	0.055	0.002	83.74	3.44	72.85	1.80	406.65	84.44
ES_52	0.113	0.009	0.015	0.001	0.056	0.002	109.07	7.79	94.76	6.47	433.07	68.31
ES_97	3.189	0.173	0.215	0.010	0.107	0.002	1454.39	41.16	1257.59	54.51	1754.94	40.42
ES_70	2.708	0.114	0.195	0.007	0.101	0.002	1330.53	30.75	1149.27	36.70	1634.72	40.94
ES_140	2.449	0.155	0.183	0.008	0.097	0.004	1257.12	44.69	1082.16	40.87	1569.42	76.00
ES_130	5.108	0.301	0.275	0.009	0.134	0.006	1837.48	48.79	1568.54	46.29	2156.33	72.23
ES_91	0.106	0.006	0.014	0.000	0.057	0.002	102.38	5.05	86.91	3.17	478.68	88.84
ES_94	0.102	0.007	0.013	0.001	0.057	0.003	98.82	6.28	82.63	3.69	509.43	119.15
ES_28	2.672	0.135	0.187	0.008	0.104	0.002	1320.75	36.68	1104.07	45.19	1692.56	38.23
ES_34	0.143	0.018	0.018	0.002	0.059	0.005	135.70	15.62	111.98	11.03	574.42	184.72
ES_106	1.274	0.054	0.112	0.004	0.082	0.002	834.02	23.84	685.53	21.53	1253.54	50.00
ES_22	3.806	0.198	0.225	0.010	0.123	0.003	1593.99	41.06	1308.27	54.25	1995.91	44.38
ES_108	0.094	0.005	0.011	0.000	0.059	0.002	91.06	4.46	73.57	2.62	577.96	85.58
ES_13	0.096	0.005	0.012	0.000	0.060	0.002	92.65	4.16	73.95	2.67	606.12	70.43
ES_6	0.113	0.011	0.014	0.001	0.061	0.006	108.97	9.94	86.58	5.39	630.88	185.05
ES_65	2.131	0.341	0.150	0.024	0.103	0.003	1158.89	104.83	900.62	130.46	1679.38	53.89
ES_17	0.164	0.008	0.018	0.001	0.065	0.002	153.90	6.85	117.56	4.80	758.34	53.66
ES_98	3.854	0.167	0.206	0.007	0.136	0.003	1604.16	34.31	1207.71	38.32	2172.58	38.89
ES_61	0.346	0.029	0.034	0.002	0.074	0.004	301.62	21.85	216.16	15.36	1028.71	99.93
ES_59	0.163	0.020	0.016	0.002	0.073	0.004	153.36	17.23	103.02	11.40	1024.38	110.38
ES_83	1.509	0.054	0.101	0.003	0.108	0.002	934.03	21.44	623.13	17.29	1762.77	33.25
ES_21	0.269	0.015	0.025	0.001	0.077	0.001	241.56	11.72	160.49	8.09	1128.66	36.12
ES_20	0.776	0.050	0.059	0.004	0.095	0.002	583.25	28.15	370.61	21.90	1530.84	36.08
ES_27	0.294	0.018	0.026	0.001	0.083	0.004	261.72	14.29	163.39	7.90	1271.47	83.36
ES_134	0.403	0.036	0.034	0.002	0.087	0.004	344.17	25.80	213.06	15.57	1361.15	79.93
ES_7	2.247	0.078	0.120	0.003	0.136	0.002	1195.92	24.15	727.77	19.82	2181.66	31.48
ES_45	1.197	0.037	0.078	0.002	0.111	0.002	799.19	16.76	483.86	10.84	1822.00	33.88
ES_38	0.475	0.021	0.036	0.001	0.095	0.004	394.84	14.09	229.36	6.58	1531.56	68.95
ES_80	0.378	0.016	0.026	0.001	0.105	0.003	325.70	11.82	166.95	5.43	1705.88	51.40
ES_3	0.148	0.009	0.010	0.000	0.113	0.004	139.92	7.56	61.10	3.04	1840.57	59.88
ES_118	0.339	0.012	0.020	0.001	0.126	0.003	296.14	9.19	124.52	3.16	2042.08	44.49
ES_139	0.380	0.025	0.021	0.001	0.128	0.007	326.74	18.16	136.94	4.81	2072.83	90.72
ES_64	0.616	0.024	0.031	0.001	0.145	0.003	487.46	14.98	196.11	6.03	2283.20	37.57
ES_1	0.144	0.009	0.008	0.000	0.124	0.007	136.50	8.13	53.83	2.44	2021.04	93.05
ES_26	0.356	0.034	0.012	0.001	0.216	0.012	309.24	25.33	76.52	6.39	2953.39	84.97
ES_95	0.117	0.028	0.004	0.001	0.234	0.013	112.70	25.25	23.45	5.47	3076.95	85.98
ES_102	-0.259	-0.096	-0.009	-0.003	0.220	0.012	-304.24	-141.39	-55.27	-20.42	2980.21	86.67
ES_99	0.124	0.131	0.003	0.003	0.295	0.011	118.32	112.04	19.57	20.59	3443.01	55.27

Table A-3. Detrital zircon data table for sample H-PC. Sample analyzed by LA-ICP-MS on 9-13-2014, 9-15-2014, and 1-28-2015. Age data are in Ma.

Sample Name	Isotopic Ratios						Apparent Ages					
	$^{207}Pb/^{235}U$	1σ abs. err.	$^{206}Pb/^{238}U$	1σ abs. err.	$^{207}Pb/^{206}Pb$	1σ abs. err.	$^{207}Pb/^{235}U$	1σ abs. err.	$^{206}Pb/^{238}U$	1σ abs. err.	$^{207}Pb/^{206}Pb$	1σ abs. err.
<10 % Discordant Samples												
H_1	11.812	0.894	0.472	0.022	0.182	0.008	2589.63	68.50	2490.19	97.45	2667.66	71.13
H_10	5.640	0.428	0.317	0.015	0.129	0.006	1922.16	63.44	1773.74	73.86	2085.49	75.42
H_11	3.704	0.268	0.276	0.012	0.097	0.004	1572.33	56.22	1572.48	59.21	1571.31	78.87
H_12	0.098	0.008	0.015	0.001	0.046	0.002	94.61	6.97	97.60	4.37	18.90	115.00
H_13	9.566	0.715	0.436	0.020	0.159	0.007	2393.93	66.50	2334.26	88.09	2444.36	73.97
H_14	4.130	0.296	0.299	0.012	0.100	0.004	1660.32	56.89	1684.73	60.78	1628.77	78.62
H_16	0.168	0.014	0.022	0.001	0.055	0.003	157.88	11.73	142.50	6.64	394.44	114.98
H_2	4.712	0.362	0.281	0.014	0.122	0.005	1769.30	62.36	1594.23	69.48	1981.87	75.96
H_3	4.171	0.317	0.303	0.014	0.100	0.004	1668.41	60.37	1707.37	70.65	1618.90	80.96
H_4	0.175	0.016	0.024	0.001	0.053	0.003	164.15	13.97	154.15	8.23	309.94	143.32
H_5	0.879	0.066	0.104	0.005	0.061	0.003	640.66	34.93	637.14	26.83	652.14	95.59
H_7	4.656	0.342	0.304	0.013	0.111	0.005	1759.41	59.56	1712.49	64.67	1814.80	78.79
H_8	0.078	0.006	0.012	0.001	0.047	0.002	76.19	5.51	76.49	3.38	65.73	107.35
H_9	0.088	0.007	0.013	0.001	0.048	0.003	85.95	6.65	84.80	4.02	116.79	120.40
H1_1	2.075	0.093	0.196	0.007	0.077	0.002	1140.45	30.24	1151.46	37.51	1118.01	56.20
H1_10	0.112	0.006	0.015	0.001	0.053	0.002	107.42	5.20	96.89	3.59	345.96	92.32
H1_11	4.162	0.188	0.292	0.011	0.103	0.003	1666.51	36.24	1650.97	52.46	1684.70	51.46
H1_12	15.842	0.704	0.561	0.020	0.205	0.006	2867.33	41.55	2872.44	81.80	2862.48	44.62
H1_13	3.208	0.145	0.233	0.008	0.100	0.003	1459.03	34.37	1350.90	43.36	1618.75	54.27
H1_14	3.458	0.157	0.265	0.010	0.095	0.003	1517.80	35.17	1516.33	49.12	1518.40	53.28
H1_15	3.869	0.173	0.283	0.010	0.099	0.003	1607.30	35.41	1607.37	50.11	1605.75	53.04
H1_16	0.107	0.006	0.016	0.001	0.048	0.002	103.57	5.22	102.87	3.82	117.76	105.82
H1_17	0.934	0.043	0.107	0.004	0.063	0.002	669.92	22.53	657.26	22.60	711.09	67.07
H1_18	2.049	0.100	0.200	0.008	0.074	0.003	1132.04	32.83	1173.87	40.69	1051.10	69.56
H1_19	5.509	0.250	0.323	0.012	0.124	0.004	1902.07	38.33	1805.75	56.39	2007.47	52.27
H1_2	3.359	0.148	0.266	0.009	0.092	0.003	1494.79	33.94	1518.70	47.18	1459.57	52.56
H1_21	4.364	0.193	0.305	0.011	0.104	0.003	1705.46	35.95	1716.23	52.87	1690.81	51.07
H1_22	0.064	0.004	0.009	0.000	0.051	0.003	62.86	3.47	58.64	2.28	224.66	116.67
H1_23	1.460	0.069	0.151	0.005	0.070	0.002	914.21	28.16	906.44	30.73	931.42	68.99
H1_24	1.753	0.083	0.172	0.006	0.074	0.002	1028.45	30.14	1021.47	35.09	1041.77	64.33
H1_4	0.089	0.006	0.014	0.001	0.046	0.003	86.96	5.76	90.40	3.95	0.00	154.10
H1_5	8.699	0.387	0.463	0.016	0.136	0.004	2306.95	39.77	2453.34	72.20	2178.41	48.10
H1_6	4.552	0.208	0.316	0.012	0.104	0.003	1740.60	37.27	1771.61	56.88	1702.11	51.29
H1_8	3.165	0.147	0.251	0.009	0.091	0.003	1448.69	35.19	1444.18	48.74	1453.82	53.51
H1_9	4.580	0.203	0.314	0.011	0.106	0.003	1745.72	36.36	1759.71	54.36	1727.56	50.60
H2_1	13.221	0.776	0.498	0.025	0.193	0.005	2695.53	53.93	2605.30	108.12	2763.73	40.66
H2_12	4.426	0.241	0.313	0.014	0.102	0.003	1717.17	44.06	1757.60	69.96	1668.02	45.49
H2_13	0.171	0.005	0.024	0.000	0.051	0.002	160.30	4.57	153.73	2.22	258.81	70.81
H2_14	1.666	0.048	0.155	0.002	0.078	0.002	995.81	18.06	928.84	13.79	1146.60	49.44
H2_14	4.491	0.243	0.314	0.014	0.104	0.003	1729.25	43.91	1758.73	69.25	1693.57	45.68
H2_15	0.095	0.005	0.015	0.001	0.047	0.001	92.58	4.98	94.65	4.30	39.43	70.26
H2_16	0.078	0.005	0.011	0.001	0.050	0.002	76.45	4.34	72.69	3.41	195.44	76.16
H2_16	4.206	0.115	0.297	0.004	0.103	0.003	1675.11	22.22	1675.72	19.23	1674.54	46.38
H2_17	3.854	0.114	0.279	0.005	0.100	0.003	1604.02	23.61	1585.03	24.78	1629.25	46.23
H2_18	4.333	0.113	0.300	0.003	0.105	0.003	1699.57	21.38	1691.29	15.86	1710.01	45.39

Table A-3 Continued

Sample Name		Isotopic Ratios							Apparent Ages			
	$^{207}Pb/^{235}U$	1σ abs. err.	$^{206}Pb/^{238}U$	1σ abs. err.	$^{207}Pb/^{206}Pb$	1σ abs. err.	$^{207}Pb/^{235}U$	1σ abs. err.	$^{206}Pb/^{238}U$	1σ abs. err.	$^{207}Pb/^{206}Pb$	1σ abs. err.
					<10 % Discordant Samples							
H2_19	3.780	0.105	0.271	0.004	0.101	0.003	1588.43	22.12	1546.00	19.33	1645.43	46.52
H2_2	2.832	0.153	0.233	0.010	0.088	0.002	1364.04	39.69	1351.46	54.63	1383.60	48.03
H2_2	4.861	0.136	0.321	0.004	0.110	0.003	1795.54	23.25	1792.82	21.07	1798.91	47.02
H2_20	4.006	0.113	0.284	0.004	0.102	0.003	1635.46	22.70	1609.20	19.17	1669.59	49.04
H2_22	0.108	0.004	0.015	0.000	0.052	0.002	104.17	3.88	96.33	2.01	287.84	93.29
H2_23	4.493	0.137	0.306	0.006	0.107	0.003	1729.62	25.03	1719.98	28.68	1741.50	46.02
H2_24	0.194	0.006	0.027	0.000	0.053	0.002	180.10	4.75	169.32	2.12	324.32	64.32
H2_25	4.303	0.123	0.298	0.005	0.105	0.003	1694.01	23.29	1680.31	22.91	1711.22	46.26
H2_26	3.886	0.103	0.282	0.003	0.100	0.003	1610.79	21.19	1602.21	15.91	1622.23	46.32
H2_27	4.025	0.106	0.270	0.003	0.108	0.003	1639.19	21.25	1541.42	16.23	1767.19	44.06
H2_3	4.207	0.108	0.295	0.003	0.103	0.003	1675.47	20.77	1666.88	13.86	1686.44	44.88
H2_3	4.599	0.245	0.313	0.014	0.107	0.003	1749.14	43.45	1755.30	67.94	1741.59	44.61
H2_4	0.226	0.013	0.033	0.002	0.050	0.001	206.48	10.73	206.71	9.67	203.64	67.66
H2_5	2.815	0.075	0.228	0.003	0.089	0.002	1359.59	19.84	1325.55	14.28	1413.72	47.37
H2_5	4.412	0.242	0.314	0.014	0.102	0.003	1714.50	44.36	1759.73	70.74	1659.50	45.76
H2_6	0.067	0.002	0.010	0.000	0.048	0.002	65.79	2.32	64.63	1.11	108.33	91.84
H2_6	4.683	0.255	0.317	0.015	0.107	0.003	1764.26	44.53	1775.27	70.71	1751.06	44.91
H2_7	16.887	0.451	0.576	0.007	0.213	0.005	2928.45	25.27	2930.63	28.40	2927.13	39.68
H2_8	0.146	0.008	0.021	0.001	0.050	0.003	138.02	6.74	135.35	3.58	184.43	136.07
H2_8	3.060	0.169	0.245	0.011	0.091	0.002	1422.68	41.35	1410.43	58.65	1440.85	47.62
H2_10	4.504	0.120	0.306	0.003	0.107	0.003	1731.76	21.81	1720.44	16.26	1745.67	46.33
H2_10	4.642	0.253	0.306	0.014	0.110	0.003	1756.77	44.55	1722.16	68.45	1797.99	46.24
H2_11	2.965	0.077	0.239	0.002	0.090	0.002	1398.74	19.64	1382.44	12.79	1423.89	47.41
H2_11	4.213	0.229	0.291	0.013	0.105	0.003	1676.54	43.66	1645.76	66.14	1715.09	45.06
H3_1	1.937	0.063	0.193	0.004	0.073	0.002	1093.87	21.62	1138.25	20.50	1006.47	50.03
H3_2	13.336	0.424	0.537	0.012	0.180	0.004	2703.76	29.62	2771.99	48.96	2653.07	34.22
H3_5	4.599	0.136	0.317	0.006	0.105	0.002	1749.14	24.41	1774.72	29.26	1718.60	36.73
H3_6	0.611	0.020	0.076	0.002	0.059	0.001	483.96	12.83	469.41	10.51	553.38	48.26
H3_7	4.598	0.146	0.304	0.006	0.110	0.002	1748.84	26.13	1712.26	31.94	1792.75	38.51
H3_9	4.996	0.168	0.349	0.009	0.104	0.002	1818.68	28.08	1929.60	40.84	1693.79	37.72
H3_10	3.747	0.162	0.266	0.010	0.102	0.002	1581.51	33.98	1520.61	49.46	1663.62	38.02
H3_11	3.015	0.089	0.245	0.005	0.089	0.002	1411.36	22.20	1414.44	23.48	1406.61	38.44
H3_12	4.484	0.149	0.312	0.007	0.104	0.002	1728.01	27.26	1749.72	36.04	1701.72	38.93
H3_14	0.924	0.030	0.108	0.002	0.062	0.001	664.40	15.49	659.44	12.37	681.14	50.08
H3_15	4.599	0.154	0.327	0.008	0.102	0.002	1749.06	27.63	1822.15	38.45	1662.68	38.36
H3_16	0.218	0.010	0.030	0.001	0.052	0.002	200.66	8.13	191.70	5.75	307.13	77.16
H4_1	4.177	0.191	0.309	0.008	0.098	0.003	1669.54	36.74	1733.35	38.96	1590.70	59.17
H4_2	4.017	0.176	0.291	0.006	0.100	0.003	1637.56	34.94	1645.62	32.03	1627.70	58.94
H4_3	0.106	0.006	0.015	0.000	0.052	0.003	102.39	5.67	94.01	2.88	302.78	109.48
H4_6	7.039	0.303	0.394	0.008	0.130	0.004	2116.31	37.57	2139.29	39.11	2094.50	54.50
H4_7	3.816	0.200	0.273	0.010	0.102	0.003	1596.23	41.27	1553.74	49.92	1653.27	58.46
H4_8	5.337	0.228	0.305	0.007	0.127	0.004	1874.76	35.92	1717.51	32.16	2054.27	54.05
H4_9	4.739	0.219	0.316	0.008	0.109	0.003	1774.21	37.99	1772.43	39.16	1776.89	57.37
H4_10	4.477	0.206	0.305	0.008	0.106	0.003	1726.68	37.49	1716.50	38.10	1739.63	57.04

Table A-3 Continued

Sample Name	Isotopic Ratios						Apparent Ages					
	$^{207}Pb/^{235}U$	1σ abs. err.	$^{206}Pb/^{238}U$	1σ abs. err.	$^{207}Pb/^{206}Pb$	1σ abs. err.	$^{207}Pb/^{235}U$	1σ abs. err.	$^{206}Pb/^{238}U$	1σ abs. err.	$^{207}Pb/^{206}Pb$	1σ abs. err.
<10 % Discordant Samples												
H4_11	4.328	0.197	0.300	0.007	0.105	0.003	1698.79	36.95	1692.74	36.43	1706.85	57.47
H4_13	4.141	0.192	0.296	0.008	0.101	0.003	1662.46	37.26	1671.61	37.82	1651.51	58.25
H4_14	13.844	0.663	0.530	0.015	0.190	0.006	2739.09	44.40	2740.21	63.41	2738.80	51.51
H4_16	4.781	0.221	0.317	0.008	0.109	0.004	1781.50	38.14	1775.87	39.55	1788.69	57.24
H5_1	0.121	0.005	0.017	0.001	0.050	0.001	116.25	4.65	111.47	4.13	215.68	46.15
H5_2	2.948	0.118	0.240	0.009	0.089	0.001	1394.23	29.83	1387.49	45.32	1404.92	28.38
H5_3	3.769	0.151	0.275	0.010	0.099	0.002	1586.10	31.72	1567.33	50.61	1611.50	28.61
H5_4	4.330	0.173	0.298	0.011	0.105	0.002	1699.17	32.52	1683.18	53.85	1719.29	27.66
H5_5	15.698	0.658	0.557	0.021	0.204	0.003	2858.58	39.26	2856.16	87.74	2860.59	26.11
H5_6	1.025	0.042	0.111	0.004	0.067	0.001	716.30	21.04	676.50	24.12	843.47	33.49
H5_7	3.724	0.159	0.266	0.010	0.101	0.002	1576.61	33.56	1522.88	52.71	1649.62	30.03
H5_10	4.311	0.172	0.299	0.011	0.105	0.002	1695.55	32.44	1687.36	53.90	1706.04	27.53
H5_11	4.326	0.177	0.296	0.011	0.106	0.002	1698.24	33.27	1672.09	55.28	1731.00	26.79
H5_12	4.173	0.167	0.294	0.011	0.103	0.002	1668.71	32.17	1662.61	53.20	1676.74	27.13
H5_13	10.946	0.444	0.426	0.016	0.186	0.003	2518.58	37.06	2287.93	71.29	2710.40	24.05
H5_14	2.720	0.115	0.225	0.009	0.088	0.002	1333.98	31.02	1310.85	44.84	1371.66	35.88
H5_15	4.556	0.213	0.307	0.013	0.108	0.002	1741.20	38.20	1726.76	65.54	1758.92	30.26
H5_16	4.275	0.200	0.297	0.013	0.104	0.002	1688.55	37.71	1675.73	63.47	1704.85	31.63
>10% Discordant Samples												
H_15	0.087	0.007	0.012	0.001	0.053	0.003	84.67	6.62	75.75	3.75	343.33	113.95
H2_7	0.110	0.006	0.015	0.001	0.054	0.002	105.80	5.76	93.98	4.43	380.65	64.40
H4_15	0.112	0.005	0.015	0.000	0.056	0.002	107.85	5.00	93.28	2.42	443.49	79.36
H2_4	2.986	0.085	0.205	0.003	0.105	0.003	1404.03	21.42	1204.13	17.37	1722.27	44.96
H2_28	0.221	0.008	0.027	0.000	0.059	0.002	202.84	6.30	171.59	2.30	583.89	82.39
H3_8	0.082	0.006	0.010	0.001	0.058	0.004	79.66	5.84	65.82	3.19	517.34	141.56
H5_8	2.386	0.096	0.168	0.006	0.103	0.002	1238.29	28.46	1002.77	34.23	1675.63	27.01
H2_1	1.369	0.047	0.114	0.002	0.087	0.003	875.67	19.78	696.37	14.30	1361.36	57.07
H1_7	9.762	0.439	0.347	0.013	0.204	0.006	2412.57	40.61	1918.57	59.73	2859.15	45.05
H4_12	0.104	0.007	0.012	0.001	0.062	0.003	100.23	6.02	77.71	3.38	676.37	88.83
H2_12	0.108	0.005	0.013	0.000	0.062	0.003	103.81	4.69	80.17	2.53	687.79	96.45
H3_13	2.690	0.091	0.171	0.004	0.114	0.003	1325.75	24.70	1020.19	21.85	1860.66	40.96
H5_9	1.252	0.075	0.103	0.006	0.088	0.001	824.24	33.27	631.28	34.68	1388.28	30.41
H2_9	0.127	0.009	0.014	0.001	0.067	0.003	121.72	8.42	88.61	4.99	829.37	98.03
H2_13	35.881	2.775	0.489	0.035	0.532	0.016	3663.19	73.66	2566.87	147.83	4332.38	43.40
H2_21	2.267	0.070	0.114	0.002	0.144	0.004	1201.99	21.64	696.62	13.54	2276.75	41.73
H2_15	0.680	0.030	0.048	0.001	0.103	0.005	526.57	17.71	301.18	6.22	1680.18	89.01
H1_20	0.782	0.037	0.049	0.002	0.115	0.003	586.39	20.66	311.09	11.70	1873.04	50.04
H_6	1.395	0.104	0.065	0.003	0.154	0.007	886.98	43.22	408.96	18.26	2395.80	72.48
H3_3	0.385	0.027	0.019	0.001	0.147	0.008	330.61	19.54	121.64	6.04	2305.80	91.60
H2_9	0.483	0.164	0.017	0.006	0.206	0.005	399.93	106.34	108.68	37.45	2873.81	39.99
H3_4	-0.663	-0.112	-0.023	-0.003	0.207	0.027	-1102.95	-409.19	-151.29	-19.81	2883.33	194.80

Table A-4. Detrital zircon data table for sample HP-DR. Sample analyzed by LA-ICP-MS on 12-12-2014. Age data are in Ma.

	Isotopic Ratios						Apparent Ages					
Sample Name	$^{207}Pb/^{235}U$	1σ abs. err.	$^{206}Pb/^{238}U$	1σ abs. err.	$^{207}Pb/^{206}Pb$	1σ abs. err.	$^{207}Pb/^{235}U$	1σ abs. err.	$^{206}Pb/^{238}U$	1σ abs. err.	$^{207}Pb/^{206}Pb$	1σ abs. err.
<10 % Discordant Samples												
D1_1	3.307	0.291	0.255	0.009	0.094	0.003	1482.78	66.43	1465.32	46.99	1507.53	60.04
D1_2	0.785	0.074	0.093	0.004	0.061	0.002	588.43	41.21	574.92	22.31	640.52	75.42
D1_3	1.944	0.203	0.182	0.012	0.077	0.002	1096.33	67.87	1078.75	66.41	1131.04	62.44
D1_4	4.040	0.371	0.291	0.013	0.101	0.003	1642.32	72.14	1645.62	64.10	1637.78	59.00
D1_5	0.241	0.022	0.034	0.001	0.052	0.002	219.63	17.52	214.62	7.83	273.27	74.39
D1_7	0.078	0.007	0.011	0.000	0.052	0.002	76.16	7.03	69.52	2.74	289.50	84.31
D1_8	3.383	0.298	0.262	0.010	0.094	0.003	1500.39	66.75	1500.42	48.74	1500.03	59.68
D1_9	0.089	0.010	0.012	0.001	0.052	0.002	86.57	8.94	78.94	4.31	302.26	92.71
D1_12	1.703	0.151	0.167	0.006	0.074	0.002	1009.77	55.22	995.93	33.83	1039.58	64.65
D1_14	6.057	0.527	0.358	0.013	0.123	0.004	1984.13	73.18	1974.67	59.66	1993.69	55.55
D2_2	3.597	0.246	0.259	0.010	0.101	0.002	1548.98	52.98	1486.54	53.38	1635.54	42.42
D2_4	3.988	0.267	0.287	0.011	0.101	0.002	1631.70	53.02	1628.17	56.83	1636.59	40.67
D2_7	2.796	0.223	0.222	0.012	0.091	0.002	1354.47	57.94	1291.79	62.71	1455.19	48.55
D2_8	5.607	0.498	0.366	0.025	0.111	0.003	1917.22	73.72	2009.50	117.49	1819.14	43.13
D2_11	2.868	0.256	0.232	0.009	0.090	0.003	1373.62	65.08	1342.61	45.08	1422.15	61.70
D2_13	0.066	0.007	0.010	0.000	0.050	0.002	64.77	6.47	61.48	2.59	188.36	96.31
D2_15	0.535	0.068	0.067	0.005	0.058	0.003	435.37	44.04	418.68	27.72	524.62	108.48
D2_16	3.847	0.333	0.272	0.009	0.103	0.003	1602.58	67.38	1549.71	46.44	1672.79	57.58
D3_2	0.215	0.016	0.031	0.001	0.050	0.001	198.04	13.00	197.29	8.36	207.36	58.61
D3_4	0.157	0.016	0.021	0.002	0.053	0.002	148.20	13.57	136.00	10.39	348.51	63.01
D3_14	0.166	0.012	0.024	0.001	0.050	0.001	155.96	10.10	152.25	6.25	213.01	55.12
D3_16	0.168	0.012	0.025	0.001	0.049	0.001	157.61	10.44	158.69	6.58	141.84	58.74
D4_3	4.581	0.194	0.289	0.009	0.115	0.001	1745.88	34.76	1635.97	47.25	1880.18	22.86
D4_5	12.485	0.468	0.470	0.013	0.193	0.002	2641.57	34.64	2484.88	57.55	2763.91	18.18
D4_11	0.099	0.008	0.015	0.001	0.048	0.002	95.50	7.36	95.21	3.87	102.83	91.99
D4_12	0.079	0.004	0.011	0.000	0.053	0.001	77.14	4.06	69.50	2.35	320.82	52.26
D4_13	3.096	0.125	0.224	0.007	0.100	0.001	1431.74	30.56	1302.52	37.61	1629.42	20.60
D4_16	5.241	0.199	0.336	0.009	0.113	0.001	1859.38	31.82	1866.51	44.63	1851.43	21.42
D5_1	1.673	0.100	0.163	0.007	0.075	0.002	998.40	37.45	972.69	37.44	1055.37	43.06
D5_2	4.117	0.227	0.298	0.013	0.100	0.001	1657.65	44.12	1683.41	64.29	1625.22	27.47
D5_7	4.651	0.223	0.303	0.010	0.111	0.002	1758.54	39.32	1706.61	50.88	1820.86	26.35
D5_10	4.340	0.227	0.302	0.012	0.104	0.002	1701.01	42.24	1700.92	57.24	1701.18	29.17
D5_11	4.585	0.233	0.308	0.012	0.108	0.002	1746.60	41.55	1729.29	57.11	1767.44	27.02
D6_2	4.419	0.214	0.300	0.012	0.107	0.001	1716.00	39.35	1691.04	59.28	1746.54	23.14
D6_3	4.023	0.197	0.281	0.012	0.104	0.001	1638.76	39.05	1598.56	58.00	1690.67	22.30
D6_4	3.617	0.151	0.257	0.008	0.102	0.001	1553.36	32.65	1474.64	42.65	1662.06	21.77
D6_5	1.893	0.085	0.180	0.006	0.076	0.001	1078.63	29.52	1065.18	34.97	1105.86	25.45
D6_6	4.092	0.226	0.283	0.013	0.105	0.001	1652.63	44.08	1608.13	67.40	1709.61	24.31
D6_7	0.916	0.051	0.102	0.005	0.065	0.001	659.99	26.75	627.94	26.49	771.05	36.09
D6_8	2.656	0.122	0.218	0.008	0.088	0.001	1316.18	33.36	1272.23	43.47	1388.45	22.70
D6_9	2.766	0.114	0.232	0.007	0.087	0.001	1346.38	30.18	1342.67	38.33	1352.23	22.53
D6_10	4.082	0.188	0.287	0.011	0.103	0.001	1650.69	36.86	1627.34	52.93	1680.48	23.46
D7_3	0.189	0.010	0.026	0.001	0.052	0.001	175.69	8.23	167.74	5.47	284.12	43.03

Table A-4 Continued

Sample Name	$^{207}Pb/^{235}U$	1σ abs. err.	$^{206}Pb/^{238}U$	1σ abs. err.	$^{207}Pb/^{206}Pb$	1σ abs. err.	$^{207}Pb/^{235}U$	1σ abs. err.	$^{206}Pb/^{238}U$	1σ abs. err.	$^{207}Pb/^{206}Pb$	1σ abs. err.
			Isotopic Ratios						Apparent Ages			
					<10 % Discordant Samples							
D7_7	0.069	0.005	0.010	0.001	0.049	0.002	67.85	5.02	65.94	3.25	135.89	72.52
D7_8	0.175	0.010	0.024	0.001	0.052	0.001	163.74	8.19	155.31	5.55	287.48	45.30
D7_9	2.740	0.165	0.218	0.011	0.091	0.001	1339.29	43.88	1272.83	57.54	1447.17	28.56
D7_10	3.860	0.179	0.271	0.009	0.103	0.001	1605.37	36.82	1547.63	46.78	1682.00	24.94
D7_12	0.182	0.010	0.025	0.001	0.053	0.001	169.59	8.71	158.67	5.81	324.77	46.99
D7_13	7.549	0.378	0.372	0.014	0.147	0.002	2178.85	43.88	2040.38	67.13	2311.93	23.51
D8_1	2.112	0.167	0.195	0.011	0.079	0.002	1152.77	53.18	1146.34	59.27	1165.04	46.35
D8_2	4.390	0.377	0.293	0.019	0.109	0.003	1710.40	68.62	1657.09	92.29	1776.48	46.05
D8_4	3.061	0.247	0.251	0.015	0.089	0.002	1423.11	59.88	1441.49	75.25	1395.87	44.91
D8_6	3.993	0.327	0.288	0.017	0.101	0.002	1632.87	64.36	1629.65	86.91	1637.18	42.82
D8_7	0.108	0.011	0.015	0.001	0.051	0.002	103.81	9.76	98.45	6.89	228.66	77.98
D8_10	0.584	0.048	0.073	0.004	0.058	0.001	467.31	30.11	455.91	25.39	523.89	54.98
D8_11	4.599	0.365	0.301	0.017	0.111	0.003	1749.17	64.06	1697.51	85.21	1811.64	41.55
D8_16	0.096	0.009	0.013	0.001	0.052	0.002	93.40	8.06	86.20	5.43	281.76	69.11
D9_1	8.323	0.835	0.391	0.023	0.154	0.005	2266.88	87.12	2128.24	106.40	2393.99	57.57
D9_4	4.461	0.429	0.317	0.017	0.102	0.003	1723.70	76.83	1772.74	81.99	1664.19	61.24
D9_5	6.292	0.629	0.353	0.020	0.129	0.005	2017.35	83.99	1947.67	96.78	2088.99	59.95
D9_6	4.395	0.425	0.319	0.017	0.100	0.003	1711.49	76.95	1784.40	82.33	1622.92	62.40
D9_8	4.299	0.419	0.300	0.016	0.104	0.004	1693.23	77.20	1693.53	80.37	1692.40	62.02
D9_10	1.807	0.176	0.160	0.008	0.082	0.003	1047.98	61.79	954.67	46.40	1247.48	67.80
D9_13	1.691	0.169	0.166	0.009	0.074	0.003	1005.01	61.80	991.20	50.77	1034.74	71.35
D9_15	4.066	0.383	0.287	0.014	0.103	0.003	1647.53	74.04	1625.62	71.41	1675.12	60.78
D9_16	1.618	0.153	0.161	0.008	0.073	0.002	977.34	57.70	964.94	44.69	1004.79	67.29
D10_3	1.794	0.137	0.174	0.007	0.075	0.002	1043.33	48.43	1035.87	39.16	1058.46	53.86
D10_4	1.962	0.148	0.190	0.008	0.075	0.002	1102.42	49.38	1123.34	41.89	1060.83	52.52
D10_6	1.986	0.152	0.187	0.008	0.077	0.002	1110.83	50.51	1102.46	42.45	1126.72	53.40
D10_7	0.081	0.008	0.011	0.001	0.052	0.002	79.04	7.10	71.76	3.77	304.27	82.64
D10_14	0.924	0.074	0.098	0.004	0.068	0.002	664.59	38.52	602.34	24.90	881.28	61.19
D10_15	3.378	0.278	0.243	0.013	0.101	0.003	1499.28	62.56	1404.52	64.84	1635.42	49.73
HDR1_1	4.962	0.224	0.326	0.010	0.110	0.004	1812.90	37.41	1817.32	47.78	1805.63	69.29
HDR1_4	3.975	0.193	0.296	0.011	0.097	0.004	1629.10	38.68	1670.62	52.19	1573.64	72.15
HDR1_5	0.197	0.010	0.027	0.001	0.052	0.002	182.29	8.08	174.25	5.61	285.10	99.33
HDR1_6	0.190	0.009	0.027	0.001	0.050	0.002	176.49	7.79	174.26	5.64	203.67	98.19
HDR1_8	0.105	0.005	0.015	0.000	0.051	0.003	101.49	4.99	95.86	3.09	233.03	118.59
HDR1_9	0.077	0.005	0.012	0.000	0.048	0.004	75.79	4.74	74.59	2.75	110.83	172.40
HDR1_11	0.313	0.016	0.043	0.002	0.053	0.002	276.22	12.37	271.27	9.50	315.62	104.21
HDR1_12	0.114	0.010	0.016	0.001	0.052	0.005	109.37	9.17	100.70	6.68	299.79	193.08
HDR1_17	13.779	0.637	0.529	0.017	0.189	0.007	2734.64	42.84	2736.19	71.07	2731.51	63.07
HDR1_18	4.277	0.193	0.296	0.009	0.105	0.004	1688.89	36.47	1671.60	44.74	1708.21	69.67
HDR1_19	4.157	0.192	0.272	0.009	0.111	0.004	1665.51	37.19	1550.84	43.92	1811.05	70.06
HDR1_21	0.081	0.006	0.012	0.000	0.047	0.004	78.62	5.37	78.79	2.85	70.60	201.43
HDR1_22	4.292	0.194	0.299	0.009	0.104	0.004	1691.73	36.53	1685.62	45.21	1697.09	69.70
HDR1_24	11.527	0.606	0.488	0.020	0.171	0.007	2566.78	48.00	2561.04	86.75	2569.30	65.04
HDR1_27	0.821	0.020	0.096	0.002	0.062	0.002	608.74	10.85	591.41	9.70	673.82	51.96
HDR1_29	3.122	0.064	0.235	0.004	0.097	0.001	1438.23	15.73	1358.15	20.83	1558.75	28.64
HDR1_30	4.814	0.113	0.319	0.006	0.109	0.002	1787.30	19.47	1786.93	30.54	1787.75	32.44

Sample Name	Isotopic Ratios						Apparent Ages					
	$^{207}Pb/^{235}U$	1σ abs. err.	$^{206}Pb/^{238}U$	1σ abs. err.	$^{207}Pb/^{206}Pb$	1σ abs. err.	$^{207}Pb/^{235}U$	1σ abs. err.	$^{206}Pb/^{238}U$	1σ abs. err.	$^{207}Pb/^{206}Pb$	1σ abs. err.
					<10 % Discordant Samples							
HDR1_31	0.086	0.003	0.012	0.000	0.052	0.002	83.45	2.49	76.24	1.46	295.09	85.95
HDR1_32	0.489	0.012	0.064	0.001	0.056	0.001	404.52	7.92	399.12	6.31	435.48	57.22
HDR1_33	7.030	0.141	0.389	0.006	0.131	0.002	2115.21	17.71	2116.93	29.42	2113.55	26.98
HDR1_34	5.650	0.158	0.346	0.009	0.119	0.002	1923.80	23.80	1914.55	40.94	1933.79	33.70
HDR1_35	5.378	0.111	0.345	0.006	0.113	0.002	1881.43	17.46	1911.58	28.08	1848.31	27.51
Teh_42	0.825	0.027	0.101	0.002	0.059	0.002	611.08	15.14	619.49	12.71	579.29	70.60
Teh_44	0.178	0.006	0.026	0.001	0.049	0.002	166.42	5.11	167.11	3.50	155.74	78.04
Teh_45	4.520	0.149	0.317	0.008	0.103	0.003	1734.73	27.01	1777.11	38.11	1683.40	48.32
					>10% Discordant Samples							
D1_10	3.188	0.288	0.197	0.008	0.118	0.004	1454.36	67.45	1157.62	44.30	1919.12	56.29
D1_11	0.542	0.059	0.019	0.001	0.204	0.009	439.85	38.18	123.19	6.19	2856.72	70.05
D1_13	0.130	0.015	0.012	0.001	0.077	0.004	124.28	13.04	78.08	4.09	1133.51	88.68
D1_15	2.767	0.261	0.200	0.010	0.100	0.003	1346.57	68.08	1174.69	51.03	1630.91	60.44
D1_16	1.217	0.149	0.071	0.006	0.125	0.004	808.41	66.18	439.66	38.96	2029.27	56.16
D1_6	0.220	0.023	0.013	0.001	0.127	0.005	201.81	19.09	80.73	4.36	2050.23	68.45
D10_1	2.622	0.251	0.195	0.014	0.097	0.003	1306.88	68.02	1149.33	74.88	1575.22	48.81
D10_11	0.216	0.018	0.025	0.001	0.063	0.002	198.76	15.13	158.89	8.02	702.31	61.95
D10_12	1.464	0.132	0.102	0.005	0.104	0.004	915.78	53.13	626.80	30.55	1696.20	63.39
D10_13	0.102	0.010	0.014	0.001	0.055	0.002	98.83	9.22	86.64	4.52	403.14	90.04
D10_16	0.232	0.024	0.014	0.001	0.119	0.005	211.72	19.66	90.19	4.99	1945.92	77.30
D10_2	0.104	0.011	0.011	0.001	0.067	0.003	100.19	10.14	71.51	5.18	850.31	76.16
D10_5	0.593	0.064	0.034	0.003	0.125	0.003	472.96	40.18	218.02	18.73	2029.57	46.36
D10_8	0.138	0.014	0.015	0.001	0.069	0.003	131.39	12.43	92.94	4.91	897.88	87.40
D2_1	0.104	0.011	0.013	0.001	0.060	0.003	100.85	10.14	80.80	5.19	605.66	90.52
D2_10	0.378	0.043	0.021	0.002	0.133	0.004	325.37	30.91	131.80	10.16	2133.08	56.91
D2_12	0.111	0.011	0.014	0.001	0.057	0.002	106.44	9.67	89.87	3.48	495.37	81.75
D2_14	1.306	0.219	0.020	0.003	0.481	0.018	848.28	92.16	125.67	17.84	4184.27	53.63
D2_3	0.180	0.014	0.018	0.001	0.074	0.002	168.41	11.76	113.33	5.23	1035.67	53.64
D2_5	0.135	0.014	0.012	0.001	0.082	0.004	128.46	12.76	76.34	4.78	1248.64	83.95
D2_6	0.177	0.018	0.017	0.001	0.074	0.003	165.39	15.78	111.03	7.37	1037.81	79.24
D2_9	0.862	0.070	0.090	0.004	0.069	0.002	631.36	37.22	558.36	25.54	902.66	61.15
D3_1	0.077	0.008	0.010	0.001	0.053	0.002	75.56	7.64	67.32	4.04	344.78	97.49
D3_10	0.257	0.021	0.011	0.001	0.166	0.004	232.39	16.78	71.86	3.92	2522.05	44.55
D3_11	3.383	0.234	0.206	0.009	0.119	0.003	1500.58	52.80	1204.96	47.75	1947.49	38.68
D3_12	0.139	0.012	0.017	0.001	0.059	0.002	132.04	10.70	109.34	6.21	563.03	65.24
D3_13	0.150	0.013	0.011	0.001	0.102	0.003	141.98	11.44	68.71	3.45	1653.56	62.12
D3_15	0.806	0.061	0.071	0.003	0.082	0.002	600.09	33.93	443.62	20.34	1246.68	50.86
D3_3	0.176	0.019	0.010	0.001	0.126	0.006	164.38	16.30	65.00	4.04	2039.99	78.71
D3_5	2.870	0.217	0.174	0.009	0.120	0.003	1373.96	55.52	1032.79	48.53	1953.17	41.95
D3_6	0.130	0.009	0.011	0.000	0.085	0.002	124.01	8.44	71.06	3.16	1315.89	47.06
D3_7	0.199	0.020	0.010	0.001	0.150	0.006	184.61	16.51	61.87	3.38	2345.64	69.43
D3_8	2.892	0.217	0.202	0.010	0.104	0.002	1379.91	55.19	1187.61	54.75	1691.65	42.60
D3_9	0.222	0.023	0.019	0.002	0.087	0.002	203.45	19.11	118.82	9.93	1349.53	53.93
D4_1	0.173	0.010	0.014	0.000	0.091	0.002	161.88	8.43	88.44	3.16	1441.23	44.90
D4_10	0.117	0.006	0.015	0.000	0.055	0.001	112.20	5.60	98.32	3.17	417.60	49.74
D4_14	0.048	0.120	0.002	0.004	0.230	0.015	47.45	110.42	9.73	24.89	3050.02	101.09
D4_15	1.546	0.092	0.124	0.007	0.091	0.001	948.83	36.17	751.72	38.57	1439.21	22.81
D4_2	0.091	0.007	0.012	0.001	0.055	0.002	88.67	6.61	77.29	3.56	407.04	78.35
D4_4	0.140	0.010	0.011	0.001	0.096	0.002	133.40	8.94	68.28	3.86	1540.58	45.58
D4_6	0.221	0.107	0.006	0.003	0.252	0.011	202.44	85.68	40.85	19.96	3195.86	66.64
D4_7	0.165	0.010	0.015	0.001	0.080	0.002	154.89	8.88	95.12	3.94	1207.04	49.45
D4_8	0.214	0.021	0.010	0.001	0.160	0.006	197.16	17.06	62.36	4.64	2454.63	57.79

Table A-4 Continued

Sample Name	Isotopic Ratios						Apparent Ages					
	^{207}Pb/^{235}U	1σ abs. err.	^{206}Pb/^{238}U	1σ abs. err.	^{207}Pb/^{206}Pb	1σ abs. err.	^{207}Pb/^{235}U	1σ abs. err.	^{206}Pb/^{238}U	1σ abs. err.	^{207}Pb/^{206}Pb	1σ abs. err.
>10% Discordant Samples												
D4_9	0.101	0.006	0.011	0.000	0.067	0.001	97.92	5.08	70.38	2.51	834.24	45.90
D5_12	0.774	0.046	0.067	0.003	0.083	0.002	582.18	25.93	419.95	18.29	1279.08	35.47
D5_13	1.651	0.105	0.118	0.006	0.101	0.002	990.07	39.32	721.30	36.16	1645.58	28.91
D5_14	0.288	0.021	0.018	0.001	0.114	0.004	257.28	16.75	117.59	5.53	1858.07	54.68
D5_15	0.739	0.041	0.071	0.003	0.075	0.002	561.68	23.86	444.11	15.59	1071.91	41.78
D5_16	0.198	0.017	0.023	0.001	0.063	0.002	183.28	14.19	144.38	9.26	719.99	62.20
D5_5	0.309	0.018	0.030	0.001	0.074	0.001	273.06	14.21	191.92	8.33	1043.04	39.23
D5_6	0.112	0.007	0.015	0.001	0.056	0.001	107.41	6.09	93.23	3.86	434.57	47.23
D5_8	0.114	0.014	0.014	0.001	0.061	0.003	109.59	12.39	86.98	7.32	633.96	100.89
D5_9	0.159	0.014	0.012	0.001	0.093	0.003	149.60	12.59	79.43	5.59	1485.24	58.00
D6_1	1.984	0.102	0.137	0.006	0.105	0.001	1109.93	34.00	827.92	34.05	1713.82	22.05
D6_11	0.112	0.009	0.013	0.001	0.063	0.002	107.38	7.95	82.61	5.10	698.95	54.89
D6_12	0.194	0.012	0.025	0.001	0.057	0.001	179.83	10.37	156.64	8.15	496.51	39.45
D6_13	0.153	0.016	0.013	0.001	0.087	0.004	144.19	14.40	81.85	6.31	1351.57	80.17
D6_14	0.102	0.008	0.011	0.001	0.068	0.002	98.19	7.61	69.27	3.54	873.54	72.23
D6_15	0.084	0.006	0.011	0.001	0.058	0.002	82.11	5.91	67.78	3.43	521.71	66.26
D6_16	0.140	0.011	0.010	0.001	0.101	0.002	133.22	10.03	64.29	4.39	1650.66	42.07
D7_1	0.312	0.030	0.022	0.001	0.103	0.004	275.71	22.90	139.86	9.41	1681.82	67.04
D7_11	0.090	0.008	0.012	0.001	0.056	0.002	87.83	7.32	75.37	4.02	441.27	82.15
D7_14	2.912	0.163	0.206	0.009	0.103	0.001	1385.07	41.40	1205.21	50.52	1674.22	24.93
D7_15	0.369	0.035	0.028	0.001	0.095	0.004	319.27	25.62	180.24	9.20	1518.31	81.21
D7_16	0.192	0.020	0.011	0.001	0.126	0.006	178.38	16.69	70.72	3.94	2046.69	83.12
D7_2	0.185	0.016	0.013	0.001	0.104	0.003	172.48	14.03	82.34	5.41	1704.77	58.30
D7_4	0.150	0.014	0.010	0.001	0.114	0.003	142.16	11.87	61.28	4.63	1865.99	44.49
D7_5	0.206	0.031	0.009	0.001	0.162	0.008	190.41	26.11	59.37	7.52	2473.37	76.75
D7_6	0.165	0.012	0.015	0.001	0.080	0.002	155.19	10.73	95.75	5.66	1197.81	45.31
D8_12	1.555	0.319	0.066	0.010	0.171	0.013	952.62	119.62	411.56	62.81	2568.67	118.36
D8_13	0.086	0.009	0.011	0.001	0.057	0.002	84.09	7.93	70.66	5.04	484.73	71.33
D8_14	0.115	0.012	0.012	0.001	0.071	0.003	110.80	11.25	75.64	5.57	953.23	79.97
D8_15	0.096	0.010	0.011	0.001	0.065	0.002	93.34	8.92	68.55	4.74	784.88	74.28
D8_3	0.138	0.014	0.012	0.001	0.083	0.003	131.66	12.00	77.64	4.71	1266.29	73.81
D8_5	0.535	0.115	0.017	0.004	0.222	0.009	434.94	73.43	111.65	22.27	2995.31	64.60
D8_8	2.997	0.247	0.200	0.012	0.108	0.003	1406.82	60.99	1177.19	65.86	1774.33	42.47
D8_9	0.211	0.018	0.027	0.002	0.056	0.001	194.19	14.71	173.44	10.39	454.67	56.01
D9_11	0.092	0.011	0.012	0.001	0.057	0.003	88.94	10.18	75.09	4.94	478.15	105.05
D9_12	0.515	0.067	0.055	0.005	0.068	0.003	422.07	43.88	344.00	33.11	873.99	74.68
D9_14	0.485	0.067	0.014	0.001	0.259	0.014	401.77	45.10	86.92	7.73	3242.34	81.64
D9_2	0.353	0.038	0.016	0.001	0.165	0.007	306.71	28.49	99.33	6.22	2504.12	67.17
D9_7	0.780	0.086	0.031	0.002	0.181	0.007	585.64	47.70	198.71	13.64	2659.56	60.83
D9_9	0.823	0.081	0.038	0.002	0.159	0.005	609.63	44.33	238.10	13.47	2440.42	56.30
HDR1_10	0.108	0.009	0.012	0.001	0.064	0.005	104.34	7.81	78.26	4.83	747.82	148.53
HDR1_13	0.274	0.014	0.012	0.000	0.165	0.008	245.80	11.42	76.87	2.74	2511.63	82.01
HDR1_14	0.268	0.014	0.012	0.000	0.159	0.008	241.10	11.18	78.14	2.71	2447.09	83.91
HDR1_15	0.066	0.005	0.011	0.000	0.042	0.004	64.49	4.90	73.08	2.70	0.00	0.00
HDR1_2	0.381	0.018	0.024	0.001	0.115	0.005	327.50	12.98	152.91	4.74	1877.78	73.15
HDR1_20	0.062	0.004	0.011	0.000	0.042	0.004	61.18	3.99	68.01	2.44	0.00	0.00
HDR1_23	2.594	0.135	0.139	0.006	0.135	0.005	1298.88	37.31	839.86	31.86	2164.35	66.73
HDR1_25	0.366	0.018	0.028	0.001	0.096	0.004	316.58	13.33	175.46	5.69	1548.78	84.65
HDR1_26	0.202	0.008	0.024	0.001	0.061	0.003	186.71	6.80	153.57	3.74	629.65	106.29
HDR1_28	0.150	0.006	0.011	0.000	0.096	0.003	141.51	5.06	72.12	2.37	1555.77	58.70
HDR1_3	0.238	0.014	0.015	0.001	0.117	0.007	216.87	11.47	94.21	3.92	1913.32	98.93
HDR1_7	0.229	0.012	0.017	0.001	0.097	0.005	209.64	9.58	109.22	3.75	1571.38	86.50

Table A-5. Detrital zircon data table for sample Si-B. Sample analyzed by LA-ICP-MS on 11-8-2014 and 11-9-2014. Age data are in Ma.

Sample Name	$^{207}Pb/^{235}U$	1σ abs. err.	$^{206}Pb/^{238}U$	1σ abs. err.	$^{207}Pb/^{206}Pb$	1σ abs. err.	$^{207}Pb/^{235}U$	1σ abs. err.	$^{206}Pb/^{238}U$	1σ abs. err.	$^{207}Pb/^{206}Pb$	1σ abs. err.
	Isotopic Ratios						Apparent Ages					
	<10 % Discordant Samples											
SK1_1	3.924	0.160	0.307	0.007	0.093	0.003	1618.55	32.42	1723.52	36.68	1485.29	54.39
SK1_2	4.264	0.177	0.309	0.008	0.100	0.003	1686.39	33.59	1734.01	39.33	1628.32	52.42
SK1_3	0.086	0.004	0.013	0.000	0.049	0.002	83.86	3.91	81.91	2.37	140.60	90.43
SK1_4	4.122	0.168	0.298	0.007	0.100	0.003	1658.72	32.77	1679.90	35.79	1632.66	53.68
SK1_5	0.057	0.003	0.009	0.000	0.044	0.002	55.95	2.81	59.98	1.64	0.00	5.77
SK1_6	1.856	0.075	0.171	0.004	0.079	0.002	1065.43	26.49	1020.14	22.36	1160.09	58.33
SK1_7	4.737	0.197	0.333	0.009	0.103	0.003	1773.89	34.28	1852.19	41.04	1683.61	53.30
SK1_9	0.371	0.016	0.052	0.001	0.052	0.002	320.60	11.94	323.81	8.53	298.15	71.30
SK1_10	0.070	0.004	0.010	0.000	0.052	0.003	68.88	3.73	62.69	1.84	290.61	115.83
SK1_11	4.116	0.184	0.296	0.008	0.101	0.003	1657.52	35.84	1671.42	40.08	1640.62	61.14
SK1_12	4.501	0.186	0.315	0.008	0.104	0.003	1731.08	33.77	1764.65	39.16	1691.41	52.56
SK1_13	3.554	0.147	0.269	0.007	0.096	0.003	1539.34	32.29	1534.74	34.53	1546.34	54.10
SK1_14	4.129	0.173	0.299	0.008	0.100	0.003	1660.08	33.62	1685.04	38.38	1629.31	53.61
SK1_15	0.065	0.003	0.009	0.000	0.050	0.002	64.12	2.72	60.35	1.50	207.96	79.62
SK1_16	4.371	0.184	0.291	0.008	0.109	0.003	1706.89	34.24	1647.31	38.09	1781.48	53.04
SK2_2	0.187	0.009	0.026	0.001	0.052	0.002	173.81	7.28	164.84	4.16	298.38	85.21
SK2_5	0.509	0.021	0.069	0.002	0.053	0.002	417.88	13.94	431.21	10.17	345.76	66.58
SK2_6	4.245	0.167	0.265	0.006	0.116	0.003	1682.84	31.80	1516.29	29.50	1897.84	52.61
SK2_7	4.400	0.174	0.317	0.007	0.101	0.003	1712.35	32.18	1773.65	35.25	1638.84	53.03
SK2_10	4.083	0.165	0.289	0.007	0.102	0.003	1650.93	32.50	1638.00	34.50	1668.08	53.91
SK2_11	0.184	0.008	0.026	0.001	0.052	0.002	171.91	7.01	165.26	4.00	265.33	82.89
SK2_13	13.227	0.523	0.516	0.012	0.186	0.005	2695.96	36.69	2680.56	50.13	2708.11	47.05
SK2_14	0.128	0.006	0.018	0.000	0.053	0.002	122.51	5.26	112.26	2.71	327.22	87.20
SK2_15	1.875	0.082	0.177	0.004	0.077	0.003	1072.15	28.66	1052.19	24.13	1113.68	69.30
SK3_1	10.786	0.439	0.420	0.013	0.186	0.005	2504.89	37.15	2258.94	58.74	2710.84	39.84
SK3_2	4.164	0.158	0.296	0.008	0.102	0.003	1666.93	30.64	1672.24	39.73	1660.35	45.32
SK3_3	3.085	0.112	0.248	0.006	0.090	0.002	1429.03	27.50	1427.49	32.13	1431.44	45.26
SK3_4	4.455	0.166	0.316	0.008	0.102	0.002	1722.63	30.44	1767.86	40.85	1668.21	43.77
SK3_6	13.917	0.575	0.525	0.017	0.192	0.005	2744.10	38.43	2718.97	69.89	2762.73	40.03
SK3_7	0.091	0.004	0.014	0.000	0.048	0.002	88.69	3.88	87.89	2.59	110.17	86.63
SK3_8	0.177	0.008	0.025	0.001	0.052	0.002	165.90	7.17	158.50	4.94	273.04	84.43
SK3_9	2.900	0.109	0.241	0.006	0.087	0.002	1381.95	28.09	1393.09	31.69	1364.90	51.04
SK3_10	3.073	0.114	0.247	0.006	0.090	0.002	1425.98	27.96	1425.01	32.44	1427.53	47.31
SK3_11	3.998	0.152	0.300	0.008	0.097	0.002	1633.74	30.39	1688.98	40.82	1563.45	44.18
SK3_12	0.069	0.003	0.010	0.000	0.052	0.001	67.85	2.52	61.47	1.61	299.33	60.45
SK3_13	2.590	0.093	0.227	0.006	0.083	0.002	1297.92	25.99	1319.34	29.35	1262.80	46.02
SK3_14	0.079	0.004	0.012	0.000	0.048	0.002	76.90	3.59	76.91	2.21	76.26	101.32
SK3_14	0.079	0.004	0.012	0.000	0.048	0.002	76.90	3.59	76.91	2.21	76.26	101.32
SK3_15	1.961	0.073	0.186	0.005	0.076	0.002	1102.32	24.81	1102.14	26.26	1102.77	49.40
SK3_16	0.070	0.004	0.010	0.000	0.052	0.002	68.63	3.44	62.57	2.14	285.44	97.02
SK4_1	1.512	0.052	0.149	0.004	0.074	0.002	935.17	20.86	893.66	22.02	1034.71	46.69
SK4_3	4.830	0.141	0.329	0.007	0.106	0.002	1790.15	24.27	1835.47	35.76	1738.09	31.93
SK4_4	0.075	0.003	0.011	0.000	0.049	0.001	73.82	2.46	70.99	1.76	166.99	60.46
SK4_5	12.068	0.388	0.496	0.013	0.177	0.003	2609.71	29.70	2595.17	55.06	2621.34	30.39
SK4_7	1.999	0.084	0.191	0.007	0.076	0.002	1115.09	28.11	1125.14	36.51	1095.94	48.95
SK4_8	1.801	0.053	0.176	0.004	0.074	0.001	1045.72	19.20	1044.66	21.71	1048.33	37.28
SK4_9	4.411	0.128	0.304	0.007	0.105	0.002	1714.34	23.76	1712.42	33.13	1717.06	32.56
SK4_10	1.652	0.059	0.165	0.004	0.072	0.002	990.17	22.26	985.93	22.66	999.97	56.65
SK4_11	13.881	0.405	0.537	0.012	0.187	0.003	2741.63	27.26	2772.96	50.09	2718.97	29.06
SK4_12	4.172	0.121	0.300	0.007	0.101	0.002	1668.57	23.44	1690.67	32.81	1641.23	32.31

Table A-5 Continued

Sample Name	Isotopic Ratios						Apparent Ages					
	$^{207}Pb/^{235}U$	1σ abs. err.	$^{206}Pb/^{238}U$	1σ abs. err.	$^{207}Pb/^{206}Pb$	1σ abs. err.	$^{207}Pb/^{235}U$	1σ abs. err.	$^{206}Pb/^{238}U$	1σ abs. err.	$^{207}Pb/^{206}Pb$	1σ abs. err.
					<10 % Discordant Samples							
SK4_15	3.005	0.101	0.247	0.006	0.088	0.002	1408.94	25.35	1424.08	32.92	1386.49	42.85
SK4_16	0.087	0.003	0.013	0.000	0.048	0.001	84.70	2.96	84.08	2.23	102.40	63.91
SK5_1	0.070	0.003	0.010	0.000	0.050	0.002	68.80	2.84	65.71	1.60	177.39	97.46
SK5_2	2.809	0.078	0.233	0.005	0.088	0.002	1358.07	20.56	1348.30	26.04	1373.31	35.29
SK5_3	0.196	0.007	0.027	0.001	0.052	0.001	181.65	5.60	174.32	4.65	277.81	51.29
SK5_5	5.233	0.141	0.328	0.007	0.116	0.002	1857.95	22.71	1827.01	34.30	1892.60	28.75
SK5_6	0.085	0.004	0.012	0.000	0.052	0.003	82.64	3.90	75.24	2.16	301.92	109.44
SK5_7	3.740	0.102	0.271	0.006	0.100	0.002	1579.89	21.70	1544.21	30.46	1627.68	29.47
SK5_9	1.905	0.050	0.180	0.004	0.077	0.001	1082.78	17.47	1069.24	20.01	1109.94	34.49
SK5_10	4.253	0.123	0.299	0.007	0.103	0.002	1684.40	23.58	1685.10	35.91	1683.36	29.28
SK5_11	4.012	0.116	0.279	0.007	0.104	0.002	1636.66	23.24	1585.82	34.00	1702.45	28.88
SK5_12	4.472	0.141	0.306	0.008	0.106	0.002	1725.81	25.76	1721.38	41.13	1731.03	28.64
SK5_14	0.106	0.004	0.015	0.000	0.052	0.002	101.97	3.55	94.64	2.12	276.68	77.42
SK5_15	3.381	0.098	0.261	0.006	0.094	0.001	1499.90	22.52	1493.44	32.85	1508.86	28.30
SK5_16	0.060	0.002	0.009	0.000	0.048	0.001	59.01	1.70	58.24	1.27	88.77	52.96
SK6_1	25.891	0.842	0.736	0.016	0.255	0.006	3342.44	31.31	3554.91	60.59	3216.99	34.14
SK6_3	0.110	0.006	0.016	0.001	0.052	0.002	106.34	5.32	99.34	3.56	265.42	98.41
SK6_6	3.995	0.125	0.296	0.006	0.098	0.002	1633.19	25.10	1672.88	29.78	1581.95	40.80
SK6_7	15.245	0.475	0.565	0.012	0.196	0.004	2830.69	29.25	2886.81	47.63	2790.54	34.54
SK6_9	5.453	0.173	0.327	0.007	0.121	0.003	1893.21	26.79	1823.25	33.09	1970.36	38.64
SK6_10	3.957	0.120	0.284	0.005	0.101	0.002	1625.39	24.32	1613.33	26.58	1640.55	40.81
SK6_11	0.097	0.005	0.014	0.000	0.050	0.002	93.87	4.26	90.81	2.73	171.89	94.72
SK6_13	0.102	0.004	0.015	0.000	0.051	0.002	98.22	3.73	93.01	2.00	226.03	83.89
SK6_14	3.923	0.117	0.285	0.005	0.100	0.002	1618.40	23.89	1615.93	26.19	1621.13	39.69
SK6_16	4.733	0.144	0.312	0.006	0.110	0.002	1773.07	25.13	1750.60	28.66	1799.15	39.79
SK7_1	4.014	0.147	0.262	0.006	0.111	0.003	1636.96	29.42	1498.78	28.63	1818.80	49.71
SK7_2	4.211	0.152	0.289	0.006	0.106	0.003	1676.08	29.10	1635.69	29.25	1726.49	49.96
SK7_3	0.650	0.025	0.081	0.002	0.058	0.002	508.55	15.04	504.03	10.03	528.32	66.75
SK7_5	3.956	0.140	0.291	0.006	0.098	0.003	1625.19	28.28	1647.52	28.84	1595.87	49.33
SK7_6	0.096	0.004	0.014	0.000	0.051	0.002	93.20	3.70	87.42	1.92	243.16	82.69
SK7_10	0.190	0.008	0.026	0.001	0.054	0.002	176.42	7.00	162.50	3.87	366.67	83.65
SK7_11	2.817	0.100	0.234	0.005	0.087	0.002	1360.07	26.30	1357.09	23.73	1364.22	52.55
SK7_13	1.763	0.100	0.173	0.007	0.074	0.003	1032.07	35.96	1027.89	39.82	1040.37	80.60
SK7_14	0.074	0.003	0.011	0.000	0.048	0.002	72.03	3.09	71.90	1.71	75.97	93.23
SK7_15	2.879	0.106	0.244	0.005	0.086	0.002	1376.45	27.36	1405.83	26.52	1330.61	54.17
SK7_16	2.764	0.099	0.227	0.005	0.088	0.002	1345.80	26.45	1319.34	24.04	1387.57	52.25
SK8_1	1.962	0.078	0.184	0.006	0.077	0.002	1102.67	26.48	1086.84	30.51	1133.87	49.71
SK8_2	0.064	0.003	0.009	0.000	0.049	0.002	62.65	3.02	60.37	2.06	150.22	96.60
SK8_3	0.239	0.010	0.034	0.001	0.051	0.002	217.23	8.16	214.40	6.46	247.82	68.56
SK8_4	2.915	0.113	0.246	0.007	0.086	0.002	1385.72	28.96	1418.93	37.80	1334.78	46.09
SK8_6	2.819	0.113	0.235	0.007	0.087	0.002	1360.59	29.71	1358.90	37.05	1363.08	50.74
SK8_7	0.151	0.009	0.020	0.001	0.054	0.002	142.52	7.97	129.90	6.09	357.95	97.46
SK8_8	3.761	0.151	0.270	0.008	0.101	0.002	1584.49	31.81	1539.23	42.90	1645.11	45.15
SK8_10	0.075	0.005	0.011	0.000	0.049	0.003	73.72	4.59	70.81	3.05	168.89	134.19
SK8_11	11.231	0.532	0.460	0.019	0.177	0.004	2542.45	43.26	2439.20	81.28	2625.76	41.28
SK8_12	4.465	0.178	0.301	0.009	0.107	0.003	1724.55	32.58	1698.12	45.77	1756.63	45.19
SK8_14	0.080	0.008	0.012	0.001	0.050	0.006	77.92	7.73	74.87	3.43	172.21	259.46
SK8_15	0.070	0.004	0.010	0.000	0.050	0.002	68.72	3.49	65.41	2.21	185.10	108.77
SK8_16	1.820	0.075	0.176	0.006	0.075	0.002	1052.56	26.51	1046.02	30.78	1065.98	50.65
SK9_1	0.262	0.009	0.037	0.001	0.051	0.001	236.37	7.25	234.70	5.77	253.09	56.06
SK9_2	17.058	0.632	0.567	0.017	0.218	0.005	2938.12	34.92	2896.15	69.60	2967.02	34.35
SK9_3	4.210	0.138	0.301	0.007	0.101	0.002	1675.88	26.46	1697.61	35.85	1648.82	39.86
SK9_4	4.165	0.156	0.293	0.009	0.103	0.002	1667.10	30.15	1655.54	43.67	1681.72	41.04
SK9_5	4.519	0.150	0.309	0.008	0.106	0.002	1734.41	27.26	1735.27	37.52	1733.41	39.87

Table A-5 Continued

Sample Name	$^{207}Pb/^{235}U$	1σ abs. err.	$^{206}Pb/^{238}U$	1σ abs. err.	$^{207}Pb/^{206}Pb$	1σ abs. err.	$^{207}Pb/^{235}U$	1σ abs. err.	$^{206}Pb/^{238}U$	1σ abs. err.	$^{207}Pb/^{206}Pb$	1σ abs. err.
	Isotopic Ratios						Apparent Ages					
<10 % Discordant Samples												
SK9_7	4.790	0.211	0.310	0.012	0.112	0.003	1783.13	36.38	1740.82	57.87	1833.05	41.23
SK9_8	3.232	0.133	0.259	0.009	0.090	0.002	1464.80	31.53	1485.36	44.73	1435.16	47.42
SK9_9	3.973	0.137	0.281	0.007	0.103	0.002	1628.76	27.58	1596.39	37.52	1670.86	39.45
SK9_11	2.876	0.097	0.238	0.006	0.088	0.002	1375.58	25.17	1376.88	31.00	1373.59	43.56
SK9_12	0.111	0.004	0.015	0.000	0.052	0.002	106.59	4.06	98.65	2.89	287.81	68.88
SK9_13	3.611	0.141	0.251	0.008	0.104	0.002	1551.91	30.62	1444.65	40.89	1701.19	43.13
SK9_14	0.262	0.011	0.036	0.001	0.052	0.002	236.38	8.53	229.71	6.17	303.33	77.95
SK9_15	4.244	0.144	0.300	0.008	0.103	0.002	1682.50	27.45	1689.04	37.85	1674.39	40.36
SK10_1	0.242	0.009	0.033	0.001	0.053	0.001	220.45	7.49	211.66	6.49	315.27	55.62
SK10_2	0.080	0.004	0.012	0.000	0.051	0.002	78.35	3.41	73.76	2.41	220.54	88.39
SK10_3	4.183	0.176	0.289	0.011	0.105	0.002	1670.77	33.95	1638.97	52.85	1710.89	43.22
SK10_4	0.262	0.010	0.037	0.001	0.051	0.001	236.65	7.78	236.38	7.09	239.25	53.73
SK10_5	4.000	0.144	0.287	0.009	0.101	0.002	1634.18	28.93	1628.37	44.66	1641.60	35.69
SK10_6	0.184	0.007	0.027	0.001	0.050	0.001	171.69	5.92	170.99	5.22	181.22	56.19
SK10_7	4.158	0.005	0.329	0.009	0.092	0.002	1665.88	6.79	1833.07	45.59	1461.09	41.29
SK10_8	0.071	0.003	0.011	0.000	0.049	0.001	69.56	2.73	67.69	2.20	134.12	67.31
SK10_9	0.219	0.008	0.031	0.001	0.051	0.001	200.83	6.73	199.35	6.11	218.16	51.08
SK10_10	0.067	0.004	0.011	0.000	0.045	0.003	65.42	4.04	68.41	2.66	0.00	112.46
SK10_11	0.179	0.007	0.026	0.001	0.050	0.001	167.34	5.89	166.53	5.16	178.71	58.08
SK10_13	0.206	0.008	0.030	0.001	0.051	0.001	190.40	6.96	187.69	5.94	224.03	65.59
SK10_14	1.648	0.058	0.169	0.005	0.071	0.001	988.80	21.88	1005.90	28.10	950.96	36.89
SK10_16	0.064	0.002	0.009	0.000	0.050	0.001	62.71	2.34	59.07	1.85	203.96	58.57
>10% Discordant Samples												
SK5_8	2.853	0.084	0.210	0.005	0.099	0.002	1369.59	21.86	1226.28	27.67	1600.56	29.16
SK2_4	10.021	0.394	0.519	0.012	0.140	0.004	2436.68	35.70	2694.11	49.08	2228.86	49.81
SK6_4	3.932	0.182	0.252	0.010	0.113	0.003	1620.31	36.84	1446.63	51.41	1853.41	39.48
SK6_2	3.890	0.128	0.250	0.006	0.113	0.002	1611.54	26.23	1437.16	29.27	1847.05	39.18
SK7_8	0.086	0.004	0.012	0.000	0.054	0.002	83.54	3.52	74.07	1.81	363.01	84.86
SK5_13	4.202	0.114	0.258	0.006	0.118	0.002	1674.40	21.99	1480.15	29.29	1927.09	27.22
SK2_3	0.200	0.010	0.025	0.001	0.057	0.003	185.52	8.84	161.88	4.32	499.01	103.95
SK3_5	2.704	0.101	0.196	0.005	0.100	0.002	1329.43	27.22	1154.05	28.06	1624.48	43.49
SK6_5	6.833	0.207	0.316	0.006	0.157	0.003	2090.07	26.47	1767.84	29.29	2423.96	36.27
SK4_14	0.796	0.026	0.081	0.002	0.071	0.002	594.78	14.43	501.09	11.88	970.82	42.88
SK6_12	4.423	0.139	0.248	0.005	0.129	0.003	1716.75	25.75	1430.37	25.71	2085.84	39.61
SK7_12	0.080	0.004	0.010	0.000	0.057	0.003	77.68	4.20	64.41	2.05	507.19	113.30
SK4_6	0.101	0.005	0.013	0.000	0.059	0.003	98.08	4.98	80.44	2.48	551.85	112.56
SK7_9	0.229	0.009	0.027	0.001	0.062	0.002	209.11	7.81	169.65	4.40	680.36	66.49
SK4_14	0.807	0.025	0.078	0.002	0.075	0.002	601.04	13.85	482.00	10.74	1080.45	40.09
SK10_12	2.315	0.094	0.161	0.006	0.104	0.002	1216.81	28.41	960.76	32.77	1704.71	32.67
SK6_8	0.092	0.004	0.011	0.000	0.061	0.002	89.53	3.64	70.57	1.85	629.30	77.72
SK2_9	0.128	0.006	0.015	0.000	0.062	0.003	121.88	5.83	95.70	2.59	669.45	95.60
SK6_15	0.018	0.004	0.002	0.001	0.059	0.002	17.91	4.43	14.05	3.49	571.56	63.56
SK4_13	2.158	0.099	0.152	0.006	0.103	0.002	1167.49	31.32	913.33	35.68	1675.77	33.85
SK4_2	6.028	0.191	0.258	0.007	0.170	0.003	1979.84	27.18	1477.85	33.50	2554.71	29.83
SK2_12	0.091	0.006	0.010	0.000	0.065	0.004	88.13	5.40	64.94	1.94	773.40	132.13
SK10_15	0.152	0.009	0.016	0.001	0.067	0.004	143.54	7.90	104.50	4.06	849.59	117.00
SK8_9	2.177	0.095	0.141	0.005	0.112	0.003	1173.64	29.97	850.94	27.35	1830.03	50.02
SK5_4	0.269	0.015	0.027	0.001	0.071	0.004	242.29	11.99	174.56	5.98	963.21	108.60
SK7_7	0.405	0.020	0.039	0.001	0.075	0.003	345.17	14.01	248.59	8.03	1059.53	72.53
SK9_16	0.135	0.006	0.014	0.000	0.068	0.003	128.97	5.38	92.77	2.77	861.45	79.71
SK8_13	6.343	0.287	0.231	0.009	0.199	0.005	2024.37	38.96	1340.00	45.78	2818.68	39.28
SK2_1	5.808	0.247	0.204	0.005	0.207	0.006	1947.67	36.15	1196.18	28.62	2879.76	49.13
SK5_17	0.214	0.013	0.019	0.001	0.083	0.004	197.12	10.42	118.92	5.53	1279.75	83.13
SK7_4	5.734	0.304	0.170	0.008	0.245	0.007	1936.44	44.90	1011.69	41.28	3150.47	43.23
SK9_6	4.293	0.159	0.147	0.004	0.212	0.005	1692.00	29.99	882.70	24.00	2922.21	37.15
SK1_8	0.038	0.081	0.003	0.006	0.096	0.004	38.28	76.67	18.72	38.31	1544.58	67.77
SK9_10	0.199	0.007	0.013	0.000	0.111	0.003	184.28	6.19	83.11	2.12	1819.60	52.07
SK2_8	0.944	0.056	0.042	0.002	0.162	0.006	675.05	28.96	267.48	12.26	2473.41	57.41
SK3_17	0.048	0.015	0.013	0.001	0.027	0.010	47.96	13.96	84.18	4.01	0.00	0.00

Table A-6. Detrital zircon data table for sample Si-LP. Sample analyzed by LA-ICP-MS on 9-9-2014, 9-11-2014, 9-12-2014, and 1-28-2015. Age data are in Ma.

Sample Name	Isotopic Ratios						Apparent Ages					
	^{207}Pb/^{235}U	1σ abs. err.	^{206}Pb/^{238}U	1σ abs. err.	^{207}Pb/^{206}Pb	1σ abs. err.	^{207}Pb/^{235}U	1σ abs. err.	^{206}Pb/^{238}U	1σ abs. err.	^{207}Pb/^{206}Pb	1σ abs. err.
<10 % Discordant Samples												
SLP_2	1.825	0.068	0.175	0.006	0.075	0.001	1054.58	24.22	1042.06	32.75	1080.87	28.52
SLP_5	3.919	0.154	0.279	0.010	0.102	0.001	1617.67	31.22	1586.81	51.89	1658.34	21.63
SLP_7	4.164	0.156	0.286	0.010	0.106	0.001	1666.87	30.21	1621.90	49.02	1724.26	25.71
SLP_10	4.549	0.169	0.313	0.011	0.105	0.001	1739.91	30.55	1754.60	52.67	1722.56	24.09
SLP_13	4.018	0.160	0.276	0.010	0.105	0.001	1637.82	31.89	1573.19	51.45	1722.10	25.66
SLP1_3	0.134	0.008	0.019	0.001	0.052	0.004	127.95	6.88	118.81	3.34	301.30	157.94
SLP1_5	0.263	0.008	0.035	0.001	0.055	0.002	237.18	6.76	221.06	4.36	400.26	73.04
SLP1_7	11.812	0.276	0.493	0.008	0.174	0.003	2589.64	21.63	2585.33	34.53	2593.14	30.33
SLP1_9	5.226	0.161	0.332	0.008	0.114	0.003	1856.81	25.98	1848.54	38.82	1866.23	42.39
SLP1_10	4.052	0.110	0.293	0.006	0.100	0.002	1644.78	21.89	1657.81	27.68	1628.30	43.51
SLP1_11	2.537	0.098	0.218	0.008	0.084	0.002	1282.78	27.67	1270.75	39.68	1303.12	42.10
SLP1_12	4.480	0.105	0.306	0.005	0.106	0.002	1727.28	19.23	1719.31	23.43	1737.08	35.70
SLP1_15	4.445	0.116	0.310	0.006	0.104	0.002	1720.81	21.38	1742.85	29.60	1694.23	36.35
SLP1_16	0.074	0.004	0.012	0.000	0.046	0.003	72.09	3.99	74.78	2.32	0.00	145.45
SLP1_19	3.928	0.091	0.284	0.004	0.100	0.002	1619.41	18.59	1610.88	22.54	1630.65	34.30
SLP2_1	3.019	0.144	0.244	0.009	0.090	0.003	1412.33	35.76	1409.43	45.15	1416.19	54.59
SLP2_2	0.874	0.037	0.100	0.003	0.063	0.002	638.01	19.91	614.73	18.45	720.78	51.29
SLP2_3	2.041	0.082	0.182	0.005	0.081	0.002	1129.17	26.97	1077.32	29.27	1229.78	43.59
SLP2_6	2.165	0.084	0.193	0.005	0.081	0.002	1170.00	26.52	1137.55	28.81	1230.03	43.10
SLP2_7	4.392	0.171	0.286	0.008	0.111	0.002	1710.85	31.73	1620.34	40.67	1823.05	38.90
SLP2_8	4.268	0.170	0.282	0.008	0.110	0.002	1687.29	32.23	1601.49	41.47	1795.16	39.94
SLP2_9	2.782	0.109	0.226	0.007	0.089	0.002	1350.81	28.94	1314.66	34.45	1408.01	40.75
SLP2_10	5.079	0.199	0.322	0.009	0.114	0.003	1832.56	32.77	1801.63	45.09	1867.39	38.98
SLP2_11	0.192	0.009	0.029	0.001	0.048	0.002	178.47	7.94	184.66	5.84	96.66	81.54
SLP2_12	1.890	0.074	0.175	0.005	0.078	0.002	1077.48	25.74	1042.19	27.11	1149.05	44.47
SLP2_13	4.394	0.174	0.287	0.008	0.111	0.003	1711.19	32.31	1628.35	41.05	1813.67	41.27
SLP2_15	2.597	0.100	0.211	0.006	0.089	0.002	1299.91	27.92	1233.96	31.10	1410.01	41.59
SLP3_4	0.687	0.032	0.084	0.003	0.059	0.002	530.76	19.22	522.84	17.85	564.52	57.98
SLP3_6	6.497	0.296	0.363	0.013	0.130	0.003	2045.42	39.31	1995.77	59.04	2095.48	44.31
SLP3_7	4.024	0.182	0.276	0.009	0.106	0.003	1639.05	36.18	1573.42	47.63	1723.88	46.20
SLP3_8	2.921	0.136	0.218	0.008	0.097	0.002	1387.40	34.67	1271.02	41.40	1570.81	47.01
SLP3_9	5.147	0.239	0.333	0.012	0.112	0.003	1843.91	38.73	1854.50	57.25	1831.59	45.77
SLP3_10	4.503	0.208	0.285	0.010	0.115	0.003	1731.58	37.76	1616.80	49.80	1872.82	47.42
SLP3_13	2.545	0.121	0.198	0.007	0.093	0.003	1285.08	34.08	1164.05	37.40	1493.13	54.40
SLP3_14	3.399	0.153	0.246	0.008	0.100	0.003	1504.20	34.72	1420.22	43.30	1624.16	46.12
SLP3_15	2.981	0.137	0.241	0.008	0.090	0.002	1402.83	34.25	1394.40	43.08	1415.26	49.77
SLP3_16	0.115	0.005	0.018	0.001	0.048	0.001	110.85	4.92	112.14	3.92	82.68	64.84
SLP4_2	3.422	0.143	0.251	0.006	0.099	0.003	1509.38	32.43	1441.43	32.41	1605.49	53.78
SLP4_3	0.291	0.012	0.042	0.001	0.050	0.002	259.37	9.34	265.93	5.96	199.81	68.43
SLP4_4	4.201	0.182	0.298	0.008	0.102	0.003	1674.25	34.93	1683.27	40.59	1662.39	53.20
SLP4_6	4.686	0.205	0.300	0.008	0.113	0.003	1764.83	36.01	1691.38	41.23	1852.35	52.99
SLP4_7	4.146	0.187	0.290	0.009	0.104	0.003	1663.34	36.17	1640.24	42.83	1692.05	54.00
SLP4_8	12.524	0.587	0.481	0.015	0.189	0.006	2644.51	43.11	2529.49	67.11	2733.24	48.58
SLP4_9	4.616	0.222	0.305	0.010	0.110	0.004	1752.21	39.35	1714.41	48.58	1797.03	58.15
SLP4_12	2.281	0.099	0.204	0.005	0.081	0.003	1206.29	30.32	1199.19	28.62	1218.41	60.71
SLP4_13	4.762	0.226	0.324	0.010	0.107	0.003	1778.30	39.07	1809.11	49.34	1741.75	58.77
SLP4_14	2.163	0.130	0.193	0.009	0.081	0.003	1169.14	40.82	1137.29	50.34	1227.99	61.89
SLP5_1	1.973	0.081	0.185	0.006	0.077	0.002	1106.42	27.38	1095.23	35.03	1128.59	44.10

Sample Name	Isotopic Ratios						Apparent Ages					
	$^{207}Pb/^{235}U$	1σ abs. err.	$^{206}Pb/^{238}U$	1σ abs. err.	$^{207}Pb/^{206}Pb$	1σ abs. err.	$^{207}Pb/^{235}U$	1σ abs. err.	$^{206}Pb/^{238}U$	1σ abs. err.	$^{207}Pb/^{206}Pb$	1σ abs. err.
<10 % Discordant Samples												
SLP5_5	6.301	0.292	0.362	0.015	0.126	0.003	2018.62	39.84	1990.48	71.54	2047.62	35.25
SLP5_6	4.218	0.165	0.285	0.010	0.107	0.002	1677.49	31.62	1618.74	47.63	1751.88	35.95
SLP5_8	4.078	0.154	0.276	0.009	0.107	0.002	1649.90	30.32	1570.25	44.09	1752.99	35.55
SLP5_9	5.502	0.220	0.338	0.011	0.118	0.002	1900.88	33.73	1878.84	55.13	1925.12	36.95
SLP5_14	13.101	0.495	0.501	0.016	0.190	0.004	2686.93	35.01	2617.07	68.02	2740.01	31.87
SLP6_1	10.375	0.551	0.475	0.011	0.158	0.006	2468.84	48.01	2504.95	49.63	2439.00	66.36
SLP6_4	13.276	0.781	0.495	0.013	0.195	0.009	2699.46	54.09	2591.85	55.64	2780.80	77.61
SLP6_7	0.174	0.011	0.025	0.001	0.050	0.002	162.52	9.62	160.43	5.98	192.77	106.76
SLP6_8	4.645	0.245	0.340	0.008	0.099	0.004	1757.46	43.22	1884.65	37.23	1609.12	73.85
SLP6_9	5.004	0.264	0.350	0.008	0.104	0.004	1820.03	43.76	1934.57	38.22	1691.06	72.94
SLP6_10	4.310	0.229	0.305	0.007	0.103	0.004	1695.27	42.86	1714.40	34.90	1671.41	73.58
SLP6_11	11.053	0.600	0.434	0.011	0.185	0.007	2527.64	49.36	2323.23	51.23	2695.84	65.03
SLP6_13	4.932	0.261	0.298	0.007	0.120	0.005	1807.75	43.76	1683.32	33.43	1954.13	71.52
SLP6_14	0.068	0.005	0.011	0.000	0.044	0.003	66.58	4.63	71.51	2.67	0.01	38.75
SLP6_15	6.533	0.404	0.396	0.014	0.120	0.005	2050.34	53.07	2150.82	64.80	1950.50	78.49
SLP7_1	0.082	0.005	0.013	0.000	0.046	0.002	80.40	4.40	83.95	2.12	3.33	82.50
SLP7_2	5.202	0.279	0.344	0.008	0.110	0.005	1852.98	44.61	1905.45	37.03	1795.21	74.85
SLP7_3	0.109	0.006	0.016	0.000	0.049	0.002	104.89	5.51	102.32	2.34	164.47	102.74
SLP7_4	3.597	0.196	0.245	0.006	0.107	0.005	1548.87	42.49	1410.45	30.21	1743.83	76.83
SLP7_5	4.179	0.221	0.293	0.006	0.104	0.004	1669.95	42.38	1654.36	30.17	1690.24	75.94
SLP7_6	10.185	0.538	0.476	0.010	0.155	0.007	2451.74	47.71	2507.90	43.36	2406.06	69.79
SLP7_8	4.441	0.244	0.310	0.008	0.104	0.005	1720.01	44.50	1739.69	36.85	1696.77	77.68
SLP7_10	3.810	0.206	0.266	0.006	0.104	0.004	1594.86	42.67	1520.90	31.59	1694.66	76.65
SLP7_12	4.794	0.255	0.305	0.007	0.114	0.005	1783.90	43.79	1716.38	32.57	1864.45	74.50
SLP7_13	3.098	0.166	0.242	0.005	0.093	0.004	1432.08	40.27	1397.70	27.11	1484.19	79.08
SLP7_14	12.264	0.653	0.498	0.011	0.179	0.008	2624.85	48.78	2606.74	46.32	2639.41	68.51
SLP7_15	2.695	0.169	0.230	0.008	0.085	0.004	1327.12	45.40	1335.37	42.06	1314.49	89.52
SLP7_16	4.712	0.281	0.321	0.010	0.107	0.005	1769.45	48.70	1793.27	47.23	1742.08	82.89
SLP8_1	2.826	0.137	0.229	0.006	0.090	0.003	1362.48	35.82	1327.74	31.04	1428.61	65.91
SLP8_2	1.631	0.085	0.161	0.005	0.074	0.003	982.26	32.18	960.05	26.06	1044.10	75.22
SLP8_5	2.698	0.135	0.225	0.006	0.087	0.003	1327.86	36.41	1307.89	32.21	1371.53	68.98
SLP8_6	4.336	0.210	0.288	0.007	0.110	0.004	1700.25	39.17	1632.77	37.00	1795.16	62.55
SLP8_8	12.838	0.620	0.494	0.013	0.190	0.007	2667.86	44.49	2587.02	54.24	2739.38	56.49
SLP8_9	4.154	0.202	0.272	0.007	0.111	0.004	1665.04	38.98	1550.28	35.92	1823.60	62.08
SLP8_10	3.860	0.197	0.264	0.008	0.107	0.004	1605.40	40.38	1512.25	39.18	1740.64	65.62
SLP8_12	3.946	0.191	0.279	0.007	0.103	0.004	1623.19	38.39	1587.97	35.91	1679.99	63.38
SLP8_13	4.027	0.197	0.276	0.007	0.107	0.004	1639.67	38.99	1570.15	36.58	1740.76	63.48
SLP8_14	0.112	0.007	0.016	0.001	0.052	0.003	107.61	6.37	99.85	3.54	296.48	112.33
SLP8_15	4.257	0.206	0.295	0.008	0.105	0.004	1685.10	38.94	1667.42	37.48	1717.98	63.01
SLP9_3	3.020	0.143	0.226	0.006	0.097	0.003	1412.56	35.48	1312.67	31.39	1566.28	63.57
SLP9_4	4.028	0.187	0.275	0.007	0.106	0.004	1639.88	37.17	1565.80	35.48	1735.88	61.14
SLP9_5	0.123	0.008	0.017	0.001	0.054	0.003	117.40	6.78	105.99	3.60	354.81	114.75
SLP9_7	1.527	0.087	0.145	0.006	0.076	0.003	941.16	34.18	871.67	31.14	1107.16	75.74
SLP9_8	2.734	0.128	0.224	0.006	0.089	0.003	1337.65	34.11	1301.42	29.12	1395.76	66.02
SLP9_9	4.099	0.193	0.273	0.007	0.109	0.004	1654.18	37.80	1557.23	35.33	1779.28	63.04
SLP9_10	3.830	0.180	0.273	0.007	0.102	0.003	1599.06	37.24	1554.73	36.72	1657.66	61.65
SLP9_12	4.007	0.184	0.285	0.007	0.102	0.003	1635.60	36.61	1618.80	34.73	1656.95	61.80
SLP9_13	4.822	0.224	0.326	0.008	0.107	0.004	1788.71	38.33	1817.13	40.56	1755.41	60.45
SLP9_16	11.227	0.532	0.462	0.013	0.176	0.006	2542.20	43.26	2447.51	55.15	2618.36	55.41

Table A-6 Continued

Sample Name	Isotopic Ratios						Apparent Ages					
	$^{207}Pb/^{235}U$	1σ abs. err.	$^{206}Pb/^{238}U$	1σ abs. err.	$^{207}Pb/^{206}Pb$	1σ abs. err.	$^{207}Pb/^{235}U$	1σ abs. err.	$^{206}Pb/^{238}U$	1σ abs. err.	$^{207}Pb/^{206}Pb$	1σ abs. err.
						>10% Discordant Samples						
SLP_15	3.215	0.118	0.241	0.008	0.097	0.001	1460.88	27.95	1389.54	42.68	1566.47	21.33
SLP9_11	2.973	0.163	0.212	0.008	0.102	0.003	1400.76	40.83	1239.37	43.40	1655.42	61.95
SLP6_5	9.369	0.511	0.384	0.010	0.177	0.007	2374.80	48.88	2095.40	48.07	2623.86	65.32
SLP2_14	2.032	0.084	0.166	0.005	0.089	0.002	1126.19	27.86	992.08	28.52	1394.38	43.90
SLP9_6	2.649	0.133	0.196	0.006	0.098	0.003	1314.27	36.44	1156.09	33.34	1582.20	63.35
SLP9_15	1.771	0.084	0.151	0.004	0.085	0.003	1034.71	30.50	909.27	22.77	1309.92	66.36
SLP1_18	1.418	0.045	0.130	0.003	0.079	0.002	896.32	18.70	786.54	18.40	1177.88	48.25
SLP5_15	2.774	0.106	0.220	0.007	0.092	0.002	1348.68	28.03	1279.61	37.10	1460.10	37.41
SLP_3	3.806	0.146	0.262	0.009	0.105	0.001	1593.95	30.44	1501.95	48.13	1718.10	22.31
SLP1_1	2.178	0.072	0.172	0.004	0.092	0.003	1173.92	22.78	1025.75	20.73	1458.62	61.94
SLP_6	4.893	0.196	0.299	0.011	0.119	0.002	1801.08	33.17	1688.54	55.25	1934.23	24.08
SLP8_16	2.203	0.151	0.173	0.009	0.093	0.003	1182.06	46.80	1030.12	51.43	1483.03	66.40
SLP6_6	0.116	0.010	0.015	0.001	0.056	0.004	111.61	9.23	97.12	4.98	432.71	157.55
SLP6_12	3.638	0.197	0.233	0.006	0.113	0.005	1557.85	42.32	1351.77	31.63	1849.40	71.50
SLP6_16	1.805	0.102	0.151	0.005	0.087	0.004	1047.11	36.30	907.40	25.72	1351.08	76.13
SLP4_5	3.126	0.146	0.212	0.007	0.107	0.003	1439.03	35.31	1241.30	36.53	1744.23	52.93
SLP1_20	0.098	0.011	0.013	0.001	0.056	0.008	95.05	9.99	81.94	4.85	437.94	282.80
SLP3_5	0.714	0.034	0.076	0.003	0.069	0.002	547.29	20.11	469.25	16.20	886.55	59.40
SLP6_2	5.074	0.265	0.353	0.008	0.104	0.004	1831.83	43.37	1948.24	36.25	1701.70	72.74
SLP4_15	4.715	0.251	0.265	0.011	0.129	0.004	1769.87	43.64	1513.33	55.28	2087.01	51.15
SLP3_11	0.098	0.007	0.013	0.000	0.057	0.003	94.97	6.03	80.54	3.16	474.05	127.01
SLP7_7	0.142	0.011	0.018	0.001	0.058	0.004	134.68	9.89	113.18	4.03	533.51	155.81
SLP6_3	2.796	0.208	0.277	0.012	0.073	0.004	1354.54	54.08	1573.97	60.28	1022.89	116.18
SLP5_7	4.488	0.177	0.280	0.009	0.116	0.003	1728.68	32.23	1589.92	46.35	1901.11	38.45
SLP5_4	2.683	0.107	0.210	0.007	0.093	0.002	1323.90	29.20	1230.61	37.89	1478.35	39.98
SLP9_2	0.076	0.006	0.010	0.000	0.057	0.004	74.25	5.19	61.53	2.34	505.41	142.89
SLP1_2	2.333	0.102	0.168	0.007	0.101	0.002	1222.48	30.58	1002.83	37.93	1634.24	37.06
SLP3_3	2.950	0.147	0.192	0.008	0.112	0.003	1394.80	37.07	1129.57	41.41	1827.03	45.00
SLP1_8	6.712	0.176	0.297	0.006	0.164	0.003	2074.22	22.93	1674.89	29.46	2498.26	32.06
SLP_16	3.884	0.144	0.254	0.009	0.111	0.001	1610.43	29.42	1459.25	44.70	1814.44	22.51
SLP_4	2.643	0.093	0.205	0.007	0.094	0.001	1312.77	25.55	1201.32	35.94	1500.02	20.05
SLP4_16	0.115	0.006	0.014	0.000	0.061	0.002	110.90	5.43	87.93	3.10	636.65	76.14
SLP5_12	3.130	0.125	0.220	0.008	0.103	0.002	1440.15	30.30	1280.35	39.60	1684.86	37.27
SLP2_5	0.145	0.006	0.016	0.000	0.067	0.002	137.33	5.60	100.82	3.09	825.82	57.03
SLP2_4	0.127	0.007	0.014	0.001	0.066	0.003	121.00	6.33	88.63	3.38	815.24	81.72
SLP8_7	25.454	1.346	0.450	0.013	0.413	0.016	3325.79	50.38	2395.71	59.48	3955.51	57.75
SLP_9	3.480	0.158	0.225	0.010	0.112	0.001	1522.65	35.19	1309.01	51.36	1833.94	22.80
SLP3_1	4.892	0.308	0.219	0.011	0.162	0.006	1800.81	51.67	1278.32	59.78	2473.71	57.24
SLP5_16	0.640	0.026	0.075	0.002	0.062	0.002	502.20	15.99	466.78	14.61	667.14	54.64
SLP_11	2.327	0.093	0.177	0.007	0.095	0.001	1220.69	27.84	1051.38	35.91	1534.05	25.09
SLP9_1	0.122	0.010	0.011	0.001	0.080	0.006	116.97	8.86	71.33	3.30	1186.38	138.22
SLP5_10	0.547	0.032	0.064	0.003	0.062	0.002	443.20	20.54	400.94	19.44	669.16	71.39
SLP4_10	0.527	0.026	0.040	0.001	0.096	0.004	429.57	17.11	250.39	7.28	1555.75	70.63
SLP5_2	3.056	0.180	0.187	0.011	0.119	0.002	1421.75	44.15	1104.41	57.07	1935.47	34.96
SLP1_17	9.024	0.396	0.229	0.010	0.286	0.005	2340.41	39.36	1330.22	49.70	3393.72	29.14
SLP8_3	0.116	0.006	0.010	0.000	0.089	0.004	111.44	5.79	61.07	2.01	1402.18	74.57
SLP7_9	4.094	0.217	0.149	0.003	0.199	0.008	1653.14	42.44	895.77	17.96	2820.10	67.24
SLP1_6	1.355	0.051	0.075	0.003	0.132	0.003	869.62	21.95	464.07	15.43	2120.05	34.33
SLP4_1	-0.097	-0.083	-0.008	-0.007	0.092	0.003	-103.51	-98.43	-49.52	-42.82	1463.69	56.25
SLP1_4	0.208	0.013	0.014	0.001	0.107	0.008	191.61	11.21	89.85	3.60	1754.50	129.80
SLP8_11	1.727	0.100	0.070	0.003	0.181	0.006	1018.81	36.55	434.70	17.02	2658.93	57.21
SLP5_3	0.105	0.005	0.015	0.001	0.052	0.002	101.40	4.60	94.45	3.38	267.99	80.78
SLP1_13	-0.282	-0.064	-0.015	-0.003	0.141	0.003	-336.14	-95.13	-94.39	-22.29	2235.01	39.19
SLP3_2	0.480	0.030	0.017	0.001	0.205	0.010	398.25	20.38	108.55	4.62	2866.93	76.98
SLP8_4	0.470	0.024	0.015	0.000	0.228	0.009	391.14	16.70	96.28	2.72	3036.82	61.12

Table A-6 Continued

Sample Name	Isotopic Ratios						Apparent Ages					
	$^{207}Pb/^{235}U$	1σ abs. err.	$^{206}Pb/^{238}U$	1σ abs. err.	$^{207}Pb/^{206}Pb$	1σ abs. err.	$^{207}Pb/^{235}U$	1σ abs. err.	$^{206}Pb/^{238}U$	1σ abs. err.	$^{207}Pb/^{206}Pb$	1σ abs. err.
					>10% Discordant Samples							
SLP1_14	1.385	0.041	0.033	0.001	0.308	0.009	882.71	17.50	207.13	3.78	3509.57	46.73
SLP_8	0.109	0.007	0.013	0.001	0.059	0.003	104.88	6.11	85.42	3.42	573.40	102.91
SLP5_11	2.355	0.093	0.067	0.002	0.255	0.005	1228.94	27.84	417.70	13.56	3216.84	32.59
SLP_1	0.071	0.003	0.009	0.000	0.057	0.001	69.86	2.90	58.57	2.08	476.30	53.49
SLP9_14	0.465	0.022	0.006	0.000	0.549	0.019	387.99	15.14	39.49	1.07	4379.10	48.46
SLP7_11	-0.588	-0.171	-0.014	-0.003	0.315	0.049	-901.38	-546.48	-87.85	-22.62	3547.58	221.14
SLP5_13	0.318	0.016	0.023	0.001	0.102	0.005	280.42	12.52	143.84	4.96	1665.30	79.98
SLP_14	0.240	0.013	0.015	0.001	0.117	0.004	218.25	10.25	94.93	3.61	1914.71	65.54
SLP3_12	4.787	0.271	0.014	0.001	2.534	0.075	1782.60	46.54	87.72	4.06	6514.30	39.31
SLP_12	0.078	0.004	0.012	0.000	0.045	0.001	75.99	3.57	79.59	3.00	0.07	39.97

Table A-7. Detrital zircon data table for sample Si-TQ. Sample analyzed by LA-ICP-MS on 11-7-2014 and 11-8-2014. Age data are in Ma.

Sample Name	Isotopic Ratios						Apparent Ages					
	$^{207}Pb/^{235}U$	1σ abs. err.	$^{206}Pb/^{238}U$	1σ abs. err.	$^{207}Pb/^{206}Pb$	1σ abs. err.	$^{207}Pb/^{235}U$	1σ abs. err.	$^{206}Pb/^{238}U$	1σ abs. err.	$^{207}Pb/^{206}Pb$	1σ abs. err.
					<10 % Discordant Samples							
STQ1_1	0.153	0.010	0.023	0.001	0.049	0.003	144.83	8.42	144.81	3.22	144.41	118.42
STQ1_2	0.071	0.005	0.012	0.000	0.044	0.003	69.46	4.41	74.01	1.86	0.07	47.97
STQ1_3	4.267	0.262	0.295	0.007	0.105	0.005	1687.04	49.28	1666.53	32.28	1712.08	89.79
STQ1_4	12.891	0.800	0.494	0.011	0.189	0.010	2671.72	56.86	2587.85	48.50	2735.34	81.62
STQ1_5	1.767	0.110	0.173	0.004	0.074	0.004	1033.26	39.60	1028.98	21.51	1041.73	100.72
STQ1_6	14.264	0.880	0.551	0.013	0.188	0.009	2767.43	56.92	2828.62	52.12	2722.62	80.64
STQ1_7	4.485	0.275	0.318	0.007	0.102	0.005	1728.17	49.72	1778.48	33.80	1667.23	90.53
STQ1_9	4.313	0.273	0.292	0.007	0.107	0.006	1695.83	50.88	1651.04	37.08	1751.10	91.25
STQ1_10	0.182	0.012	0.028	0.001	0.047	0.003	169.74	9.95	177.50	4.00	62.44	124.71
STQ1_11	6.511	0.399	0.377	0.008	0.125	0.006	2047.38	52.53	2061.73	37.96	2032.43	86.54
STQ1_12	4.419	0.282	0.306	0.008	0.105	0.005	1715.91	51.42	1718.58	40.72	1712.10	90.94
STQ1_14	2.137	0.144	0.197	0.006	0.079	0.004	1160.86	45.57	1159.44	30.06	1162.91	108.62
STQ1_16	1.955	0.129	0.185	0.005	0.077	0.004	1100.02	43.31	1092.07	26.37	1115.18	107.11
STQ2_1	3.179	0.100	0.246	0.006	0.094	0.002	1452.11	24.00	1418.80	29.05	1501.05	37.89
STQ2_4	4.593	0.151	0.313	0.007	0.106	0.002	1748.05	27.07	1757.44	35.88	1736.67	41.28
STQ2_5	0.085	0.005	0.012	0.000	0.051	0.003	83.13	4.43	78.30	2.26	224.06	125.84
STQ2_6	4.907	0.153	0.318	0.007	0.112	0.002	1803.47	25.97	1780.80	35.08	1829.61	36.03
STQ2_7	22.299	0.754	0.646	0.016	0.250	0.006	3196.82	32.33	3211.23	62.83	3187.65	34.98
STQ2_10	0.074	0.007	0.012	0.000	0.045	0.005	72.27	6.23	76.05	2.49	0.79	180.25
STQ2_13	0.081	0.004	0.011	0.000	0.053	0.003	79.47	3.98	71.95	1.86	311.60	117.43
STQ3_14	0.192	0.007	0.027	0.001	0.052	0.002	178.13	5.89	170.52	3.14	280.41	70.78
STQ3_15	4.377	0.127	0.302	0.003	0.105	0.003	1708.00	23.78	1701.38	16.94	1716.22	44.37
STQ3_16	1.770	0.052	0.174	0.002	0.074	0.002	1034.62	18.83	1034.87	10.91	1034.20	49.27
STQ4_1	3.111	0.096	0.249	0.004	0.091	0.002	1435.34	23.41	1434.00	21.61	1437.75	45.03
STQ4_3	4.261	0.130	0.296	0.005	0.104	0.002	1685.82	24.73	1671.83	23.76	1703.68	43.35
STQ4_4	4.347	0.134	0.307	0.005	0.103	0.002	1702.35	25.09	1727.16	24.88	1672.35	44.20
STQ4_5	4.354	0.131	0.306	0.005	0.103	0.002	1703.73	24.58	1723.26	24.21	1680.20	42.59
STQ4_6	4.727	0.143	0.319	0.005	0.108	0.003	1772.12	25.11	1783.53	24.88	1759.11	42.97

99

Table A-7 Continued

Sample Name	Isotopic Ratios						Apparent Ages					
	$^{207}Pb/^{235}U$	1σ abs. err.	$^{206}Pb/^{238}U$	1σ abs. err.	$^{207}Pb/^{206}Pb$	1σ abs. err.	$^{207}Pb/^{235}U$	1σ abs. err.	$^{206}Pb/^{238}U$	1σ abs. err.	$^{207}Pb/^{206}Pb$	1σ abs. err.
						<10 % Discordant Samples						
STQ4_7	0.106	0.004	0.015	0.000	0.050	0.001	101.92	3.49	98.56	2.03	181.88	68.76
STQ4_9	4.666	0.142	0.314	0.005	0.108	0.003	1761.25	25.17	1758.29	24.93	1765.16	43.06
STQ4_10	0.460	0.018	0.059	0.001	0.056	0.002	384.12	12.52	372.15	7.81	457.37	76.69
STQ4_11	4.155	0.126	0.295	0.005	0.102	0.002	1665.22	24.49	1667.85	24.06	1662.32	42.57
STQ4_12	1.760	0.054	0.170	0.003	0.075	0.002	1030.84	19.68	1014.54	15.58	1066.04	47.35
STQ4_14	4.220	0.132	0.294	0.005	0.104	0.002	1677.85	25.33	1659.66	26.20	1701.09	42.87
STQ4_15	4.652	0.156	0.322	0.007	0.105	0.003	1758.71	27.56	1801.69	32.84	1708.43	44.55
STQ5_1	0.077	0.009	0.011	0.000	0.049	0.007	75.19	8.33	73.42	2.91	132.20	292.82
STQ5_2	4.230	0.115	0.298	0.007	0.103	0.001	1679.95	22.11	1681.65	36.50	1678.13	23.00
STQ5_3	1.953	0.053	0.183	0.004	0.078	0.001	1099.40	18.02	1081.32	23.13	1135.67	31.36
STQ5_4	2.806	0.076	0.234	0.005	0.087	0.002	1357.05	20.05	1353.46	27.36	1363.00	33.48
STQ5_6	4.256	0.131	0.280	0.007	0.110	0.002	1684.84	25.03	1592.76	35.53	1801.74	38.10
STQ5_7	4.343	0.100	0.303	0.006	0.104	0.001	1701.61	18.89	1706.76	30.49	1695.56	21.02
STQ5_8	1.939	0.060	0.186	0.005	0.076	0.002	1094.81	20.66	1097.09	25.78	1090.61	42.16
STQ5_9	4.395	0.130	0.319	0.009	0.100	0.001	1711.40	24.18	1782.41	42.19	1625.84	24.32
STQ5_10	12.159	0.311	0.492	0.011	0.179	0.002	2616.72	23.72	2578.93	47.44	2646.35	22.70
STQ5_11	1.791	0.044	0.179	0.004	0.072	0.001	1042.03	16.02	1064.17	21.41	996.21	25.76
STQ5_12	3.878	0.091	0.283	0.006	0.099	0.001	1609.01	18.81	1607.10	29.48	1611.80	21.75
STQ5_14	0.097	0.005	0.014	0.000	0.049	0.002	94.21	4.42	91.92	2.65	153.05	112.63
STQ5_15	19.263	0.692	0.548	0.019	0.255	0.003	3055.10	34.11	2816.51	78.00	3216.23	19.20
STQ5_16	4.388	0.105	0.303	0.006	0.105	0.001	1710.15	19.57	1706.49	31.59	1714.93	21.89
STQ6_1	4.298	0.127	0.306	0.008	0.102	0.001	1693.00	24.13	1719.46	38.84	1660.56	25.85
STQ6_4	3.754	0.113	0.282	0.007	0.097	0.001	1582.99	23.79	1599.50	36.35	1561.22	28.77
STQ6_5	3.073	0.097	0.246	0.007	0.091	0.001	1426.09	24.00	1418.98	35.27	1436.87	28.90
STQ6_6	4.646	0.139	0.319	0.008	0.106	0.002	1757.55	24.65	1785.99	40.32	1724.05	26.38
STQ6_7	2.066	0.062	0.186	0.005	0.081	0.001	1137.68	20.38	1099.68	25.74	1211.05	31.58
STQ6_8	4.467	0.136	0.316	0.008	0.102	0.001	1724.87	24.88	1771.92	41.00	1668.41	26.31
STQ6_10	8.013	0.250	0.387	0.011	0.150	0.002	2232.49	27.83	2108.15	49.69	2348.72	23.48
STQ6_11	4.502	0.135	0.309	0.008	0.106	0.002	1731.32	24.65	1737.90	39.29	1723.53	27.56
STQ6_13	0.079	0.004	0.011	0.000	0.051	0.002	76.82	3.67	71.44	2.23	247.72	104.60
STQ6_14	4.063	0.126	0.283	0.008	0.104	0.002	1646.81	24.92	1606.35	38.35	1699.00	27.20
STQ6_15	4.291	0.129	0.299	0.008	0.104	0.002	1691.67	24.41	1686.95	38.21	1697.69	27.72
STQ6_16	4.351	0.129	0.306	0.008	0.103	0.001	1703.01	24.28	1720.09	38.95	1682.23	26.14
STQ7_2	0.107	0.006	0.016	0.000	0.049	0.002	103.19	5.18	100.68	3.09	161.99	112.34
STQ7_3	0.151	0.007	0.022	0.001	0.049	0.002	142.50	6.07	142.08	3.99	149.90	90.78
STQ7_4	4.065	0.153	0.298	0.008	0.099	0.002	1647.25	30.27	1680.55	40.37	1605.36	44.63
STQ7_5	0.100	0.007	0.015	0.001	0.050	0.004	96.99	6.29	92.81	3.29	201.58	155.49
STQ7_7	4.389	0.170	0.300	0.009	0.106	0.003	1710.23	31.48	1692.01	42.96	1732.93	43.17
STQ7_8	10.078	0.387	0.460	0.013	0.159	0.004	2441.91	34.91	2438.62	57.90	2444.95	39.90
STQ7_11	4.589	0.175	0.310	0.008	0.107	0.003	1747.20	31.33	1741.89	41.51	1753.88	46.06
STQ7_12	0.159	0.006	0.023	0.001	0.049	0.001	149.83	5.60	149.53	4.19	155.03	66.14
STQ7_13	0.092	0.007	0.014	0.001	0.049	0.004	89.13	6.86	87.05	3.57	145.84	188.14
STQ7_14	2.379	0.124	0.189	0.008	0.091	0.003	1236.34	36.65	1117.41	43.66	1450.39	59.60
STQ7_15	0.530	0.021	0.068	0.002	0.056	0.002	432.10	13.62	425.37	11.25	468.51	59.40
STQ8_1	4.517	0.212	0.303	0.007	0.108	0.004	1734.13	38.25	1708.04	36.16	1765.10	67.51
STQ8_2	4.580	0.212	0.315	0.008	0.105	0.004	1745.65	37.95	1766.07	36.66	1720.64	66.70
STQ8_3	2.472	0.118	0.219	0.006	0.082	0.003	1263.74	33.81	1278.68	29.61	1237.71	72.15
STQ8_4	4.532	0.211	0.311	0.007	0.106	0.004	1736.91	38.01	1744.80	36.66	1726.77	66.79
STQ8_5	4.882	0.234	0.334	0.009	0.106	0.004	1799.21	39.64	1857.54	42.88	1731.62	67.04
STQ8_6	0.076	0.005	0.012	0.000	0.047	0.003	74.62	4.66	74.62	2.57	73.85	140.78
STQ8_7	4.364	0.202	0.303	0.007	0.104	0.004	1705.49	37.61	1706.90	35.21	1703.12	67.25
STQ8_10	1.396	0.077	0.137	0.005	0.074	0.003	887.33	32.02	829.57	29.14	1033.50	76.14
STQ8_11	5.190	0.243	0.360	0.009	0.105	0.004	1850.91	39.14	1981.84	41.34	1706.15	67.65
STQ8_12	0.084	0.004	0.012	0.000	0.051	0.002	81.62	4.19	76.68	2.26	227.96	102.03

Table A-7 Continued

Sample Name	Isotopic Ratios						Apparent Ages					
	$^{207}Pb/^{235}U$	1σ abs. err.	$^{206}Pb/^{238}U$	1σ abs. err.	$^{207}Pb/^{206}Pb$	1σ abs. err.	$^{207}Pb/^{235}U$	1σ abs. err.	$^{206}Pb/^{238}U$	1σ abs. err.	$^{207}Pb/^{206}Pb$	1σ abs. err.
<10 % Discordant Samples												
STQ8_13	2.092	0.105	0.193	0.005	0.079	0.003	1146.16	34.02	1135.28	29.12	1166.12	78.93
STQ8_14	4.508	0.218	0.304	0.008	0.107	0.004	1732.40	39.34	1712.73	40.39	1755.60	67.40
STQ9_1	5.059	0.206	0.331	0.006	0.111	0.004	1829.19	33.88	1841.57	28.80	1815.39	60.74
STQ9_2	4.281	0.172	0.302	0.005	0.103	0.004	1689.63	32.48	1698.76	25.14	1678.57	61.61
STQ9_3	4.350	0.255	0.300	0.014	0.105	0.004	1702.91	47.30	1691.02	67.75	1717.83	62.72
STQ9_4	20.229	0.812	0.619	0.011	0.237	0.008	3102.37	38.12	3106.63	42.04	3099.83	53.09
STQ9_5	1.979	0.092	0.192	0.005	0.075	0.003	1108.30	31.03	1132.08	27.48	1062.21	74.24
STQ9_6	24.074	1.011	0.724	0.015	0.241	0.008	3271.41	40.13	3510.82	54.50	3128.01	54.34
STQ9_7	4.339	0.175	0.303	0.005	0.104	0.004	1700.89	32.76	1704.92	26.15	1696.17	61.42
STQ9_8	4.381	0.184	0.306	0.007	0.104	0.004	1708.74	34.19	1722.55	32.29	1692.09	61.01
STQ9_9	4.679	0.189	0.314	0.005	0.108	0.004	1763.52	33.16	1759.85	26.45	1768.10	61.10
STQ9_10	3.395	0.150	0.262	0.006	0.094	0.003	1503.35	34.00	1499.51	31.88	1509.03	65.24
STQ9_11	3.751	0.161	0.271	0.006	0.101	0.003	1582.36	33.80	1543.40	31.22	1634.93	61.79
STQ9_12	0.257	0.017	0.035	0.001	0.053	0.003	232.35	13.76	221.77	8.42	341.04	136.35
STQ9_14	3.527	0.165	0.257	0.008	0.099	0.003	1533.38	36.28	1476.90	38.54	1612.44	62.24
STQ9_16	0.103	0.006	0.016	0.000	0.047	0.003	99.65	5.58	101.82	3.01	48.39	132.06
STQ10_1	0.206	0.009	0.028	0.000	0.054	0.002	190.51	7.71	176.53	2.84	367.70	91.61
STQ10_3	4.286	0.169	0.300	0.004	0.104	0.003	1690.66	32.03	1690.20	21.81	1691.45	60.91
STQ10_4	4.232	0.216	0.311	0.011	0.099	0.003	1680.20	41.00	1745.25	51.70	1600.13	64.29
STQ10_5	4.174	0.178	0.305	0.007	0.099	0.003	1668.87	34.40	1717.22	32.11	1608.78	62.14
STQ10_6	2.367	0.096	0.210	0.003	0.082	0.003	1232.55	28.41	1231.04	17.76	1235.42	66.10
STQ10_7	10.066	0.430	0.478	0.009	0.153	0.005	2440.84	38.73	2517.42	40.92	2377.81	59.71
STQ10_8	3.806	0.162	0.276	0.006	0.100	0.003	1593.91	33.63	1571.62	29.72	1623.73	61.31
STQ10_9	0.194	0.010	0.027	0.001	0.051	0.002	179.69	8.52	174.41	5.37	250.06	92.77
STQ10_10	2.997	0.118	0.255	0.004	0.085	0.003	1406.78	29.63	1466.61	19.75	1317.48	63.32
STQ10_11	5.327	0.224	0.322	0.006	0.120	0.004	1873.28	35.38	1798.13	30.46	1957.88	60.72
STQ10_13	3.547	0.145	0.267	0.004	0.096	0.003	1537.80	31.91	1526.75	21.86	1553.25	64.88
STQ10_15	5.845	0.243	0.354	0.007	0.120	0.004	1953.06	35.36	1953.30	31.85	1953.00	59.49
>10% Discordant Samples												
STQ4_13	0.198	0.010	0.026	0.001	0.055	0.003	183.40	8.42	164.73	3.95	431.65	110.52
STQ8_15	0.522	0.028	0.061	0.002	0.062	0.003	426.53	18.45	381.47	11.32	677.19	92.22
STQ6_2	0.215	0.007	0.028	0.001	0.056	0.001	197.60	5.66	176.38	4.54	459.39	41.60
STQ10_14	5.344	0.317	0.294	0.013	0.132	0.005	1875.86	49.47	1660.12	66.43	2124.19	58.56
STQ5_13	0.101	0.003	0.013	0.000	0.054	0.001	97.58	2.62	86.28	1.93	383.55	44.72
STQ10_12	0.199	0.012	0.026	0.001	0.056	0.003	184.55	9.91	163.11	4.45	468.93	123.56
STQ7_10	11.119	0.435	0.415	0.012	0.194	0.005	2533.18	35.82	2238.63	55.29	2778.64	39.34
STQ2_11	0.090	0.004	0.012	0.000	0.055	0.002	87.46	3.71	76.69	2.01	392.06	89.28
STQ7_9	0.088	0.006	0.012	0.000	0.055	0.004	85.75	5.41	74.98	2.84	397.58	138.78
STQ2_2	0.058	0.004	0.010	0.001	0.042	0.002	57.22	3.94	64.43	3.33	0.00	0.04
STQ8_9	0.117	0.006	0.015	0.000	0.055	0.002	112.72	5.52	98.27	3.04	429.08	87.56
STQ4_2	2.362	0.084	0.181	0.004	0.095	0.002	1231.20	24.94	1070.36	24.00	1525.45	44.78
STQ7_6	0.293	0.011	0.035	0.001	0.060	0.002	260.68	8.63	224.04	5.67	604.82	56.92
STQ2_9	3.115	0.127	0.208	0.007	0.108	0.002	1436.33	30.87	1219.53	38.74	1773.74	36.68
STQ9_13	0.535	0.024	0.059	0.001	0.066	0.003	435.34	15.93	367.39	8.16	813.07	79.44
STQ9_13	0.529	0.024	0.058	0.001	0.066	0.003	430.84	15.76	361.97	8.01	818.34	79.13
STQ8_16	0.118	0.011	0.015	0.001	0.058	0.003	112.88	9.69	94.20	7.51	526.39	101.03
STQ1_15	0.220	0.018	0.037	0.002	0.043	0.003	202.23	14.92	235.81	9.80	0.00	9.48
STQ2_3	0.129	0.006	0.016	0.000	0.060	0.003	123.47	5.49	99.68	2.64	609.80	95.45
STQ6_9	4.522	0.168	0.240	0.008	0.137	0.002	1734.97	30.38	1387.39	42.36	2184.27	25.22
STQ9_15	0.104	0.006	0.012	0.000	0.061	0.003	100.40	5.71	79.81	2.87	622.27	109.95
STQ5_5	3.295	0.183	0.191	0.010	0.125	0.002	1479.88	42.31	1126.63	56.37	2031.03	23.26
STQ4_8	1.636	0.092	0.116	0.006	0.102	0.003	984.14	35.02	706.56	34.00	1668.96	45.46
STQ7_16	2.104	0.113	0.125	0.006	0.122	0.003	1150.11	36.33	759.64	33.97	1986.19	43.38

Table A-7 Continued

Sample Name		Isotopic Ratios						Apparent Ages					
	$^{207}Pb/^{235}U$	1σ abs. err.	$^{206}Pb/^{238}U$	1σ abs. err.	$^{207}Pb/^{206}Pb$	1σ abs. err.	$^{207}Pb/^{235}U$	1σ abs. err.	$^{206}Pb/^{238}U$	1σ abs. err.	$^{207}Pb/^{206}Pb$	1σ abs. err.
						>10% Discordant Samples							
STQ10_2	0.241	0.015	0.020	0.001	0.086	0.004	219.50	12.08	130.09	5.83	1335.28	77.14
STQ1_13	0.137	0.009	0.011	0.000	0.087	0.005	130.30	8.06	73.01	1.85	1364.07	105.36
STQ8_8	1.752	0.132	0.090	0.006	0.141	0.005	1027.86	47.56	557.32	34.69	2235.30	63.26
STQ1_8	0.391	0.026	0.027	0.001	0.105	0.006	334.79	18.56	171.14	3.97	1718.87	101.49
STQ6_3	0.173	0.009	0.013	0.000	0.099	0.005	162.33	8.09	81.30	2.84	1606.75	90.99
STQ2_12	6.561	0.280	0.158	0.006	0.300	0.007	2054.15	36.92	948.26	31.51	3471.57	36.48
STQ7_1	1.256	0.073	0.021	0.001	0.431	0.010	825.95	32.36	134.97	7.05	4019.20	35.89
STQ10_16	4.142	0.239	0.008	0.000	3.937	0.146	1662.55	46.07	49.00	2.06	7103.45	48.17

Table A-8. Detrital zircon data table for sample Si-KM. Sample analyzed by LA-ICP-MS on 12-22-2014. Age data are in Ma.

Sample Name		Isotopic Ratios						Apparent Ages					
	$^{207}Pb/^{235}U$	1σ abs. err.	$^{206}Pb/^{238}U$	1σ abs. err.	$^{207}Pb/^{206}Pb$	1σ abs. err.	$^{207}Pb/^{235}U$	1σ abs. err.	$^{206}Pb/^{238}U$	1σ abs. err.	$^{207}Pb/^{206}Pb$	1σ abs. err.
						<10 % Discordant Samples							
K1_2	2.860	0.253	0.230	0.013	0.090	0.003	1371.47	64.42	1332.44	66.74	1431.92	55.15
K1_3	0.077	0.008	0.011	0.001	0.050	0.002	75.47	7.66	71.36	4.80	206.37	88.20
K1_4	3.862	0.332	0.278	0.015	0.101	0.003	1605.72	67.11	1582.30	74.24	1635.74	52.14
K1_5	0.802	0.075	0.099	0.006	0.059	0.002	598.20	41.54	609.64	34.96	554.06	68.46
K1_6	10.567	0.939	0.459	0.026	0.167	0.005	2485.80	79.22	2437.19	115.39	2525.01	47.58
K1_7	0.203	0.021	0.028	0.002	0.052	0.002	187.62	17.28	179.24	11.92	293.40	78.89
K1_9	0.220	0.021	0.032	0.002	0.050	0.002	202.31	16.92	201.48	11.63	210.93	73.18
K1_10	4.690	0.423	0.305	0.018	0.112	0.003	1765.53	72.86	1715.03	89.16	1824.97	51.33
K1_11	3.884	0.371	0.270	0.018	0.104	0.003	1610.27	74.33	1542.85	91.38	1698.75	52.68
K1_12	0.104	0.012	0.016	0.001	0.048	0.002	100.66	10.71	99.87	6.72	118.19	102.64
K1_13	0.141	0.013	0.021	0.001	0.049	0.001	133.93	11.51	133.87	7.92	133.86	70.75
K1_14	4.388	0.384	0.298	0.017	0.107	0.003	1710.04	69.86	1683.59	81.94	1741.75	51.33
K1_15	4.147	0.359	0.293	0.016	0.103	0.003	1663.71	68.51	1654.95	78.54	1673.95	51.97
K1_16	4.145	0.362	0.277	0.015	0.108	0.003	1663.17	68.97	1578.13	75.15	1771.44	52.62
K2_1	2.100	0.146	0.191	0.009	0.080	0.002	1148.66	46.64	1127.73	50.33	1188.29	43.14
K2_2	2.801	0.190	0.213	0.011	0.095	0.002	1355.77	49.61	1246.92	55.99	1531.74	36.90
K2_3	0.082	0.007	0.011	0.001	0.052	0.001	79.92	6.17	72.54	4.08	306.45	62.78
K2_4	1.536	0.101	0.161	0.007	0.069	0.001	944.94	39.58	963.67	41.49	901.45	40.23
K2_6	4.009	0.280	0.276	0.014	0.105	0.002	1636.10	55.21	1570.08	71.34	1721.93	37.04
K2_7	4.079	0.270	0.286	0.013	0.103	0.002	1650.16	52.51	1621.75	66.55	1686.43	36.76
K2_8	14.815	1.015	0.520	0.026	0.207	0.004	2803.43	63.17	2700.28	108.14	2878.40	33.19
K2_9	1.987	0.156	0.180	0.010	0.080	0.002	1111.27	51.74	1065.55	53.13	1201.75	53.77
K2_10	2.046	0.153	0.185	0.010	0.080	0.002	1131.11	49.64	1092.62	53.68	1205.64	46.74
K2_11	4.313	0.293	0.307	0.015	0.102	0.002	1695.88	54.44	1726.02	74.22	1658.72	36.57
K2_12	0.058	0.004	0.009	0.000	0.046	0.001	56.91	4.31	57.89	3.10	15.51	64.91
K2_13	0.196	0.019	0.027	0.002	0.054	0.002	182.11	15.71	169.23	10.10	352.59	85.90
K2_14	0.182	0.015	0.026	0.001	0.052	0.001	169.61	12.56	162.63	9.05	268.01	64.46
K2_15	0.159	0.012	0.024	0.001	0.047	0.001	149.78	10.11	154.68	7.99	72.68	54.49
K2_16	2.610	0.192	0.215	0.012	0.088	0.002	1303.56	52.63	1256.22	64.23	1382.23	38.49
K3_2	16.050	1.480	0.569	0.045	0.205	0.004	2879.79	84.55	2902.04	181.21	2864.09	32.27

Table A-8 Continued

Sample Name	Isotopic Ratios						Apparent Ages					
	$^{207}Pb/^{235}U$	1σ abs. err.	$^{206}Pb/^{238}U$	1σ abs. err.	$^{207}Pb/^{206}Pb$	1σ abs. err.	$^{207}Pb/^{235}U$	1σ abs. err.	$^{206}Pb/^{238}U$	1σ abs. err.	$^{207}Pb/^{206}Pb$	1σ abs. err.
						<10 % Discordant Samples						
K3_3	1.576	0.146	0.167	0.013	0.069	0.001	960.87	56.15	993.87	72.58	885.86	41.49
K3_4	0.112	0.012	0.015	0.001	0.053	0.002	107.86	10.55	97.32	8.03	347.20	69.75
K3_5	4.676	0.434	0.326	0.026	0.104	0.002	1762.91	74.74	1818.49	123.92	1697.45	37.18
K3_6	4.049	0.381	0.298	0.024	0.098	0.002	1644.00	73.86	1682.31	118.26	1595.15	37.21
K3_7	3.770	0.373	0.269	0.023	0.102	0.002	1586.35	76.46	1534.04	115.97	1656.37	37.55
K3_8	0.108	0.013	0.016	0.001	0.049	0.002	104.19	11.54	102.77	9.07	136.58	96.01
K3_9	3.426	0.327	0.257	0.021	0.097	0.002	1510.41	72.44	1475.24	107.04	1559.87	38.46
K3_10	3.970	0.383	0.290	0.024	0.099	0.002	1628.05	75.42	1639.22	119.41	1613.43	37.18
K3_11	5.204	0.499	0.342	0.028	0.110	0.002	1853.33	78.56	1898.41	133.79	1802.92	37.43
K3_12	0.110	0.011	0.016	0.001	0.050	0.001	105.96	10.34	101.34	8.48	211.01	66.96
K3_13	0.182	0.018	0.025	0.002	0.053	0.001	170.01	15.43	158.97	13.06	326.23	55.82
K3_14	3.292	0.312	0.257	0.021	0.093	0.002	1479.21	71.31	1476.36	106.02	1483.09	39.15
K3_15	8.587	0.821	0.432	0.035	0.144	0.003	2295.18	83.39	2316.08	157.19	2276.43	35.61
K3_16	4.588	0.440	0.327	0.027	0.102	0.002	1747.02	77.00	1822.23	129.60	1657.95	37.47
K4_1	4.459	0.336	0.306	0.015	0.106	0.003	1723.37	60.59	1722.62	73.57	1724.69	47.11
K4_3	1.587	0.119	0.160	0.008	0.072	0.002	965.02	45.76	958.68	44.09	979.94	50.75
K4_4	12.026	0.927	0.487	0.025	0.179	0.005	2606.42	69.83	2558.50	108.25	2644.23	42.47
K4_5	4.373	0.334	0.317	0.016	0.100	0.003	1707.31	61.30	1777.30	78.82	1622.88	47.11
K4_6	14.323	1.086	0.543	0.027	0.191	0.005	2771.37	69.52	2795.24	113.27	2754.40	41.30
K4_7	3.569	0.267	0.268	0.013	0.096	0.002	1542.57	57.69	1533.09	66.98	1555.99	46.57
K4_9	4.856	0.372	0.330	0.017	0.107	0.003	1794.70	62.55	1838.92	81.44	1744.09	46.50
K4_10	4.095	0.316	0.296	0.015	0.100	0.003	1653.27	61.15	1671.95	74.14	1630.02	49.39
K4_11	0.080	0.008	0.011	0.001	0.051	0.002	78.58	7.53	73.02	4.40	251.68	97.39
K4_12	13.320	0.996	0.549	0.027	0.176	0.004	2702.58	68.30	2822.62	111.91	2614.38	41.23
K4_13	1.936	0.149	0.194	0.010	0.072	0.002	1093.48	50.29	1143.22	52.85	996.18	53.39
K4_14	4.751	0.355	0.331	0.016	0.104	0.003	1776.23	60.83	1844.58	78.21	1697.22	45.95
K4_16	4.051	0.311	0.289	0.015	0.102	0.003	1644.50	60.70	1634.63	73.30	1657.55	47.67
K5_1	1.771	0.150	0.171	0.006	0.075	0.003	1034.74	53.55	1015.58	35.48	1074.98	68.15
K5_3	0.248	0.021	0.036	0.001	0.050	0.002	224.65	16.82	227.79	8.20	191.28	78.64
K5_4	3.877	0.327	0.276	0.011	0.102	0.003	1608.96	65.83	1571.39	53.56	1658.04	61.49
K5_5	1.765	0.151	0.177	0.007	0.072	0.003	1032.60	54.09	1049.94	38.89	995.56	68.71
K5_7	4.347	0.360	0.305	0.011	0.103	0.003	1702.26	66.25	1718.11	53.83	1682.36	61.14
K5_8	2.744	0.229	0.224	0.008	0.089	0.003	1340.47	60.40	1300.97	43.42	1403.63	63.73
K5_9	4.097	0.341	0.285	0.010	0.104	0.004	1653.66	65.68	1615.30	51.32	1702.29	61.16
K5_10	10.130	0.832	0.471	0.016	0.156	0.005	2446.71	73.16	2488.85	70.51	2411.46	55.98
K5_12	3.669	0.302	0.272	0.009	0.098	0.003	1564.69	63.73	1549.75	47.88	1584.46	61.73
K5_13	1.877	0.158	0.183	0.007	0.075	0.003	1073.09	54.27	1081.17	35.80	1056.21	68.72
K5_14	4.676	0.385	0.329	0.011	0.103	0.003	1762.95	66.60	1835.79	55.10	1677.24	60.95
K5_15	3.580	0.315	0.256	0.012	0.101	0.003	1545.10	67.52	1470.24	60.63	1648.61	61.26
K5_16	2.435	0.209	0.204	0.008	0.086	0.003	1252.90	59.95	1198.83	44.40	1346.56	65.04
K6_3	2.634	0.237	0.225	0.010	0.085	0.003	1310.23	64.20	1306.83	51.44	1315.74	66.12
K6_4	3.833	0.351	0.290	0.013	0.096	0.003	1599.71	71.13	1640.59	66.95	1546.25	64.14
K6_6	2.109	0.190	0.199	0.009	0.077	0.003	1151.75	60.26	1169.13	46.64	1119.13	68.06
K6_7	4.000	0.369	0.287	0.014	0.101	0.004	1634.14	72.30	1627.32	67.63	1642.90	63.95
K6_8	3.016	0.276	0.250	0.011	0.088	0.003	1411.71	67.56	1436.83	58.88	1373.96	66.37
K6_9	12.050	1.090	0.487	0.022	0.179	0.006	2608.29	81.46	2559.55	93.76	2646.33	56.53
K6_10	0.092	0.010	0.014	0.001	0.049	0.002	89.60	9.35	87.60	4.96	143.21	106.29
K6_11	4.125	0.457	0.290	0.022	0.103	0.004	1659.25	86.75	1640.18	109.52	1683.43	64.54
K6_12	7.665	0.718	0.402	0.020	0.138	0.005	2192.50	80.80	2179.71	93.01	2204.45	59.11

Table A-8 Continued

Sample Name	Isotopic Ratios						Apparent Ages					
	$^{207}Pb/^{235}U$	1σ abs. err.	$^{206}Pb/^{238}U$	1σ abs. err.	$^{207}Pb/^{206}Pb$	1σ abs. err.	$^{207}Pb/^{235}U$	1σ abs. err.	$^{206}Pb/^{238}U$	1σ abs. err.	$^{207}Pb/^{206}Pb$	1σ abs. err.
						<10 % Discordant Samples						
K6_13	2.942	0.276	0.246	0.012	0.087	0.003	1392.87	68.69	1420.38	63.92	1350.94	66.17
K6_14	3.515	0.326	0.264	0.013	0.097	0.003	1530.62	70.82	1509.22	64.58	1560.29	64.68
K6_16	2.809	0.259	0.232	0.011	0.088	0.003	1357.94	66.67	1343.38	57.21	1380.89	65.66
K7_3	2.105	0.173	0.180	0.006	0.085	0.003	1150.49	55.18	1068.72	32.61	1308.71	61.47
K7_4	0.164	0.015	0.025	0.001	0.047	0.002	154.62	12.83	161.22	6.25	55.42	85.43
K7_5	0.157	0.014	0.024	0.001	0.048	0.002	148.23	11.99	151.14	5.13	102.69	84.09
K7_6	0.092	0.008	0.014	0.001	0.046	0.002	89.25	7.56	92.68	3.19	0.11	87.35
K7_7	1.807	0.155	0.181	0.006	0.072	0.003	1048.17	54.68	1073.49	33.96	996.46	69.71
K7_8	0.177	0.018	0.026	0.001	0.050	0.002	165.19	15.28	164.30	8.04	178.70	94.86
K7_9	3.936	0.322	0.290	0.009	0.099	0.003	1621.16	64.26	1641.15	43.99	1595.94	60.32
K7_10	1.825	0.151	0.182	0.006	0.073	0.002	1054.39	52.93	1076.59	32.39	1009.39	65.36
K7_11	3.951	0.328	0.299	0.010	0.096	0.003	1624.25	65.12	1686.82	49.00	1544.74	60.64
K7_12	2.058	0.169	0.201	0.007	0.074	0.002	1135.03	54.61	1181.21	34.97	1048.44	63.86
K7_13	1.780	0.147	0.180	0.006	0.072	0.002	1038.16	52.23	1067.07	31.00	978.47	65.85
K7_14	4.094	0.340	0.301	0.010	0.099	0.003	1653.01	65.70	1695.57	48.89	1599.97	60.64
K7_15	0.074	0.009	0.011	0.001	0.047	0.003	72.25	8.30	73.59	4.13	28.83	125.60
K7_16	2.562	0.220	0.223	0.008	0.083	0.003	1289.73	60.78	1297.75	39.90	1277.05	66.93
K8_1	2.879	0.270	0.254	0.012	0.082	0.003	1376.42	68.40	1457.18	63.36	1253.80	65.26
K8_3	3.705	0.348	0.277	0.013	0.097	0.003	1572.39	72.38	1575.08	65.52	1569.29	64.15
K8_4	0.087	0.010	0.013	0.001	0.049	0.002	84.77	9.57	83.22	4.98	129.33	115.12
K8_6	3.865	0.359	0.287	0.013	0.098	0.003	1606.48	72.28	1628.86	66.28	1577.75	63.18
K8_7	3.734	0.373	0.283	0.016	0.096	0.003	1578.76	76.97	1604.33	80.41	1545.27	64.75
K8_8	2.710	0.273	0.227	0.013	0.087	0.003	1331.22	72.00	1317.22	67.98	1354.33	67.42
K8_9	0.180	0.018	0.026	0.001	0.049	0.002	168.13	15.58	168.45	9.02	164.16	87.29
K8_10	1.870	0.186	0.186	0.010	0.073	0.003	1070.67	63.86	1101.60	56.15	1008.73	70.96
K8_11	3.912	0.379	0.291	0.015	0.098	0.003	1616.25	75.54	1646.15	76.51	1578.03	63.67
K8_12	3.848	0.366	0.280	0.014	0.100	0.003	1602.94	73.86	1593.48	70.16	1615.89	63.10
K8_13	9.299	0.917	0.452	0.025	0.149	0.005	2367.89	86.63	2402.71	108.87	2338.51	59.32
K8_14	1.600	0.156	0.169	0.009	0.069	0.002	970.34	59.19	1004.87	48.62	893.50	71.91
K8_15	3.595	0.359	0.270	0.016	0.097	0.003	1548.53	76.43	1541.19	79.24	1559.06	63.35
K8_16	3.830	0.366	0.282	0.014	0.098	0.003	1599.11	74.13	1603.34	71.03	1594.05	63.73
K9_1	0.076	0.009	0.011	0.001	0.050	0.002	74.36	8.00	71.22	4.99	176.20	99.82
K9_3	1.709	0.151	0.175	0.010	0.071	0.002	1011.85	54.94	1037.98	53.17	955.35	60.64
K9_4	2.579	0.237	0.234	0.014	0.080	0.002	1294.69	65.06	1357.54	74.23	1191.58	58.76
K9_6	1.803	0.143	0.172	0.008	0.076	0.002	1046.64	50.59	1023.69	42.55	1094.52	55.23
K9_7	0.090	0.009	0.013	0.001	0.050	0.002	87.92	8.36	84.63	5.06	177.72	88.07
K9_8	0.075	0.007	0.011	0.001	0.048	0.002	73.62	6.75	72.56	4.33	107.87	80.18
K9_9	1.646	0.132	0.164	0.008	0.073	0.002	988.18	49.53	980.73	41.54	1004.41	57.01
K9_10	0.081	0.008	0.012	0.001	0.050	0.002	78.96	7.89	75.81	4.53	174.97	97.51
K9_12	3.902	0.320	0.286	0.014	0.099	0.003	1614.18	64.19	1623.68	68.45	1601.48	53.08
K9_13	13.165	1.071	0.530	0.025	0.180	0.005	2691.56	74.00	2741.08	103.69	2654.30	47.34
K9_14	3.012	0.248	0.254	0.012	0.086	0.002	1410.63	60.80	1458.88	63.63	1338.16	54.17
K9_15	0.065	0.006	0.009	0.000	0.050	0.002	63.57	5.60	59.96	3.18	201.11	78.95
K9_16	0.178	0.017	0.025	0.001	0.051	0.002	166.30	14.84	159.92	9.34	257.78	83.75
K10_1	2.727	0.226	0.241	0.015	0.082	0.002	1335.74	59.89	1391.44	75.78	1247.44	47.53
K10_2	0.080	0.009	0.011	0.001	0.052	0.002	77.83	8.18	71.25	4.86	284.73	102.32
K10_3	3.976	0.326	0.295	0.018	0.098	0.002	1629.25	64.44	1668.90	87.26	1578.31	45.07
K10_4	0.243	0.020	0.036	0.002	0.049	0.001	220.68	16.25	228.95	13.19	133.20	60.28
K10_5	4.197	0.364	0.299	0.019	0.102	0.003	1673.52	68.73	1685.63	95.94	1658.26	45.85
K10_6	0.654	0.054	0.083	0.005	0.057	0.001	511.05	32.74	516.56	29.11	486.36	57.18
K10_8	3.438	0.286	0.245	0.015	0.102	0.002	1513.24	63.32	1414.70	77.19	1653.89	44.63
K10_9	3.568	0.292	0.259	0.016	0.100	0.002	1542.47	62.98	1487.00	79.64	1619.24	43.61
K10_10	0.122	0.011	0.016	0.001	0.054	0.002	116.77	10.31	105.48	6.79	353.38	74.15
K10_11	2.761	0.234	0.242	0.015	0.083	0.002	1344.96	61.23	1397.61	79.38	1262.04	46.39
K10_12	3.976	0.331	0.282	0.017	0.102	0.002	1629.33	65.30	1603.29	86.32	1663.01	44.61
K10_13	0.555	0.046	0.074	0.005	0.054	0.001	448.53	29.61	463.08	27.29	374.43	53.46

Table A-8 Continued

	Isotopic Ratios						Apparent Ages					
Sample Name	$^{207}Pb/^{235}U$	1σ abs. err.	$^{206}Pb/^{238}U$	1σ abs. err.	$^{207}Pb/^{206}Pb$	1σ abs. err.	$^{207}Pb/^{235}U$	1σ abs. err.	$^{206}Pb/^{238}U$	1σ abs. err.	$^{207}Pb/^{206}Pb$	1σ abs. err.
						>10% Discordant Samples						
K10_16	4.157	0.089	0.332	0.007	0.091	0.001	1665.55	17.32	1846.50	31.46	1444.43	15.80
K6_15	0.250	0.032	0.032	0.002	0.058	0.003	226.68	25.79	199.98	14.51	513.56	117.51
K5_11	0.274	0.028	0.033	0.002	0.060	0.003	246.24	22.25	211.18	11.01	594.77	94.44
K1_1	0.081	0.008	0.011	0.001	0.056	0.002	78.68	7.76	67.38	4.43	435.90	81.26
K4_15	3.884	0.311	0.232	0.013	0.121	0.003	1610.36	62.75	1347.27	66.36	1974.21	47.23
K9_11	2.742	0.247	0.188	0.011	0.106	0.003	1340.05	64.90	1112.37	60.70	1724.63	53.01
K8_5	3.439	0.358	0.214	0.014	0.117	0.004	1513.24	78.69	1250.19	71.82	1904.07	61.78
K7_1	0.091	0.009	0.011	0.001	0.058	0.003	88.51	8.62	72.70	3.49	539.68	92.31
K6_1	0.322	0.030	0.037	0.002	0.064	0.002	283.40	22.86	232.04	10.05	731.90	78.50
K10_14	4.315	0.103	0.367	0.007	0.085	0.001	1696.25	19.50	2017.58	34.85	1319.22	24.58
K2_5	2.925	0.196	0.189	0.009	0.112	0.002	1388.52	49.57	1115.55	48.76	1836.96	36.57
K4_8	0.167	0.026	0.019	0.002	0.062	0.004	156.45	22.72	124.47	14.23	673.68	128.62
K1_8	5.327	0.532	0.255	0.017	0.152	0.005	1873.27	81.95	1461.70	88.89	2365.65	54.90
K10_15	7.126	0.210	0.496	0.014	0.104	0.001	2127.35	25.87	2596.55	59.84	1700.35	15.84
K5_2	0.239	0.034	0.027	0.002	0.065	0.004	217.55	27.32	169.36	12.64	776.96	136.88
K9_2	11.066	1.389	0.349	0.030	0.230	0.011	2528.69	110.62	1927.62	140.33	3053.62	73.99
K9_5	0.117	0.012	0.013	0.001	0.064	0.002	112.41	10.54	85.33	5.42	731.97	75.26
K5_6	2.187	0.190	0.146	0.006	0.109	0.004	1176.97	58.92	877.37	35.50	1779.00	61.40
K4_2	6.345	0.534	0.260	0.016	0.177	0.004	2024.73	71.24	1487.54	81.69	2628.21	41.38
K6_5	0.288	0.032	0.026	0.002	0.079	0.004	256.71	24.57	167.51	9.50	1178.34	89.63
K6_2	0.344	0.041	0.029	0.002	0.085	0.004	300.51	30.34	187.34	12.12	1308.88	94.98
K8_2	0.200	0.024	0.016	0.001	0.091	0.004	185.27	20.46	102.45	7.11	1439.26	90.47
K7_2	0.057	0.160	0.004	0.012	0.095	0.003	56.27	143.00	28.07	74.79	1523.19	66.18
K3_1	0.099	0.026	0.006	0.002	0.116	0.005	96.00	23.95	39.82	9.82	1896.28	69.01
K10_7	0.312	0.032	0.016	0.001	0.139	0.006	275.82	24.72	104.35	7.08	2211.20	69.04

Table A-9. Detrital zircon data table for sample CB-BS. Sample analyzed by LA-ICP-MS on 11-10-2014. Age data are in Ma.

	Isotopic Ratios						Apparent Ages					
Sample Name	$^{207}Pb/^{235}U$	1σ abs. err.	$^{206}Pb/^{238}U$	1σ abs. err.	$^{207}Pb/^{206}Pb$	1σ abs. err.	$^{207}Pb/^{235}U$	1σ abs. err.	$^{206}Pb/^{238}U$	1σ abs. err.	$^{207}Pb/^{206}Pb$	1σ abs. err.
						<10 % Discordant Samples						
CBBS1_1	7.962	0.405	0.389	0.019	0.148	0.001	2226.77	44.89	2119.01	89.70	2327.41	15.91
CBBS1_3	2.631	0.061	0.218	0.005	0.087	0.001	1309.23	16.97	1272.16	24.84	1370.47	16.69
CBBS1_5	3.036	0.147	0.226	0.007	0.097	0.002	1416.66	23.27	1313.63	19.39	1575.15	31.79
CBBS1_7	1.697	0.047	0.152	0.004	0.081	0.001	1007.22	17.44	910.02	20.10	1225.17	27.27
CBBS1_8	0.057	0.002	0.008	0.000	0.050	0.001	56.62	1.52	53.89	1.18	173.46	38.91
CBBS1_10	0.058	0.002	0.009	0.000	0.047	0.001	56.85	1.59	56.61	1.21	66.97	44.68
CBBS1_11	3.458	0.088	0.264	0.006	0.095	0.001	1517.72	19.88	1508.51	32.82	1530.59	13.43
CBBS1_12	0.133	0.004	0.019	0.000	0.051	0.001	126.94	3.88	121.27	3.02	234.41	47.34
CBBS1_16	0.077	0.003	0.011	0.000	0.050	0.001	75.39	2.92	72.38	2.42	171.74	51.10
CBBS2_1	2.547	0.073	0.211	0.006	0.087	0.001	1285.66	20.71	1236.31	30.57	1369.08	17.27
CBBS2_2	0.647	0.028	0.079	0.003	0.059	0.001	506.50	16.95	489.55	18.58	583.80	35.87
CBBS2_3	3.928	0.157	0.284	0.011	0.100	0.001	1619.47	31.81	1612.70	55.49	1628.29	15.30
CBBS2_8	4.047	0.078	0.271	0.005	0.108	0.001	1643.74	15.47	1543.58	23.33	1774.30	15.91
CBBS2_9	2.455	0.063	0.197	0.005	0.091	0.001	1259.01	18.48	1157.33	24.91	1437.25	20.14
CBBS2_10	2.291	0.086	0.190	0.006	0.087	0.001	1209.49	26.09	1122.78	34.54	1367.77	31.19
CBBS2_11	0.055	0.002	0.008	0.000	0.049	0.001	54.83	1.71	52.52	1.01	157.02	58.53

Table A-9 Continued

Sample Name	$^{207}Pb/^{235}U$	1σ abs. err.	$^{206}Pb/^{238}U$	1σ abs. err.	$^{207}Pb/^{206}Pb$	1σ abs. err.	$^{207}Pb/^{235}U$	1σ abs. err.	$^{206}Pb/^{238}U$	1σ abs. err.	$^{207}Pb/^{206}Pb$	1σ abs. err.
			Isotopic Ratios						Apparent Ages			
					<10 % Discordant Samples							
CBBS2_12	3.535	0.101	0.245	0.007	0.105	0.001	1535.09	22.44	1412.19	34.23	1708.77	17.26
CBBS2_13	2.979	0.124	0.217	0.009	0.099	0.001	1402.19	31.05	1266.86	45.92	1614.39	19.84
CBBS2_15	11.816	0.518	0.518	0.020	0.165	0.003	2589.95	40.23	2690.78	84.50	2511.61	32.11
CBBS2_16	0.582	0.026	0.073	0.003	0.058	0.001	465.55	16.68	455.09	17.25	516.99	46.48
CBBS3_1	4.709	0.145	0.315	0.006	0.108	0.002	1768.89	25.48	1766.37	31.67	1771.46	38.07
CBBS3_2	3.025	0.097	0.244	0.005	0.090	0.002	1413.95	24.13	1405.33	26.92	1426.51	42.55
CBBS3_3	2.141	0.069	0.197	0.004	0.079	0.002	1162.24	22.12	1159.01	23.44	1167.81	43.25
CBBS3_4	0.203	0.008	0.028	0.001	0.053	0.001	187.91	6.34	175.54	4.56	345.83	58.34
CBBS3_6	4.593	0.135	0.329	0.006	0.101	0.002	1748.06	24.21	1833.87	29.05	1646.49	38.81
CBBS3_7	4.493	0.131	0.309	0.006	0.106	0.002	1729.60	23.97	1733.57	28.29	1724.39	36.73
CBBS3_9	0.075	0.003	0.011	0.000	0.050	0.002	73.29	3.25	69.43	1.90	200.53	94.66
CBBS3_10	1.894	0.056	0.182	0.003	0.075	0.002	1078.90	19.63	1079.54	18.70	1077.15	42.32
CBBS3_12	4.623	0.141	0.310	0.006	0.108	0.002	1753.36	25.13	1741.84	30.83	1766.69	37.59
CBBS3_13	3.483	0.148	0.241	0.009	0.105	0.002	1523.29	33.03	1393.24	44.87	1708.53	39.04
CBBS3_14	3.025	0.097	0.244	0.005	0.090	0.002	1414.00	24.07	1406.12	28.15	1425.45	39.46
CBBS3_16	5.282	0.187	0.347	0.009	0.110	0.002	1866.02	29.73	1922.50	44.84	1803.27	37.65
CBBS4_1	2.588	0.089	0.224	0.006	0.084	0.002	1297.20	24.96	1300.44	33.29	1291.92	37.74
CBBS4_3	2.748	0.087	0.212	0.005	0.094	0.002	1341.49	23.20	1241.05	28.73	1505.62	32.80
CBBS4_4	3.119	0.106	0.248	0.007	0.091	0.002	1437.47	25.90	1430.56	36.28	1447.80	34.85
CBBS4_5	4.363	0.147	0.301	0.008	0.105	0.002	1705.30	27.46	1695.95	40.52	1716.89	35.86
CBBS4_7	5.035	0.154	0.364	0.009	0.100	0.002	1825.27	25.62	2002.67	41.47	1628.54	32.95
CBBS4_8	2.915	0.090	0.240	0.006	0.088	0.002	1385.83	22.96	1388.09	30.21	1382.43	34.15
CBBS4_9	8.245	0.273	0.424	0.011	0.141	0.003	2258.31	29.54	2278.57	49.37	2240.08	35.97
CBBS4_10	4.115	0.136	0.290	0.008	0.103	0.002	1657.35	26.69	1641.55	39.65	1677.53	32.38
CBBS4_12	0.108	0.004	0.015	0.000	0.053	0.002	104.17	3.88	94.32	2.75	335.92	64.68
CBBS4_14	2.698	0.097	0.213	0.006	0.092	0.002	1328.03	26.23	1245.52	33.15	1463.80	39.67
CBBS4_16	3.185	0.132	0.248	0.008	0.093	0.003	1453.41	31.59	1425.74	41.75	1494.18	53.09
CBBS5_1	1.974	0.076	0.189	0.005	0.076	0.002	1106.78	25.53	1115.25	29.57	1090.50	58.22
CBBS5_2	3.192	0.085	0.253	0.005	0.092	0.002	1455.30	20.43	1454.21	26.79	1457.22	31.78
CBBS5_3	4.220	0.164	0.272	0.009	0.113	0.002	1677.85	31.40	1550.01	46.81	1841.96	37.20
CBBS5_6	5.574	0.244	0.324	0.013	0.125	0.002	1912.09	36.94	1811.29	64.49	2023.57	28.90
CBBS5_7	0.120	0.006	0.018	0.001	0.049	0.002	115.49	5.57	115.08	4.30	124.35	97.93
CBBS5_8	3.174	0.110	0.232	0.007	0.099	0.002	1450.94	26.30	1345.68	36.43	1609.02	32.81
CBBS5_10	1.754	0.046	0.170	0.003	0.075	0.001	1028.53	16.71	1010.01	18.42	1068.48	33.63
CBBS5_11	4.904	0.159	0.337	0.009	0.106	0.002	1802.86	27.02	1870.39	45.16	1725.95	30.98
CBBS5_12	3.225	0.098	0.239	0.006	0.098	0.002	1463.21	23.30	1380.49	30.62	1585.74	34.22
CBBS5_14	2.032	0.058	0.185	0.004	0.080	0.001	1126.27	19.27	1092.64	22.63	1192.03	35.18
CBBS5_16	4.633	0.130	0.313	0.006	0.107	0.002	1755.20	23.11	1754.51	31.71	1756.32	35.94
CBBS6_1	3.004	0.146	0.236	0.010	0.092	0.002	1408.68	36.27	1366.96	53.94	1472.48	37.87
CBBS6_3	4.156	0.193	0.294	0.012	0.103	0.002	1665.48	37.28	1660.67	60.47	1671.65	37.47
CBBS6_4	2.970	0.142	0.240	0.010	0.090	0.002	1399.88	35.80	1386.43	53.72	1420.53	39.08
CBBS6_6	0.109	0.006	0.015	0.001	0.053	0.002	104.73	5.22	95.33	4.06	324.39	77.20
CBBS6_8	3.005	0.150	0.245	0.011	0.089	0.002	1408.96	37.25	1414.78	57.09	1400.27	40.37
CBBS6_9	4.192	0.193	0.292	0.012	0.104	0.002	1672.44	37.14	1649.09	59.57	1701.97	37.76
CBBS6_10	4.010	0.230	0.280	0.015	0.104	0.002	1636.24	45.62	1590.56	74.62	1695.57	41.65
CBBS6_12	2.776	0.136	0.231	0.010	0.087	0.002	1349.01	35.82	1340.47	52.89	1362.69	41.59
CBBS6_13	4.220	0.204	0.292	0.013	0.105	0.002	1678.01	38.90	1650.53	62.96	1712.65	38.70
CBBS6_14	0.373	0.019	0.050	0.002	0.054	0.001	321.77	13.82	313.05	13.43	385.52	59.17
CBBS7_1	0.172	0.005	0.024	0.000	0.053	0.001	161.29	4.27	150.73	2.96	319.17	48.86
CBBS7_2	2.788	0.097	0.234	0.007	0.086	0.002	1352.40	25.57	1355.93	35.63	1346.73	36.57
CBBS7_3	3.691	0.114	0.259	0.007	0.103	0.002	1569.36	24.40	1487.00	33.60	1681.87	31.79
CBBS7_5	4.341	0.115	0.303	0.006	0.104	0.002	1701.25	21.69	1706.37	28.79	1694.86	33.05

Table A-9 Continued

Sample Name	Isotopic Ratios						Apparent Ages					
	$^{207}Pb/^{235}U$	1σ abs. err.	$^{206}Pb/^{238}U$	1σ abs. err.	$^{207}Pb/^{206}Pb$	1σ abs. err.	$^{207}Pb/^{235}U$	1σ abs. err.	$^{206}Pb/^{238}U$	1σ abs. err.	$^{207}Pb/^{206}Pb$	1σ abs. err.
<10 % Discordant Samples												
CBBS7_6	3.497	0.112	0.255	0.007	0.100	0.002	1526.62	24.91	1462.01	34.64	1617.27	32.46
CBBS7_8	3.330	0.101	0.252	0.006	0.096	0.002	1488.19	23.51	1446.27	29.68	1548.35	38.86
CBBS7_10	6.747	0.184	0.342	0.007	0.143	0.003	2078.83	23.89	1894.98	33.29	2266.17	30.92
CBBS7_12	3.716	0.128	0.269	0.008	0.100	0.002	1574.89	27.11	1536.66	39.76	1626.40	33.79
CBBS7_16	4.420	0.112	0.305	0.005	0.105	0.002	1716.14	20.72	1715.91	25.75	1716.34	33.61
CBBS8_2	1.745	0.047	0.171	0.004	0.074	0.001	1025.41	17.31	1014.94	22.34	1047.78	29.55
CBBS8_3	3.829	0.084	0.265	0.005	0.105	0.001	1598.92	17.58	1514.49	25.83	1712.04	21.11
CBBS8_4	2.037	0.155	0.176	0.012	0.084	0.003	1127.88	50.46	1043.93	67.41	1293.29	74.26
CBBS8_6	1.648	0.035	0.165	0.003	0.072	0.001	988.89	13.40	985.08	15.06	997.33	30.79
CBBS8_8	2.009	0.059	0.178	0.004	0.082	0.002	1118.70	19.69	1056.15	24.16	1242.29	36.20
CBBS8_10	5.020	0.104	0.326	0.005	0.112	0.002	1822.72	17.37	1817.90	26.30	1828.21	24.34
CBBS8_11	4.196	0.085	0.295	0.005	0.103	0.001	1673.32	16.52	1668.93	24.41	1678.80	23.08
CBBS8_13	4.179	0.083	0.294	0.005	0.103	0.001	1669.83	16.21	1661.59	23.95	1680.18	22.23
CBBS9_1	1.051	0.036	0.110	0.003	0.069	0.001	729.50	17.46	671.13	19.57	913.27	28.76
CBBS9_3	1.351	0.044	0.130	0.004	0.075	0.001	868.10	18.74	789.58	19.94	1074.17	35.93
CBBS9_5	0.155	0.004	0.022	0.000	0.052	0.001	146.36	3.39	137.64	2.66	289.99	35.01
CBBS9_8	3.353	0.109	0.245	0.008	0.099	0.001	1493.39	25.11	1414.83	39.18	1606.77	18.47
CBBS9_10	2.132	0.050	0.180	0.004	0.086	0.001	1159.11	16.19	1066.93	20.74	1335.77	20.25
CBBS9_11	0.448	0.009	0.058	0.001	0.056	0.000	376.06	6.44	366.43	6.82	435.80	16.60
CBBS9_12	3.261	0.072	0.230	0.005	0.103	0.001	1471.81	17.00	1331.95	23.61	1679.76	18.36
CBBS9_14	4.629	0.190	0.321	0.007	0.105	0.003	1754.57	33.62	1792.88	35.81	1708.82	57.26
CBBS9_15	4.341	0.181	0.311	0.008	0.101	0.003	1701.23	33.77	1747.15	37.17	1644.69	57.34
CBBS9_16	0.417	0.016	0.055	0.001	0.055	0.002	354.26	11.55	343.98	6.31	421.71	68.96
CBBS9_17	3.273	0.125	0.254	0.005	0.093	0.003	1474.66	29.25	1458.98	24.06	1496.85	56.77
CBBS9_18	0.457	0.018	0.058	0.001	0.057	0.002	382.33	12.37	363.47	6.85	497.67	68.04
CBBS9_19	2.069	0.083	0.179	0.004	0.084	0.003	1138.55	27.23	1058.90	21.02	1293.23	60.87
CBBS9_20	4.016	0.166	0.278	0.007	0.105	0.003	1637.52	33.13	1582.24	33.84	1708.82	56.57
CBBS9_21	4.652	0.177	0.327	0.006	0.103	0.003	1758.71	31.26	1824.28	28.60	1681.24	55.52
CBBS9_22	4.002	0.163	0.285	0.007	0.102	0.003	1634.62	32.53	1617.33	33.31	1656.51	55.92
CBBS9_24	10.240	0.414	0.471	0.011	0.158	0.005	2456.67	36.74	2486.85	46.31	2431.40	51.87
>10% Discordant Samples												
CBBS9_6	3.148	0.065	0.223	0.004	0.102	0.001	1444.40	15.68	1298.38	22.24	1666.45	14.47
CBBS1_15	3.523	0.130	0.238	0.008	0.107	0.002	1532.47	28.85	1376.51	39.29	1754.95	31.10
CBBS6_2	3.451	0.173	0.235	0.011	0.107	0.002	1516.12	38.70	1360.21	55.11	1741.28	40.66
CBBS8_16	1.293	0.042	0.124	0.004	0.075	0.001	842.46	18.39	755.59	20.27	1078.85	30.80
CBBS5_13	4.403	0.163	0.267	0.009	0.119	0.002	1712.92	30.16	1527.31	44.30	1948.31	33.16
CBBS1_9	3.033	0.041	0.216	0.003	0.102	0.001	1415.96	10.36	1262.21	13.50	1655.49	12.66
CBBS8_15	3.048	0.068	0.217	0.004	0.102	0.001	1419.82	16.83	1265.02	23.55	1660.30	15.50
CBBS1_2	3.098	0.067	0.217	0.004	0.104	0.001	1432.23	16.45	1265.98	23.42	1688.69	13.01
CBBS4_6	3.137	0.101	0.217	0.006	0.105	0.002	1441.83	24.61	1267.43	30.50	1709.45	31.88
CBBS2_5	0.073	0.004	0.010	0.000	0.054	0.002	71.28	3.84	62.52	2.13	375.95	96.56
CBBS2_4	9.067	0.178	0.371	0.007	0.177	0.002	2344.83	17.75	2034.29	30.58	2627.22	14.31
CBBS5_9	0.077	0.004	0.010	0.000	0.055	0.003	75.48	4.04	65.40	2.50	407.80	108.84
CBBS2_7	2.841	0.054	0.202	0.004	0.102	0.001	1366.46	14.08	1184.05	18.82	1664.39	13.41
CBBS1_6	8.111	0.201	0.350	0.008	0.168	0.001	2243.46	22.12	1932.37	39.07	2540.79	13.07
CBBS8_9	0.218	0.008	0.027	0.001	0.059	0.002	200.33	6.48	169.80	4.82	576.80	56.41
CBBS9_2	1.451	0.039	0.126	0.003	0.084	0.001	910.26	15.86	763.26	16.44	1286.05	26.21
CBBS9_9	0.078	0.004	0.010	0.000	0.057	0.003	75.84	4.02	63.58	2.04	481.69	95.69
CBBS2_6	2.420	0.065	0.175	0.005	0.100	0.001	1248.51	19.00	1040.70	24.81	1627.29	12.28
CBBS8_14	2.440	0.055	0.176	0.004	0.101	0.001	1254.58	16.13	1045.57	20.51	1633.59	13.95
CBBS9_23	2.851	0.120	0.192	0.005	0.107	0.003	1369.03	31.13	1134.05	26.10	1756.99	56.53
CBBS7_11	0.068	0.003	0.009	0.000	0.057	0.002	67.06	2.92	55.41	2.11	505.09	58.55
CBBS4_2	5.276	0.203	0.270	0.008	0.142	0.003	1865.02	32.33	1539.67	42.67	2249.93	40.94
CBBS7_13	5.057	0.173	0.263	0.007	0.139	0.003	1828.93	28.67	1504.95	37.88	2220.67	34.74
CBBS6_11	5.483	0.263	0.273	0.012	0.146	0.003	1897.94	40.33	1557.27	59.44	2294.18	35.27

Table A-9 Continued

Sample Name	Isotopic Ratios						Apparent Ages					
	$^{207}Pb/^{235}U$	1σ abs. err.	$^{206}Pb/^{238}U$	1σ abs. err.	$^{207}Pb/^{206}Pb$	1σ abs. err.	$^{207}Pb/^{235}U$	1σ abs. err.	$^{206}Pb/^{238}U$	1σ abs. err.	$^{207}Pb/^{206}Pb$	1σ abs. err.
						>10% Discordant Samples						
CBBS1_14	2.329	0.093	0.165	0.005	0.102	0.002	1221.20	27.95	984.06	30.32	1668.62	39.87
CBBS3_5	7.641	0.492	0.312	0.018	0.177	0.006	2189.73	56.19	1752.84	86.68	2627.99	54.67
CBBS6_5	1.833	0.134	0.138	0.010	0.097	0.002	1057.24	47.05	831.68	55.05	1558.10	39.73
CBBS7_14	2.473	0.071	0.166	0.004	0.108	0.002	1264.25	20.68	989.67	20.57	1767.60	32.67
CBBS5_5	0.462	0.117	0.048	0.012	0.070	0.002	385.88	78.18	299.64	74.82	942.55	69.41
CBBS9_4	0.095	0.003	0.011	0.000	0.063	0.001	92.38	2.98	70.66	1.69	697.32	50.00
CBBS9_7	0.495	0.018	0.049	0.002	0.073	0.002	408.26	12.48	310.72	9.39	1005.34	41.76
CBBS1_13	1.979	0.038	0.139	0.002	0.103	0.001	1108.40	12.84	840.30	12.60	1680.54	19.32
CBBS9_13	1.576	0.050	0.116	0.004	0.098	0.001	960.65	19.60	708.77	20.99	1592.64	10.76
CBBS2_14	0.311	0.016	0.032	0.001	0.071	0.002	275.00	12.20	200.55	9.08	968.22	44.14
CBBS5_15	0.097	0.003	0.011	0.000	0.067	0.001	93.72	3.18	67.35	2.01	831.14	42.95
CBBS4_13	2.513	0.084	0.152	0.004	0.120	0.002	1275.66	23.96	913.22	23.15	1952.37	33.48
CBBS6_15	0.533	0.041	0.048	0.004	0.081	0.002	434.12	26.56	301.22	21.69	1218.73	42.87
CBBS6_16	1.423	0.105	0.101	0.007	0.103	0.002	898.74	43.01	617.84	41.76	1672.23	40.31
CBBS7_4	0.093	0.005	0.009	0.000	0.072	0.003	90.36	4.44	60.50	2.42	974.04	76.84
CBBS8_1	1.626	0.044	0.104	0.003	0.114	0.001	980.46	16.98	637.22	15.19	1856.63	21.29
CBBS1_4	0.135	0.005	0.012	0.000	0.080	0.002	128.35	4.41	78.45	1.94	1192.42	52.23
CBBS6_7	0.238	0.014	0.020	0.001	0.085	0.003	216.97	11.04	130.40	6.42	1305.38	59.49
CBBS7_9	0.250	0.015	0.021	0.001	0.086	0.004	226.92	12.11	134.78	6.60	1337.32	77.59
CBBS8_5	4.583	0.134	0.170	0.005	0.196	0.002	1746.14	24.08	1010.07	25.60	2792.68	18.52
CBBS8_12	1.909	0.067	0.081	0.003	0.170	0.003	1084.13	23.27	503.79	15.78	2560.60	27.71
CBBS3_8	2.331	0.083	0.086	0.002	0.198	0.005	1221.86	24.93	529.18	13.01	2806.36	38.65
CBBS4_15	29.085	3.177	0.260	0.028	0.811	0.016	3456.37	101.94	1490.05	143.69	4941.56	28.21
CBBS8_7	1.102	0.031	0.049	0.001	0.164	0.002	754.42	14.97	307.20	7.77	2495.10	21.88
CBBS3_15	2.166	0.107	0.071	0.003	0.222	0.007	1170.27	33.64	440.21	16.47	2997.07	52.23
CBBS3_11	0.596	0.026	0.019	0.001	0.231	0.008	474.81	16.67	119.31	3.50	3061.92	57.06
CBBS7_7	0.730	0.022	0.019	0.000	0.283	0.006	556.76	13.04	119.35	2.65	3382.09	34.33

Table A-10. Detrital zircon data table for sample CB-BBM. Data from Hutto et al., (2009). Analyses performed at the LaserChron Center at the University of Arizona.

Sample Name	Isotopic Ratios						Apparent Ages					
	$^{207}Pb/^{235}U$	1σ abs. err.	$^{206}Pb/^{238}U$	1σ abs. err.	$^{207}Pb/^{206}Pb$	1σ abs. err.	$^{207}Pb/^{235}U$	1σ abs. err.	$^{206}Pb/^{238}U$	1σ abs. err.	$^{207}Pb/^{206}Pb$	1σ abs. err.
						<10 % Discordant Samples						
F1-39	0.056	0.049	0.009	0.019	21.401	0.046	55.11	2.64	55.57	1.03	35.25	109.31
F1-90	0.058	0.121	0.009	0.022	20.858	0.119	57.56	6.78	56.63	1.25	96.42	282.70
F1-96	0.058	0.053	0.009	0.012	21.241	0.052	56.82	2.95	56.91	0.69	53.25	124.00
F1-66	0.053	0.152	0.009	0.027	23.275	0.150	52.58	7.79	57.58	1.57	-169.73	374.09
F1-45	0.052	0.135	0.009	0.030	24.247	0.132	51.05	6.74	58.19	1.76	-272.54	336.50
F1-56	0.054	0.141	0.009	0.018	23.988	0.140	53.14	7.30	59.97	1.04	-245.32	355.01
F1-81	0.031	0.604	0.010	0.009	43.036	0.604	31.03	18.46	62.14	0.53	-2025.97	2472.38
F1-53	0.054	0.250	0.010	0.045	24.764	0.246	53.35	13.00	62.16	2.76	-326.59	640.46
F1-36	0.071	0.040	0.010	0.012	20.230	0.038	69.21	2.67	66.37	0.79	168.38	89.07
F1-23	0.069	0.162	0.011	0.053	21.845	0.153	68.20	10.71	70.57	3.73	-14.11	372.54
F1-22	0.069	0.216	0.011	0.036	21.946	0.213	68.04	14.20	70.72	2.55	-25.21	520.22
F1-24	0.077	0.186	0.011	0.031	20.504	0.183	75.18	13.45	73.26	2.24	136.85	433.06
F1-42	0.078	0.141	0.011	0.019	20.290	0.140	76.12	10.37	73.43	1.39	161.42	328.93
F1-87	0.077	2.747	0.011	0.054	20.499	2.746	75.46	202.39	73.52	3.95	137.44	0.00

Table A-10 Continued

Sample Name	Isotopic Ratios						Apparent Ages					
	$^{207}Pb/^{235}U$	1σ abs. err.	$^{206}Pb/^{238}U$	1σ abs. err.	$^{207}Pb/^{206}Pb$	1σ abs. err.	$^{207}Pb/^{235}U$	1σ abs. err.	$^{206}Pb/^{238}U$	1σ abs. err.	$^{207}Pb/^{206}Pb$	1σ abs. err.
<10 % Discordant Samples												
F1-32	0.066	0.149	0.012	0.030	24.340	0.146	65.34	9.43	75.19	2.21	-282.28	373.60
F1-72	0.072	0.098	0.012	0.052	22.484	0.084	70.74	6.73	75.40	3.86	-84.26	205.86
F1-33	0.054	0.809	0.012	0.017	30.385	0.809	53.24	41.99	76.03	1.31	-883.07	2826.52
F1-11	0.077	0.049	0.012	0.019	21.711	0.046	75.67	3.60	78.06	1.46	0.75	110.16
F1-59	0.093	0.098	0.014	0.046	20.177	0.087	90.57	8.53	87.42	3.95	174.45	203.96
F1-67	0.091	0.036	0.014	0.013	21.476	0.033	88.65	3.03	90.96	1.20	26.89	79.56
F1-30	0.095	0.044	0.015	0.024	21.262	0.038	92.17	3.92	93.78	2.21	50.83	89.82
F1-1	0.103	0.077	0.016	0.039	20.957	0.066	100.00	7.31	100.62	3.91	85.25	156.75
F1-95	0.122	0.120	0.016	0.021	18.047	0.118	116.52	13.23	101.80	2.07	428.80	264.72
F1-10	0.192	0.229	0.016	0.026	11.499	0.227	178.04	37.34	102.22	2.65	1359.69	443.33
F1-31	0.185	0.403	0.016	0.023	12.149	0.403	172.71	64.15	104.47	2.36	1252.98	822.28
F1-82	0.120	0.135	0.018	0.011	20.460	0.134	115.47	14.71	114.20	1.25	141.83	316.39
F1-29	0.141	0.130	0.023	0.024	22.425	0.128	133.76	16.34	145.96	3.49	-77.82	314.50
F1-43	0.156	0.046	0.024	0.016	20.843	0.043	147.36	6.28	150.44	2.33	98.11	101.72
F1-94	0.093	0.473	0.024	0.035	35.893	0.472	90.28	40.86	154.18	5.29	-1392.35	1600.40
F1-37	0.163	0.049	0.024	0.024	20.563	0.043	153.14	6.98	154.63	3.68	130.05	100.73
F1-15	0.175	0.040	0.026	0.019	20.672	0.036	163.45	6.07	166.63	3.06	117.63	84.12
F1-99	0.183	0.036	0.027	0.030	20.147	0.021	170.43	5.68	169.89	4.98	177.92	48.28
F1-69	0.180	0.052	0.027	0.022	20.479	0.047	167.98	7.98	170.00	3.61	139.65	110.06
F1-35	0.184	0.072	0.027	0.023	20.073	0.068	171.13	11.30	170.02	3.91	186.46	158.12
F1-78	0.183	0.022	0.027	0.012	20.333	0.018	170.54	3.48	171.55	2.10	156.47	42.98
F1-77	0.192	0.052	0.028	0.016	19.837	0.049	178.28	8.48	175.60	2.72	213.99	114.49
F1-65	0.193	0.105	0.029	0.028	20.380	0.102	179.35	17.34	181.50	4.98	151.05	238.95
F1-54	0.515	0.049	0.067	0.045	18.024	0.018	421.59	16.82	419.74	18.33	431.71	41.14
F1-14	0.687	0.046	0.087	0.017	17.498	0.042	531.18	18.97	539.11	9.00	497.24	93.54
F1-63	0.841	0.085	0.089	0.013	14.672	0.084	619.60	39.42	552.44	6.94	873.27	174.15
F1-85	0.783	0.021	0.097	0.007	17.044	0.020	586.97	9.41	595.29	4.04	554.90	43.35
F1-51	1.552	0.029	0.161	0.016	14.273	0.024	951.21	17.90	960.31	14.10	930.19	49.88
F1-93	1.729	0.032	0.171	0.025	13.605	0.020	1019.52	20.32	1015.63	23.12	1027.85	40.03
F1-97	1.869	0.033	0.182	0.028	13.401	0.017	1070.26	21.60	1076.11	27.35	1058.35	35.09
F1-57	2.061	0.025	0.193	0.016	12.918	0.018	1136.06	16.80	1138.31	16.90	1131.75	36.78
F1-79	1.869	0.026	0.175	0.021	12.878	0.016	1070.19	17.34	1037.26	20.22	1137.91	30.92
F1-47	2.088	0.037	0.191	0.021	12.636	0.031	1144.89	25.57	1128.76	21.43	1175.58	61.26
F1-28	2.255	0.017	0.204	0.015	12.454	0.008	1198.28	12.09	1195.01	16.47	1204.17	16.19
F1-91	2.202	0.025	0.193	0.014	12.099	0.021	1181.54	17.64	1138.62	14.51	1260.98	41.22
F1-83	2.698	0.023	0.228	0.018	11.666	0.015	1327.90	17.26	1325.41	21.33	1331.90	29.08
F1-62	2.830	0.050	0.234	0.042	11.425	0.027	1363.48	37.55	1357.98	51.55	1372.09	51.99
F1-61	2.913	0.018	0.239	0.013	11.320	0.012	1385.38	13.37	1382.46	15.80	1389.86	23.63
F1-9	2.977	0.032	0.244	0.031	11.299	0.010	1401.76	24.41	1407.23	38.56	1393.42	19.24
F1-7	3.017	0.021	0.246	0.019	11.252	0.011	1411.82	16.27	1418.68	23.56	1401.47	20.37
F1-89	2.996	0.026	0.244	0.022	11.243	0.014	1406.49	19.90	1408.84	27.59	1402.91	27.64
F1-26	3.108	0.039	0.250	0.035	11.085	0.016	1434.79	29.98	1437.99	45.63	1430.03	31.30
F1-12	3.057	0.020	0.246	0.014	11.084	0.014	1422.09	15.00	1416.69	17.30	1430.15	26.94
F1-55	3.015	0.021	0.239	0.017	10.948	0.012	1411.34	16.12	1383.37	21.29	1453.79	23.63
F1-16	3.213	0.023	0.254	0.018	10.908	0.015	1460.26	18.09	1459.95	23.91	1460.71	27.58
F1-46	3.052	0.031	0.240	0.022	10.844	0.023	1420.75	24.07	1386.93	27.33	1471.78	42.88
F1-74	3.128	0.057	0.245	0.031	10.808	0.048	1439.72	44.02	1413.85	38.72	1478.13	91.76

Table A-10 Continued

Sample Name	Isotopic Ratios						Apparent Ages					
	$^{207}Pb/^{235}U$	1σ abs. err.	$^{206}Pb/^{238}U$	1σ abs. err.	$^{207}Pb/^{206}Pb$	1σ abs. err.	$^{207}Pb/^{235}U$	1σ abs. err.	$^{206}Pb/^{238}U$	1σ abs. err.	$^{207}Pb/^{206}Pb$	1σ abs. err.
					<10 % Discordant Samples							
F1-8	2.476	0.025	0.193	0.020	10.762	0.015	1265.15	18.05	1139.20	21.20	1486.17	27.47
F1-50	3.303	0.058	0.257	0.034	10.719	0.047	1481.78	45.11	1473.35	45.31	1493.86	88.04
F1-48	3.291	0.022	0.249	0.015	10.452	0.016	1478.83	16.93	1435.58	19.30	1541.42	29.58
F1-52	2.975	0.075	0.225	0.062	10.413	0.042	1401.13	56.91	1306.33	73.20	1548.46	78.94
F1-27	3.762	0.028	0.272	0.016	9.965	0.023	1584.76	22.21	1550.60	22.19	1630.50	41.85
F1-86	4.140	0.027	0.296	0.021	9.873	0.017	1662.28	21.89	1673.70	30.22	1647.86	31.92
F1-20	4.134	0.033	0.295	0.028	9.835	0.018	1660.99	26.83	1665.68	40.37	1655.04	33.17
F1-98	4.149	0.030	0.296	0.025	9.823	0.017	1663.96	24.29	1669.27	36.18	1657.26	30.79
F1-6	4.215	0.036	0.299	0.033	9.781	0.014	1677.02	29.54	1686.59	49.12	1665.05	26.15
F1-21	4.180	0.024	0.296	0.022	9.761	0.009	1670.06	19.26	1670.88	32.23	1669.00	15.77
F1-80	4.080	0.027	0.288	0.017	9.727	0.022	1650.36	22.17	1630.71	23.77	1675.45	39.93
F1-49	3.540	0.042	0.249	0.040	9.707	0.014	1536.15	33.39	1434.39	51.06	1679.18	26.20
F1-5	4.267	0.047	0.299	0.043	9.648	0.019	1687.04	38.87	1684.28	64.33	1690.46	34.34
F1-38	4.332	0.020	0.303	0.014	9.633	0.015	1699.56	16.88	1704.64	21.27	1693.30	27.15
F1-92	4.189	0.041	0.292	0.024	9.614	0.033	1671.80	33.23	1651.89	35.27	1696.87	59.91
F1-2	4.200	0.039	0.292	0.035	9.598	0.017	1673.94	31.96	1653.20	51.04	1700.01	31.54
F1-3	4.352	0.029	0.302	0.024	9.582	0.016	1703.22	23.73	1703.39	35.78	1702.99	29.36
F1-75	4.303	0.030	0.299	0.028	9.580	0.011	1693.88	24.66	1686.06	41.39	1703.56	19.90
F1-73	4.353	0.032	0.302	0.024	9.559	0.021	1703.49	26.53	1700.17	36.32	1707.56	38.66
F1-60	4.235	0.015	0.293	0.009	9.551	0.012	1680.81	12.05	1658.20	12.87	1709.12	21.60
F1-88	4.421	0.026	0.306	0.021	9.547	0.016	1716.23	21.71	1721.50	31.12	1709.78	29.81
F1-40	4.430	0.031	0.305	0.020	9.502	0.024	1717.89	25.30	1717.30	29.40	1718.61	43.20
F1-34	4.441	0.035	0.306	0.031	9.485	0.016	1720.04	28.70	1718.64	46.62	1721.74	28.67
F1-68	4.490	0.037	0.308	0.034	9.472	0.015	1729.17	30.95	1733.19	51.82	1724.31	27.57
F1-19	4.447	0.041	0.305	0.019	9.456	0.037	1721.05	34.39	1715.87	28.47	1727.35	67.79
F1-70	4.660	0.025	0.314	0.022	9.290	0.013	1760.17	21.10	1760.48	33.58	1759.80	23.22
F1-64	4.819	0.023	0.320	0.016	9.148	0.016	1788.29	19.09	1788.58	24.68	1787.94	29.71
F1-76	4.953	0.030	0.326	0.023	9.066	0.018	1811.33	25.01	1817.28	37.06	1804.47	32.95
F1-4	4.885	0.023	0.320	0.022	9.029	0.007	1799.74	19.23	1789.27	34.06	1811.88	12.18
F1-41	5.325	0.020	0.337	0.015	8.722	0.012	1872.82	16.77	1871.42	24.69	1874.35	22.36
F1-25	5.698	0.022	0.351	0.013	8.487	0.018	1931.09	18.85	1938.12	21.59	1923.54	31.55
F1-18	6.157	0.043	0.365	0.039	8.167	0.018	1998.41	37.77	2004.45	67.53	1992.16	32.36
F1-17	0.427	0.250	0.025	0.040	8.147	0.247	361.37	76.16	160.81	6.40	1996.41	445.76
F1-84	6.278	0.031	0.356	0.007	7.816	0.030	2015.37	27.12	1962.58	12.18	2069.89	53.06
F1-100	10.829	0.022	0.476	0.015	6.057	0.017	2508.54	20.49	2508.54	30.13	2508.52	27.92
F1-58	12.954	0.031	0.507	0.028	5.398	0.014	2676.31	29.43	2644.34	60.74	2700.55	22.79
F1-13	13.971	0.028	0.534	0.020	5.267	0.019	2747.74	26.29	2756.81	45.54	2741.07	31.09
F1-71	14.803	0.027	0.545	0.023	5.072	0.015	2802.67	26.12	2802.33	52.95	2802.91	23.76

Table A-11. Detrital zircon data table for sample CZ. Data from Hutto et al., (2009). Analyses performed at the LaserChron Center at the University of Arizona.

Sample Name	Isotopic Ratios $^{207}Pb/^{235}U$	1σ abs. err.	$^{206}Pb/^{238}U$	1σ abs. err.	$^{207}Pb/^{206}Pb$	1σ abs. err.	Apparent Ages $^{207}Pb/^{235}U$	1σ abs. err.	$^{206}Pb/^{238}U$	1σ abs. err.	$^{207}Pb/^{206}Pb$	1σ abs. err.
						<10 % Discordant Samples						
B1-39	0.052	0.338	21.914	0.333	0.008	0.062	53.04	3.30	51.45	16.98	-21.76	825.11
B1-14	0.055	0.045	21.850	0.042	0.009	0.016	55.77	0.87	54.20	2.38	-14.74	102.19
B1-54	0.056	0.081	22.020	0.080	0.009	0.012	57.11	0.70	55.06	4.32	-33.43	193.50
B1-36	0.064	0.413	19.226	0.413	0.009	0.019	57.18	1.09	62.89	25.19	285.99	981.99
B1-2	0.058	0.070	21.152	0.066	0.009	0.022	57.20	1.28	57.34	3.89	63.24	157.29
B1-47	0.059	0.090	21.299	0.087	0.009	0.024	58.48	1.38	58.20	5.11	46.65	208.60
B1-51	0.054	0.405	23.569	0.398	0.009	0.070	59.22	4.14	53.39	21.04	-201.04	1034.15
B1-81	0.062	0.200	21.987	0.195	0.010	0.044	63.89	2.82	61.51	11.94	-29.86	476.70
B1-31	0.075	0.181	18.636	0.176	0.010	0.043	64.68	2.74	73.06	12.77	356.82	400.22
B1-26	0.060	0.110	23.359	0.109	0.010	0.012	64.70	0.75	58.72	6.25	-178.69	272.40
B1-63	0.058	0.228	26.315	0.225	0.011	0.036	71.20	2.57	57.43	12.74	-485.09	604.10
B1-64	0.109	0.111	14.044	0.104	0.011	0.040	71.24	2.83	105.14	11.14	963.29	213.17
B1-71	0.054	0.368	28.639	0.367	0.011	0.030	71.59	2.10	53.18	19.07	-715.26	1050.52
B1-24	0.076	0.105	20.434	0.100	0.011	0.033	72.55	2.35	74.73	7.55	144.87	234.21
B1-37	0.071	0.080	22.347	0.077	0.012	0.019	73.93	1.38	69.81	5.37	-69.36	189.11
B1-45	0.066	0.141	24.214	0.139	0.012	0.021	74.05	1.55	64.69	8.83	-269.17	355.03
B1-13	0.067	0.136	23.973	0.131	0.012	0.034	74.34	2.50	65.57	8.62	-243.75	333.34
B1-95	0.075	0.085	21.458	0.082	0.012	0.022	74.70	1.65	73.33	5.98	28.91	195.85
B1-69	0.074	0.140	21.838	0.140	0.012	0.013	74.83	1.00	72.22	9.79	-13.36	339.11
B1-19	0.082	0.141	19.712	0.139	0.012	0.019	74.97	1.42	79.86	10.81	228.62	323.41
B1-4	0.074	0.053	21.699	0.039	0.012	0.036	75.03	2.72	72.85	3.74	2.07	93.37
B1-50	0.075	0.030	21.584	0.027	0.012	0.012	75.18	0.90	73.37	2.10	14.83	65.19
B1-80	0.071	0.107	23.005	0.103	0.012	0.031	75.88	2.35	69.62	7.21	-140.62	254.40
B1-89	0.098	0.114	16.642	0.111	0.012	0.028	76.09	2.15	95.27	10.39	606.78	240.01
B1-60	0.070	0.157	23.614	0.156	0.012	0.010	76.40	0.73	68.33	10.35	-205.81	394.16
B1-29	0.079	0.034	21.139	0.018	0.012	0.029	77.44	2.22	77.05	2.51	64.73	42.44
B1-42	0.115	0.162	15.033	0.161	0.013	0.020	80.20	1.58	110.36	16.92	822.78	337.22
B1-90	0.111	0.193	16.123	0.191	0.013	0.033	83.18	2.72	106.93	19.63	674.95	410.92
B1-56	0.080	0.124	22.904	0.121	0.013	0.026	85.58	2.23	78.57	9.37	-129.82	300.18
B1-73	0.089	0.054	20.993	0.048	0.014	0.025	86.49	2.14	86.30	4.48	81.16	114.29
B1-97	0.089	0.065	21.672	0.054	0.014	0.036	90.00	3.20	86.98	5.42	5.07	130.80
B1-9	0.102	0.030	19.370	0.027	0.014	0.014	92.03	1.23	98.95	2.87	268.86	62.67
B1-35	0.096	0.056	20.946	0.051	0.015	0.023	93.21	2.08	92.96	4.96	86.47	121.39
B1-52	0.101	0.204	20.038	0.203	0.015	0.015	94.25	1.42	98.02	19.03	190.52	476.67
B1-82	0.102	0.040	21.463	0.033	0.016	0.023	101.97	2.34	99.01	3.77	28.31	78.24
B1-3	0.131	0.108	20.022	0.101	0.019	0.037	121.44	4.46	124.96	12.69	192.40	236.17
B1-17	0.156	0.081	21.226	0.081	0.024	0.005	153.00	0.77	147.21	11.08	54.94	192.74
B1-77	0.170	0.074	20.713	0.072	0.025	0.018	162.16	2.87	159.05	10.93	112.98	170.20
B1-10	0.179	0.027	20.056	0.023	0.026	0.013	165.30	2.07	166.83	4.10	188.45	54.53
B1-23	0.172	0.045	20.972	0.041	0.026	0.018	166.40	2.91	161.08	6.70	83.56	98.11
B1-43	0.198	0.142	18.510	0.133	0.027	0.049	169.41	8.26	183.73	23.83	372.03	300.36
B1-91	0.233	0.052	17.137	0.049	0.029	0.019	184.14	3.43	212.79	10.04	543.01	106.60
B1-1	0.204	0.098	20.408	0.090	0.030	0.038	191.84	7.20	188.57	16.83	147.80	211.56
B1-85	0.216	0.074	20.791	0.070	0.033	0.023	206.85	4.60	198.78	13.35	104.06	166.52
B1-75	0.225	0.069	21.182	0.067	0.035	0.015	218.71	3.29	205.76	12.89	59.79	161.00
B1-55	0.327	0.047	19.324	0.045	0.046	0.012	288.78	3.33	287.20	11.69	274.29	103.66
B1-68	0.460	0.050	18.502	0.035	0.062	0.036	386.33	13.39	384.44	15.93	373.06	78.06
B1-16	0.540	0.225	16.434	0.221	0.064	0.044	402.14	17.23	438.47	80.45	633.94	481.41
B1-20	0.548	0.024	17.912	0.015	0.071	0.020	443.56	8.36	443.89	8.77	445.59	32.54
B1-58	0.669	0.038	17.731	0.031	0.086	0.022	532.04	10.98	520.12	15.35	468.10	68.59
B1-59	0.787	0.043	16.870	0.042	0.096	0.010	592.86	5.66	589.64	19.19	577.24	90.70
B1-28	0.846	0.020	16.569	0.014	0.102	0.015	623.99	8.98	622.31	9.44	616.20	29.24

Table A-11 Continued

Sample Name	$^{207}Pb/^{235}U$	1σ abs. err.	$^{206}Pb/^{238}U$	1σ abs. err.	$^{207}Pb/^{206}Pb$	1σ abs. err.	$^{207}Pb/^{235}U$	1σ abs. err.	$^{206}Pb/^{238}U$	1σ abs. err.	$^{207}Pb/^{206}Pb$	1σ abs. err.
			Isotopic Ratios						Apparent Ages			
						<10 % Discordant Samples						
B1-27	1.821	0.035	13.431	0.015	0.177	0.032	1052.70	30.98	1053.06	23.13	1053.79	30.34
B1-32	1.874	0.038	13.211	0.033	0.180	0.018	1064.76	17.47	1072.07	25.05	1086.94	66.91
B1-8	1.874	0.024	13.128	0.014	0.178	0.020	1058.20	19.52	1071.82	16.13	1099.64	27.83
B1-33	1.925	0.018	13.073	0.007	0.183	0.017	1080.74	16.72	1089.83	12.23	1108.01	14.54
B1-96	2.123	0.026	12.786	0.023	0.197	0.011	1158.36	11.45	1156.21	17.69	1152.17	46.15
B1-88	1.913	0.030	12.644	0.020	0.175	0.022	1042.12	20.69	1085.76	19.74	1174.37	40.26
B1-72	2.536	0.056	11.395	0.032	0.210	0.045	1226.71	50.38	1282.51	40.48	1377.22	62.38
B1-40	2.947	0.025	11.174	0.014	0.239	0.021	1380.65	26.47	1394.10	19.20	1414.72	26.21
B1-74	3.085	0.037	11.121	0.019	0.249	0.031	1432.46	39.95	1428.96	28.00	1423.74	36.51
B1-5	2.924	0.019	11.109	0.017	0.236	0.008	1363.69	9.96	1388.13	14.25	1425.90	32.47
B1-18	2.757	0.022	11.037	0.019	0.221	0.012	1285.33	13.75	1343.86	16.67	1438.28	36.23
B1-34	2.796	0.042	10.953	0.018	0.222	0.038	1292.96	44.17	1354.40	31.19	1452.76	33.88
B1-22	2.966	0.022	10.902	0.018	0.235	0.012	1358.07	14.33	1398.91	16.50	1461.69	34.81
B1-99	3.261	0.067	10.744	0.063	0.254	0.022	1459.68	28.87	1471.81	52.18	1489.33	120.05
B1-92	3.211	0.046	10.598	0.039	0.247	0.024	1421.96	30.50	1459.75	35.50	1515.18	73.81
B1-12	3.611	0.031	10.305	0.011	0.270	0.029	1540.20	40.14	1551.96	24.81	1568.00	20.06
B1-25	3.278	0.051	10.181	0.046	0.242	0.022	1397.37	27.26	1475.84	39.57	1590.54	85.92
B1-6	3.318	0.020	10.120	0.019	0.244	0.007	1405.08	8.96	1485.29	15.90	1601.77	35.64
B1-83	3.858	0.041	10.057	0.029	0.281	0.028	1598.32	40.06	1604.87	32.88	1613.47	54.66
B1-84	3.775	0.048	10.033	0.018	0.275	0.044	1564.45	61.26	1587.39	38.38	1617.98	34.26
B1-62	4.209	0.021	9.775	0.010	0.298	0.019	1683.30	27.70	1675.74	17.21	1666.27	17.58
B1-76	4.218	0.026	9.749	0.020	0.298	0.016	1682.58	23.99	1677.57	21.13	1671.29	36.99
B1-87	3.314	0.027	9.681	0.022	0.233	0.016	1348.63	19.84	1484.40	21.18	1684.14	40.07
B1-94	4.267	0.018	9.678	0.014	0.300	0.012	1689.02	17.38	1687.10	15.09	1684.71	26.08
B1-15	4.053	0.019	9.651	0.012	0.284	0.015	1610.02	20.80	1644.95	15.55	1689.86	22.71
B1-7	4.349	0.021	9.617	0.017	0.303	0.012	1707.72	17.40	1702.62	17.13	1696.34	31.71
B1-70	4.221	0.032	9.562	0.015	0.293	0.028	1655.21	40.87	1678.14	25.89	1706.91	26.69
B1-61	4.107	0.027	9.557	0.023	0.285	0.015	1614.75	21.71	1655.64	22.18	1707.91	41.42
B1-93	4.330	0.035	9.553	0.009	0.300	0.034	1691.41	50.43	1699.14	28.92	1708.68	16.38
B1-66	4.056	0.021	9.534	0.007	0.280	0.020	1593.75	27.68	1645.52	16.98	1712.28	13.06
B1-46	4.386	0.029	9.529	0.021	0.303	0.020	1706.78	30.44	1709.72	24.11	1713.31	38.47
B1-100	3.512	0.067	9.482	0.015	0.241	0.065	1394.47	82.01	1529.85	53.10	1722.41	27.77
B1-11	4.468	0.026	9.384	0.011	0.304	0.024	1711.43	35.77	1725.01	21.59	1741.51	19.25
B1-65	4.197	0.028	9.372	0.019	0.285	0.021	1618.04	30.48	1673.48	23.27	1743.70	34.36
B1-30	4.262	0.039	9.346	0.030	0.289	0.025	1636.04	35.55	1686.09	31.73	1748.89	54.40
B1-78	4.629	0.017	9.318	0.008	0.313	0.015	1754.67	22.27	1754.52	14.00	1754.31	15.39
B1-48	4.609	0.034	9.289	0.023	0.310	0.025	1743.08	38.79	1750.85	28.43	1760.12	41.52
B1-38	4.339	0.058	9.221	0.020	0.290	0.054	1642.59	78.59	1700.87	47.83	1773.45	37.24
B1-44	3.939	0.022	9.052	0.014	0.259	0.017	1482.83	22.92	1621.80	18.03	1807.14	25.46
B1-57	5.214	0.018	8.510	0.013	0.322	0.013	1798.36	20.40	1854.84	15.37	1918.75	22.42
B1-53	5.495	0.091	8.075	0.088	0.322	0.025	1798.71	38.47	1899.85	78.51	2012.19	156.16
B1-21	6.845	0.016	7.517	0.010	0.373	0.012	2044.31	20.85	2091.51	14.00	2138.28	18.19
B1-49	5.685	0.047	7.512	0.015	0.310	0.044	1739.36	67.08	1929.08	40.25	2139.52	26.76
B1-79	7.980	0.017	6.833	0.013	0.395	0.012	2148.26	21.74	2228.79	15.77	2303.63	21.99
B1-41	9.518	0.041	6.321	0.020	0.436	0.035	2334.20	68.93	2389.30	37.40	2436.61	34.57
B1-67	14.358	0.027	4.965	0.018	0.517	0.020	2686.42	43.50	2773.68	25.47	2837.79	29.52

Table A-12. Detrital zircon data table for sample QC. Sample analyzed by LA-ICP-MS on 11-11-2014 and 12-10-2014.

Sample Name	Isotopic Ratios						Apparent Ages					
	$^{207}Pb/^{235}U$	1σ abs. err.	$^{206}Pb/^{238}U$	1σ abs. err.	$^{207}Pb/^{206}Pb$	1σ abs. err.	$^{207}Pb/^{235}U$	1σ abs. err.	$^{206}Pb/^{238}U$	1σ abs. err.	$^{207}Pb/^{206}Pb$	1σ abs. err.
					<10 % Discordant Samples							
Q1_1	0.107	0.005	0.016	0.001	0.788	0.049	103.17	4.58	100.47	3.86	165.62	66.13
Q1_2	2.676	0.118	0.216	0.009	0.926	0.090	1321.78	32.03	1262.58	45.91	1418.96	31.55
Q1_3	0.395	0.023	0.052	0.003	0.946	0.055	337.92	16.84	324.96	17.62	427.86	42.27
Q1_4	1.576	0.071	0.150	0.006	0.829	0.076	960.64	27.76	899.54	32.28	1103.14	49.96
Q1_5	3.564	0.148	0.259	0.010	0.903	0.100	1541.48	32.45	1482.26	49.00	1623.55	32.93
Q1_6	1.875	0.082	0.187	0.007	0.834	0.073	1072.46	28.66	1103.26	37.81	1010.23	48.32
Q1_7	2.895	0.115	0.239	0.008	0.910	0.088	1380.49	29.59	1381.26	44.07	1379.16	31.36
Q1_8	0.076	0.005	0.011	0.001	0.615	0.048	74.22	4.56	73.56	3.43	95.25	116.26
Q1_10	2.888	0.122	0.230	0.009	0.881	0.091	1378.90	31.48	1334.65	44.83	1447.97	37.65
Q1_11	3.790	0.156	0.279	0.010	0.899	0.099	1590.55	32.58	1585.78	51.34	1596.74	33.33
Q1_12	9.334	0.364	0.441	0.015	0.923	0.154	2371.36	35.14	2353.70	68.90	2386.46	25.32
Q1_13	9.308	0.376	0.416	0.015	0.922	0.162	2368.84	36.35	2242.27	68.70	2479.52	26.09
Q1_14	1.985	0.086	0.184	0.007	0.914	0.078	1110.48	28.81	1090.51	39.14	1149.67	34.43
Q1_15	0.900	0.041	0.101	0.004	0.862	0.065	651.70	21.90	618.93	23.69	766.72	48.46
Q1_16	1.968	0.081	0.182	0.007	0.911	0.079	1104.65	27.26	1075.17	36.37	1163.03	33.20
Q2_1	2.514	0.099	0.214	0.008	0.908	0.085	1276.20	28.34	1250.05	39.89	1320.33	31.77
Q2_2	3.131	0.123	0.246	0.009	0.898	0.092	1440.38	29.88	1420.30	44.21	1469.98	32.52
Q2_3	1.714	0.071	0.167	0.006	0.892	0.074	1013.62	26.18	995.27	33.65	1053.29	37.14
Q2_4	1.656	0.066	0.165	0.006	0.890	0.073	991.76	24.77	982.35	31.62	1012.44	36.22
Q2_5	2.511	0.104	0.215	0.008	0.885	0.085	1275.33	29.74	1255.34	41.59	1308.98	37.14
Q2_6	3.107	0.122	0.248	0.009	0.906	0.091	1434.45	29.79	1430.20	44.67	1440.57	31.47
Q2_7	1.848	0.073	0.178	0.006	0.898	0.075	1062.55	25.86	1057.75	34.20	1072.21	34.80
Q2_8	0.100	0.004	0.015	0.001	0.856	0.050	97.24	3.79	93.97	3.28	177.80	48.65
Q2_9	1.768	0.070	0.171	0.006	0.904	0.075	1033.69	25.41	1018.13	33.08	1066.56	33.84
Q2_11	2.971	0.121	0.240	0.009	0.908	0.090	1400.18	30.40	1384.64	45.04	1423.73	32.15
Q2_12	4.117	0.161	0.276	0.009	0.902	0.108	1657.78	31.36	1568.94	47.83	1772.06	30.43
Q2_13	1.675	0.066	0.168	0.006	0.900	0.072	999.22	24.67	999.83	32.08	997.68	34.37
Q2_14	2.076	0.102	0.181	0.008	0.854	0.083	1140.76	33.07	1073.41	42.28	1271.00	49.05
Q2_15	0.750	0.032	0.088	0.003	0.826	0.062	568.48	18.16	544.73	18.52	664.43	50.10
Q2_16	0.450	0.019	0.056	0.002	0.893	0.058	377.00	13.23	352.28	12.84	531.60	41.15
Q3_1	4.270	0.131	0.299	0.009	0.933	0.104	1687.57	24.85	1686.79	42.66	1688.17	20.17
Q3_2	0.192	0.007	0.026	0.001	0.867	0.054	178.46	5.96	162.75	5.33	391.53	40.39
Q3_4	1.655	0.055	0.170	0.005	0.906	0.070	991.43	20.89	1014.52	29.04	940.28	28.65
Q3_5	6.003	0.195	0.360	0.011	0.943	0.121	1976.35	27.84	1981.89	52.44	1970.20	19.09
Q3_6	4.102	0.126	0.290	0.008	0.949	0.103	1654.63	24.73	1641.50	42.20	1670.98	17.81
Q3_8	1.802	0.061	0.162	0.005	0.920	0.081	1046.20	21.99	969.04	28.71	1210.66	26.09
Q3_9	2.625	0.081	0.224	0.007	0.934	0.085	1307.56	22.35	1304.51	34.17	1312.18	21.23
Q3_10	1.815	0.060	0.176	0.005	0.832	0.075	1050.77	21.57	1047.36	28.41	1057.48	36.90
Q3_12	1.971	0.063	0.184	0.006	0.932	0.077	1105.69	21.30	1091.30	30.21	1133.71	22.96
Q3_13	4.277	0.137	0.297	0.009	0.928	0.105	1688.99	26.01	1674.96	44.33	1706.08	21.82
Q3_14	1.230	0.031	0.123	0.003	0.853	0.073	814.45	14.02	747.54	15.15	1001.92	26.50
Q3_15	1.614	0.059	0.154	0.005	0.844	0.076	975.58	22.57	921.35	26.33	1099.76	38.52
Q4_1	2.257	0.085	0.196	0.007	0.934	0.083	1199.06	26.11	1151.11	36.72	1274.77	25.93
Q4_2	2.358	0.098	0.205	0.008	0.900	0.083	1229.97	29.12	1203.02	41.38	1265.76	34.91
Q4_3	3.816	0.145	0.271	0.010	0.934	0.101	1596.21	30.14	1548.08	48.48	1649.18	24.98
Q4_4	0.487	0.020	0.062	0.002	0.879	0.057	402.83	13.45	387.16	13.75	480.41	42.35
Q4_5	0.060	0.003	0.009	0.000	0.878	0.050	59.17	2.43	55.39	2.10	201.09	46.44
Q4_7	1.585	0.060	0.158	0.006	0.931	0.072	964.17	23.17	945.26	30.62	995.29	27.72
Q4_9	0.110	0.004	0.016	0.001	0.862	0.049	105.81	3.99	104.27	3.65	126.33	46.89
Q4_10	1.785	0.069	0.172	0.006	0.931	0.075	1040.14	24.80	1025.85	33.89	1058.15	28.14

Table A-12 Continued

Sample Name	$^{207}Pb/^{235}U$	1σ abs. err.	$^{206}Pb/^{238}U$	1σ abs. err.	$^{207}Pb/^{206}Pb$	1σ abs. err.	$^{207}Pb/^{235}U$	1σ abs. err.	$^{206}Pb/^{238}U$	1σ abs. err.	$^{207}Pb/^{206}Pb$	1σ abs. err.
			Isotopic Ratios						Apparent Ages			
					<10 % Discordant Samples							
Q5_1	0.659	0.038	0.083	0.004	0.984	0.057	513.79	22.89	515.54	24.83	505.78	26.24
Q5_2	0.179	0.012	0.026	0.001	0.974	0.051	167.17	9.89	162.95	8.67	227.04	38.99
Q5_4	1.902	0.121	0.167	0.010	0.985	0.082	1081.90	41.34	997.78	52.29	1255.26	23.99
Q5_5	3.650	0.216	0.274	0.014	0.984	0.097	1560.45	46.17	1560.01	71.82	1560.85	22.93
Q5_6	0.079	0.006	0.011	0.001	0.980	0.051	77.55	5.53	71.80	4.73	258.27	36.60
Q5_7	0.569	0.037	0.071	0.004	0.975	0.058	457.45	23.48	440.70	23.05	542.28	36.34
Q5_8	1.833	0.109	0.177	0.009	0.982	0.075	1057.34	38.43	1049.29	50.19	1073.80	25.77
Q5_9	4.633	0.275	0.311	0.016	0.985	0.108	1755.31	48.32	1744.62	79.80	1767.87	21.35
Q5_11	1.911	0.122	0.173	0.010	0.979	0.080	1084.83	41.56	1028.31	52.17	1199.95	28.95
Q5_12	0.539	0.035	0.066	0.004	0.979	0.059	437.88	22.92	411.47	22.51	579.00	32.65
Q5_14	1.646	0.106	0.153	0.009	0.986	0.078	987.95	39.92	918.58	49.59	1145.19	23.98
Q5_16	0.487	0.033	0.063	0.004	0.978	0.056	403.03	22.19	394.32	22.34	453.08	35.11
Q6_1	2.262	0.095	0.205	0.007	0.981	0.080	1200.55	29.19	1201.81	36.97	1198.32	21.50
Q6_2	1.147	0.046	0.124	0.004	0.983	0.067	775.73	21.58	751.00	22.38	847.62	22.41
Q6_3	1.467	0.114	0.147	0.011	0.989	0.073	916.78	45.71	881.90	59.84	1001.74	23.80
Q6_4	1.443	0.069	0.151	0.005	0.970	0.069	906.93	28.36	907.89	29.13	904.62	34.10
Q6_5	3.957	0.165	0.292	0.010	0.980	0.098	1625.49	33.15	1652.32	47.33	1590.97	21.46
Q6_6	1.718	0.067	0.165	0.005	0.983	0.075	1015.27	24.83	986.10	27.49	1078.78	21.91
Q6_7	1.975	0.078	0.189	0.006	0.983	0.076	1106.87	26.18	1116.40	30.90	1088.23	22.14
Q6_8	1.712	0.072	0.168	0.005	0.978	0.074	1013.16	26.59	1000.67	27.63	1040.30	28.42
Q6_9	1.595	0.066	0.161	0.005	0.980	0.072	968.37	25.43	963.24	28.31	980.09	24.24
Q6_10	0.393	0.017	0.052	0.002	0.977	0.055	336.36	12.05	325.89	9.89	409.49	30.15
Q6_13	1.481	0.074	0.144	0.006	0.976	0.075	922.60	29.84	865.63	33.52	1061.43	26.01
Q6_14	2.134	0.095	0.194	0.007	0.976	0.080	1159.88	30.41	1145.18	36.26	1187.49	25.93
Q6_15	2.309	0.095	0.205	0.006	0.980	0.082	1215.20	28.69	1204.18	33.94	1234.85	24.16
Q6_16	3.901	0.161	0.280	0.009	0.981	0.101	1613.87	32.82	1591.56	45.87	1643.14	20.58
Q7_1	4.504	0.198	0.309	0.006	1.185	0.106	1731.78	35.92	1735.82	29.89	1726.97	29.86
Q7_2	2.292	0.102	0.206	0.004	1.185	0.081	1209.73	30.93	1207.87	21.78	1213.14	32.62
Q7_3	1.319	0.098	0.138	0.007	0.973	0.069	854.27	42.16	832.65	42.14	910.93	50.87
Q7_4	12.676	0.568	0.507	0.011	1.147	0.181	2655.87	41.30	2643.82	46.06	2665.13	27.02
Q7_6	3.043	0.144	0.242	0.006	1.073	0.091	1418.37	35.65	1394.63	32.55	1454.28	31.48
Q7_8	3.747	0.216	0.262	0.011	0.995	0.104	1581.52	45.12	1498.65	54.49	1693.94	31.67
Q7_9	2.483	0.125	0.223	0.006	1.049	0.081	1267.08	35.80	1296.68	33.76	1217.26	34.88
Q7_10	5.624	0.272	0.341	0.009	1.062	0.120	1919.83	40.92	1892.76	44.37	1949.27	30.14
Q7_11	0.098	0.007	0.014	0.001	0.997	0.052	94.75	6.25	87.99	3.65	268.66	62.50
Q7_12	0.106	0.007	0.016	0.000	1.094	0.050	102.67	6.12	99.36	2.88	180.34	63.94
Q7_13	0.376	0.018	0.052	0.001	1.084	0.052	324.38	13.44	329.77	8.20	286.00	40.87
Q7_14	1.904	0.089	0.184	0.004	1.112	0.075	1082.57	30.60	1087.22	23.34	1073.32	34.27
Q7_15	9.784	0.477	0.436	0.013	1.044	0.163	2414.64	43.92	2331.14	56.33	2485.88	27.27
Q7_16	1.662	0.084	0.155	0.005	1.029	0.078	994.31	31.65	926.27	26.92	1147.68	33.20
Q8_1	2.232	0.150	0.206	0.007	1.111	0.079	1191.12	46.15	1205.85	37.42	1164.69	47.57
Q8_2	1.766	0.125	0.170	0.006	1.090	0.075	1033.11	44.92	1012.11	34.26	1078.04	52.17
Q8_3	2.092	0.144	0.192	0.007	1.092	0.079	1146.29	46.30	1130.79	37.28	1175.94	48.64
Q8_4	4.288	0.306	0.298	0.012	1.053	0.105	1691.07	57.10	1678.96	60.40	1706.31	44.75
Q8_5	4.107	0.285	0.289	0.011	1.073	0.103	1655.79	55.22	1635.60	54.81	1681.68	44.52
Q8_6	1.933	0.133	0.190	0.007	1.086	0.074	1092.58	45.10	1121.07	37.59	1036.45	49.02
Q8_7	1.872	0.126	0.177	0.006	1.106	0.077	1071.13	43.67	1048.75	33.34	1117.19	47.70
Q8_8	2.092	0.141	0.193	0.007	1.114	0.079	1146.08	45.15	1136.56	35.12	1164.33	47.66
Q8_9	1.879	0.126	0.180	0.006	1.110	0.076	1073.65	43.46	1068.00	33.50	1085.33	47.54
Q8_10	2.257	0.161	0.213	0.009	1.056	0.077	1198.83	48.92	1242.39	45.63	1121.35	48.80
Q8_11	2.255	0.153	0.207	0.007	1.108	0.079	1198.36	46.74	1214.42	38.01	1169.71	48.45
Q8_12	1.559	0.115	0.157	0.007	1.039	0.072	954.07	44.78	941.59	38.21	983.19	51.61

	Isotopic Ratios						Apparent Ages					
Sample Name	$^{207}Pb/^{235}U$	1σ abs. err.	$^{206}Pb/^{238}U$	1σ abs. err.	$^{207}Pb/^{206}Pb$	1σ abs. err.	$^{207}Pb/^{235}U$	1σ abs. err.	$^{206}Pb/^{238}U$	1σ abs. err.	$^{207}Pb/^{206}Pb$	1σ abs. err.
						<10 % Discordant Samples						
Q8_13	0.532	0.039	0.069	0.003	1.076	0.056	433.19	25.74	429.61	16.13	452.45	61.44
Q8_14	2.011	0.137	0.184	0.006	1.100	0.079	1119.34	45.30	1087.73	35.14	1181.44	48.24
Q8_15	1.803	0.127	0.179	0.007	1.081	0.073	1046.39	44.91	1059.55	36.42	1019.21	50.99
Q8_16	0.112	0.010	0.016	0.001	1.003	0.052	107.67	9.01	100.59	5.49	267.38	74.14
Q9_1	0.587	0.036	0.075	0.002	1.075	0.057	469.00	22.88	464.26	14.45	492.35	51.35
Q9_2	2.118	0.141	0.196	0.008	1.008	0.078	1154.81	44.78	1156.40	45.18	1151.95	44.03
Q9_3	1.714	0.102	0.169	0.005	1.085	0.073	1013.67	37.31	1008.75	28.86	1024.42	44.15
Q9_4	0.175	0.011	0.026	0.001	1.047	0.050	163.83	9.83	162.33	5.76	185.74	57.80
Q9_5	4.507	0.319	0.330	0.017	0.991	0.099	1732.21	57.14	1839.09	81.56	1605.55	38.87
Q9_6	3.986	0.229	0.295	0.009	1.106	0.098	1631.40	45.58	1666.12	42.49	1587.02	39.30
Q9_7	0.498	0.032	0.066	0.002	1.049	0.055	410.41	21.18	410.50	14.02	410.08	52.56
Q9_8	2.003	0.182	0.188	0.014	0.975	0.077	1116.55	59.66	1108.38	74.66	1132.58	49.03
Q9_9	0.208	0.015	0.029	0.001	0.991	0.052	191.78	12.68	184.38	8.95	283.97	56.37
Q9_10	1.869	0.122	0.179	0.006	1.067	0.076	1070.18	42.22	1060.88	33.11	1089.31	51.42
Q9_11	0.192	0.014	0.025	0.001	1.002	0.055	178.73	11.77	162.19	7.22	403.54	59.08
Q9_12	1.983	0.144	0.186	0.009	0.998	0.077	1109.70	47.77	1099.71	46.60	1129.44	51.75
Q9_13	1.754	0.105	0.172	0.005	1.079	0.074	1028.73	37.99	1025.71	29.87	1035.28	44.57
Q9_14	1.756	0.104	0.172	0.005	1.086	0.074	1029.32	37.57	1020.49	29.07	1048.27	43.90
Q9_15	2.248	0.150	0.201	0.008	1.015	0.081	1196.21	45.96	1179.77	44.28	1226.14	46.44
Q9_16	4.448	0.260	0.305	0.009	1.103	0.106	1721.25	47.34	1714.72	44.16	1729.30	40.00
Q10_1	1.795	0.082	0.175	0.006	0.996	0.075	1043.56	29.35	1037.46	30.25	1056.56	28.74
Q10_2	1.695	0.075	0.173	0.005	1.007	0.071	1006.49	27.96	1029.14	27.37	957.70	30.36
Q10_4	3.152	0.147	0.248	0.008	0.999	0.092	1445.58	35.44	1430.15	38.97	1468.53	30.75
Q10_6	4.234	0.203	0.295	0.010	0.989	0.104	1680.73	38.72	1666.67	50.33	1698.51	27.32
Q10_7	1.850	0.086	0.179	0.005	0.999	0.075	1063.45	30.29	1061.75	29.83	1067.15	32.19
Q10_8	0.081	0.005	0.012	0.000	0.979	0.049	79.52	5.01	76.59	3.03	168.68	64.09
Q10_11	1.869	0.086	0.179	0.006	0.998	0.076	1070.29	29.83	1063.03	30.31	1085.33	29.75
Q10_13	2.962	0.136	0.245	0.008	0.996	0.088	1397.85	34.24	1415.12	40.06	1371.79	27.93
Q10_15	1.649	0.092	0.165	0.006	0.976	0.072	989.03	34.56	985.76	34.96	996.49	40.07
Q10_16	1.784	0.087	0.170	0.005	0.996	0.076	1039.59	31.12	1010.13	29.24	1102.25	34.73
Q10_17	2.324	0.117	0.211	0.007	0.985	0.080	1219.74	35.22	1232.76	38.97	1196.97	33.59
Q10_18	3.113	0.141	0.248	0.007	1.004	0.091	1435.80	34.28	1427.12	37.69	1448.87	29.30
Q10_19	4.416	0.208	0.310	0.010	0.994	0.103	1715.35	38.21	1739.69	48.90	1685.96	28.30
Q10_21	1.870	0.113	0.162	0.008	0.970	0.084	1070.70	39.12	969.48	41.52	1283.28	36.58
Q10_22	1.952	0.087	0.185	0.006	1.002	0.077	1098.98	29.52	1093.77	30.12	1109.51	28.58
Q10_23	1.807	0.103	0.173	0.006	0.979	0.076	1048.14	36.64	1027.56	35.37	1091.50	43.29
Q10_24	0.575	0.033	0.071	0.002	0.988	0.059	461.40	21.12	442.75	14.94	555.60	50.66
Q10_25	2.295	0.109	0.209	0.007	0.992	0.080	1210.89	33.19	1221.87	36.07	1191.57	31.19
Q10_26	4.255	0.190	0.301	0.009	1.000	0.102	1684.61	36.16	1697.92	45.60	1668.27	25.96
						>10 % Discordant Samples						
Q3_16	1.501	0.045	0.137	0.003	0.820	0.079	930.81	18.05	829.33	19.04	1179.51	33.46
Q10_3	0.176	0.010	0.023	0.001	0.977	0.056	164.38	8.37	146.34	5.50	433.10	43.78
Q6_11	3.089	0.152	0.218	0.009	0.978	0.103	1429.90	37.16	1271.84	47.60	1673.73	22.67
Q10_20	0.077	0.005	0.010	0.000	0.982	0.054	75.36	4.60	65.83	2.50	389.41	59.38
Q10_5	1.164	0.074	0.112	0.006	0.969	0.075	783.78	33.97	684.22	32.26	1078.97	38.35
Q4_8	0.603	0.023	0.066	0.002	0.915	0.066	479.40	14.71	412.01	14.21	803.57	32.36
Q6_12	1.835	0.099	0.151	0.007	0.980	0.088	1058.10	34.94	907.39	39.53	1383.72	23.80
Q10_9	0.342	0.027	0.040	0.003	0.973	0.061	298.43	20.42	255.41	17.37	650.34	42.78
Q10_10	1.220	0.070	0.112	0.005	0.977	0.079	809.65	31.70	683.47	30.00	1174.62	31.21
Q5_3	2.014	0.148	0.155	0.011	0.987	0.094	1120.27	48.80	929.47	58.64	1511.60	23.63
Q10_14	2.486	0.132	0.176	0.007	0.980	0.102	1268.04	37.61	1044.95	39.53	1669.50	27.45
Q4_6	2.211	0.095	0.162	0.006	0.876	0.099	1184.52	29.59	965.82	34.59	1598.11	38.18
Q1_9	0.796	0.035	0.075	0.003	0.909	0.077	594.33	19.65	463.92	17.79	1129.50	36.11
Q7_5	4.347	0.218	0.224	0.007	1.042	0.141	1702.41	40.50	1303.05	34.71	2236.57	29.62
Q5_10	0.235	0.015	0.025	0.001	0.977	0.067	214.31	12.21	161.61	8.68	841.74	31.86
Q5_15	0.235	0.016	0.025	0.001	0.972	0.068	214.01	13.12	159.96	8.97	860.08	38.62

Table A-12 Continued

Sample Name	Isotopic Ratios $^{207}Pb/^{235}U$	1σ abs. err.	$^{206}Pb/^{238}U$	1σ abs. err.	$^{207}Pb/^{206}Pb$	1σ abs. err.	Apparent Ages $^{207}Pb/^{235}U$	1σ abs. err.	$^{206}Pb/^{238}U$	1σ abs. err.	$^{207}Pb/^{206}Pb$	1σ abs. err.
					>10 % Discordant Samples							
Q2_10	0.262	0.013	0.027	0.001	0.768	0.070	236.62	10.74	171.91	7.14	940.53	66.02
Q3_3	1.206	0.054	0.095	0.004	0.961	0.093	803.31	24.61	582.26	24.24	1477.78	23.31
Q3_11	0.192	0.011	0.018	0.001	0.659	0.076	178.60	9.60	117.07	5.44	1097.61	87.64
Q3_7	12.937	0.686	0.309	0.014	0.759	0.304	2675.06	48.75	1735.47	68.38	3488.92	52.95
Q10_12	0.162	0.306	0.008	0.015	1.000	0.147	152.22	237.54	51.35	97.73	2307.71	26.57
Q7_7	0.763	0.061	0.030	0.002	0.980	0.182	575.54	34.65	192.95	12.90	2671.64	31.27
Q5_13	0.931	0.145	0.025	0.003	0.972	0.271	668.21	73.47	158.80	21.71	3310.28	59.42

APPENDIX B

FRACTIONATION FACTOR CORRECTED ISOTOPIC RATIOS AND APPARENT

AGES OF PEIXE, FC1, AND 91500 ZIRCON SECONDARY STANDARDS

Table B-1. Data for the 91500 zircon standard.

Sample Name	Isotopic Ratios						Apparent Ages					
	$^{207}Pb/^{235}U$	1σ abs. err.	$^{206}Pb/^{238}U$	1σ abs. err.	$^{207}Pb/^{206}Pb$	1σ abs. err.	$^{207}Pb/^{235}U$	1σ abs. err.	$^{206}Pb/^{238}U$	1σ abs. err.	$^{207}Pb/^{206}Pb$	1σ abs. err.
Analyzed on 4/9/2014												
91500_a	1.862	0.064	0.181	0.005	0.074	0.002	1067.82	22.47	1074.26	25.79	1054.74	45.50
91500_b	1.863	0.063	0.182	0.005	0.074	0.002	1068.02	21.98	1078.74	25.07	1046.25	44.82
91500_c	1.788	0.060	0.177	0.004	0.073	0.002	1041.16	21.60	1052.08	23.71	1018.76	45.96
91500_d	1.806	0.063	0.177	0.005	0.074	0.002	1047.57	22.42	1052.41	24.66	1037.94	47.80
91500_e	1.656	0.070	0.172	0.005	0.070	0.002	991.86	26.24	1021.48	25.60	927.86	62.16
91500_f	1.826	0.075	0.181	0.005	0.073	0.002	1054.79	26.54	1071.28	25.77	1021.75	59.70
91500_g	1.797	0.061	0.177	0.005	0.074	0.002	1044.44	22.05	1052.16	24.88	1028.41	46.53
91500_h	1.880	0.060	0.179	0.004	0.076	0.002	1074.23	20.83	1061.40	22.42	1100.45	44.46
91500_i	1.812	0.068	0.175	0.005	0.075	0.002	1049.70	24.34	1042.13	25.00	1064.71	53.67
91500_J	1.776	0.066	0.178	0.005	0.072	0.002	1036.72	23.84	1058.35	25.15	990.61	52.54
91500_k	1.948	0.078	0.189	0.006	0.075	0.002	1097.65	26.56	1116.23	31.59	1060.07	51.68
91500_L	1.752	0.067	0.174	0.005	0.073	0.002	1027.72	24.36	1032.21	27.14	1017.26	51.29
Analyzed on 1/29/2015												
91500_a	1.713	0.146	0.163	0.010	0.076	0.005	1013.27	53.11	973.27	56.70	1093.30	127.79
91500_b	1.723	0.143	0.162	0.010	0.077	0.005	1017.15	51.81	968.20	53.93	1116.61	124.54
91500_c	1.687	0.056	0.167	0.004	0.073	0.002	1003.64	20.85	997.64	19.90	1016.11	64.97
91500_d	1.966	0.066	0.174	0.004	0.082	0.003	1104.10	22.33	1035.28	20.81	1241.70	64.55

Table B-2. Data for the FC-1 zircon standard.

Sample Name	Isotopic Ratios						Apparent Ages					
	$^{207}Pb/^{235}U$	1σ abs. err.	$^{206}Pb/^{238}U$	1σ abs. err.	$^{207}Pb/^{206}Pb$	1σ abs. err.	$^{207}Pb/^{235}U$	1σ abs. err.	$^{206}Pb/^{238}U$	1σ abs. err.	$^{207}Pb/^{206}Pb$	1σ abs. err.
Analyzed on 4/9/2014												
FC1_a	1.945	0.065	0.188	0.005	0.075	0.001	1096.64	22.09	1108.41	26.97	1073.40	38.35
FC1_b	1.954	0.067	0.188	0.005	0.076	0.002	1099.98	22.63	1109.12	27.51	1082.00	40.18
FC1_c	2.043	0.085	0.195	0.007	0.076	0.002	1129.92	27.87	1148.56	36.19	1094.76	42.41
FC1_d	2.017	0.063	0.190	0.004	0.077	0.002	1121.28	20.83	1120.77	23.64	1122.72	38.64
FC1_e	1.979	0.079	0.196	0.005	0.073	0.002	1108.26	26.57	1151.45	26.79	1025.40	56.88
FC1_f	1.983	0.064	0.187	0.004	0.077	0.002	1109.63	21.70	1104.87	21.90	1119.53	45.37
FC1_g	1.987	0.059	0.199	0.004	0.072	0.001	1110.98	19.71	1169.91	23.82	997.46	36.16
FC1_h	1.959	0.078	0.191	0.007	0.074	0.001	1101.60	26.39	1128.51	35.34	1048.92	37.20
FC1_i	1.944	0.070	0.191	0.005	0.074	0.002	1096.45	23.78	1127.06	25.61	1035.40	49.58
FC1_J	1.967	0.100	0.192	0.005	0.074	0.003	1104.31	33.51	1132.37	27.22	1050.08	78.63
Analyzed on 4/10/2014												
FC1_a	2.079	0.064	0.192	0.004	0.078	0.002	1141.99	21.01	1134.37	22.37	1156.52	38.56
FC1_b	1.967	0.060	0.191	0.004	0.075	0.001	1104.19	20.36	1126.63	21.56	1060.27	39.30
FC1_c	2.036	0.069	0.191	0.005	0.077	0.001	1127.55	22.93	1127.51	28.14	1127.19	36.78
FC1_d	2.168	0.074	0.204	0.006	0.077	0.001	1170.90	23.36	1199.10	30.06	1118.70	35.37
FC1_e	2.068	0.074	0.194	0.005	0.077	0.002	1138.11	24.08	1143.07	25.58	1128.60	45.59
FC1_f	1.989	0.073	0.190	0.005	0.076	0.002	1111.92	24.58	1119.43	26.67	1097.22	46.36
FC1_G	1.959	0.060	0.190	0.004	0.075	0.002	1101.44	20.32	1120.14	20.49	1064.93	40.58
FC1_h	2.008	0.061	0.196	0.004	0.074	0.002	1118.23	20.34	1155.05	20.83	1047.58	40.34
FC1_i	2.055	0.057	0.195	0.004	0.077	0.001	1133.81	18.72	1145.93	19.33	1110.93	36.51
FC1_J	2.054	0.065	0.200	0.005	0.075	0.001	1133.70	21.49	1174.53	25.94	1056.59	37.27
FC1_k	1.900	0.068	0.185	0.005	0.075	0.002	1080.96	23.50	1091.65	27.10	1058.56	44.20
FC1_L	1.941	0.113	0.192	0.006	0.073	0.003	1095.19	38.31	1130.30	34.21	1024.80	81.84
FC1_n	1.918	0.161	0.199	0.004	0.070	0.005	1087.44	54.61	1167.87	22.60	930.88	141.66
FC1_o	1.928	0.195	0.193	0.004	0.072	0.006	1090.74	65.52	1139.09	22.34	997.55	165.08
FC1_p	1.913	0.193	0.196	0.004	0.071	0.006	1085.57	65.30	1154.46	22.22	944.10	166.39

Table B-2 Continued

	Isotopic Ratios						Apparent Ages					
Sample Name	$^{207}Pb/^{235}U$	1σ abs. err.	$^{206}Pb/^{238}U$	1σ abs. err.	$^{207}Pb/^{206}Pb$	1σ abs. err.	$^{207}Pb/^{235}U$	1σ abs. err.	$^{206}Pb/^{238}U$	1σ abs. err.	$^{207}Pb/^{206}Pb$	1σ abs. err.
						Analyzed on 4/11/2014						
FC1_a	2.013	0.075	0.192	0.003	0.076	0.002	1119.95	25.02	1130.40	15.31	1074.70	15.90
FC1_b	1.993	0.076	0.190	0.003	0.076	0.002	1113.23	25.35	1124.02	15.41	1058.98	22.65
FC1_c	1.912	0.150	0.185	0.005	0.075	0.005	1085.43	51.05	1094.23	27.76	1114.08	20.38
FC1_d	1.625	0.124	0.164	0.004	0.072	0.005	979.79	46.79	981.58	19.58	1016.83	12.26
FC1_e	1.970	0.113	0.191	0.006	0.075	0.003	1105.46	38.07	1129.13	31.31	1186.99	27.58
FC1_f	2.003	0.115	0.195	0.006	0.074	0.003	1116.40	38.10	1150.10	31.09	1146.06	26.83
FC1_g	1.879	0.111	0.176	0.008	0.077	0.003	1073.71	38.58	1044.42	41.23	1258.01	38.58
FC1_h	1.867	0.108	0.181	0.008	0.075	0.003	1069.39	37.59	1072.23	40.85	1094.55	21.45
FC1_i	1.988	0.079	0.188	0.006	0.077	0.001	1111.55	26.37	1108.72	34.06	1157.08	21.82
FC1_J	1.936	0.077	0.185	0.006	0.076	0.001	1093.62	26.25	1092.65	33.71	1139.85	22.47
FC1_k	1.988	0.077	0.193	0.006	0.075	0.001	1111.48	25.86	1138.13	33.63	1097.92	20.07
FC1_l	2.027	0.078	0.197	0.006	0.075	0.001	1124.73	25.98	1157.67	34.08	1123.67	21.21
FC1_m	2.155	0.083	0.194	0.006	0.081	0.002	1166.82	26.44	1141.19	32.89	1242.12	18.91
FC1_n	1.968	0.076	0.194	0.006	0.073	0.001	1104.68	25.60	1145.55	33.22	1030.18	15.45
FC1_o	1.990	0.063	0.193	0.004	0.075	0.002	1111.97	21.10	1140.22	21.10	1050.77	13.61
FC1_p	2.021	0.064	0.196	0.004	0.075	0.002	1122.65	21.23	1153.83	21.26	1077.57	15.45
FC1_q	1.952	0.076	0.194	0.004	0.074	0.002	1099.25	25.79	1142.14	21.58	1076.43	16.66
FC1_r	1.915	0.075	0.189	0.004	0.074	0.002	1086.17	25.68	1117.23	21.22	1064.72	16.58
						Analyzed on 9/9/2014						
FC1_a	1.893	0.107	0.179	0.010	0.077	0.001	1078.69	36.80	1062.29	53.02	1112.26	32.39
FC1_b	1.880	0.090	0.179	0.008	0.076	0.001	1073.96	31.37	1063.08	45.13	1096.41	26.64
FC1_c	2.061	0.081	0.194	0.005	0.077	0.002	1136.11	26.37	1142.67	29.62	1123.09	43.48
FC1_d	1.958	0.077	0.184	0.005	0.077	0.002	1101.06	26.22	1088.25	28.82	1125.93	43.93
						Analyzed on 9/11/2014						
FC1_a	1.968	0.096	0.192	0.007	0.074	0.002	1104.47	32.36	1131.11	39.41	1051.95	53.44
FC1_b	1.850	0.086	0.182	0.007	0.074	0.002	1063.39	30.34	1076.95	35.40	1035.22	52.04
FC1_c	1.987	0.089	0.182	0.005	0.079	0.002	1111.03	29.67	1077.19	28.28	1177.25	59.10
FC1_d	2.022	0.086	0.197	0.005	0.074	0.002	1122.90	28.55	1160.02	26.88	1051.14	60.29
						Analyzed on 9/15/2014						
FC1_a	1.925	0.106	0.187	0.005	0.074	0.003	1089.93	36.02	1107.47	27.31	1054.75	80.11
FC1_b	1.945	0.104	0.186	0.005	0.076	0.003	1096.83	35.32	1098.31	24.60	1093.61	79.40
FC1_c	1.924	0.115	0.185	0.006	0.075	0.003	1089.49	39.32	1096.30	33.28	1076.60	86.55
FC1_d	1.858	0.105	0.183	0.005	0.074	0.003	1066.22	36.57	1082.39	27.47	1033.97	84.60
FC1_e	1.738	0.087	0.172	0.005	0.074	0.003	1022.84	31.76	1025.04	26.88	1030.01	69.91
FC1_f	1.813	0.089	0.180	0.005	0.074	0.003	1050.06	31.64	1066.29	26.52	1028.35	69.30
FC1_a	1.958	0.140	0.187	0.008	0.076	0.003	1101.11	46.85	1107.45	41.33	1087.73	84.73
FC1_b	1.936	0.138	0.184	0.008	0.076	0.003	1093.46	46.58	1090.85	40.72	1097.79	84.17
FC1_d	1.987	0.105	0.187	0.008	0.077	0.002	1111.03	35.03	1106.67	44.61	1119.35	47.94
FC1_e	2.026	0.076	0.186	0.005	0.079	0.002	1124.23	25.22	1097.92	29.62	1175.31	41.93
FC1_f	1.996	0.056	0.193	0.003	0.075	0.002	1114.29	18.84	1136.12	16.96	1071.83	40.25
FC1_a	1.901	0.075	0.184	0.007	0.075	0.001	1081.52	25.82	1089.70	35.71	1065.46	29.82
FC1_b	1.928	0.077	0.184	0.007	0.076	0.001	1090.73	26.31	1086.80	36.37	1098.96	28.93
FC1_c	1.949	0.076	0.190	0.007	0.074	0.001	1098.21	25.97	1122.86	36.65	1050.05	29.43
						Analyzed on 11/7/2014						
FC1_a	1.948	0.119	0.191	0.004	0.074	0.004	1097.80	40.20	1124.79	21.87	1044.06	98.37
FC1_b	1.938	0.120	0.186	0.004	0.076	0.004	1094.28	40.49	1098.65	22.20	1084.99	98.77
FC1_c	1.980	0.060	0.185	0.004	0.078	0.002	1108.79	20.22	1095.57	21.01	1134.64	40.67
FC1_d	1.906	0.059	0.185	0.004	0.075	0.002	1083.22	20.51	1095.42	21.06	1058.58	44.64
FC1_g	1.897	0.059	0.185	0.003	0.074	0.002	1080.21	20.51	1093.69	18.20	1053.57	46.05
FC1_h	2.053	0.061	0.201	0.003	0.074	0.002	1133.19	19.95	1178.94	16.09	1047.00	46.11
FC1_i	1.998	0.046	0.193	0.004	0.075	0.001	1114.91	15.33	1137.61	21.22	1071.22	21.11
FC1_j	1.977	0.047	0.193	0.004	0.074	0.001	1107.72	15.83	1136.43	22.14	1052.08	21.49

Table B-2 Continued

Sample Name	Isotopic Ratios						Apparent Ages					
	$^{207}Pb/^{235}U$	1σ abs. err.	$^{206}Pb/^{238}U$	1σ abs. err.	$^{207}Pb/^{206}Pb$	1σ abs. err.	$^{207}Pb/^{235}U$	1σ abs. err.	$^{206}Pb/^{238}U$	1σ abs. err.	$^{207}Pb/^{206}Pb$	1σ abs. err.
Analyzed on 11/8/2014												
FC1_a	2.114	0.063	0.202	0.005	0.076	0.001	1153.52	20.21	1184.57	27.57	1095.80	29.17
FC1_b	2.018	0.062	0.188	0.005	0.078	0.001	1121.54	20.61	1109.13	27.05	1145.82	29.82
FC1_c	1.978	0.073	0.187	0.005	0.077	0.002	1108.10	24.75	1107.54	26.86	1109.55	48.15
FC1_d	1.974	0.073	0.190	0.005	0.075	0.002	1106.60	24.53	1120.71	26.60	1079.32	48.71
FC1_e	2.018	0.096	0.195	0.005	0.075	0.003	1121.72	31.75	1147.01	26.69	1072.36	73.96
FC1_f	2.061	0.096	0.196	0.005	0.076	0.003	1136.09	31.40	1154.27	25.27	1100.83	73.21
FC1_i	1.987	0.152	0.197	0.013	0.073	0.003	1111.18	50.32	1157.24	69.12	1022.36	68.30
FC1_j	1.942	0.076	0.191	0.003	0.074	0.002	1095.59	25.96	1125.14	14.26	1037.57	66.75
FC1_k	1.802	0.073	0.185	0.004	0.071	0.002	1046.26	26.14	1095.73	24.23	945.10	58.70
FC1_l	1.765	0.072	0.180	0.004	0.071	0.002	1032.79	26.15	1066.42	23.72	962.98	59.70
FC1_m	1.956	0.078	0.193	0.004	0.073	0.002	1100.50	26.51	1140.04	23.75	1023.85	59.73
FC1_n	2.068	0.104	0.198	0.004	0.076	0.004	1138.13	33.93	1167.24	23.49	1083.74	96.59
Analyzed on 11/9/2014												
FC1_a	1.889	0.070	0.183	0.005	0.075	0.002	1077.28	24.19	1084.43	25.79	1062.96	47.74
FC1_b	2.035	0.076	0.197	0.005	0.075	0.002	1127.24	25.09	1159.74	28.03	1065.25	47.90
FC1_c	1.993	0.060	0.188	0.004	0.077	0.001	1112.98	20.10	1109.00	23.01	1121.15	38.29
FC1_d	2.152	0.063	0.202	0.004	0.077	0.001	1165.62	20.25	1188.71	23.92	1123.36	37.64
FC1_e	1.898	0.055	0.180	0.004	0.076	0.001	1080.31	19.00	1069.42	23.12	1102.15	34.23
FC1_g	1.985	0.060	0.196	0.004	0.073	0.002	1110.46	20.23	1155.85	19.65	1022.11	44.19
FC1_h	2.071	0.062	0.198	0.004	0.076	0.002	1139.39	20.39	1166.70	18.96	1087.22	45.03
FC1_i	1.908	0.070	0.183	0.004	0.076	0.002	1084.02	23.98	1084.22	20.22	1083.06	56.29
FC1_j	1.880	0.067	0.181	0.004	0.075	0.002	1073.99	23.45	1072.94	19.46	1075.56	55.11
FC1_k	2.237	0.089	0.213	0.007	0.076	0.002	1192.71	27.65	1244.78	35.02	1099.36	48.57
FC1_l	2.076	0.081	0.199	0.006	0.076	0.002	1140.93	26.55	1170.69	32.28	1084.61	48.09
FC1_o	2.038	0.080	0.194	0.007	0.076	0.001	1128.23	26.46	1144.86	36.75	1096.28	37.08
FC1_p	2.048	0.072	0.197	0.006	0.075	0.001	1131.62	23.69	1157.90	32.28	1081.48	35.35
Analyzed on 11/10/2014												
FC1_a	1.515	0.041	0.149	0.004	0.074	0.001	936.50	16.57	895.95	21.02	1033.16	21.29
FC1_b	1.374	0.037	0.135	0.003	0.074	0.001	878.01	15.79	815.52	19.53	1039.04	18.03
FC1_c	1.554	0.022	0.152	0.002	0.074	0.000	955.71	8.38	914.51	9.70	1051.77	14.91
FC1_d	1.536	0.019	0.151	0.002	0.074	0.000	951.88	9.06	905.16	11.24	1061.52	12.55
FC1_e	1.898	0.059	0.187	0.004	0.074	0.002	1080.25	20.34	1103.93	21.10	1032.32	41.69
FC1_f	1.922	0.061	0.189	0.004	0.074	0.002	1088.71	21.09	1115.79	22.60	1034.47	42.41
FC1_g	1.958	0.060	0.187	0.005	0.076	0.001	1101.09	20.42	1103.39	24.56	1096.64	35.40
FC1_h	1.855	0.059	0.176	0.004	0.077	0.001	1065.08	20.63	1042.93	24.50	1110.84	35.12
FC1_i	1.856	0.049	0.177	0.004	0.076	0.001	1065.66	17.33	1052.47	19.76	1093.09	33.30
FC1_j	1.894	0.052	0.179	0.004	0.077	0.001	1078.91	18.18	1060.80	21.21	1116.02	33.82
FC1_k	1.879	0.095	0.180	0.008	0.076	0.002	1073.73	32.89	1069.20	45.02	1083.04	42.34
FC1_l	1.934	0.087	0.185	0.007	0.076	0.002	1092.88	29.65	1092.24	40.03	1094.29	39.76
FC1_m	1.831	0.053	0.173	0.004	0.077	0.001	1056.81	18.80	1027.89	20.77	1116.92	37.70
FC1_n	1.987	0.047	0.191	0.003	0.075	0.001	1111.17	16.00	1126.30	16.09	1081.57	34.95
FC1_o	2.005	0.037	0.189	0.003	0.077	0.001	1117.31	12.47	1117.25	14.01	1117.41	26.99
FC1_p	1.908	0.037	0.183	0.003	0.076	0.001	1083.96	12.95	1081.24	14.45	1089.42	28.95
FC1_q	1.432	0.029	0.140	0.002	0.074	0.001	902.43	12.22	846.77	14.01	1041.27	21.04
FC1_r	1.516	0.040	0.145	0.003	0.076	0.001	936.76	16.00	872.26	18.85	1091.68	25.08
FC1_a	1.950	0.076	0.193	0.007	0.073	0.001	1098.28	25.75	1138.87	36.16	1018.57	31.76
FC1_b	1.955	0.076	0.188	0.007	0.076	0.001	1100.30	25.83	1108.09	35.33	1084.79	31.63
FC1_c	1.938	0.075	0.186	0.006	0.076	0.001	1094.15	25.75	1097.18	34.53	1087.93	34.02
FC1_g	1.872	0.070	0.182	0.006	0.075	0.001	1071.32	24.36	1078.45	34.18	1056.74	27.04
FC1_h	1.889	0.070	0.182	0.006	0.075	0.001	1077.35	24.28	1080.41	33.93	1071.05	27.29

Table B-2 Continued

Sample Name	Isotopic Ratios						Apparent Ages					
	$^{207}Pb/^{235}U$	1σ abs. err.	$^{206}Pb/^{238}U$	1σ abs. err.	$^{207}Pb/^{206}Pb$	1σ abs. err.	$^{207}Pb/^{235}U$	1σ abs. err.	$^{206}Pb/^{238}U$	1σ abs. err.	$^{207}Pb/^{206}Pb$	1σ abs. err.
Analyzed on 12/10/2014												
FC1_a	1.928	0.113	0.186	0.010	0.075	0.001	1090.91	38.30	1098.28	51.79	1076.02	23.52
FC1_b	1.938	0.113	0.185	0.009	0.076	0.001	1094.45	38.21	1094.51	51.45	1094.11	23.23
FC1_c	2.061	0.081	0.197	0.006	0.076	0.001	1136.03	26.50	1159.44	30.77	1091.61	23.86
FC1_d	1.888	0.074	0.182	0.005	0.075	0.001	1076.86	25.86	1077.78	29.92	1075.03	22.43
FC1_e	1.973	0.095	0.189	0.005	0.076	0.001	1106.19	32.09	1115.81	26.75	1087.39	34.69
FC1_f	1.903	0.085	0.184	0.004	0.075	0.001	1082.10	29.17	1087.70	19.70	1070.90	33.45
FC1_g	1.986	0.132	0.193	0.006	0.075	0.002	1110.62	43.93	1135.26	33.66	1062.88	48.27
FC1_h	2.065	0.138	0.188	0.006	0.079	0.002	1137.23	44.59	1112.80	33.52	1184.35	47.28
FC1_i	2.024	0.114	0.193	0.005	0.076	0.002	1123.65	37.63	1139.69	29.00	1092.88	41.29
FC1_j	1.942	0.109	0.188	0.005	0.075	0.002	1095.82	36.95	1110.27	27.20	1067.34	41.91
FC1_k	1.946	0.085	0.188	0.005	0.075	0.001	1096.97	28.96	1111.25	28.79	1068.94	29.37
FC1_l	1.911	0.084	0.184	0.005	0.075	0.001	1084.77	28.72	1089.30	28.88	1075.91	28.35
Analyzed on 12/11/2014												
FC1_a	2.029	0.173	0.200	0.011	0.074	0.002	1125.29	56.50	1175.27	56.45	1029.13	56.05
FC1_b	2.029	0.174	0.197	0.010	0.075	0.002	1125.16	56.77	1161.15	55.98	1055.40	56.51
FC1_c	2.032	0.133	0.197	0.009	0.075	0.001	1126.13	43.51	1159.73	48.61	1061.78	39.46
FC1_d	2.029	0.131	0.201	0.009	0.073	0.001	1125.20	43.12	1179.80	48.57	1021.17	39.60
FC1_e	2.066	0.193	0.210	0.017	0.071	0.001	1137.69	62.11	1229.61	89.10	966.09	40.49
FC1_f	2.068	0.192	0.208	0.016	0.072	0.001	1138.29	61.65	1220.16	87.33	985.16	41.09
FC1_g	2.059	0.155	0.206	0.010	0.072	0.002	1135.27	50.24	1208.08	54.46	999.03	51.12
FC1_i	2.053	0.170	0.203	0.007	0.073	0.002	1133.22	55.00	1192.38	38.51	1021.11	66.94
FC1_j	1.985	0.167	0.196	0.007	0.073	0.002	1110.52	55.19	1156.21	40.09	1021.64	67.14
FC1_k	1.978	0.178	0.197	0.009	0.073	0.003	1108.05	58.82	1160.96	45.74	1005.59	69.10
FC1_l	1.991	0.179	0.199	0.009	0.073	0.003	1112.62	59.08	1167.63	46.29	1006.62	69.20
FC1_m	1.972	0.159	0.204	0.006	0.070	0.002	1106.02	52.94	1199.44	31.83	927.35	64.94
FC1_n	1.895	0.153	0.194	0.006	0.071	0.002	1079.39	52.39	1142.36	30.81	955.06	64.82
FC1_o	1.910	0.177	0.194	0.009	0.071	0.002	1084.58	60.02	1142.30	48.73	970.94	68.14
FC1_p	1.896	0.174	0.195	0.009	0.071	0.002	1079.77	59.37	1147.82	47.47	945.42	68.31
FC1_q	1.923	0.151	0.191	0.008	0.073	0.002	1089.12	51.02	1127.48	44.71	1012.84	55.74
FC1_r	1.862	0.146	0.188	0.008	0.072	0.002	1067.83	50.50	1112.73	44.01	976.87	56.34
FC1_s	1.847	0.146	0.187	0.011	0.072	0.002	1062.23	50.68	1104.24	57.16	976.81	47.27
FC1_t	1.967	0.156	0.197	0.011	0.073	0.002	1104.19	52.06	1157.30	60.20	1000.90	47.27
Analyzed on 12/12/2014												
FC1_a	1.899	0.167	0.182	0.007	0.075	0.002	1080.59	56.87	1080.12	36.32	1081.21	63.09
FC1_b	1.985	0.175	0.188	0.007	0.077	0.002	1110.46	57.96	1110.68	36.94	1109.68	63.68
FC1_c	1.919	0.168	0.180	0.006	0.077	0.003	1087.67	56.81	1069.27	34.01	1124.70	63.32
FC1_e	1.959	0.132	0.188	0.007	0.076	0.002	1101.52	44.38	1107.99	40.54	1089.11	44.37
FC1_f	1.893	0.130	0.184	0.008	0.074	0.002	1078.62	44.66	1090.90	42.29	1054.25	44.32
FC1_g	2.058	0.072	0.197	0.005	0.076	0.001	1134.89	23.51	1156.62	25.12	1093.59	22.73
FC1_h	1.936	0.069	0.187	0.005	0.075	0.001	1093.65	23.53	1103.81	25.61	1073.50	22.21
FC1_i	2.019	0.114	0.189	0.008	0.078	0.001	1121.89	37.77	1114.28	43.82	1136.72	33.92
FC1_j	1.991	0.098	0.189	0.007	0.076	0.001	1112.42	32.81	1117.83	35.71	1101.91	30.73
FC1_k	1.883	0.082	0.183	0.006	0.075	0.001	1075.24	28.54	1082.97	34.74	1059.52	23.64
FC1_l	1.916	0.082	0.186	0.006	0.075	0.001	1086.66	28.10	1100.03	34.23	1059.91	23.29
FC1_m	1.911	0.087	0.185	0.006	0.075	0.001	1085.09	29.85	1093.80	31.49	1067.65	29.10
FC1_n	1.872	0.082	0.183	0.005	0.074	0.001	1071.38	28.74	1085.75	29.54	1042.27	28.80
FC1_o	1.970	0.157	0.188	0.011	0.076	0.002	1105.29	52.39	1109.39	58.41	1097.40	46.78
FC1_p	1.821	0.146	0.176	0.010	0.075	0.002	1053.01	51.33	1042.76	56.64	1074.50	45.62
FC1_q	1.951	0.188	0.187	0.010	0.076	0.003	1098.79	62.68	1103.58	52.98	1088.81	67.25
FC1_r	1.996	0.191	0.198	0.010	0.073	0.003	1114.05	62.64	1162.08	54.17	1020.98	67.72
FC1_s	1.873	0.146	0.183	0.008	0.074	0.002	1071.59	50.34	1081.02	44.17	1081.91	18.38
FC1_t	1.943	0.173	0.189	0.012	0.075	0.002	1096.02	58.09	1115.02	62.56	1064.63	17.77

Table B-2 Continued

Sample Name	$^{207}Pb/^{235}U$	1σ abs. err.	$^{206}Pb/^{238}U$	1σ abs. err.	$^{207}Pb/^{206}Pb$	1σ abs. err.	$^{207}Pb/^{235}U$	1σ abs. err.	$^{206}Pb/^{238}U$	1σ abs. err.	$^{207}Pb/^{206}Pb$	1σ abs. err.
			Isotopic Ratios						Apparent Ages			
						Analyzed on 1/28/2015						
FC1_a	1.955	0.111	0.181	0.009	0.078	0.003	1100.15	37.50	1071.57	48.60	1155.59	63.60
FC1_c	1.941	0.051	0.185	0.002	0.076	0.002	1095.45	17.40	1094.87	9.96	1096.83	50.50
FC1_d	1.883	0.048	0.180	0.002	0.076	0.002	1075.20	16.83	1066.48	9.21	1093.16	48.84
FC1_e	1.954	0.045	0.190	0.003	0.075	0.001	1099.88	15.36	1118.96	15.87	1062.46	37.57
FC1_f	1.939	0.045	0.187	0.003	0.075	0.001	1094.52	15.42	1105.91	15.63	1072.10	38.55
FC1_g	2.009	0.090	0.191	0.006	0.076	0.003	1118.72	29.97	1126.65	30.86	1100.93	76.10
FC1_h	1.971	0.088	0.186	0.006	0.077	0.003	1105.61	29.73	1097.55	30.06	1119.09	75.74
FC1_i	1.882	0.034	0.184	0.003	0.074	0.001	1074.63	11.96	1088.40	13.84	1046.81	30.51
FC1_j	1.854	0.034	0.185	0.003	0.073	0.001	1064.87	11.99	1091.84	14.32	1010.03	29.48
						Analyzed on 1/29/2015						
FC1_a	2.043	0.167	0.188	0.011	0.078	0.005	1130.02	54.21	1111.32	60.79	1158.75	119.69
FC1_b	2.050	0.168	0.189	0.011	0.078	0.005	1132.23	54.39	1117.64	61.43	1152.90	119.71
FC1_c	1.871	0.058	0.184	0.004	0.074	0.002	1070.82	20.28	1088.94	22.12	1033.44	51.44
FC1_d	1.942	0.056	0.189	0.004	0.074	0.002	1095.79	19.31	1116.90	19.97	1053.42	50.48

Table B-3. Data for the Peixe zircon standard.

Sample Name	$^{207}Pb/^{235}U$	1σ abs. err.	$^{206}Pb/^{238}U$	1σ abs. err.	$^{207}Pb/^{206}Pb$	1σ abs. err.	$^{207}Pb/^{235}U$	1σ abs. err.	$^{206}Pb/^{238}U$	1σ abs. err.	$^{207}Pb/^{206}Pb$	1σ abs. err.
			Isotopic Ratios						Apparent Ages			
						Analyzed on 9/9/2014						
PX_a	0.737	0.029	0.089	0.003	0.060	0.001	560.60	17.09	550.81	18.20	600.89	43.03
PX_b	0.707	0.027	0.088	0.003	0.058	0.001	542.73	16.16	541.53	17.70	548.10	38.87
PX_c	0.673	0.029	0.083	0.003	0.059	0.002	522.83	17.67	511.17	15.66	573.48	56.37
						Analyzed on 9/11/2014						
PX_a	0.737	0.035	0.089	0.003	0.060	0.002	560.82	20.17	550.81	18.65	601.19	60.28
PX_b	0.768	0.037	0.092	0.003	0.061	0.002	578.79	20.97	566.83	18.92	625.55	65.23
PX_c	0.678	0.033	0.084	0.003	0.058	0.002	525.41	19.62	520.59	16.51	545.73	68.66
PX_d	0.728	0.031	0.090	0.002	0.058	0.002	555.59	17.80	558.11	13.09	544.62	64.71
						Analyzed on 9/12/2014						
PX_a	0.722	0.040	0.092	0.002	0.057	0.002	552.01	23.14	566.49	13.36	492.36	92.19
PX_b	0.734	0.042	0.092	0.003	0.058	0.003	559.04	24.04	564.97	14.89	534.63	92.43
PX_c	0.664	0.036	0.087	0.002	0.056	0.002	516.86	21.73	535.99	11.38	433.91	94.66
PX_e	0.686	0.035	0.087	0.002	0.057	0.002	530.24	20.69	538.84	13.70	506.31	82.67
						Analyzed on 9/13/2014						
PX_a	0.719	0.052	0.088	0.004	0.059	0.003	550.10	30.39	544.37	21.76	572.97	94.43
PX_b	0.700	0.052	0.086	0.004	0.059	0.003	538.52	30.63	532.62	22.25	562.66	97.10
PX_c	0.815	0.045	0.099	0.004	0.060	0.002	605.09	24.84	610.00	26.12	586.50	60.75
PX_d	0.801	0.044	0.095	0.004	0.061	0.002	597.13	24.28	583.04	24.93	650.76	57.11
PX_e	0.851	0.029	0.098	0.002	0.063	0.002	625.36	16.01	601.76	11.59	678.44	45.96
PX_f	0.793	0.030	0.099	0.002	0.058	0.002	593.04	16.64	609.21	13.35	531.53	64.17
						Analyzed on 9/15/2014						
PX_b	0.668	0.032	0.089	0.002	0.054	0.002	519.31	19.38	549.15	13.89	390.81	75.97
PX_c	0.702	0.030	0.085	0.003	0.060	0.001	540.17	17.86	523.83	18.97	610.18	44.81
PX_d	0.730	0.031	0.089	0.003	0.060	0.001	556.34	18.22	547.29	19.58	593.95	46.27

Table B-3 Continued

Sample Name	Isotopic Ratios						Apparent Ages					
	$^{207}Pb/^{235}U$	1σ abs. err.	$^{206}Pb/^{238}U$	1σ abs. err.	$^{207}Pb/^{206}Pb$	1σ abs. err.	$^{207}Pb/^{235}U$	1σ abs. err.	$^{206}Pb/^{238}U$	1σ abs. err.	$^{207}Pb/^{206}Pb$	1σ abs. err.
Analyzed on 11/7/2014												
PX_a	0.842	0.059	0.105	0.003	0.058	0.004	620.05	32.11	642.76	18.71	537.37	126.78
PX_b	0.836	0.056	0.104	0.003	0.059	0.003	616.80	30.36	635.07	14.70	549.61	122.55
PX_e	0.752	0.025	0.092	0.001	0.060	0.002	569.23	14.53	564.77	8.40	587.18	62.94
PX_f	0.752	0.027	0.089	0.002	0.061	0.002	569.12	15.30	548.09	9.77	654.21	63.54
PX_g	0.761	0.033	0.094	0.003	0.059	0.002	574.80	18.94	579.34	17.17	557.38	69.04
PX_h	0.751	0.026	0.093	0.002	0.058	0.002	568.64	14.69	575.18	9.69	543.09	62.82
PX_i	0.754	0.024	0.090	0.002	0.061	0.002	570.40	13.72	557.07	12.33	624.19	55.72
PX_j	0.725	0.022	0.087	0.002	0.060	0.002	553.79	13.00	539.92	11.38	611.57	55.05
Analyzed on 11/8/2014												
PX_a	0.752	0.025	0.089	0.002	0.061	0.001	569.62	14.51	550.29	13.96	647.72	48.59
PX_b	0.773	0.027	0.094	0.002	0.060	0.002	581.54	15.39	577.05	14.57	599.29	56.05
PX_c	0.791	0.033	0.092	0.003	0.062	0.002	591.49	18.54	568.71	15.54	680.22	66.10
PX_d	0.785	0.033	0.095	0.003	0.060	0.002	588.45	18.58	583.84	15.85	606.63	68.39
PX_e	0.843	0.043	0.094	0.003	0.065	0.003	620.68	23.25	577.99	14.88	778.82	87.17
PX_f	0.795	0.039	0.096	0.002	0.060	0.003	593.77	21.72	589.34	13.35	609.98	88.57
PX_g	0.698	0.031	0.092	0.002	0.055	0.002	537.59	18.59	567.23	11.41	414.03	86.85
PX_h	0.698	0.031	0.091	0.002	0.056	0.002	537.88	18.55	559.36	11.12	448.14	86.38
PX_i	0.663	0.029	0.090	0.001	0.054	0.002	516.22	17.51	554.02	8.23	352.43	89.47
PX_j	0.693	0.030	0.088	0.001	0.057	0.002	534.64	17.59	544.04	7.83	494.96	84.50
PX1_k	0.679	0.030	0.088	0.002	0.056	0.002	526.38	18.25	543.44	13.40	453.85	78.05
PX1_l	0.658	0.030	0.088	0.002	0.054	0.002	513.18	18.20	545.48	14.17	372.63	78.65
Analyzed on 11/9/2014												
PX_a	0.747	0.028	0.092	0.002	0.059	0.002	566.33	15.94	568.29	13.65	558.57	55.04
PX_b	0.760	0.028	0.092	0.002	0.060	0.002	573.76	16.00	570.26	13.57	587.80	54.46
PX_c	0.736	0.022	0.090	0.002	0.060	0.001	560.26	12.99	553.09	11.73	589.93	45.03
PX_d	0.785	0.025	0.095	0.002	0.060	0.001	588.35	14.16	583.88	13.49	606.07	45.38
PX_e	0.747	0.020	0.094	0.002	0.057	0.001	566.30	11.52	581.04	11.38	507.36	38.46
PX_f	0.753	0.020	0.093	0.002	0.059	0.001	569.98	11.55	572.37	10.98	560.26	39.52
PX_g	0.767	0.024	0.095	0.002	0.059	0.001	578.02	13.62	582.67	10.34	559.24	51.41
PX_h	0.744	0.023	0.092	0.002	0.059	0.001	564.87	13.53	566.30	10.18	558.54	52.37
PX_i	0.780	0.029	0.097	0.002	0.058	0.002	585.56	16.16	595.92	11.39	544.95	62.75
PX_j	0.788	0.029	0.094	0.002	0.061	0.002	590.04	16.47	578.83	11.54	632.78	61.96
PX_k	0.842	0.034	0.101	0.003	0.061	0.002	620.15	18.61	619.15	18.03	611.98	57.01
PX_l	0.779	0.031	0.094	0.003	0.060	0.002	584.64	17.78	578.27	16.96	609.30	56.12
PX_m	0.785	0.026	0.095	0.002	0.060	0.001	588.40	14.95	587.88	13.48	590.44	52.55
PX_n	0.763	0.026	0.094	0.002	0.059	0.001	575.57	14.73	578.67	13.54	563.39	51.14
PX_o	0.725	0.025	0.090	0.003	0.058	0.001	553.80	14.89	558.46	16.01	534.59	42.20
PX_p	0.792	0.028	0.096	0.003	0.060	0.001	592.36	15.90	588.81	17.19	605.91	41.91
PX_a	0.708	0.028	0.089	0.003	0.058	0.001	543.83	16.29	547.28	17.00	529.48	46.15
PX_b	0.697	0.026	0.086	0.003	0.059	0.001	536.88	15.64	530.32	16.33	564.92	40.41
PX_c	0.684	0.028	0.085	0.003	0.059	0.001	529.31	16.90	523.61	17.55	553.47	45.75
Px_e	0.742	0.023	0.090	0.002	0.060	0.001	563.86	13.14	556.02	10.18	595.11	48.19
Px_f	0.746	0.024	0.092	0.002	0.059	0.001	566.11	13.97	568.31	11.18	556.79	52.68
PX_g	0.706	0.022	0.086	0.002	0.060	0.001	542.36	13.08	531.43	12.10	588.69	43.80
PX_h	0.720	0.023	0.088	0.002	0.059	0.001	550.78	13.38	545.83	12.32	571.39	46.41
PX_i	0.699	0.020	0.083	0.002	0.061	0.001	537.94	11.87	513.17	10.74	644.74	41.25
PX_j	0.747	0.022	0.090	0.002	0.060	0.001	566.40	12.97	556.76	11.82	605.66	47.31
PX_k	0.642	0.030	0.083	0.003	0.056	0.001	503.41	18.22	513.23	19.89	459.13	51.29
PX_l	0.725	0.033	0.087	0.003	0.061	0.001	553.33	19.39	535.33	20.39	628.21	50.50
PX_n	0.742	0.019	0.085	0.001	0.064	0.001	563.71	10.85	524.29	8.30	726.07	40.23
PX_m	0.722	0.018	0.089	0.001	0.059	0.001	551.78	10.48	551.23	8.25	553.96	41.82
PX_o	0.552	0.013	0.070	0.001	0.057	0.001	446.02	8.21	434.59	7.40	505.40	31.68
PX_p	0.540	0.016	0.068	0.001	0.057	0.001	438.53	10.19	426.40	7.82	502.74	46.88

Table B-3 Continued

Sample Name	Isotopic Ratios						Apparent Ages					
	$^{207}Pb/^{235}U$	1σ abs. err.	$^{206}Pb/^{238}U$	1σ abs. err.	$^{207}Pb/^{206}Pb$	1σ abs. err.	$^{207}Pb/^{235}U$	1σ abs. err.	$^{206}Pb/^{238}U$	1σ abs. err.	$^{207}Pb/^{206}Pb$	1σ abs. err.
Analyzed on 11/11/2014												
PX_a	0.756	0.030	0.092	0.003	0.060	0.001	571.94	17.38	565.38	19.22	597.94	37.62
PX_b	0.758	0.030	0.092	0.003	0.059	0.001	572.67	17.30	569.54	19.12	584.97	38.84
PX_c	0.753	0.029	0.093	0.003	0.059	0.001	569.95	16.94	571.78	18.84	562.47	37.73
PX_d	0.760	0.030	0.094	0.003	0.059	0.001	573.83	16.98	576.84	18.96	561.72	37.40
PX_e	0.711	0.022	0.089	0.003	0.058	0.001	545.55	13.02	549.20	15.15	529.92	28.50
PX_f	0.807	0.026	0.097	0.003	0.061	0.001	601.00	14.55	594.81	16.80	623.96	32.17
Analyzed on 12/10/2014												
PX_a	0.703	0.045	0.086	0.005	0.059	0.001	540.29	26.28	534.03	27.11	566.54	36.31
PX_b	0.710	0.044	0.085	0.004	0.061	0.001	544.97	25.97	525.17	26.05	628.41	35.58
PX_c	0.698	0.032	0.086	0.003	0.059	0.001	537.74	19.07	530.61	16.10	568.18	36.26
PX_d	0.726	0.033	0.087	0.003	0.060	0.001	553.92	19.30	539.23	16.30	614.84	35.21
PX_e	0.700	0.040	0.084	0.003	0.061	0.001	538.64	23.56	518.83	16.26	623.51	46.69
PX_f	0.715	0.040	0.089	0.002	0.058	0.001	547.75	23.45	551.17	14.61	533.65	50.28
PX_g	0.761	0.056	0.092	0.003	0.060	0.002	574.51	31.63	568.99	19.85	596.59	60.83
PX_h	0.762	0.055	0.092	0.003	0.060	0.002	575.17	31.45	564.42	19.33	618.10	60.34
PX_i	0.774	0.052	0.090	0.003	0.062	0.002	581.82	29.27	558.26	19.48	675.00	55.87
PX_j	0.708	0.044	0.089	0.003	0.058	0.001	543.48	26.11	551.09	16.98	511.81	53.63
PX_k	0.811	0.048	0.084	0.003	0.070	0.002	603.06	26.62	518.38	17.39	935.91	50.56
Analyzed on 12/11/2014												
PX_a	0.691	0.062	0.086	0.005	0.058	0.002	533.40	36.83	532.28	27.91	537.18	68.62
PX_b	0.731	0.065	0.091	0.005	0.058	0.002	557.10	37.67	560.41	28.45	542.57	68.69
PX_c	0.720	0.052	0.089	0.004	0.059	0.002	550.51	30.43	549.78	25.67	553.43	55.02
PX_d	0.759	0.055	0.093	0.004	0.059	0.002	573.56	31.04	574.67	26.32	569.05	54.46
PX_e	0.788	0.076	0.100	0.008	0.057	0.001	590.26	42.35	611.50	46.43	509.18	55.15
PX_f	0.776	0.075	0.098	0.008	0.058	0.002	583.00	42.03	601.48	45.42	511.38	56.99
PX_g	0.826	0.067	0.101	0.005	0.059	0.002	611.47	36.38	623.16	29.95	568.88	65.86
PX_h	0.812	0.065	0.098	0.005	0.060	0.002	603.63	35.96	604.44	29.35	601.06	64.42
PX_i	0.794	0.070	0.100	0.004	0.058	0.002	593.70	38.68	615.13	22.36	512.09	80.18
PX_j	0.776	0.068	0.098	0.004	0.057	0.002	583.47	38.08	602.62	21.61	509.12	80.17
PX_k	0.762	0.072	0.096	0.004	0.057	0.002	575.13	40.89	593.78	26.04	502.05	82.79
PX_l	0.746	0.071	0.096	0.004	0.056	0.002	565.62	40.54	591.19	26.28	464.07	83.36
PX_m	0.724	0.065	0.094	0.003	0.056	0.002	552.96	37.61	580.81	19.61	440.64	82.80
PX_n	0.695	0.061	0.089	0.003	0.057	0.002	535.62	36.09	550.14	18.00	475.03	80.34
PX_o	0.704	0.070	0.092	0.004	0.056	0.002	540.98	40.68	564.94	26.07	441.87	85.13
PX_p	0.734	0.072	0.094	0.005	0.056	0.002	559.16	41.58	581.39	26.69	470.28	84.38
PX_q	0.784	0.086	0.094	0.006	0.061	0.003	588.01	47.80	577.47	35.84	729.38	85.19
PX_r	0.819	0.079	0.098	0.005	0.060	0.002	607.68	42.99	604.14	30.01	620.54	83.94
Analyzed on 12/12/2014												
PX_a	0.704	0.064	0.089	0.003	0.057	0.002	540.91	37.56	548.36	20.49	509.25	73.13
PX_b	0.722	0.066	0.089	0.003	0.059	0.002	552.06	38.10	551.51	20.03	553.98	73.30
PX_c	0.719	0.064	0.092	0.003	0.057	0.002	549.86	36.99	568.40	18.44	473.78	72.75
PX_d	0.729	0.066	0.090	0.003	0.059	0.002	556.01	37.95	553.37	18.59	566.81	73.57
PX_e	0.727	0.053	0.090	0.004	0.059	0.002	554.99	30.75	555.71	22.54	552.41	56.44
PX_f	0.767	0.055	0.091	0.004	0.061	0.002	578.28	31.26	559.58	22.29	652.78	54.39
PX_g	0.775	0.035	0.094	0.003	0.060	0.001	582.86	19.85	577.99	16.03	601.91	38.48
PX_h	0.754	0.034	0.091	0.003	0.060	0.001	570.40	19.72	562.48	15.48	602.12	39.54
PX_i	0.769	0.044	0.098	0.004	0.057	0.001	579.05	25.05	605.26	22.21	477.56	46.21
Analyzed on 12/12/2014												
PX_j	0.778	0.044	0.095	0.004	0.059	0.001	584.12	24.80	587.00	21.57	573.02	43.57
PX_k	0.777	0.041	0.094	0.004	0.060	0.001	583.57	23.05	580.11	20.82	597.01	40.85
PX_l	0.737	0.039	0.090	0.003	0.060	0.001	560.42	22.61	552.93	19.87	590.87	42.02
PX_m	0.723	0.039	0.092	0.003	0.057	0.001	552.59	22.93	566.99	18.95	493.68	45.28
PX_n	0.729	0.039	0.091	0.003	0.058	0.001	556.22	22.83	559.03	18.44	544.77	44.51
PX_o	0.724	0.062	0.091	0.005	0.058	0.002	552.90	35.72	560.81	32.15	520.66	59.81

Table B-3 Continued

Sample Name		Isotopic Ratios								Apparent Ages				
	$^{207}Pb/^{235}U$	1σ abs. err.	$^{206}Pb/^{238}U$	1σ abs. err.	$^{207}Pb/^{206}Pb$	1σ abs. err.	$^{207}Pb/^{235}U$	1σ abs. err.	$^{206}Pb/^{238}U$	1σ abs. err.	$^{207}Pb/^{206}Pb$	1σ abs. err.		
Analyzed on 12/12/2014														
PX_p	0.791	0.067	0.096	0.006	0.059	0.002	591.90	37.23	593.80	33.08	584.81	59.89		
PX_q	0.781	0.080	0.094	0.005	0.060	0.002	586.22	44.49	581.85	31.16	602.62	80.04		
PX_r	0.750	0.077	0.093	0.005	0.058	0.002	568.38	43.74	573.69	30.68	546.65	82.03		
PX_s	0.705	0.059	0.089	0.004	0.057	0.002	542.06	34.65	549.66	24.41	509.66	68.35		
PX_t	0.717	0.061	0.091	0.004	0.057	0.002	548.85	35.19	562.14	25.39	493.47	68.67		
Analyzed on 1/28/2015														
PX_a	0.714	0.034	0.088	0.003	0.059	0.002	547.37	19.88	541.92	18.98	568.41	72.94		
PX_b	0.777	0.037	0.093	0.003	0.061	0.002	583.63	20.65	570.42	19.97	633.68	69.44		
PX_c	0.782	0.026	0.091	0.001	0.063	0.002	586.56	14.89	558.90	8.68	695.37	73.91		
PX_d	0.827	0.029	0.092	0.002	0.065	0.002	612.21	15.89	565.97	9.40	787.45	75.33		
PX_e	0.741	0.022	0.091	0.002	0.059	0.002	563.10	12.94	562.01	9.38	567.68	69.23		
PX_f	0.744	0.024	0.090	0.002	0.060	0.002	564.75	14.15	554.26	11.39	607.40	70.61		
PX_g	0.749	0.037	0.091	0.003	0.060	0.003	567.50	21.29	561.15	17.49	590.42	99.25		
PX_h	0.706	0.034	0.088	0.003	0.058	0.003	542.61	20.13	543.86	16.16	534.71	99.08		
PX_i	0.691	0.024	0.088	0.002	0.057	0.003	533.65	14.11	542.17	10.36	497.38	95.08		
PX_j	0.659	0.032	0.092	0.002	0.052	0.003	513.87	19.47	565.12	14.61	291.97	144.40		
Analyzed on 1/29/2015														
PX_a	0.583	0.020	0.075	0.002	0.057	0.001	466.59	13.03	463.79	11.54	480.41	51.62		
PX_b	0.528	0.018	0.071	0.002	0.054	0.001	430.75	11.99	444.13	11.01	359.80	50.71		
PX_c	0.479	0.023	0.068	0.003	0.051	0.002	397.37	15.98	426.73	15.67	229.93	69.83		
PX_d	0.575	0.021	0.072	0.002	0.058	0.002	461.33	13.39	450.30	10.67	516.66	57.84		
PX_e	0.435	0.016	0.059	0.002	0.054	0.001	366.56	11.60	367.54	9.19	360.43	61.66		
PX_f	0.456	0.013	0.059	0.001	0.056	0.001	381.27	8.83	371.94	6.19	438.31	48.28		
PX_g	0.469	0.014	0.059	0.001	0.058	0.001	390.55	9.94	367.66	7.63	528.49	47.92		
PX_h	0.503	0.015	0.060	0.001	0.060	0.001	413.39	10.10	377.15	6.41	621.09	51.42		
PX_i	0.457	0.013	0.057	0.001	0.059	0.001	382.34	9.09	354.33	5.78	555.62	49.91		
PX_j	0.441	0.013	0.057	0.001	0.056	0.001	371.15	8.96	358.72	6.25	449.48	49.69		
PX_k	0.441	0.012	0.055	0.001	0.058	0.001	371.16	8.67	346.67	6.66	527.07	42.97		
PX_l	0.453	0.013	0.056	0.001	0.059	0.001	379.20	9.18	348.58	6.40	570.74	47.66		

APPENDIX C

NORMALIZED AGE DISTRIBUTION PLOTS FOR DETRITAL ZIRCON SAMPLES

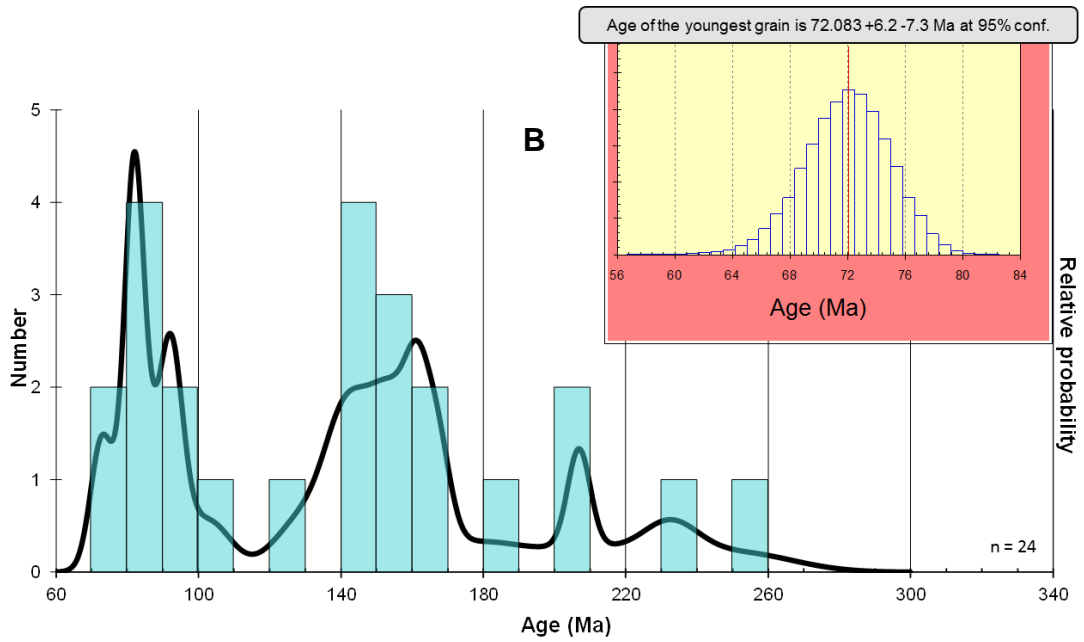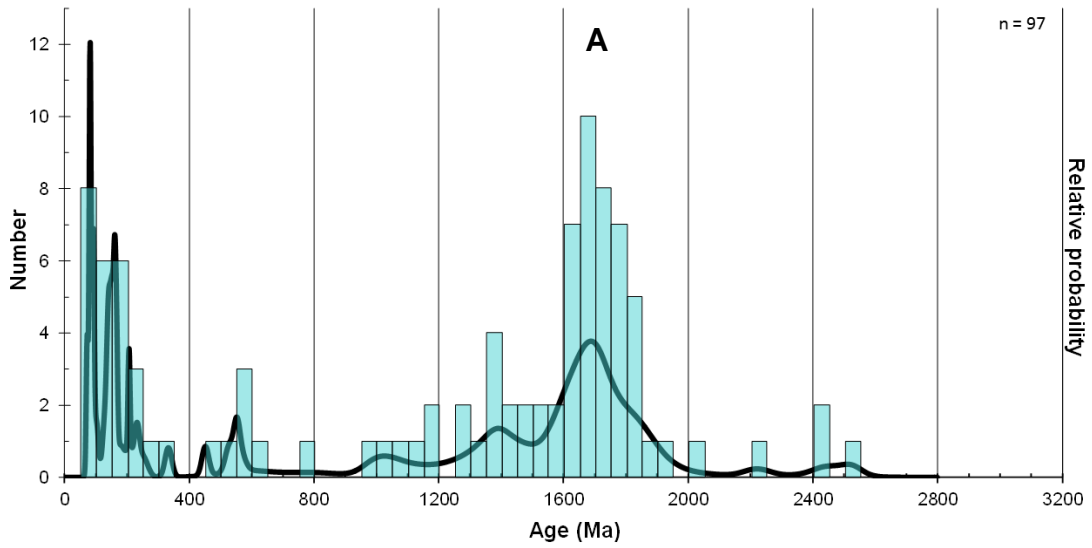**AND ASSOCIATED YOUNGEST DETRITAL ZIRCON PLOTS**

Figure C-1. A) Normalized age distribution for sample Teh. B) Normalized age distribution for sample Teh between 60-340 Ma and an associated youngest detrital zircon grain plot.
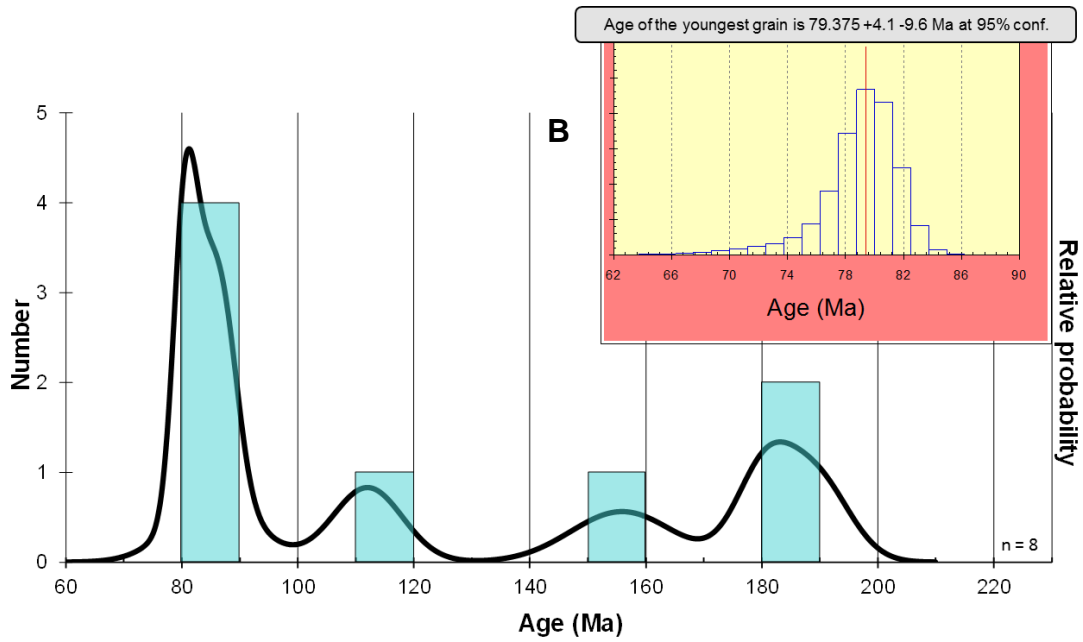
Figure C-2. A) Normalized age distribution for sample Se-E. B) Normalized age distribution for Se-E values between 60-230 Ma and associated youngest detrital zircon grain plot.

Figure C-3. A) Normalized age distribution for sample HP-PC. B) Normalized age distribution for HP-PC values between 40-280 Ma and associated youngest detrital zircon grain plot.
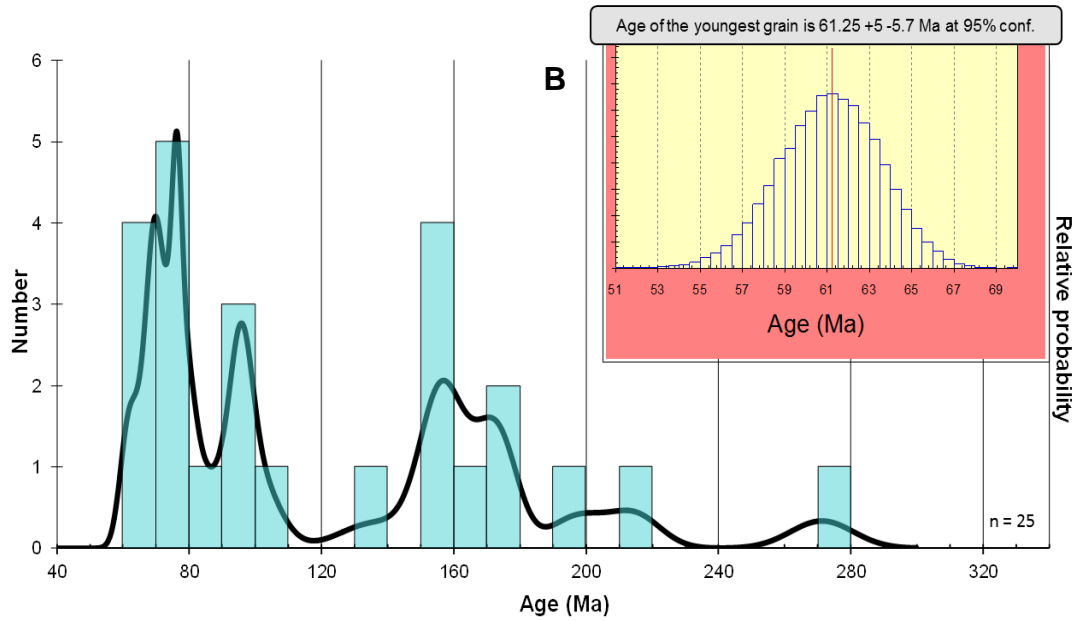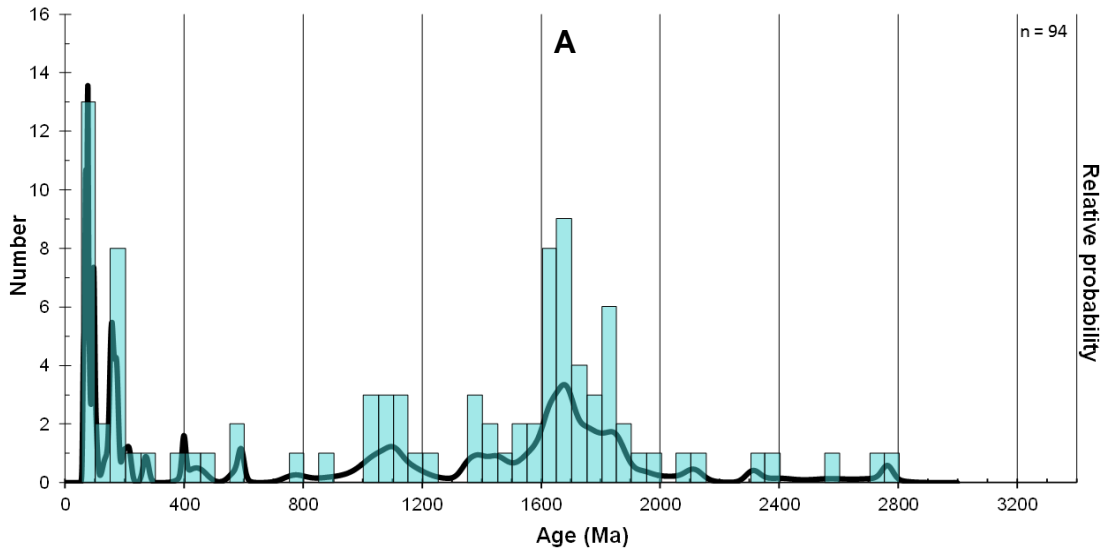
Figure C-4. A) Normalized age distribution for sample HP-DR. B) Normalized age distribution for HP-DR values between 40-330 Ma and associated youngest detrital zircon grain plot.
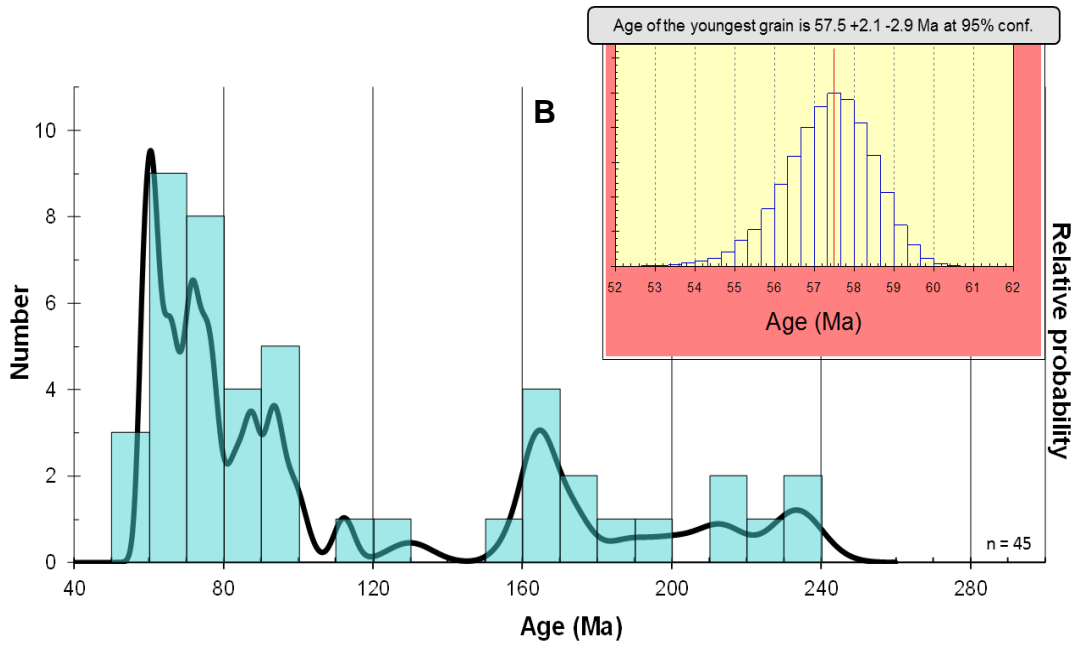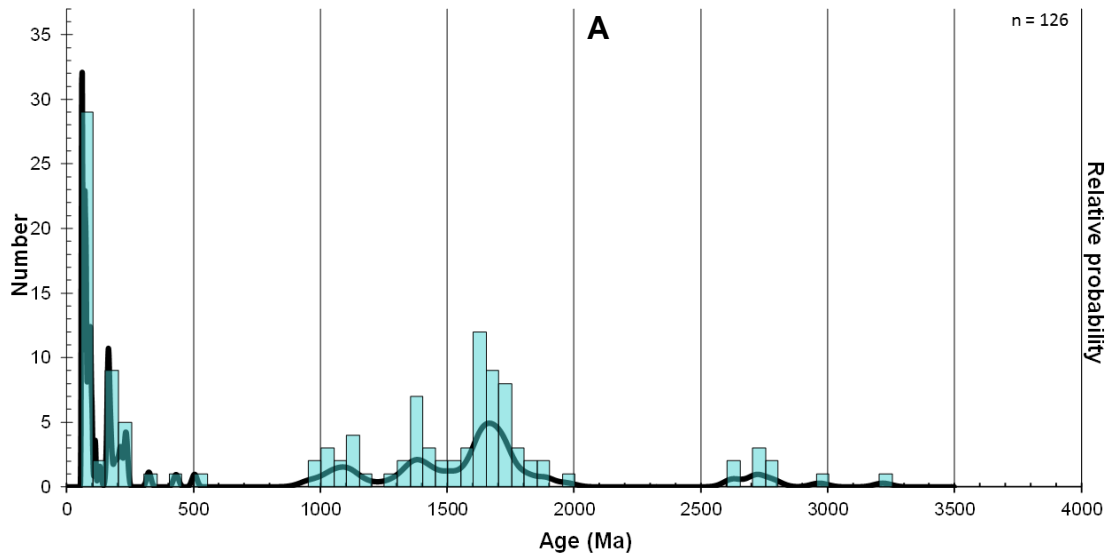
Figure C-5. A) Normalized age distribution for sample Si-B. B) Normalized age distribution for Si-B values between 40-300 Ma and associated youngest detrital zircon grain plot.
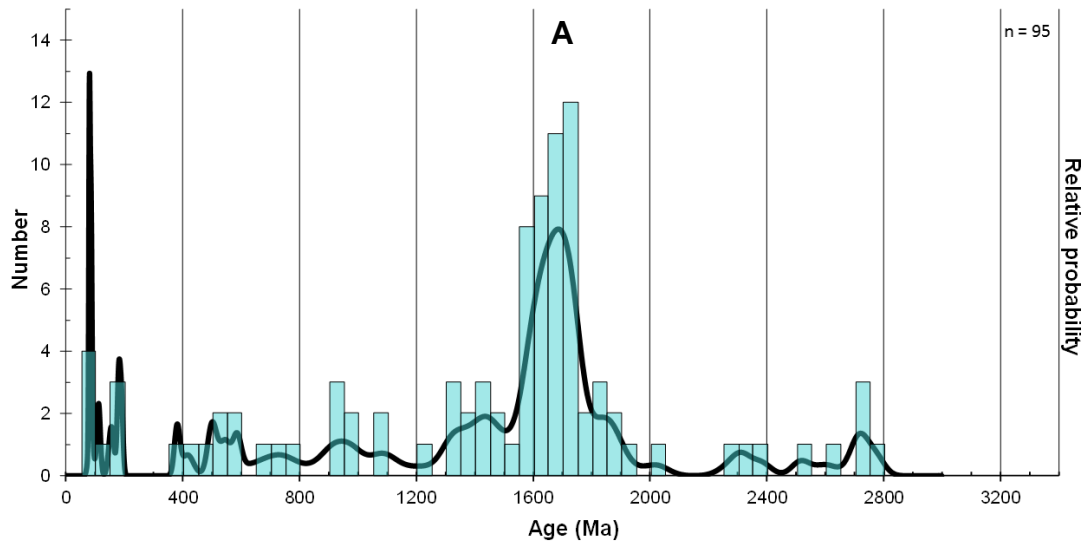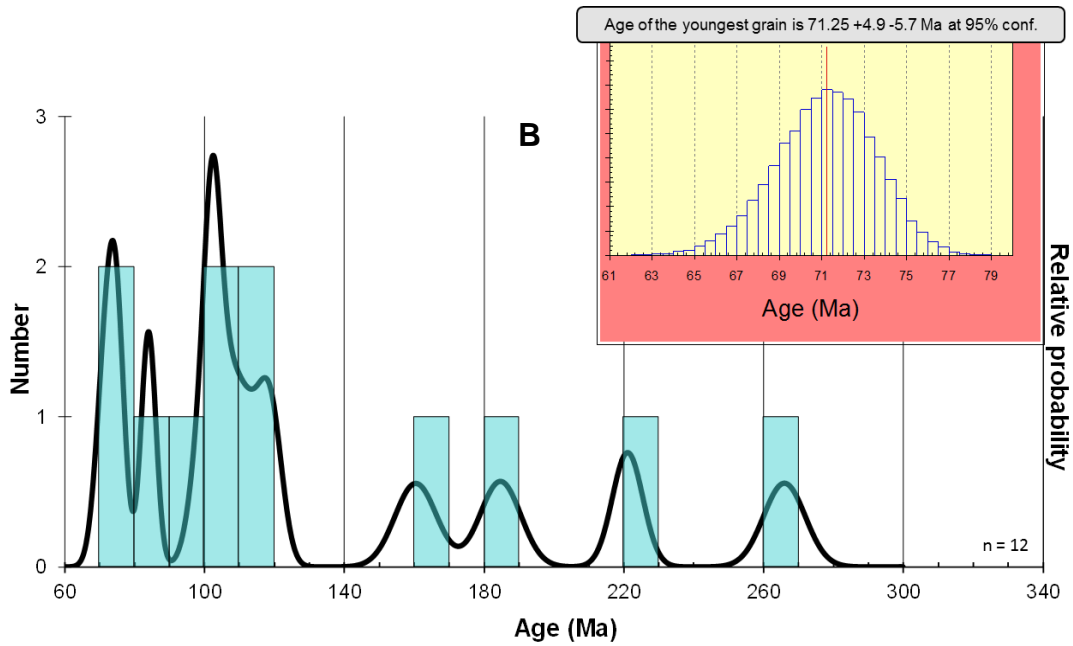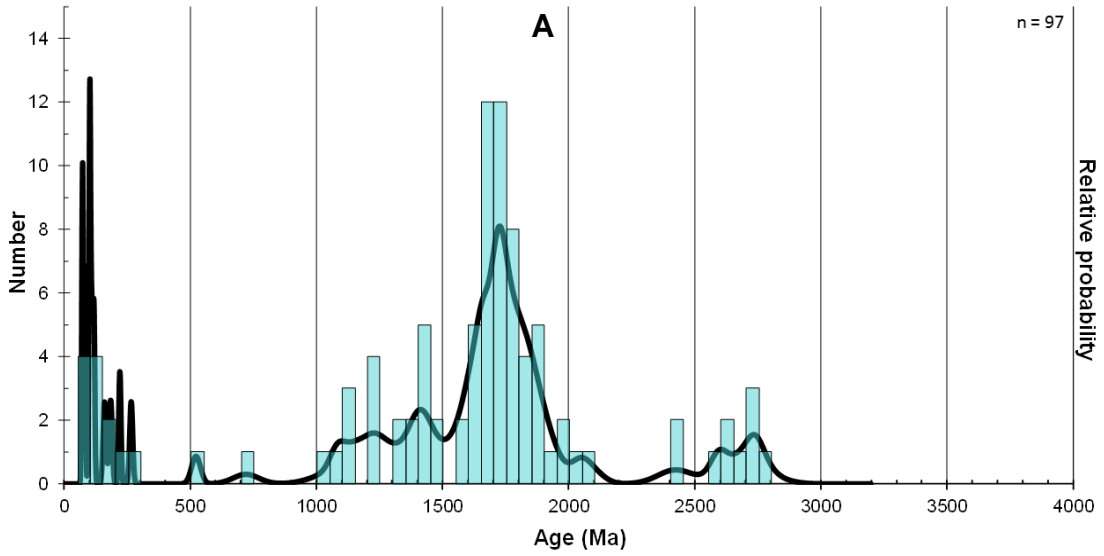
Figure C-6. A) Normalized age distribution for sample Si-LP. B) Normalized age distribution for Si-LP values between 60-340 Ma and associated youngest detrital zircon grain plot.
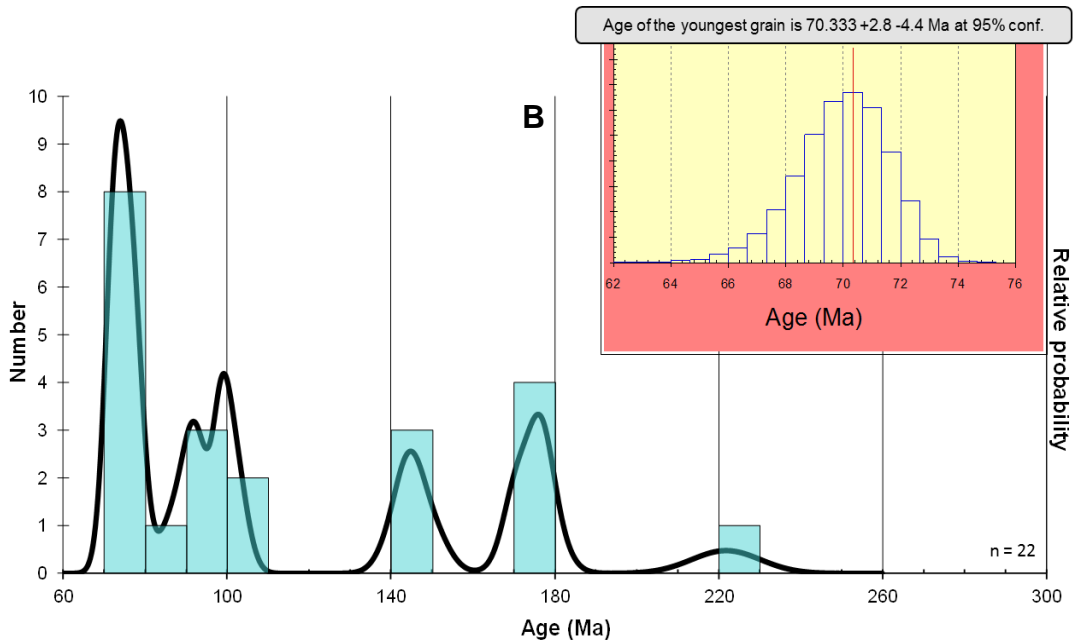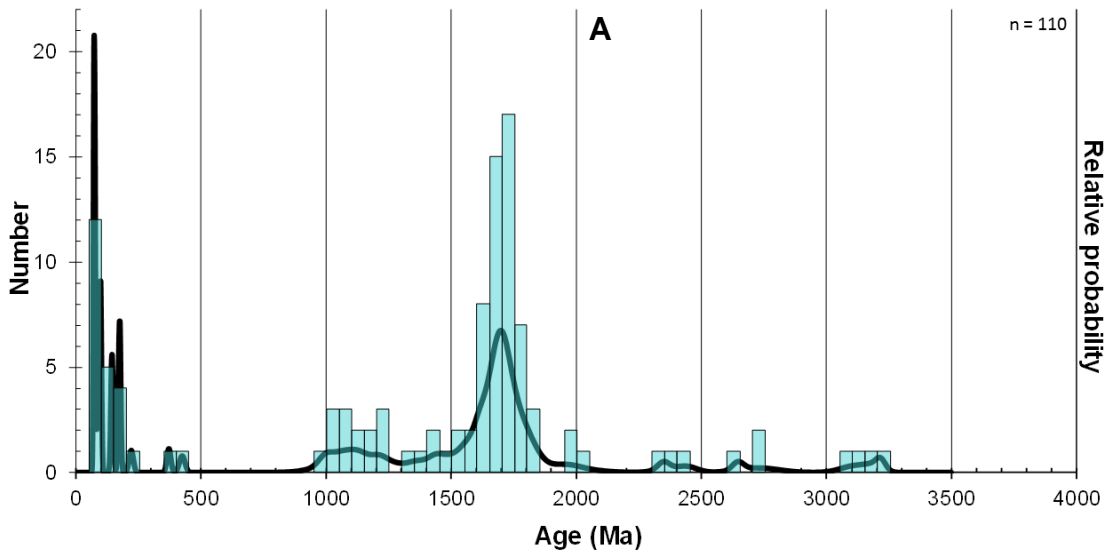
Figure C-7. A) Normalized age distribution for sample Si-TQ. B) Normalized age distribution for Si-TQ values between 60-300 Ma and associated youngest detrital zircon grain plot.

133
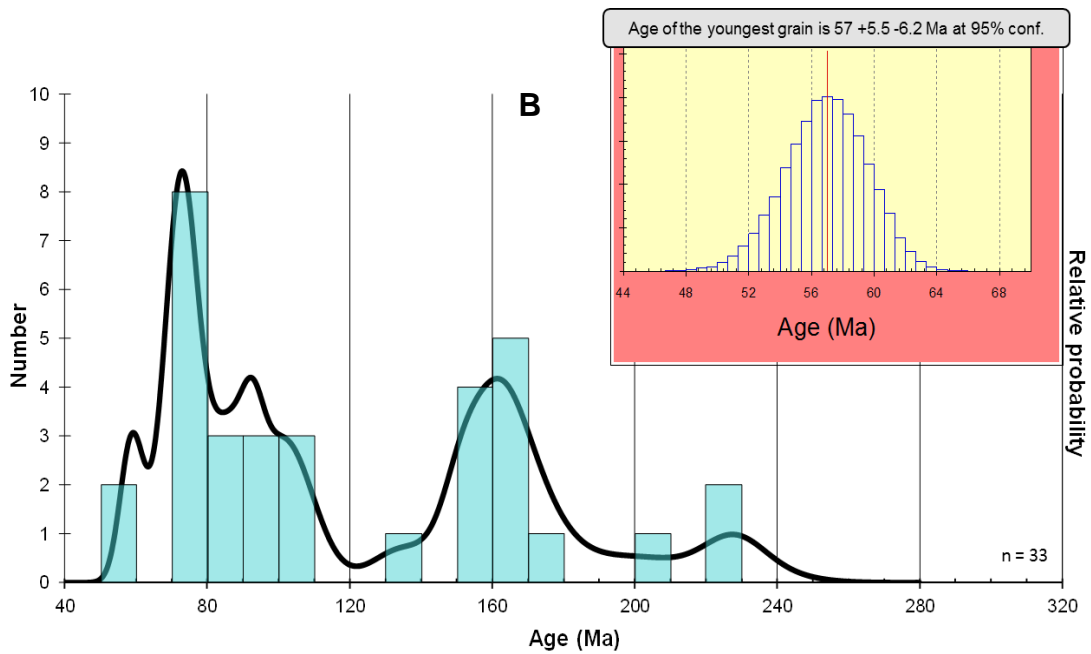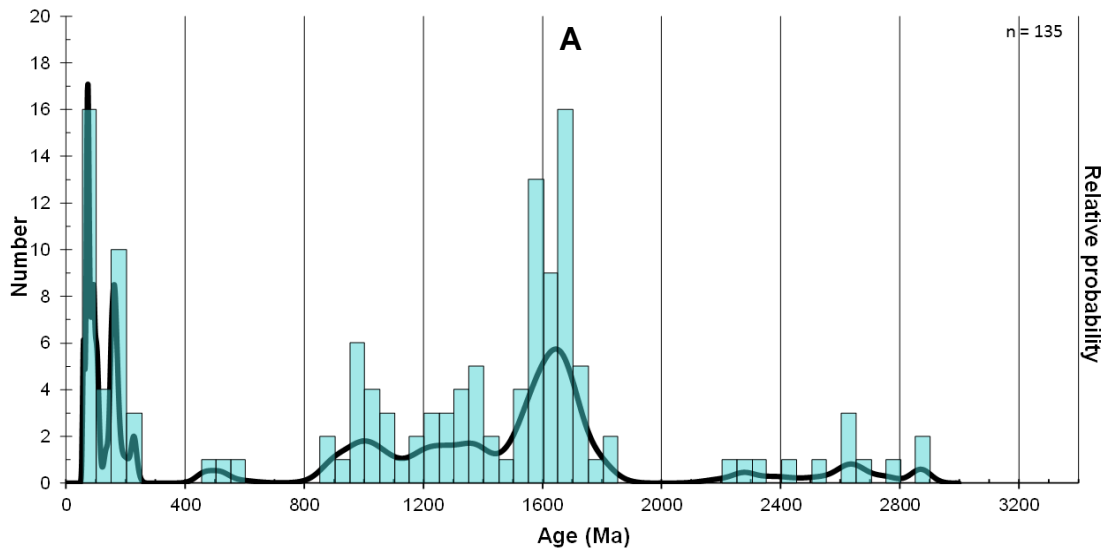
Figure C-8. A) Normalized age distribution for sample Si-KM. B) Normalized age distribution for Si-KM values between 40-320 Ma and associated youngest detrital zircon grain plot.
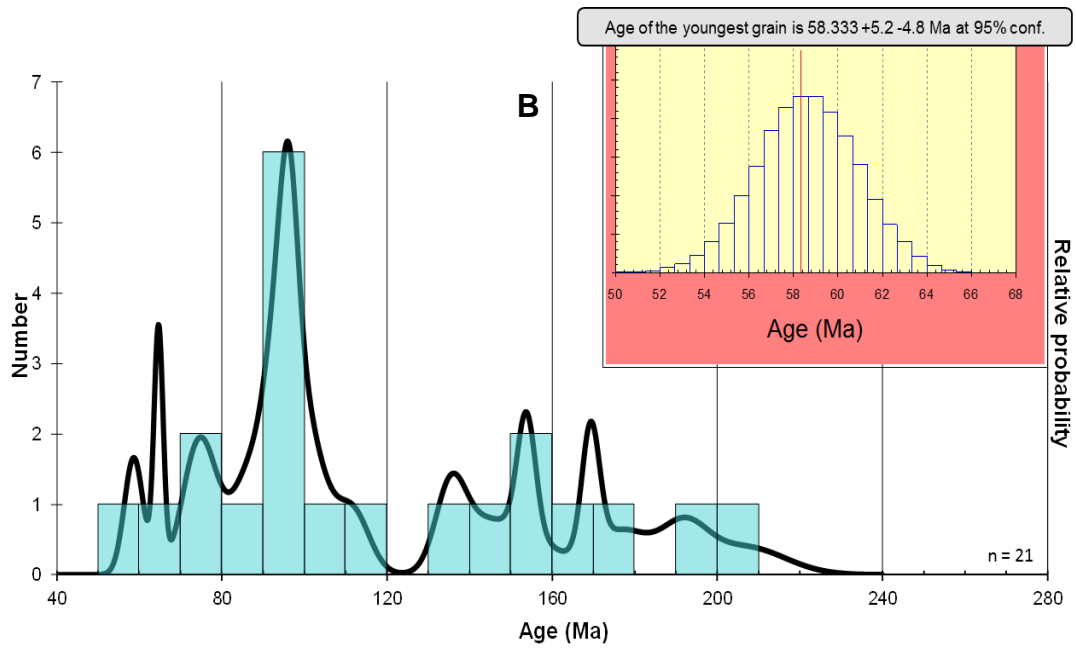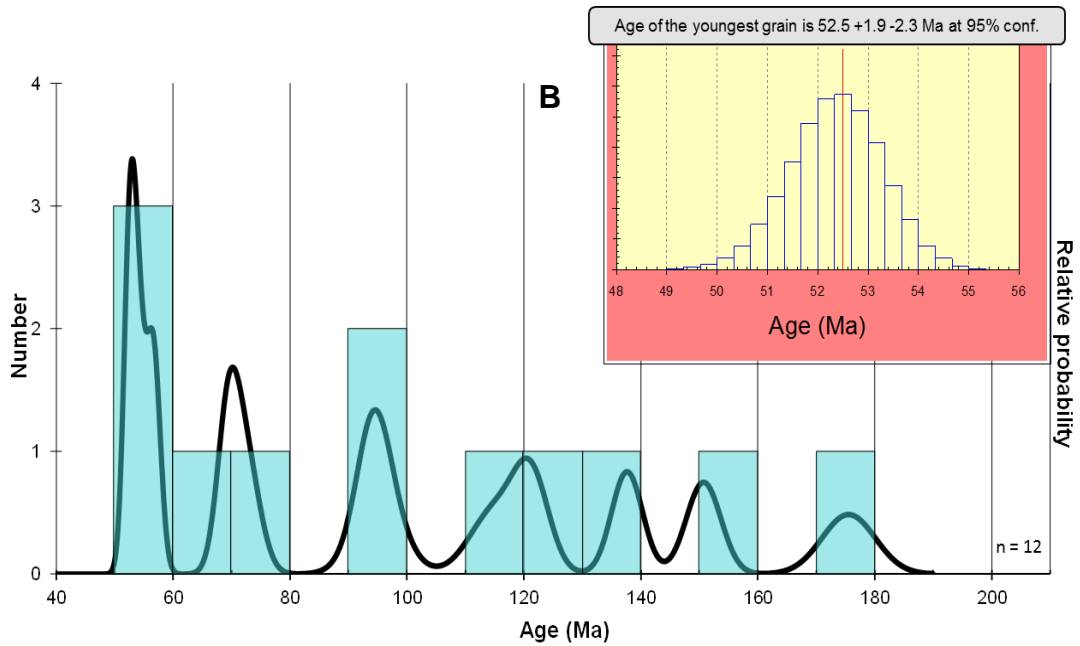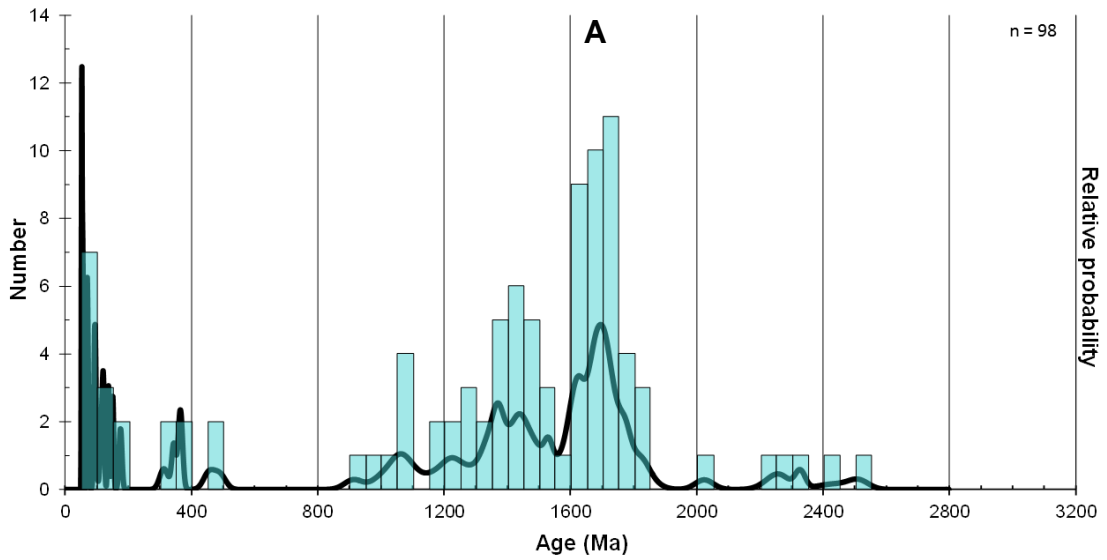
Figure C-9. A) Normalized age distribution for sample CB-BS. B) Normalized age distribution for CB-BS values between 40-210 Ma and associated youngest detrital zircon grain plot.
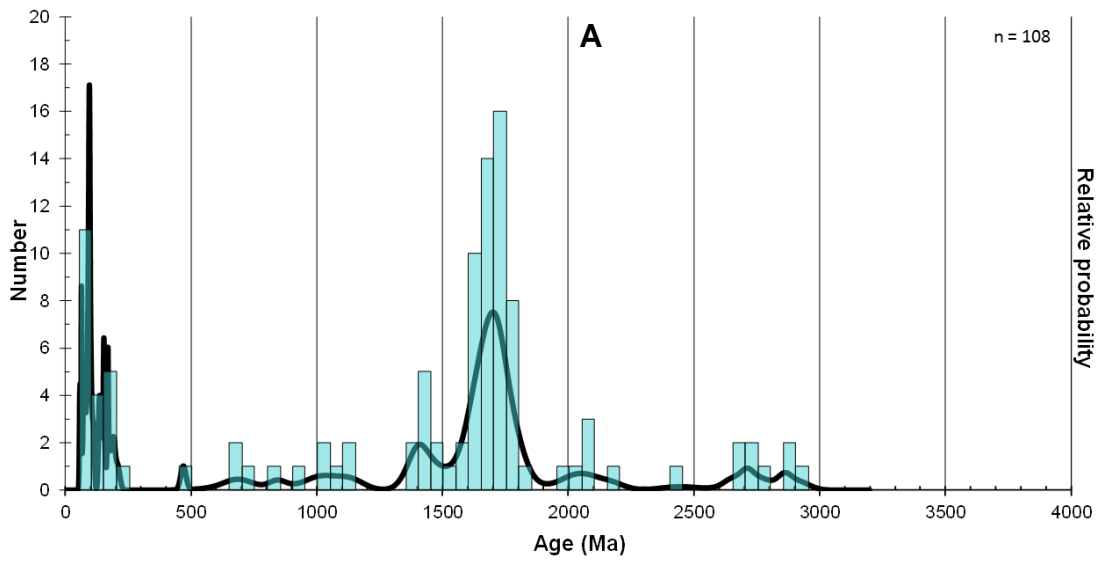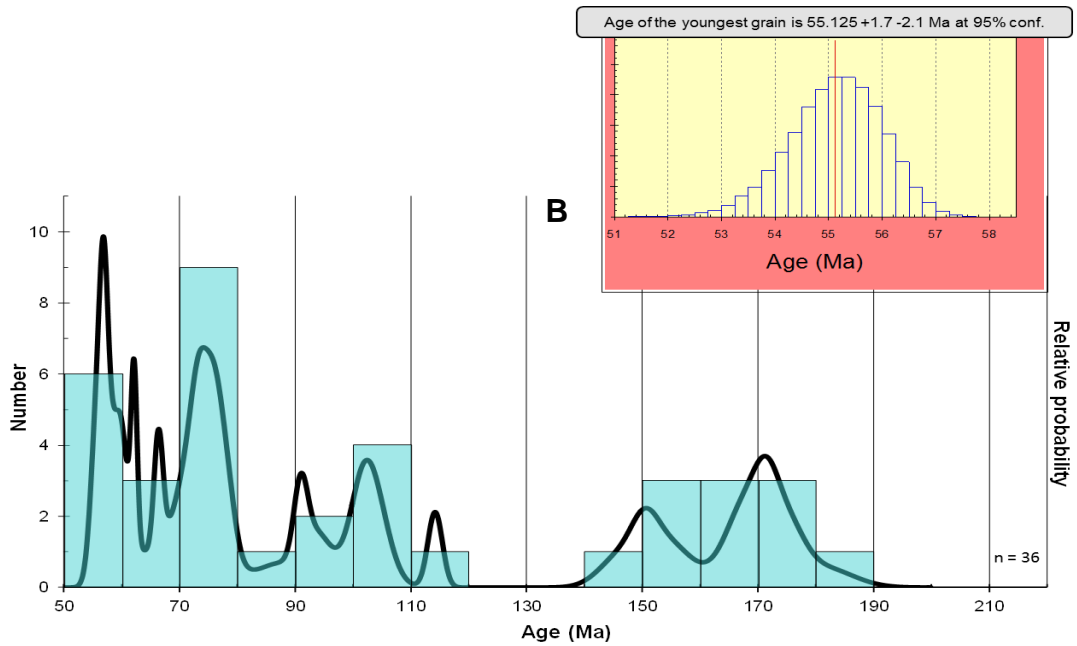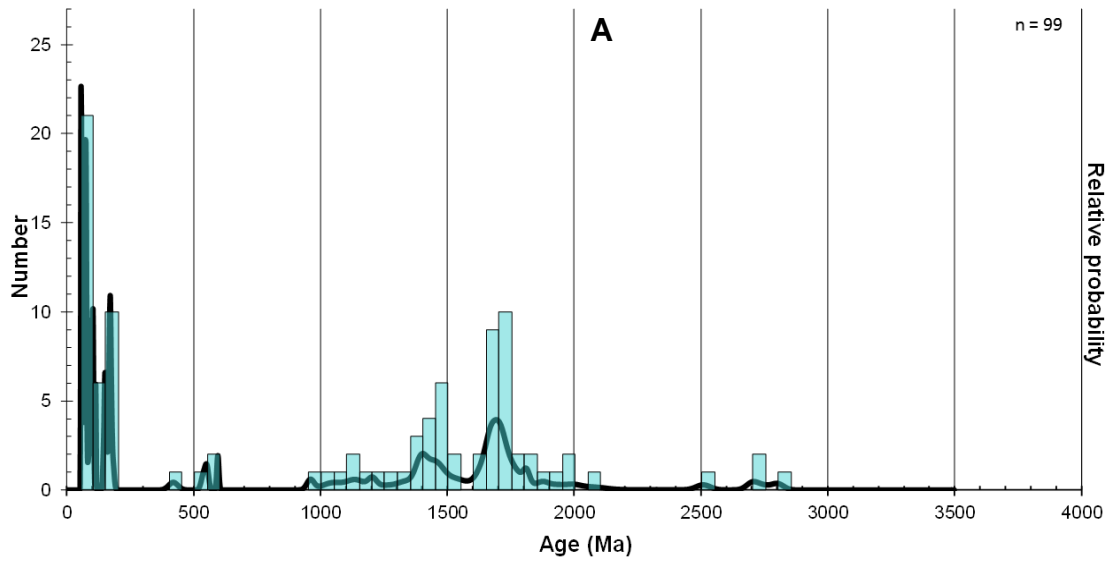
Figure C-10. A) Normalized age distribution for sample CB-BBM. B) Normalized age distribution for CB-BBM values between 50-220 Ma and associated youngest detrital zircon grain plot.
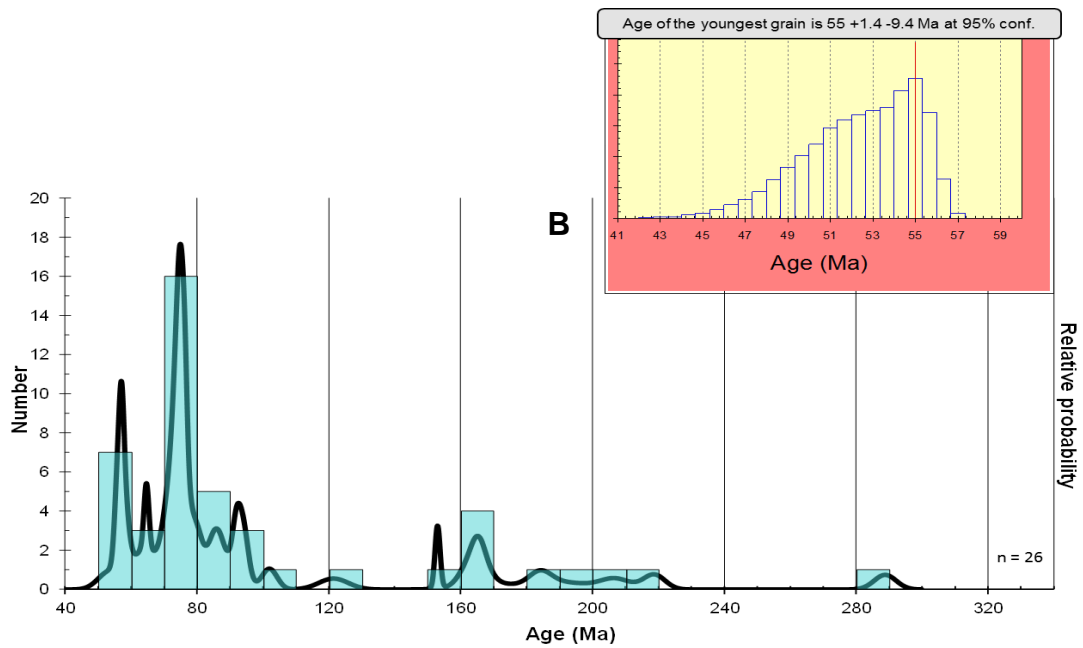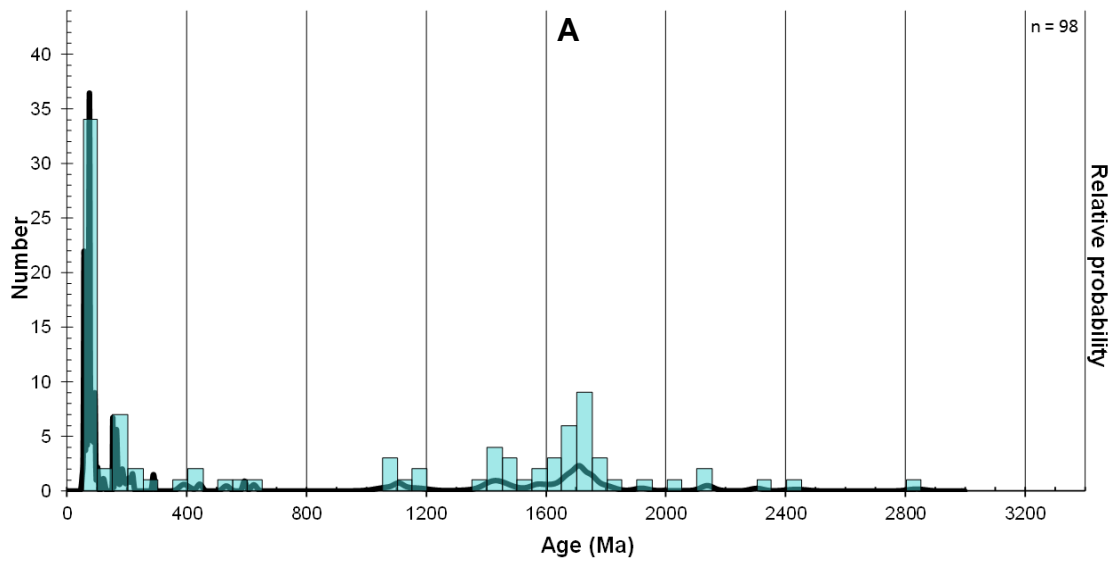
Figure C-11. A) Normalized age distribution for sample CZ. B) Normalized age distribution for CB-BBM values between 40-340 Ma and associated youngest detrital zircon grain plot.
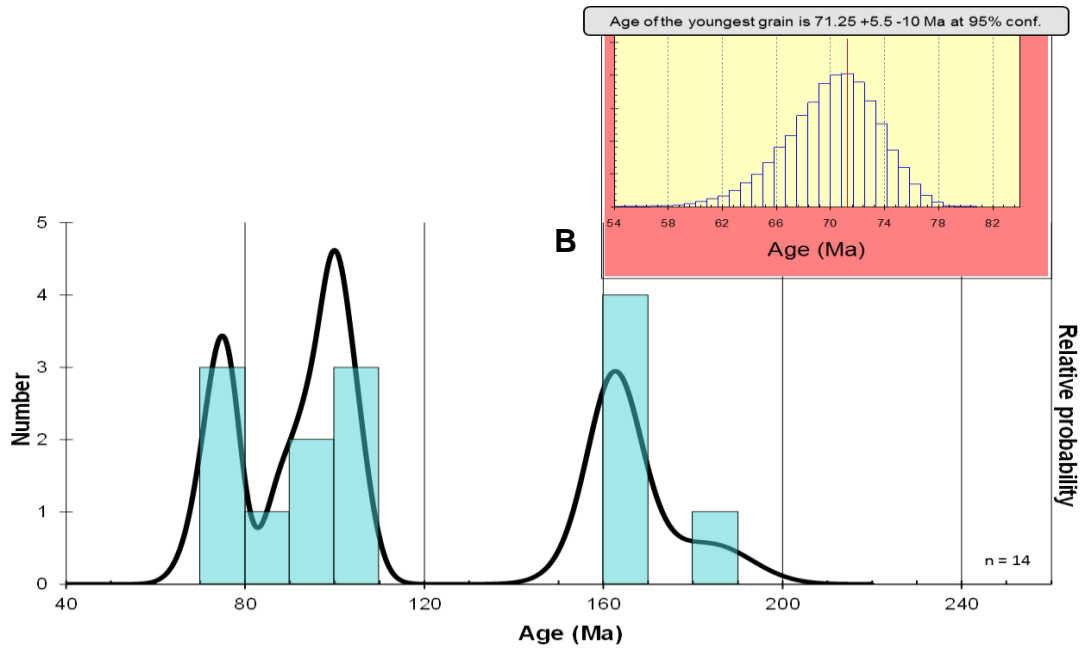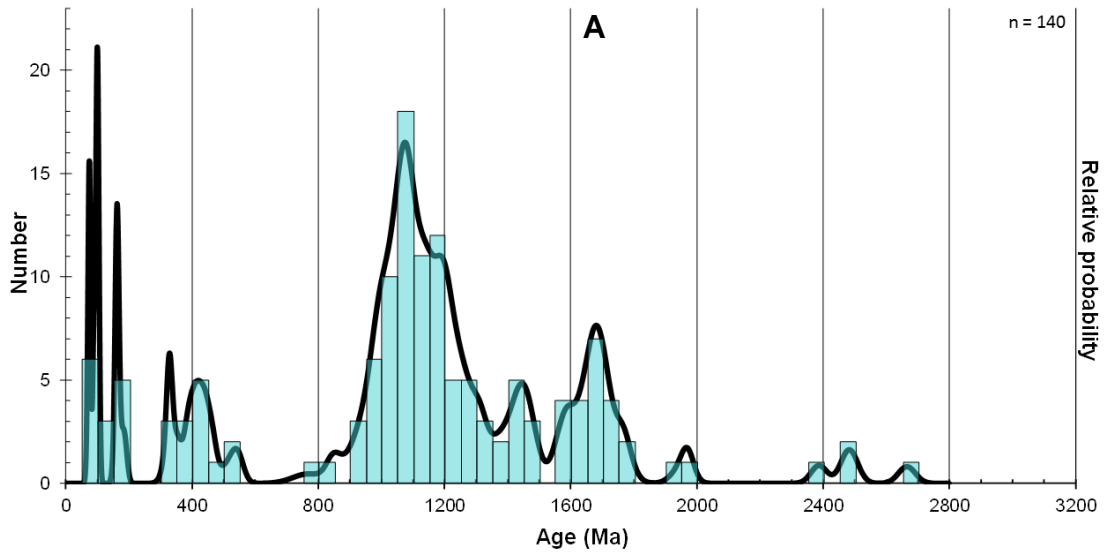
Figure C-12. A) Normalized age distribution for sample QC. B) Normalized age distribution for QC values between 40-260 Ma and associated youngest detrital zircon grain plot.

138

# APPENDIX D

DETRITAL ZIRCON SHAPE DATA AND ASSOCIATED GRAIN MAPS

Table D-1. Detrital zircon shape data for sample Teh. Grain map numbers correspond with Figure D-1.

Sample Name	Grain Map #	Area (µm²)	Perimeter Length (µm)	Major Axis (µm)	Minor Axis (µm)	Aspect Ratio
			<10% Discordant Samples			
TH_7	525	467285.1	2774.7	1042	571	1.82
TH_26	268	465323.1	2608.8	804.7	736.3	1.09
TH_29	222	602336.8	3742.1	1471.3	521.2	2.82
TH_30	433	329944.5	2299.4	866.3	484.9	1.79
TH_31	215	270103.2	2069.9	742.7	463	1.60
TH_33	918	475460.2	2718.1	806.4	750.7	1.07
TH_34	149	578138.6	3309.1	1072.5	686.4	1.56
TH_35	143	311305.4	2131.7	693.5	571.5	1.21
TH_36	131	435893	2628.2	944.9	587.3	1.61
TH_38	344	247540.1	1967.7	705.8	446.6	1.58
TH_39	355	545765.5	3156.4	1242.9	559.1	2.22
TH_43	425	300514.4	2189	662.6	577.4	1.15
TH_47	364	708939.2	4840.2	1275.8	707.5	1.80
TH_48	302	604298.8	4489.1	1606.4	479	3.35
TH_52	690	355123.6	2396.2	940.6	480.7	1.96
TH_53	671	403846.8	2657.4	996.8	515.9	1.93
TH_56	693	421177.9	2985.5	1202.4	446	2.70
TH_57	680	424447.9	2533.9	849.4	636.2	1.34
TH_58	668	296590.3	2329.3	879.9	429.2	2.05
TH_60	619	330598.5	2314.3	870.5	483.6	1.80
TH_62	945	258985.2	2099.9	830.5	397.1	2.09
TH_63	965	348910.6	2246.4	737.9	602	1.23
TH_67	876	263890.2	2131.7	855	393	2.18
TH_68	905	533339.4	4358.4	2042.8	332.4	6.15
TH_70	820	385534.8	2306.3	751	653.6	1.15
TH_71	817	330925.5	2410.4	979.2	430.3	2.28
TH_72	1106	351853.6	2429.8	917.8	488.1	1.88
TH_76	1135	351853.6	2315.1	785.4	570.4	1.38
TH_77	1092	294301.3	2129.9	746.5	502	1.49
TH_78	1086	332887.5	2342.5	891.1	475.7	1.87
TH_79	1197	478076.2	2616.8	872.5	697.7	1.25
TH_82	1288	391420.8	2378.6	818.1	609.1	1.34
TH_83	1325	384880.8	2666.2	1059.9	462.3	2.29
TH_84	798	307708.4	2103.5	662.9	591.1	1.12
TH_87	810	378340.7	2459.8	904.9	532.3	1.70
TH_89	792	366568.7	2453.5	905.4	515.5	1.76
TH_91	887	316864.4	2251.5	793.7	508.3	1.56
TH_92	894	389785.8	2701.6	1115.2	445	2.51
TH_93	827	441125	2657.4	880.4	638	1.38
TH_94	753	518297.4	3863	1384.8	476.5	2.91
TH_95	933	346294.6	2504.7	1022.2	431.3	2.37
TH_96	1004	390112.8	2807.5	1203.3	412.8	2.91
TH_97	1088	329617.5	2285.1	694.6	604.2	1.15
TH_98	1187	569309.6	3146.9	1252.8	578.6	2.17
TH_100	1145	313921.4	2167.9	718.9	556	1.29
TH_101	1213	565058.6	3366.5	1063.1	676.8	1.57
TH_103	1323	436874	2589.4	792.9	701.5	1.13
TH_106	1345	236422.1	1839.8	632	476.3	1.33

Table D-1 Continued

Sample Name	Grain Map #	Area (µm²)	Perimeter Length (µm)	Major Axis (µm)	Minor Axis (µm)	Aspect Ratio
			<10% Discordant Samples			
TH_107	1357	309343.4	2235.8	739.7	532.4	1.39
TH_108	1368	243616.1	1972	737.6	420.5	1.75
TH_109	1371	533666.4	2770.3	924.7	734.8	1.26
TH_110	1349	325039.5	2444	951.7	434.9	2.19
TH_111	1346	403192.8	2481.7	938.9	546.8	1.72
TH_112	1360	395671.8	2451	887.1	567.9	1.56
TH_115	1365	310978.4	2219	815.5	485.6	1.68
TH_118	1293	387496.8	2648.6	1079.3	457.1	2.36
TH_120	1028	449300.1	2825.8	1053	543.3	1.94
TH_122	987	422158.9	2612.4	949	566.4	1.68
TH_125	857	353488.6	2242	705.4	638	1.11
TH_127	1007	524837.4	2968.7	1024.3	652.4	1.57
TH_130	769	440798	2630	869.2	645.7	1.35
Teh_1	715	466631.1	2868.2	957.3	620.6	1.54
Teh_2	796	258004.2	2071.8	599.9	547.6	1.10
Teh_3	800	439817	2676.8	901.7	621.1	1.45
Teh_5	705	289723.3	2386.7	975.3	378.2	2.58
Teh_8	957	393382.8	2520.7	738.1	678.6	1.09
Teh_10	906	544784.5	3132.7	1189.8	583	2.04
Teh_12	881	423139.9	2674.2	912.7	590.3	1.55
Teh_13	123	606914.8	3757.4	1502.6	514.3	2.92
Teh_14	1039	310324.4	2166	781.4	505.6	1.55
Teh_15	991	368530.7	2614.3	1090.9	430.1	2.54
Teh_16	1060	357739.6	2282.6	765.6	595	1.29
Teh_17	1105	299533.4	2095.5	730.7	521.9	1.40
Teh_18	1150	276316.2	1988.8	684.1	514.3	1.33
Teh_19	1205	533666.4	2981.1	836.9	811.9	1.03
Teh_20	1189	320788.5	2187.2	793.4	514.8	1.54
Teh_21	1292	477749.2	2907.7	1141.3	533	2.14
Teh_22	1326	356431.6	2654.8	1062.6	427.1	2.49
Teh_23	1266	246886.1	1871.6	620.1	506.9	1.22
Teh_24	1263	238057.1	1844.2	619	489.6	1.26
Teh_25	1225	420850.9	2610.6	992.9	539.7	1.84
Teh_26	1230	502601.3	3130.1	1072.4	596.7	1.80
Teh_27	1251	352834.6	2318.7	706	636.4	1.11
Teh_29	1066	373762.7	2502.1	857.8	554.8	1.55
Teh_30	1203	322423.5	2187.2	698.8	587.5	1.19
Teh_31	1237	461072.1	2621.2	809.6	725.1	1.12
Teh_32	1131	381283.8	2514.5	766.6	633.3	1.21
Teh_33	1221	336484.5	2300.1	779	550	1.42
Teh_35	1236	322750.5	2212.8	691	594.7	1.16
Teh_37	1294	322423.5	2410.4	920.6	445.9	2.06
Teh_38	1254	297898.4	2174.1	774.9	489.5	1.58
Teh_39	1308	298225.4	2232.2	854.8	444.2	1.92
Teh_40	228	406789.8	2722.8	1152.1	449.6	2.56
Teh_41	1256	251464.2	1935.9	715.2	447.7	1.60
Teh_42	1195	802134.7	3936.1	1570.4	650.3	2.41
Teh_44	1147	365914.7	2476.6	715.4	651.2	1.10
Teh_45	1244	431642	2677.5	804.7	683	1.18
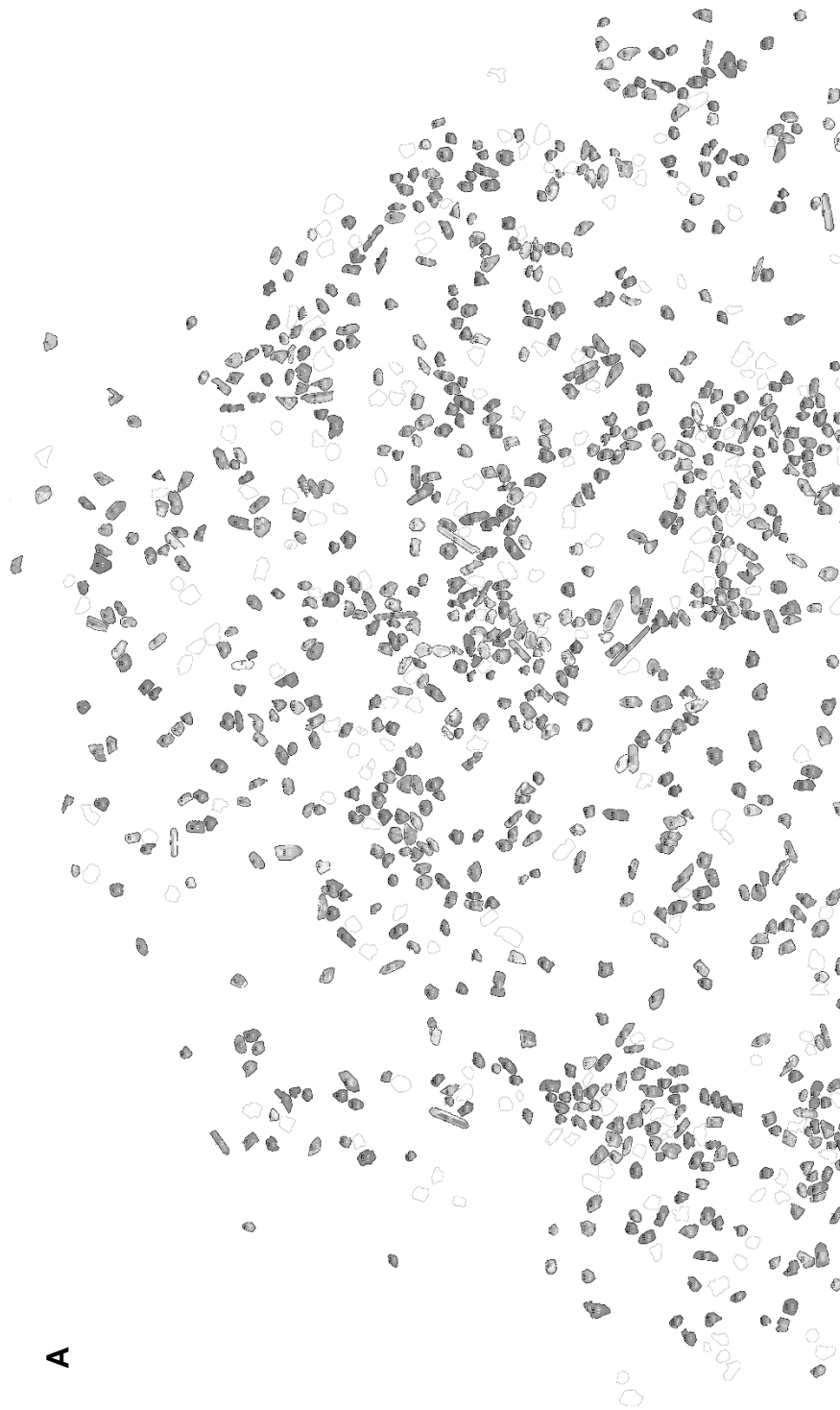
Figure D-1. Grain map generated for sample Teh. Upper image (A) and lower image (B) are shown. The joining area of images A-B contain overlapping grains.

B

Figure D-1 Continued

Table D-2. Detrital zircon shape data for sample Se-E. Grain map numbers correspond with Figure D-2.

Sample Name	Grain Map #	Area (µm²)	Perimeter Length (µm)	Major Axis (µm)	Minor Axis (µm)	Aspect Ratio
			<10% Discordant Samples			
ES_2	214	6461.5	324.6	94	87.5	1.07
ES_4	78	9407.8	457.2	161.1	74.3	2.17
ES_5	64	4856	278.3	94	65.7	1.43
ES_8	44	3639.5	231.9	72.2	64.2	1.12
ES_9	40	3839	262.2	99.9	48.9	2.04
ES_10	73	8564.2	358.2	109.8	99.3	1.11
ES_11	100	3937.1	250.2	73.9	67.8	1.09
ES_12	117	2756.6	205.7	73.1	48	1.52
ES_14	74	4620.5	284.1	112.6	52.2	2.16
ES_15	46	4672.9	270.2	88.1	67.5	1.31
ES_16	60	2583.3	205.7	73.4	44.8	1.64
ES_19	306	3191.5	223	81.3	50	1.63
ES_23	65	1223	135	41.4	37.6	1.10
ES_24	75	4941	297	109.5	57.4	1.91
ES_25	51	4614	277.9	102.4	57.4	1.78
ES_29	912	4950.8	279	86.8	72.6	1.20
ES_30	886	7615.9	372.9	151.5	64	2.37
ES_31	921	6265.3	332.4	105.6	75.6	1.40
ES_32	891	5408.6	303.2	115.6	59.6	1.94
ES_33	909	6164	323.5	120.8	65	1.86
ES_35	864	5591.7	291.9	102.2	69.7	1.47
ES_36	842	4676.1	277	94.1	63.3	1.49
ES_37	952	6317.7	339.2	124	64.9	1.91
ES_39	1027	5725.8	305.8	111.2	65.6	1.70
ES_40	1072	4254.3	261.5	85.4	63.4	1.35
ES_41	1048	6628.3	310.9	105.9	79.7	1.33
ES_42	1081	14201.7	465.3	143.9	125.6	1.15
ES_43	1111	5464.2	279.4	93.3	74.6	1.25
ES_44	1188	7831.7	390.6	155.3	64.2	2.42
ES_46	1104	5941.6	297.2	100.8	75.1	1.34
ES_47	1054	6419	308.1	95.8	85.3	1.12
ES_48	1011	8613.2	358.2	120.3	91.1	1.32
ES_49	1085	4708.8	274.7	102.2	58.7	1.74
ES_50	1119	5209.1	329.2	139.4	47.6	2.93
ES_53	1230	5075.1	293.9	116.4	55.5	2.10
ES_54	1266	8197.9	418.2	173.3	60.2	2.88
ES_55	1233	4757.9	266.8	92.5	65.5	1.41
ES_56	1118	7478.5	428.8	180.6	52.7	3.43
ES_58	1003	3878.2	254.4	81.1	60.9	1.33
ES_60	1063	4025.4	249.6	83.7	61.2	1.37
ES_62	798	5261.5	282.9	95.9	69.9	1.37
ES_63	788	2998.6	216.5	74.5	51.2	1.46
ES_66	736	6608.7	366.8	149.8	56.2	2.67
ES_67	655	9849.3	482.1	204.2	61.4	3.33
ES_68	784	5487.1	284.7	88.6	78.8	1.12
ES_69	643	4113.7	254.1	85.1	61.6	1.38
ES_72	680	3861.9	247	89.5	54.9	1.63
ES_73	681	5732.3	298	115.3	63.3	1.82

Table D-2 Continued

| Sample Name	Grain Map #	Area (μm^2)	Perimeter Length (μm)	Major Axis (μm)	Minor Axis (μm)	Aspect Ratio
			<10% Discordant Samples			
ES_74	124	8783.3	394.9	162.5	68.8	2.36
ES_75	181	5294.2	284.7	96.9	69.5	1.39
ES_76	206	4198.7	261.7	99	54	1.83
ES_77	238	9241.1	435.2	183.7	64	2.87
ES_78	276	6595.6	341.4	134.6	62.4	2.16
ES_79	1037	4963.9	270.1	87.3	72.4	1.21
ES_81	142	8168.5	360.7	130.2	79.9	1.63
ES_82	112	6396.1	352.9	143.3	56.8	2.52
ES_84	225	7625.7	368.2	140.6	69	2.04
ES_86	262	7851.3	357.5	124	80.6	1.54
ES_87	279	3940.4	253.6	95.3	52.6	1.81
ES_88	411	7301.9	379.6	148.4	62.6	2.37
ES_89	432	5863.1	323.9	115.3	64.8	1.78
ES_90	505	5346.5	281.7	100.8	67.5	1.49
ES_92	573	4764.4	263.6	92	65.9	1.40
ES_93	560	3168.6	218.5	73.3	55.1	1.33
ES_96	466	8119.4	338.1	108.1	95.7	1.13
ES_100	710	7419.7	339.6	125	75.6	1.65
ES_101	755	5137.2	274.5	95.9	68.2	1.41
ES_103	315	6327.5	332.1	130.5	61.7	2.12
ES_104	870	5964.5	308.8	116.1	65.4	1.78
ES_105	895	6128	323.4	126.6	61.7	2.05
ES_107	971	4963.9	273.7	97.5	64.8	1.50
ES_109	972	12929.6	483.1	178.7	92.1	1.94
ES_110	1051	2773	195.3	60.3	58.6	1.03
ES_111	1047	5752	327.4	133.2	55	2.42
ES_112	1032	1903.1	183.7	75.4	32.1	2.35
ES_113	1153	4479.9	274.9	105.8	53.9	1.96
ES_114	1150	7972.3	363.9	138.8	73.1	1.90
ES_115	1216	3253.7	219.6	79.1	52.4	1.51
ES_116	1276	6942.2	368.7	155.2	56.9	2.73
ES_117	1332	7920	439	187.4	53.8	3.48
ES_119	1371	7337.9	365.2	143.8	65	2.21
ES_120	1404	2194.2	185.9	70.1	39.8	1.76
ES_122	1252	4313.1	269.4	102.4	53.6	1.91
ES_123	1235	2537.5	192.3	58.8	55	1.07
ES_124	1197	3845.5	272.4	109.7	44.6	2.46
ES_125	1159	3770.3	237.9	80.8	59.4	1.36
ES_126	1093	7583.2	355.2	120.3	80.3	1.50
ES_127	851	5588.5	323	124.9	57	2.19
ES_129	920	4640.2	275.3	95	62.2	1.53
ES_132	814	5271.3	283.6	96.8	69.4	1.39
ES_133	54	7050.2	426.8	150.6	59.6	2.53
ES_135	735	5379.2	305.2	110.3	62.1	1.78
ES_136	777	4107.1	260.6	96.4	54.2	1.78
ES_137	636	4584.6	255.8	83.3	70.1	1.19
ES_138	702	4699	351.1	103.6	57.8	1.79
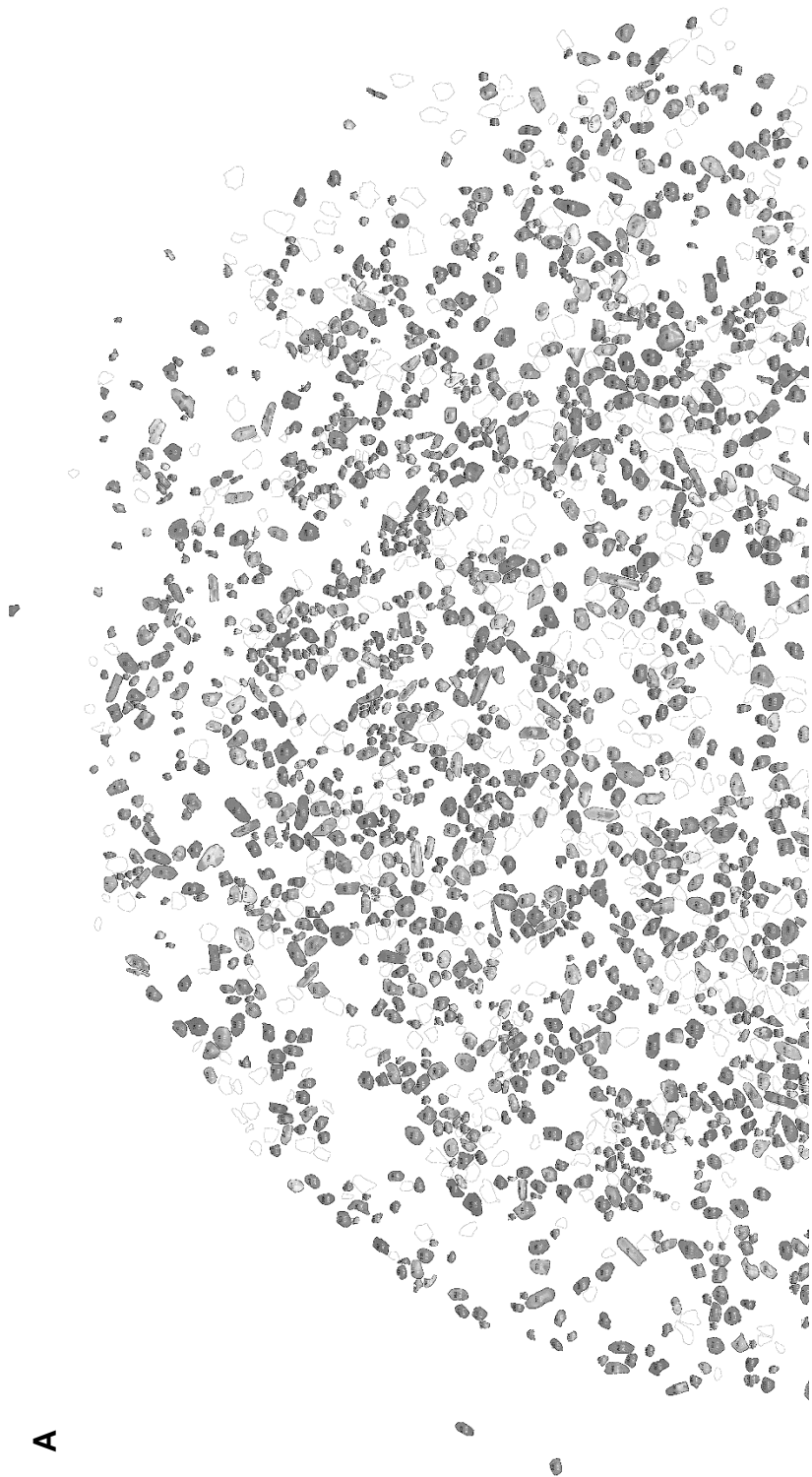
Figure D-2. Grain map generated for sample Se-E. Upper image (A) and lower image (B) are shown. The joining area of images A-B contain overlapping grains.
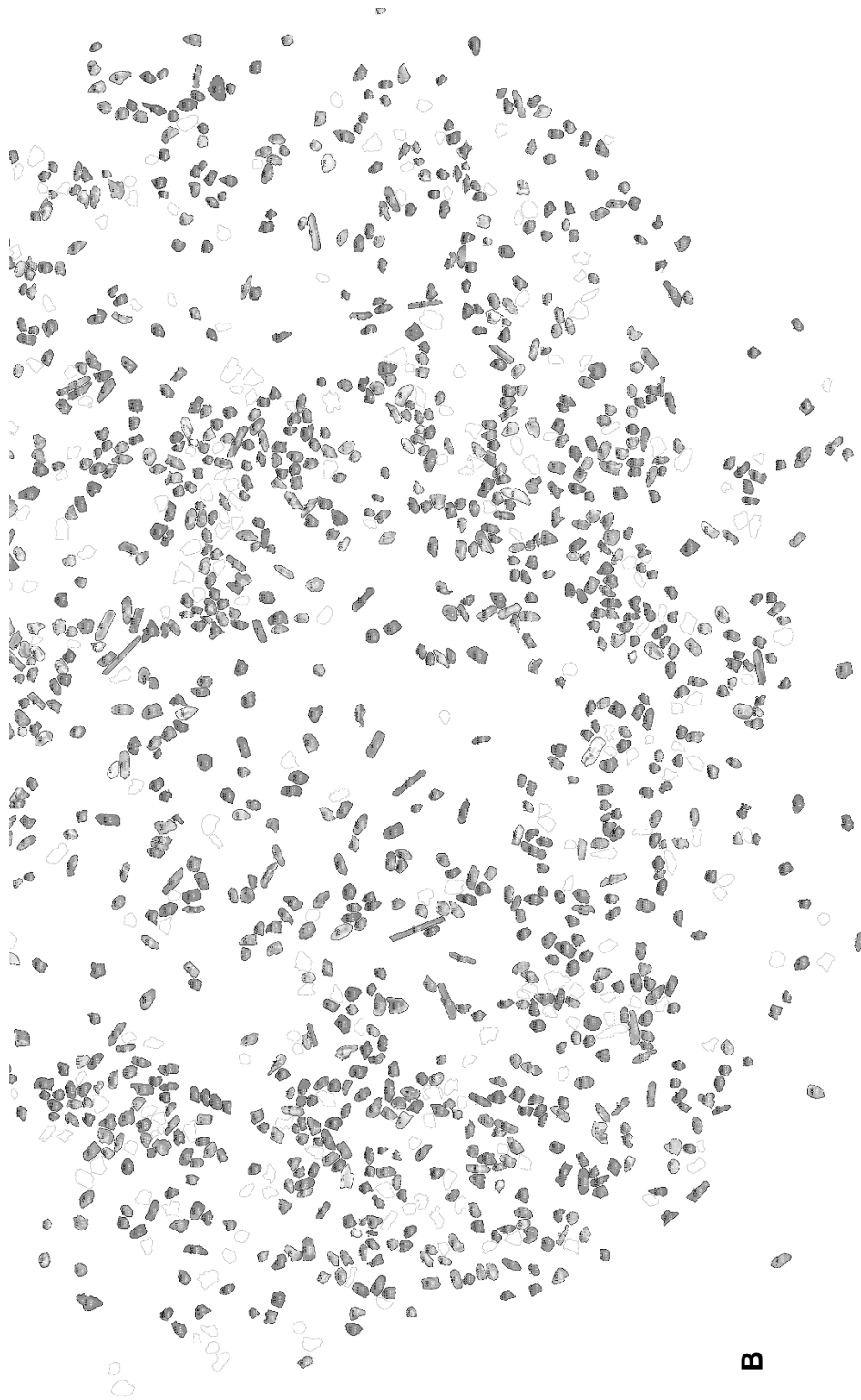
B
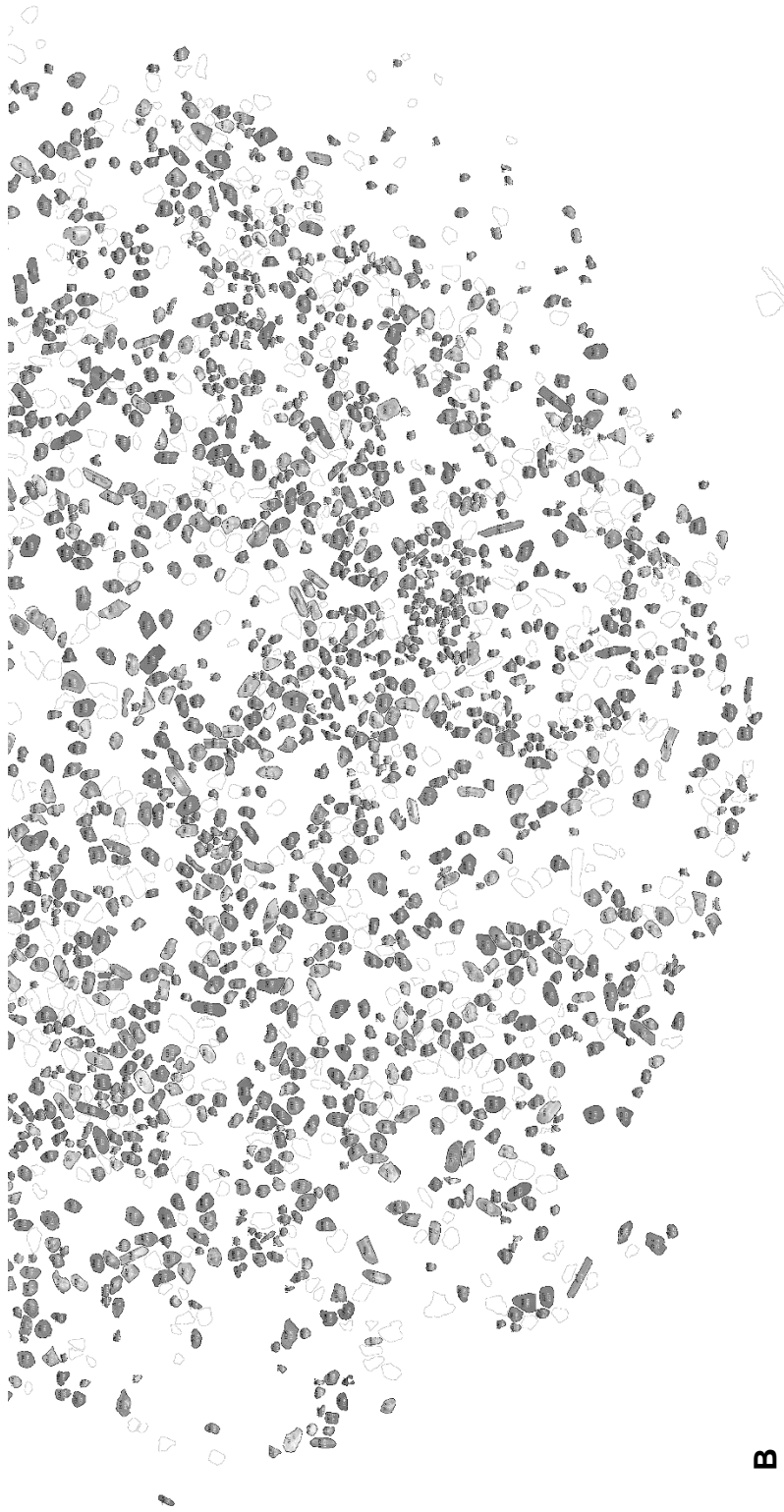
Figure D-2 Continued

Table D-3. Detrital zircon shape data for sample HP-PC. Grain map numbers correspond with Figure D-3.

Sample Name	Grain Map #	Area (µm^2)	Perimeter Length (µm)	Major Axis (µm)	Minor Axis (µm)	Aspect Ratio
			<10% Discordant Samples			
H_1	5	14913.5	483.5	179.5	105.8	1.70
H_2	10	9566.2	446.4	140.4	86.8	1.62
H_3	13	12744.1	525.2	219.7	73.8	2.98
H_4	24	9339.2	408.7	155.4	76.5	2.03
H_5	29	7500.5	356.9	132.2	72.3	1.83
H_7	60	7280	369.6	134.9	68.7	1.96
H_8	77	7387	343.7	101.8	92.4	1.10
H_9	33	8800.9	374.6	140.1	80	1.75
H_10	14	10224.4	423.2	136.4	95.4	1.43
H_11	11	15724.2	592.9	199.4	100.4	1.99
H_12	20	11401.6	546	239.2	60.7	3.94
H_13	7	6832.5	318.1	104.3	83.4	1.25
H_14	6	7325.4	350.3	115.2	80.9	1.42
H_16	97	7004.4	348.4	110.7	80.6	1.37
H2_1	110	11544.2	448.4	167.8	87.6	1.92
H2_2	133	10383.3	385.9	122.8	107.7	1.14
H2_3	136	9514.3	458	177.1	68.4	2.59
H2_4	167	7001.1	337.4	109.5	81.4	1.35
H2_5	170	11067.6	433.6	121.5	116	1.05
H2_6	193	10778.9	406.8	131.1	104.7	1.25
H2_8	134	8311.2	364.7	118.7	89.1	1.33
H2_10	88	7597.8	337.4	116.5	83.1	1.40
H2_11	55	8862.5	402.9	165.8	68	2.44
H2_12	38	8158.8	366.1	128.1	81.1	1.58
H2_14	75	7095.2	362.8	123.1	73.4	1.68
H2_15	172	13013.2	535.8	227.2	72.9	3.12
H2_16	177	14547	630	284.9	65	4.38
H3_1	213	11359.4	423.8	143	101.1	1.41
H3_2	180	6864.9	322.8	106.9	81.8	1.31
H3_5	207	7302.7	334.6	109.3	85	1.29
H3_6	246	6213.1	324.2	102.5	77.2	1.33
H3_7	279	11187.5	413.7	133.5	106.7	1.25
H3_9	306	9942.3	432.7	131.7	96.1	1.37
H3_10	314	10620.1	407.8	151.4	89.3	1.70
H3_11	335	8535	362.8	108.6	100.1	1.08
H3_12	271	8340.4	366.8	134.2	79.1	1.70
H3_14	324	8197.7	362	132.3	78.9	1.68
H3_15	325	11213.5	467.1	195.6	73	2.68
H3_16	338	10941.1	405.8	135.6	102.7	1.32
H4_1	407	32177.9	827.9	337.6	121.3	2.78
H4_2	403	9219.2	387	125.4	93.6	1.34
H4_3	370	8878.7	388.7	115.4	98	1.18
H4_6	364	8833.3	403.5	124	90.7	1.37
H4_7	345	8982.5	391.9	137.5	83.2	1.65
H4_8	272	7892.9	353.9	126.5	79.4	1.59
H4_9	269	8035.6	370.6	128.5	79.6	1.61
H4_10	267	8687.4	394	148.1	74.7	1.98
H4_11	226	11145.4	445.5	173.9	81.6	2.13

Table D-3 Continued

Sample Name	Grain Map #	Area (µm^2)	Perimeter Length (µm)	Major Axis (µm)	Minor Axis (µm)	Aspect Ratio
			<10% Discordant Samples			
H4_13	291	11842.6	473.5	184.3	81.8	2.25
H4_14	229	9102.4	394.9	142.9	81.1	1.76
H4_16	171	13629.3	493.3	176.7	98.2	1.80
H5_1	103	12108.5	516.3	195.6	78.8	2.48
H5_2	119	11096.7	411.5	129.4	109.2	1.18
H5_3	290	12565.7	444.2	141.2	113.3	1.25
H5_4	273	6482.3	309	108.8	75.8	1.44
H5_5	258	7831.3	337.8	105.2	94.8	1.11
H5_6	123	11067.6	421.8	150.2	93.8	1.60
H5_7	69	7704.8	336.5	117.7	83.3	1.41
H5_10	105	9446.2	404	147	81.8	1.80
H5_11	106	8807.3	383.2	127.2	88.1	1.44
H5_12	89	8025.8	347.4	122.6	83.4	1.47
H5_13	65	12348.4	439.8	133.2	118.1	1.13
H5_14	299	11823.1	441.7	146.4	102.8	1.42
H5_15	278	7665.9	362.2	132.9	73.4	1.81
H5_16	264	8674.4	389.2	110.4	100	1.10
H1_1	507	12795.9	442.2	160.5	101.5	1.58
H1_2	497	8061.5	353.7	128.5	79.9	1.61
H1_3	505	9579.1	404.8	129.2	94.4	1.37
H1_4	481	15691.7	693.5	310.6	64.3	4.83
H1_5	469	8042.1	389.2	104.5	98	1.07
H1_6	456	8771.7	362.6	120.5	92.7	1.30
H1_8	449	8849.5	439.5	124.7	90.4	1.38
H1_9	429	8220.4	341.6	108.6	96.4	1.13
H1_10	446	7302.7	352.2	120	77.5	1.55
H1_11	436	5237.1	287.5	92.9	71.7	1.30
H1_12	415	12783	460.5	132.8	122.6	1.08
H1_13	427	7974	370.5	115.5	87.9	1.31
H1_14	360	10016.9	394.7	126.5	100.8	1.25
H1_15	317	7435.7	340.6	122.7	77.1	1.59
H1_16	330	7691.8	361.9	129	75.9	1.70
H1_17	321	7211.9	340.6	119.5	76.8	1.56
H1_18	268	6245.6	332.4	122.6	64.9	1.89
H1_19	239	7069.2	340.6	105.2	85.6	1.23
H1_21	311	9455.9	391.7	134.3	89.6	1.50
H1_22	337	5969.9	295.2	91.2	83.3	1.09
H1_23	353	6021.8	328.9	121	63.3	1.91
H1_24	371	5752.7	294.3	105	69.7	1.51
H2_2	444	7552.4	335.5	107.1	89.7	1.19
H2_3	457	5551.6	288.6	87.7	80.6	1.09
H2_5	412	8016.1	365.5	118.2	86.4	1.37
H2_6	459	10305.5	453.7	179.3	73.2	2.45
H2_7	441	5156	281.7	85.7	76.6	1.12
H2_8	423	10817.9	470.3	185	74.5	2.48
H2_10	430	4974.4	293.9	93	68.1	1.37
H2_11	417	6702.8	334.2	103	82.8	1.24
H2_13	401	9903.4	402.2	150.6	83.7	1.80
H2_14	425	6647.7	324.7	105.4	80.3	1.31
H2_16	461	11998.2	486.9	199.4	76.6	2.60

Table D-3 Continued

Sample Name	Grain Map #	Area (µm^2)	Perimeter Length (µm)	Major Axis (µm)	Minor Axis (µm)	Aspect Ratio
			<10% Discordant Samples			
H2_17	460	5006.8	269.1	90.6	70.4	1.29
H2_18	476	13130	467.2	170.2	98.2	1.73
H2_19	479	6586.1	330.4	117	71.6	1.63
H2_20	482	5279.2	281.4	84.8	79.3	1.07
H2_22	487	10448.2	423.9	141.5	94	1.51
H2_23	493	31597.5	879	394.9	101.9	3.88
H2_24	492	9874.2	448.6	165.5	75.9	2.18
H2_25	491	7821.5	340.3	119.3	83.5	1.43
H2_26	490	13690.9	502.1	189.5	92	2.06
H2_27	503	8278.8	355.3	103.2	102.2	1.01
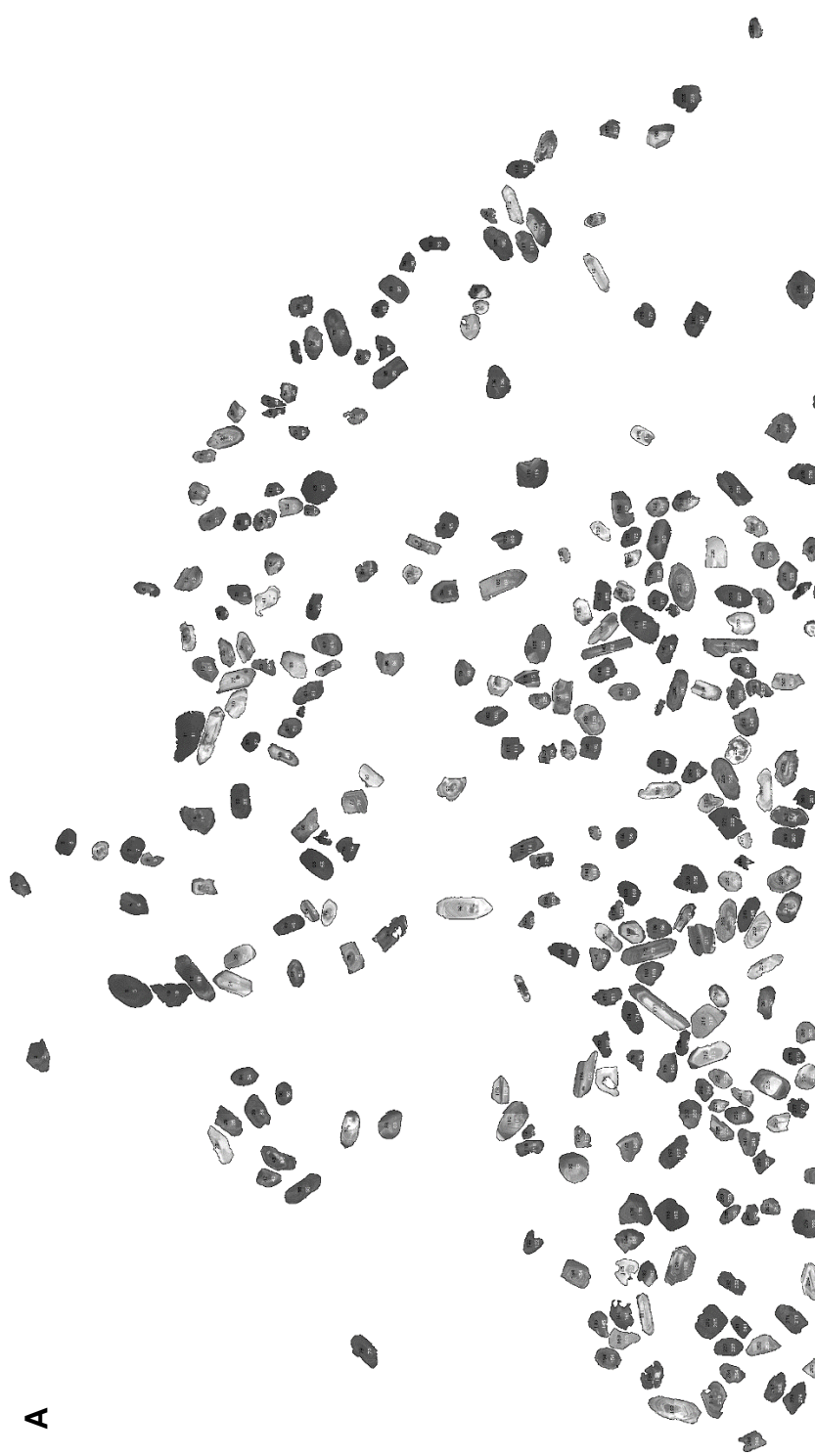
Figure D-3. Grain map generated for sample HP-PC. Upper image (A) and lower image (B) are shown. The joining area of images A-B contain overlapping grains.

B

Figure D-3 Continued

Table D-4. Detrital zircon shape data for sample HP-DR. Grain map numbers correspond with Figure D-4.

Sample Name	Grain Map #	Area (µm²)	Perimeter Length (µm)	Major Axis (µm)	Minor Axis (µm)	Aspect Ratio
		<10% Discordant Samples				
D1_1	11	3432.8	233.7	83.8	52.1	1.61
D1_2	16	4075.2	254.5	95	54.6	1.74
D1_3	34	4824.8	315.6	135.2	45.4	2.98
D1_4	29	4406.2	323.7	132.1	42.5	3.11
D1_5	21	4558.7	274.2	101.1	57.4	1.76
D1_7	41	4386.7	275.7	110	50.8	2.17
D1_8	50	5350.4	289.6	90.4	75.3	1.20
D1_9	48	5756	295	97.7	75	1.30
D1_14	62	5457.5	304.8	121.4	57.2	2.12
D2_2	109	6427.6	404.6	183.1	44.7	4.10
D2_4	119	4925.3	266.8	82.4	76.1	1.08
D2_7	144	4068.8	257.5	93.3	55.5	1.68
D2_8	111	4643.1	279.9	105.8	55.9	1.89
D2_11	61	5493.1	288.6	103.7	67.4	1.54
D2_13	92	8981.1	455.5	157.1	72.8	2.16
D2_15	59	4763.1	266.6	80.7	75.2	1.07
D2_16	56	4925.3	345.2	150.4	41.7	3.61
D3_2	198	4231	257.5	93.2	57.8	1.61
D3_4	127	5947.4	300.8	100.4	75.5	1.33
D3_14	232	4993.5	274.7	84.3	75.4	1.12
D3_16	242	4162.9	262.9	81	65.4	1.24
D4_3	239	3754	246.9	76.8	62.3	1.23
D4_5	329	3007.8	214.4	80.6	47.5	1.70
D4_11	210	5541.8	286	100.8	70	1.44
D4_12	270	6164.8	298.6	97.2	80.7	1.20
D4_13	181	3844.9	250.6	97	50.4	1.92
D4_16	102	3812.4	236.5	75.1	64.6	1.16
D5_1	78	3092.1	212.5	71.4	55.1	1.30
D5_2	107	3900	249.1	89.4	55.5	1.61
D5_7	216	4237.5	272.3	92.7	58.2	1.59
D5_10	217	5889	310.1	95	78.9	1.20
D5_11	182	3075.9	208.9	68.6	57.1	1.20
D6_2	314	4114.2	242.5	85.6	61.2	1.40
D6_3	325	2722.2	203.2	73	47.5	1.54
D6_4	320	3815.7	240.5	88.3	55	1.61
D6_5	304	5334.2	289.8	94.6	71.8	1.32
D6_6	333	5272.5	297.3	117.2	57.3	2.05
D6_7	364	2608.7	197.5	63	52.7	1.20
D6_8	372	6252.4	358.9	147.4	54	2.73
D6_9	359	4925.3	307.4	121.2	51.7	2.34
D6_10	355	6275.1	369.7	148.6	53.8	2.76
D7_3	431	4948.1	327.3	136.6	46.1	2.96
D7_7	530	5710.5	305.5	110.3	65.9	1.67
D7_8	470	4085	266.6	98.8	52.7	1.87
D7_9	505	3952	259.4	102.1	49.3	2.07
D7_10	558	3290	225.3	71.7	58.4	1.23
D7_12	565	4085	257.6	92.3	56.4	1.64
D7_13	541	3228.4	231.7	89.1	46.2	1.93

Table D-4 Continued

| Sample Name	Grain Map #	Area (µm^2)	Perimeter Length (µm)	Major Axis (µm)	Minor Axis (µm)	Aspect Ratio
			<10% Discordant Samples			
D8_1	666	4633.3	269.2	94.6	62.4	1.52
D8_2	656	5953.9	335.7	128.6	58.9	2.18
D8_4	654	4730.7	263.9	87.1	69.1	1.26
D8_6	649	3672.9	244	87.3	53.6	1.63
D8_7	639	6599.6	375.4	159.3	52.7	3.02
D8_10	641	5253	317.3	127.1	52.6	2.42
D8_11	612	2774.2	200	60.5	58.4	1.04
D8_16	549	5973.4	322.5	114.3	66.5	1.72
D9_1	564	3510.7	253.1	102	43.8	2.33
D9_4	590	4649.5	273.4	104.9	56.4	1.86
D9_5	601	3361.4	215.9	68.3	62.7	1.09
D9_6	599	3818.9	258.4	103.5	47	2.20
D9_8	635	5425	355.5	155.9	44.3	3.52
D9_10	579	5973.4	302.9	108.3	70.2	1.54
D9_13	547	5159	312.6	124	53	2.34
D9_15	458	4282.9	263.3	101	54	1.87
D9_16	417	6713.1	329.6	128.6	66.5	1.93
D10_3	375	4594.4	261.4	89.8	65.1	1.38
D10_4	357	6800.7	318.1	110.4	78.4	1.41
D10_6	287	5330.9	289.3	106.7	63.6	1.68
D10_7	337	5366.6	314	124.2	55	2.26
D10_14	418	5113.5	324.3	126.7	51.4	2.46
D10_15	544	3614.5	241.6	91.1	50.5	1.80
HDR1_1	51	6333.5	395.1	177.8	45.3	3.92
HDR1_4	95	2845.5	202.8	62.8	57.7	1.09
HDR1_5	84	3945.5	244.1	80.4	62.5	1.29
HDR1_6	97	3562.6	255.8	95.3	47.6	2.00
HDR1_8	113	4033.1	270.7	100.7	51	1.97
HDR1_9	118	4023.3	271.1	109.4	46.8	2.34
HDR1_11	153	6336.7	377.2	166.3	48.5	3.43
HDR1_12	193	9850.7	413	144.6	86.7	1.67
HDR1_17	208	3968.2	256.4	89.5	56.5	1.58
HDR1_18	250	4282.9	285.5	114.4	47.7	2.40
HDR1_19	259	3971.4	267	106.6	47.5	2.24
HDR1_21	272	5090.8	292.3	107.8	60.1	1.79
HDR1_22	244	3731.3	234.8	84	56.6	1.48
HDR1_24	283	4678.7	276.2	96.3	61.9	1.56
HDR1_27	249	1190.8	132	47.5	31.9	1.49
HDR1_29	472	3721.6	255	92.8	51.1	1.82
HDR1_30	494	7066.8	367.2	147.5	61	2.42
HDR1_31	526	3380.9	251.2	75.4	57.1	1.32
HDR1_32	512	3247.9	220	79.2	52.2	1.52
HDR1_33	504	4776.1	292.2	118.5	51.3	2.31
HDR1_34	534	3202.4	225.3	79.1	51.5	1.54
HDR1_35	573	3231.6	214.9	66.6	61.8	1.08

Figure D-4. Grain map generated for sample HP-DR. Upper image (A) and lower image (B) are shown. The joining area of images A-B contain overlapping grains.
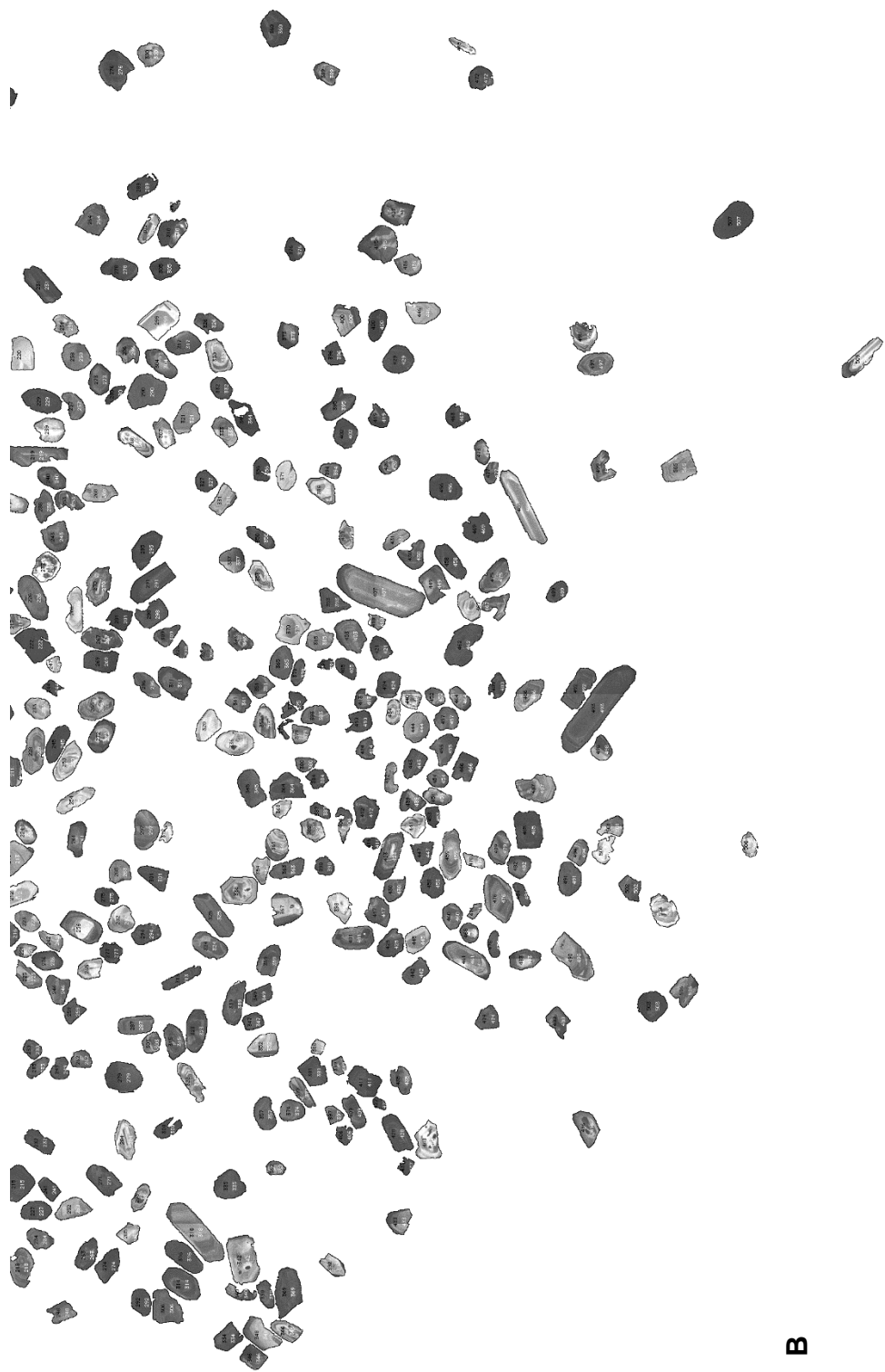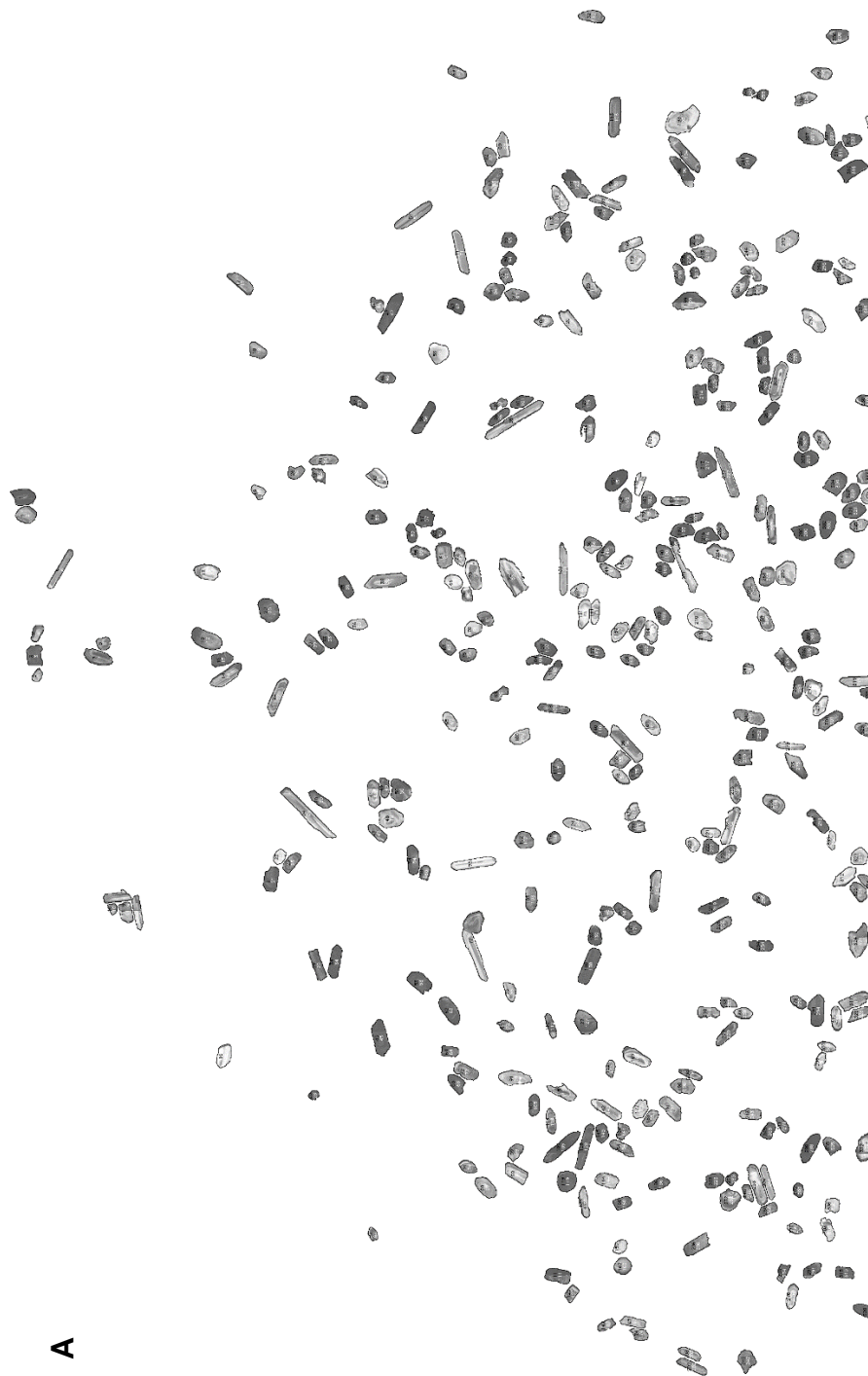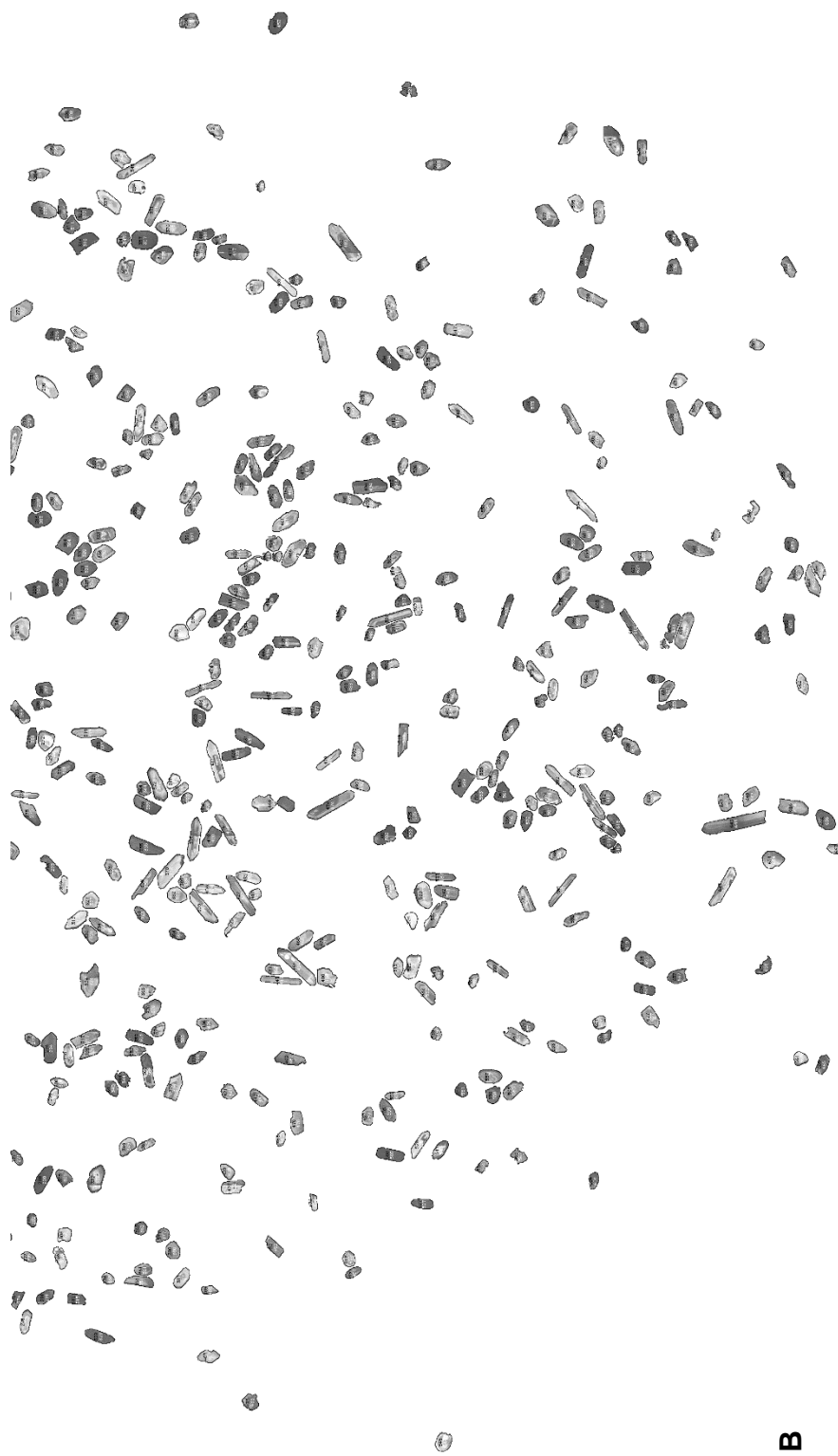
B

Figure D-4 Continued

Table D-5. Detrital zircon shape data for sample Si-B. Grain map numbers correspond with Figure D-5.

Sample Name	Grain Map #	Area (µm^2)	Perimeter Length (µm)	Major Axis (µm)	Minor Axis (µm)	Aspect Ratio
			<10% Discordant Samples			
SK1_1	153	39208.9	842.6	290.4	171.9	1.69
SK1_2	162	9229	375.1	130.3	90.2	1.44
SK1_3	170	11165	437.5	158	89.9	1.76
SK1_4	137	10681.8	424.4	127.9	106.4	1.20
SK1_5	123	9358.8	400.3	146.2	81.5	1.79
SK1_6	134	5435	280.3	87.9	78.8	1.12
SK1_7	108	6271.6	312	108.2	73.8	1.47
SK1_9	49	5318.2	282.5	87	77.8	1.12
SK1_11	76	6472.7	320.5	118.5	69.5	1.71
SK1_12	82	7345	331	108.6	86.1	1.26
SK1_13	74	11022.3	417.7	149.5	93.9	1.59
SK1_14	107	18519.7	608.7	237	99.5	2.38
SK1_16	142	23465	609.9	236.2	126.5	1.87
SK2_2	105	8123.2	380.6	142.5	72.6	1.96
SK2_5	39	18646.2	520.4	163.1	145.6	1.12
SK2_6	41	6625.1	336.3	130.6	64.6	2.02
SK2_7	52	9728.4	405.8	126.2	98.1	1.29
SK2_10	80	16003.3	528	188.5	108.1	1.74
SK2_11	89	7040.1	319.5	111.3	80.6	1.38
SK2_13	54	7380.6	324	111.4	84.3	1.32
SK2_14	45	9527.4	392.7	140.6	86.3	1.63
SK2_15	50	6916.9	319.8	109.7	80.2	1.37
SK3_1	125	15182.9	474	160.8	120.2	1.34
SK3_2	117	23478	623.1	181.8	164.4	1.11
SK3_3	124	10996.4	432.9	168.7	83	2.03
SK3_4	97	7406.6	341.5	109.4	86.2	1.27
SK3_6	59	23455.3	618	218.4	136.8	1.60
SK3_7	71	10078.7	417	138.5	92.7	1.49
SK3_8	55	17627.9	573.9	223	100.7	2.21
SK3_9	47	15370.9	538.5	170	115.1	1.48
SK3_10	30	14427.3	488.9	184.3	99.7	1.85
SK3_11	32	12092.5	444.9	158.3	97.3	1.63
SK3_12	20	18276.5	691.8	218.6	106.4	2.05
SK3_13	3	12935.6	437	143.4	114.9	1.25
SK3_14	2	22132.2	646.2	218.6	128.9	1.70
SK3_14	4	13551.7	482.3	161.5	106.8	1.51
SK3_15	12	38800.3	818.9	320.2	154.3	2.08
SK3_16	16	9154.5	373.3	116.2	100.3	1.16
SK4_1	27	8395.6	373.6	124.1	86.2	1.44
SK4_3	13	11904.4	436.4	147	103.1	1.43
SK4_4	9	18542.4	583.7	227.1	103.9	2.19
SK4_5	51	14939.6	496	189.2	100.5	1.88
SK4_7	67	16194.6	523.2	187.5	110	1.70
SK4_8	81	21756	577.9	188	147.4	1.28
SK4_9	79	14946.1	516.6	192	99.1	1.94
SK4_10	119	18493.8	602.1	225.9	104.2	2.17
SK4_11	141	21149.6	807.9	185.2	145.4	1.27
SK4_12	146	24525.4	640.3	213.6	146.2	1.46

Table D-5 Continued

Sample Name	Grain Map #	Area (μm^2)	Perimeter Length (μm)	Major Axis (μm)	Minor Axis (μm)	Aspect Ratio
			<10% Discordant Samples			
SK4_15	177	22553.8	622.5	226.7	126.7	1.79
SK4_16	144	24467	699.5	280.9	110.9	2.53
SK5_1	132	71841.3	1426.5	541.5	168.9	3.21
SK5_2	120	14025.2	466.1	145.2	123	1.18
SK5_3	158	19015.9	580.7	220.3	109.9	2.00
SK5_5	148	19872	649.6	210.4	120.3	1.75
SK5_6	180	11265.5	452.5	167	85.9	1.94
SK5_7	201	28497.8	799.6	330	109.9	3.00
SK5_9	212	10908.8	422.6	159.5	87.1	1.83
SK5_11	226	14978.6	538.5	189	100.9	1.87
SK5_12	252	26023.6	735.4	291.6	113.6	2.57
SK5_14	176	20919.4	642.6	242	110.1	2.20
SK5_15	211	36870.8	847.5	316.9	148.1	2.14
SK5_16	174	11823.3	475	161.3	93.3	1.73
SK6_1	186	17585.8	526.1	189.5	118.1	1.60
SK6_3	187	12050.3	533.6	225.3	68.1	3.31
SK6_6	172	23974.1	712.4	269.4	113.3	2.38
SK6_7	154	8593.5	365.6	116.8	93.7	1.25
SK6_9	193	19259.1	554.7	198.4	123.6	1.61
SK6_11	173	6715.9	309.9	100.3	85.3	1.18
SK6_13	192	14978.6	564.1	234.7	81.2	2.89
SK6_14	188	8317.8	372.1	141.5	74.8	1.89
SK6_16	185	14845.6	489.6	167.9	112.6	1.49
SK7_1	245	27012.6	709.3	206.7	166.4	1.24
SK7_2	269	23101.8	776.9	259.8	113.2	2.30
SK7_3	302	12955	452.7	170.6	96.7	1.76
SK7_5	308	11910.9	467.1	136.6	111	1.23
SK7_6	332	14034.9	472	166	107.6	1.54
SK7_10	275	7704.9	346.9	122.4	80.1	1.53
SK7_11	280	10085.1	427.1	158.3	81.1	1.95
SK7_13	253	14086.8	558.2	245.3	73.1	3.36
SK7_14	320	22722.4	745	210.4	137.5	1.53
SK7_15	336	19859	732.1	308.7	81.9	3.77
SK7_16	342	15915.7	522.8	161	125.8	1.28
SK8_1	331	15909.2	515.4	181	111.9	1.62
SK8_2	340	12685.9	448.9	167.4	96.5	1.73
SK8_3	344	20744.3	585.7	210.3	125.6	1.67
SK8_4	351	9783.6	403	148.3	84	1.77
SK8_6	362	42912.1	1059	304	179.7	1.69
SK8_7	370	24671.3	751.7	256.2	122.6	2.09
SK8_8	368	18565.1	597.6	193.8	121.9	1.59
SK8_10	358	8463.7	375.7	134.5	80.1	1.68
SK8_11	359	14884.5	494	160.3	118.3	1.36
SK8_12	364	15315.8	472	155.2	125.6	1.24
SK8_14	350	9465.8	396.1	129.3	93.2	1.39
SK8_15	337	31144	779	320.4	123.8	2.59
SK8_16	343	17673.3	544.8	208.8	107.8	1.94
SK9_1	349	9232.3	382	134	87.7	1.53
SK9_2	352	10270	423.1	132.2	98.9	1.34
SK9_3	346	11638.5	427.2	136.1	108.9	1.25

Table D-5 Continued

| Sample Name	Grain Map #	Area (µm^2)	Perimeter Length (µm)	Major Axis (µm)	Minor Axis (µm)	Aspect Ratio
			<10% Discordant Samples			
SK9_4	341	16713.5	500.5	163.3	130.3	1.25
SK9_5	347	13671.7	507.1	204.4	85.2	2.40
SK9_7	357	26912.1	782.8	198.1	173	1.15
SK9_8	363	7786	345.4	107.8	91.9	1.17
SK9_9	329	27956.3	803.6	340.7	104.5	3.26
SK9_11	326	6466.2	350.2	131.7	62.5	2.11
SK9_12	323	12063.3	483.8	200.3	76.7	2.61
SK9_13	338	15075.8	484.5	160.7	119.4	1.35
SK9_14	348	17864.7	533	160.2	142	1.13
SK9_15	353	13914.9	490.3	185.9	95.3	1.95
SK10_1	292	19580.1	545.7	192.3	129.7	1.48
SK10_2	276	20874	655.5	263.8	100.8	2.62
SK10_3	298	10396.5	412.2	153.8	86.1	1.79
SK10_4	307	6255.4	295.2	95.7	83.2	1.15
SK10_5	300	13444.7	475.8	154.5	110.8	1.39
SK10_6	281	16687.5	538.4	180.7	117.6	1.54
SK10_7	313	17469	535.7	181.4	122.6	1.48
SK10_8	288	42532.7	994.8	380.2	142.4	2.67
SK10_9	257	11291.5	463.8	138	104.1	1.33
SK10_10	241	12562.7	482.2	184.4	86.7	2.13
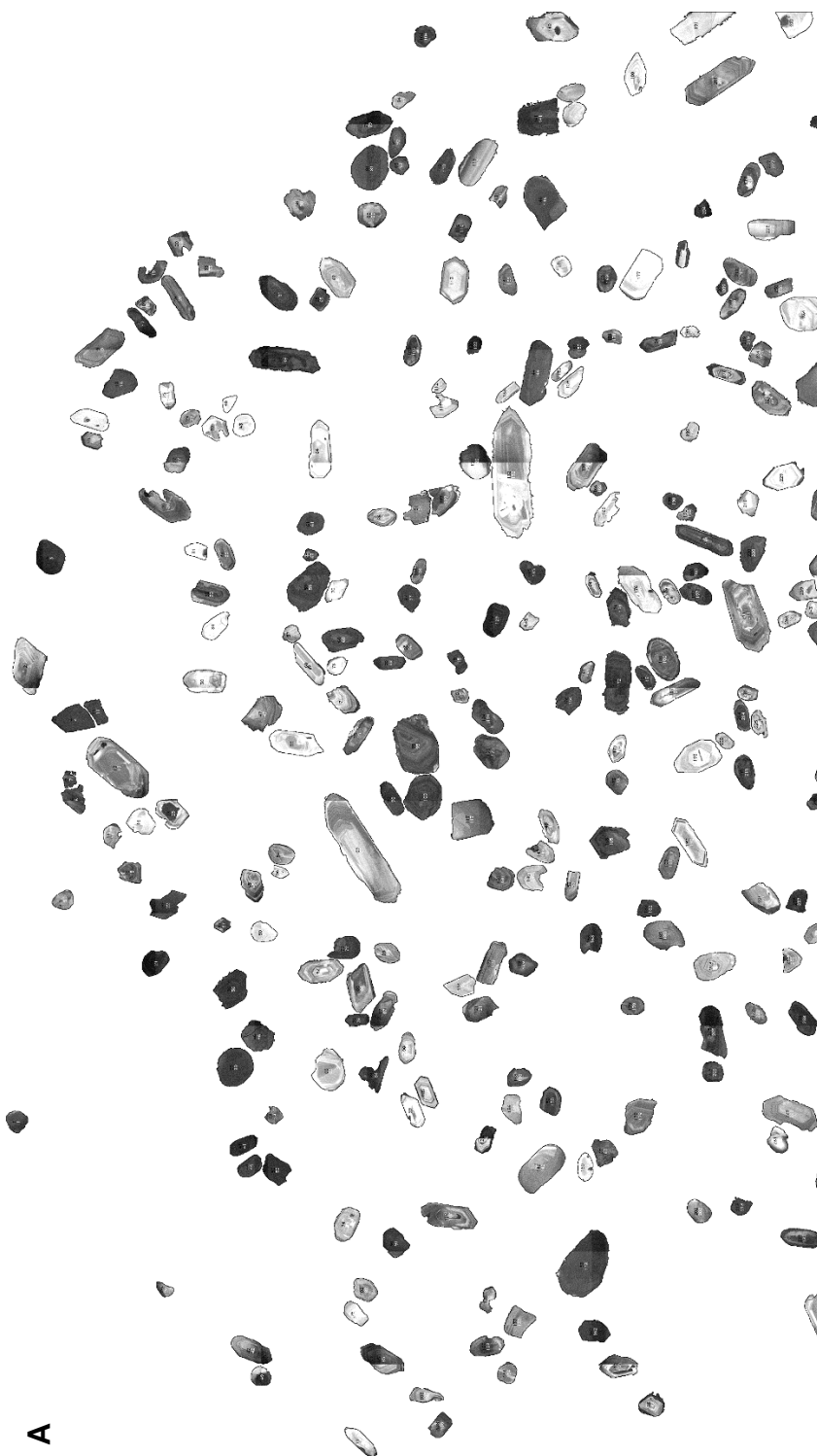
Figure D-5. Grain map generated for sample SI-B. Upper image (A) and lower image (B) are shown. The joining area of images A-B contain overlapping grains.
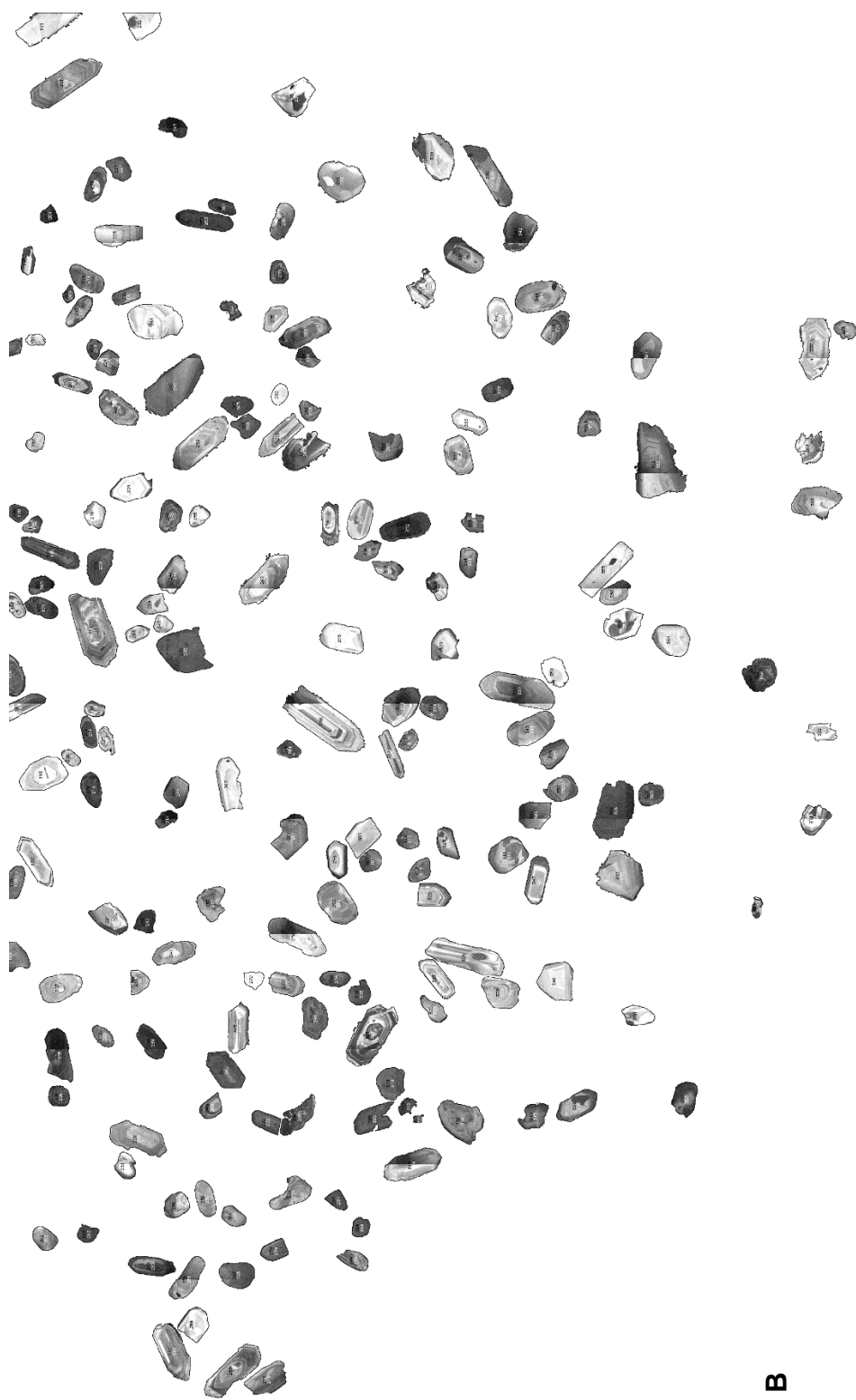
Figure D-5 Continued

Table D-6. Detrital zircon shape data for sample Si-LP. Grain map numbers correspond with Figure D-6.

Sample Name	Grain Map #	Area (μm^2)	Perimeter Length (μm)	Major Axis (μm)	Minor Axis (μm)	Aspect Ratio
			<10% Discordant Samples			
SLP_2	20	10645.2	399.3	129	105.1	1.23
SLP_5	36	5720.3	312.1	88.4	82.4	1.07
SLP_7	65	6652.1	325.7	113.7	74.5	1.53
SLP_10	54	8061	362	109.2	94	1.16
SLP_13	106	8515.5	407.9	122.9	88.2	1.39
SLP1_3	60	24809.7	648.3	191.4	165.1	1.16
SLP1_5	101	9353.1	408.2	141.7	84	1.69
SLP1_7	130	8882.4	368.6	133.6	84.6	1.58
SLP1_9	154	9460.3	397	148.2	81.3	1.82
SLP1_10	142	7288.4	346.5	123.3	75.3	1.64
SLP1_11	144	11378.9	409.1	132.8	109.1	1.22
SLP1_12	156	7398.8	348.4	119.2	79	1.51
SLP1_15	124	9992.7	468	168.8	75.4	2.24
SLP1_16	125	7483.2	429.6	123.6	77.1	1.60
SLP2_1	90	27845.1	745.7	271.2	130.7	2.07
SLP2_2	40	7515.6	374.1	137.2	69.8	1.97
SLP2_3	98	10625.8	435.2	160.7	84.2	1.91
SLP2_6	200	10460.2	409.3	139.3	95.6	1.46
SLP2_7	181	10064.1	413.5	149.5	85.7	1.74
SLP2_8	192	4980.1	274.6	86.7	73.1	1.19
SLP2_9	239	9746	393.8	123.4	100.5	1.23
SLP2_10	229	6820.9	350.7	122.4	71	1.72
SLP2_11	274	7450.7	328.5	105.8	89.6	1.18
SLP2_12	234	8577.2	396.2	124.9	87.5	1.43
SLP2_13	242	11366	424.4	137.1	105.6	1.30
SLP2_15	286	10132.3	406.8	156.8	82.3	1.91
SLP3_4	275	12833.4	532.5	158.3	103.2	1.53
SLP3_6	165	9382.4	418.2	163.3	73.2	2.23
SLP3_7	143	13385.3	495.6	167.7	101.6	1.65
SLP3_8	111	13395	466.3	160	106.6	1.50
SLP3_9	69	6671.5	400.4	137.7	61.7	2.23
SLP3_10	76	6223.5	328.4	105.2	75.3	1.40
SLP3_13	187	10651.7	453.6	173.3	78.3	2.21
SLP3_14	237	9733	423.9	161.3	76.8	2.10
SLP3_15	240	10554.3	585.3	119.3	112.6	1.06
SLP3_16	250	9038.2	456.3	171.2	67.2	2.55
SLP4_2	221	8733.1	383.2	109.9	101.2	1.09
SLP4_3	264	10116.1	411.6	132.1	97.5	1.35
SLP4_4	197	7307.8	335.9	107.5	86.5	1.24
SLP4_6	152	9927.8	390.2	122.6	103.1	1.19
SLP4_7	146	6872.8	329.7	114.9	76.2	1.51
SLP4_8	121	7479.9	363.9	113	84.3	1.34
SLP4_9	122	5885.9	309.3	110.9	67.6	1.64
SLP4_12	95	7781.8	365.5	109	90.9	1.20
SLP4_13	94	9671.3	409.6	114.6	107.5	1.07
SLP4_14	93	8866.2	378.3	136.6	82.6	1.65
SLP5_1	190	12852.9	502.7	149.8	109.3	1.37
SLP5_5	380	11002.4	571.8	137	102.3	1.34

Table D-6 Continued

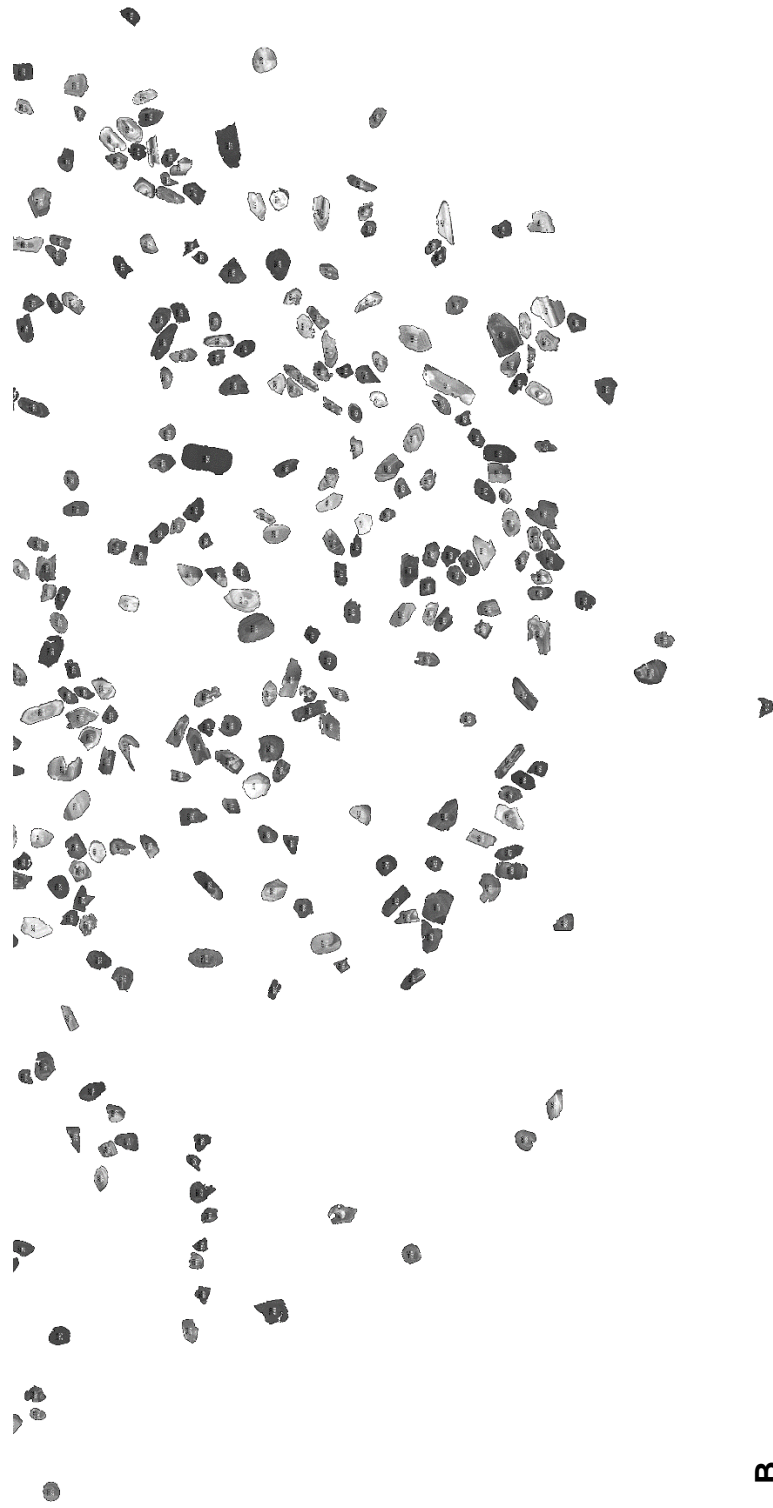| Sample Name	Grain Map #	Area (μm^2)	Perimeter Length (μm)	Major Axis (μm)	Minor Axis (μm)	Aspect Ratio
			<10% Discordant Samples			
SLP5_6	141	8791.5	377.6	121.4	92.2	1.32
SLP5_8	489	3694.5	278.7	96.8	48.6	1.99
SLP5_9	480	9375.9	444.7	152.9	78.1	1.96
SLP5_14	478	9405.1	430.5	146.3	81.8	1.79
SLP6_1	350	10440.7	428.6	156.4	85	1.84
SLP6_4	348	10577.1	464.9	169.2	79.6	2.13
SLP6_7	372	12762	458.3	158.1	102.8	1.54
SLP6_8	385	8395.4	352.8	124.7	85.7	1.46
SLP6_9	343	23358.5	646.8	242.1	122.8	1.97
SLP6_10	327	6996.2	338.1	114.1	78.1	1.46
SLP6_11	341	7548.1	352.2	115.1	83.5	1.38
SLP6_13	409	7768.9	493.5	123.5	80.1	1.54
SLP6_14	382	11226.4	428.3	125.3	114.1	1.10
SLP6_15	376	10521.9	411.9	124.9	107.3	1.16
SLP7_1	419	6366.4	336.1	107	75.7	1.41
SLP7_2	437	7746.1	361.6	136.8	72.1	1.90
SLP7_3	441	9788.2	443.8	149.7	83.3	1.80
SLP7_4	450	6512.5	331.2	115.7	71.7	1.61
SLP7_5	468	9197.3	466.2	136	86.1	1.58
SLP7_6	464	7382.5	343.3	119.1	78.9	1.51
SLP7_8	492	11885.4	517.7	131.2	115.3	1.14
SLP7_10	475	8015.6	369.7	113.3	90.1	1.26
SLP7_12	503	8216.9	364.2	129.9	80.6	1.61
SLP7_13	500	4649	282.6	92.3	64.1	1.44
SLP7_14	497	12336.7	564.7	170	92.4	1.84
SLP7_15	487	8765.5	413	166.1	67.2	2.47
SLP7_16	510	11635.4	461.7	145.6	101.7	1.43
SLP8_1	451	18914	713	276.9	87	3.18
SLP8_2	440	12875.6	461.9	159.6	102.7	1.55
SLP8_5	502	7330.6	378.3	111.8	83.5	1.34
SLP8_6	444	8567.5	371.1	137	79.6	1.72
SLP8_8	427	6122.9	347.6	107	72.9	1.47
SLP8_9	369	9061	391.1	129.8	88.9	1.46
SLP8_10	362	6519	355.5	142.6	58.2	2.45
SLP8_12	370	8934.3	402.4	109.5	103.9	1.05
SLP8_13	386	11275.1	431	137.4	104.5	1.31
SLP8_14	405	8976.5	463.1	157.4	72.6	2.17
SLP8_15	377	7103.3	370.2	133.3	67.9	1.96
SLP9_3	315	9233	380	139.8	84.1	1.66
SLP9_4	306	8155.2	400.5	132.4	78.4	1.69
SLP9_5	288	8483.1	371.7	110.1	98.1	1.12
SLP9_7	256	7113.1	357.7	126.1	71.8	1.76
SLP9_8	345	6765.7	341.7	112.4	76.6	1.47
SLP9_9	317	5450.9	285.3	94.7	73.3	1.29
SLP9_10	363	5493.1	318.7	108.1	64.7	1.67
SLP9_12	392	10901.7	494.8	182.4	76.1	2.40
SLP9_13	397	8843.4	494.6	168.5	66.8	2.52
SLP9_16	302	6915	339.7	115.7	76.1	1.52
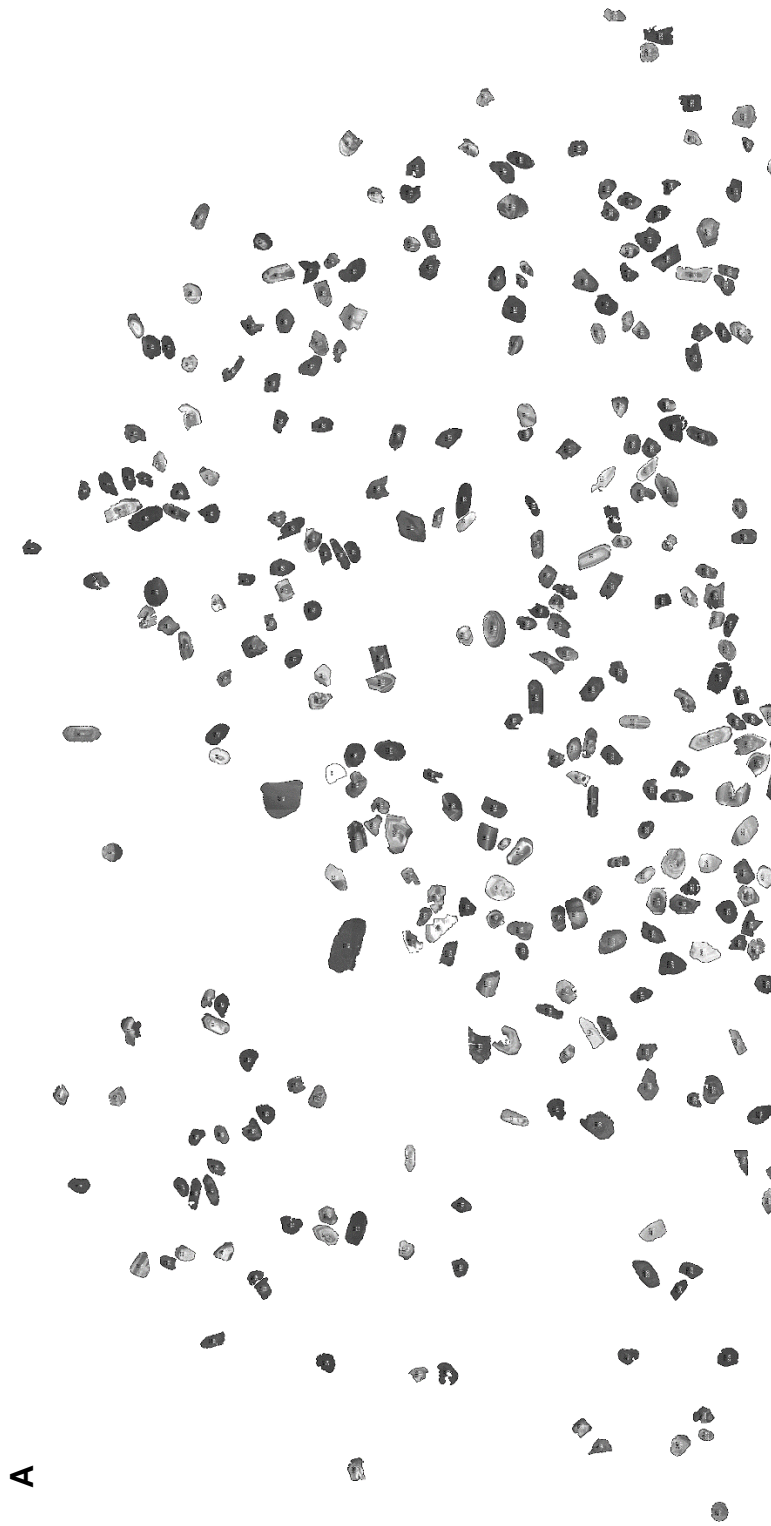
Figure D-6. Grain map generated for sample Si-LP. Upper image (A) and lower image (B) are shown. The joining area of images A-B contain overlapping grains.

B

Figure D-6 Continued

Table D-7. Detrital zircon shape data for sample Si-TQ. Grain map numbers correspond with Figure D-7.

Sample Name	Grain Map #	Area (µm^2)	Perimeter Length (µm)	Major Axis (µm)	Minor Axis (µm)	Aspect Ratio
			<10% Discordant Samples			
STQ1_1	120	10301.1	410	130	100.9	1.29
STQ1_2	80	13908	515.9	188.9	93.8	2.01
STQ1_3	112	7652	342	121.3	80.3	1.51
STQ1_4	124	9310.9	378.9	137.3	86.3	1.59
STQ1_5	138	10271.9	391.4	134.8	97	1.39
STQ1_6	116	8041.6	354.6	124.2	82.4	1.51
STQ1_7	107	7064.4	328.5	109.9	81.8	1.34
STQ1_9	63	18284.2	565.7	178.1	130.7	1.36
STQ1_10	45	11346.5	478.1	134.1	107.8	1.24
STQ1_11	7	11314	453.8	151.1	95.3	1.59
STQ1_12	21	16394.8	727	166.6	125.3	1.33
STQ1_14	43	8022.1	385.7	139.7	73.1	1.91
STQ1_16	50	7220.2	321	101	91	1.11
STQ2_1	100	21956	643.3	207.5	134.7	1.54
STQ2_4	64	6580.6	324.9	110.8	75.6	1.47
STQ2_5	48	8707.1	408	158	70.2	2.25
STQ2_6	41	9187.6	376	123.7	94.6	1.31
STQ2_7	25	14907.9	519.2	191.8	98.9	1.94
STQ2_10	23	14817	497.4	170.4	110.7	1.54
STQ2_13	61	9869.3	419.1	163.5	76.9	2.13
STQ3_14	206	7707.2	357.1	116	84.6	1.37
STQ3_15	200	11992.5	528.9	187.1	81.6	2.29
STQ4_1	113	15229.3	568.7	169.9	114.1	1.49
STQ4_3	151	8375.9	380.7	107.3	99.4	1.08
STQ4_4	169	11469.8	454.1	151	96.7	1.56
STQ4_5	168	12758.7	511.3	197	82.4	2.39
STQ4_6	187	12245.8	465.2	181.8	85.7	2.12
STQ4_7	222	26293.3	682	245.3	136.5	1.80
STQ4_9	234	7275.4	330.8	115.3	80.3	1.44
STQ4_10	238	7041.6	358.1	143.9	62.3	2.31
STQ4_11	262	10249.2	441.5	124.9	104.5	1.20
STQ4_12	256	9934.3	397.3	131.5	96.2	1.37
STQ4_14	285	10482.9	405.3	147.7	90.4	1.63
STQ4_15	290	13667.7	527.7	222.3	78.3	2.84
STQ5_1	122	15959.7	520.1	203.6	99.8	2.04
STQ5_2	136	9905	405.9	135	93.4	1.45
STQ5_3	156	11255.6	663.2	195.4	73.3	2.67
STQ5_4	185	9612.9	389.1	148.1	82.6	1.79
STQ5_6	167	19410.8	646.1	241.3	102.4	2.36
STQ5_7	171	8028.6	338.9	107.1	95.5	1.12
STQ5_8	243	16057.1	583.1	181.3	112.7	1.61
STQ5_9	241	16722.7	589.6	234.5	90.8	2.58
STQ5_10	232	10888.7	407.2	145.4	95.4	1.52
STQ5_11	267	9836.9	382.7	136.4	91.8	1.49
STQ5_12	261	12047.7	436.1	147.9	103.7	1.43
STQ5_14	265	10554.3	420.7	160.7	83.6	1.92
STQ5_15	275	10379	412.1	151.6	87.2	1.74
STQ5_16	274	11560.8	456.2	165.1	89.2	1.85

Table D-7 Continued

Sample Name	Grain Map #	Area (µm^2)	Perimeter Length (µm)	Major Axis (µm)	Minor Axis (µm)	Aspect Ratio
			<10% Discordant Samples			
STQ6_1	279	12486	486.9	186.3	85.3	2.18
STQ6_4	292	6908.5	328.2	113.6	77.4	1.47
STQ6_5	289	7557.8	345.6	112.8	85.3	1.32
STQ6_6	300	6973.5	339.7	103.7	85.6	1.21
STQ6_7	298	9359.6	400.1	127.7	93.3	1.37
STQ6_8	299	11258.8	408	129.2	111	1.16
STQ6_10	281	29711.9	683.2	232.6	162.6	1.43
STQ6_11	286	8223.4	341.8	109.9	95.3	1.15
STQ6_13	263	42171.9	1042.9	405.6	132.4	3.06
STQ6_14	231	12534.7	498.5	192.8	82.8	2.33
STQ6_15	237	6827.4	322.5	99.1	87.8	1.13
STQ6_16	217	10158.3	405.7	148.2	87.3	1.70
STQ7_2	170	10745.9	423.5	160.6	85.2	1.88
STQ7_3	145	10207	387.5	124.6	104.3	1.19
STQ7_4	155	7671.5	345	124.2	78.7	1.58
STQ7_5	190	7781.8	364.3	137.4	72.1	1.91
STQ7_7	220	9265.5	416.9	143.1	82.5	1.73
STQ7_8	228	7642.2	347.4	105.9	91.9	1.15
STQ7_12	268	9505.7	396.8	113.8	106.4	1.07
STQ7_13	183	8252.6	367.8	133.2	78.9	1.69
STQ7_14	164	7671.5	350.1	125.9	77.6	1.62
STQ7_15	186	10629	416.9	156.6	86.4	1.81
STQ8_1	161	8785	401.6	151.1	74	2.04
STQ8_2	149	11268.6	446.1	162.3	88.4	1.84
STQ8_3	146	7106.6	320.4	105.9	85.4	1.24
STQ8_4	135	10911.5	422	142.3	97.6	1.46
STQ8_5	137	7298.1	341.8	118.8	78.2	1.52
STQ8_6	110	13106.1	524	210.2	79.4	2.65
STQ8_7	98	12304.2	484.6	183.9	85.2	2.16
STQ8_10	71	6619.6	314	101	83.4	1.21
STQ8_11	49	11307.5	428.3	158.2	91	1.74
STQ8_12	74	18907.6	701.8	305.8	78.7	3.89
STQ8_13	46	15865.6	531.1	179.5	112.6	1.59
STQ8_14	39	10336.8	423.9	125.8	104.6	1.20
STQ9_1	18	6230	309.8	102.3	77.5	1.32
STQ9_2	6	7307.8	348.1	132.2	70.4	1.88
STQ9_3	3	7463.7	345.6	126.6	75.1	1.69
STQ9_4	1	12417.8	431.6	156.4	101.1	1.55
STQ9_5	26	8804.5	367.9	137.4	81.6	1.68
STQ9_6	31	6583.9	319.1	99	84.6	1.17
STQ9_7	24	9479.8	413.9	143.4	84.2	1.70
STQ9_8	14	6713.7	319.5	107.3	79.7	1.35
STQ9_9	9	11239.3	473.7	191.7	74.6	2.57
STQ9_10	15	11206.9	481.8	179.3	79.6	2.25
STQ9_11	2	33646.6	840.8	300.3	142.7	2.10
STQ9_12	16	5691.1	285.2	92.7	78.2	1.19
STQ9_14	28	8687.6	369.8	131	84.5	1.55
STQ9_16	12	15781.2	533.5	193.8	103.7	1.87
STQ10_1	76	9775.2	383.7	114	109.1	1.04
STQ10_3	33	10012.2	431	144.3	88.4	1.63

Table D-7 Continued

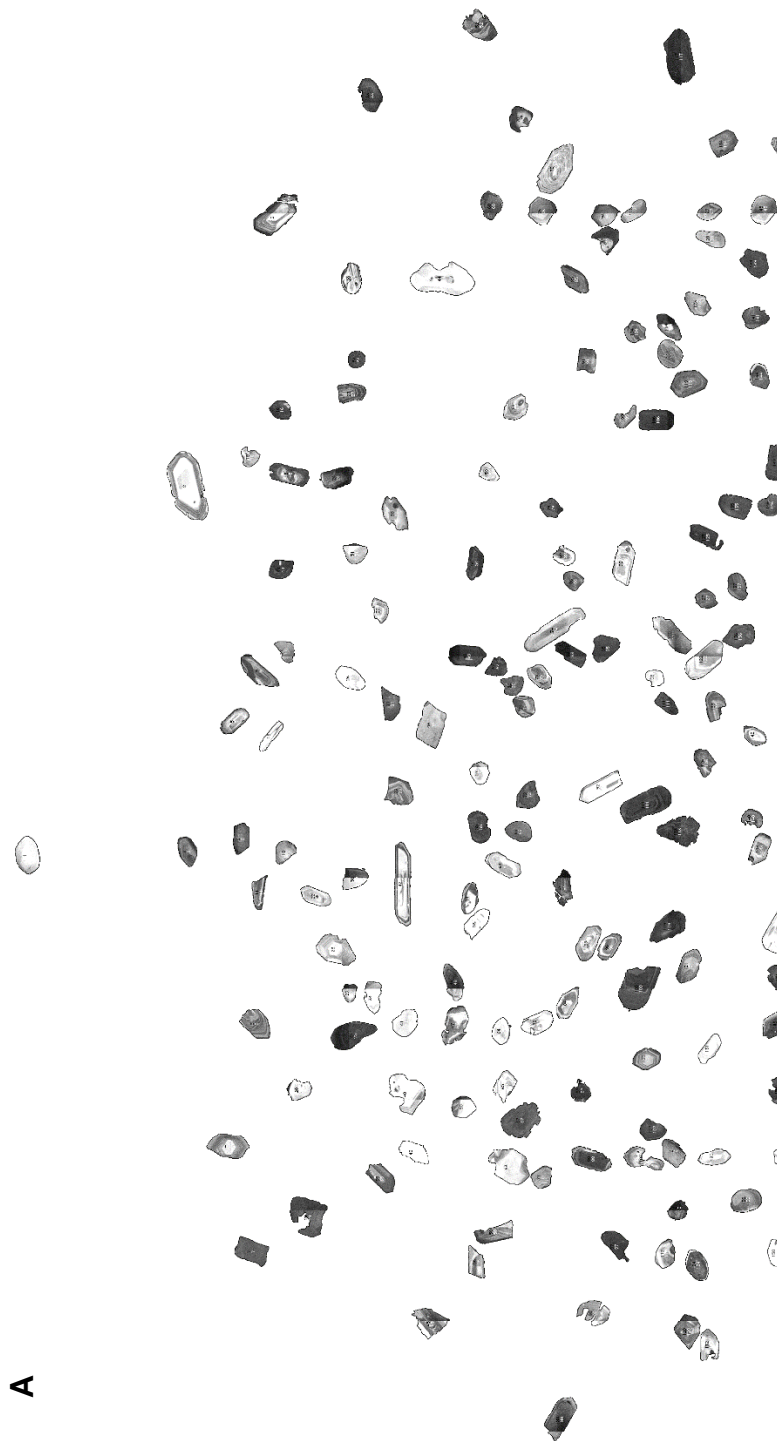| Sample Name	Grain Map #	Area (μm^2)	Perimeter Length (μm)	Major Axis (μm)	Minor Axis (μm)	Aspect Ratio
			<10% Discordant Samples			
STQ10_4	94	7642.2	354.8	108.8	89.4	1.22
STQ10_5	85	8557.7	389.6	145.8	74.8	1.95
STQ10_6	115	9512.2	369	121.7	99.5	1.22
STQ10_7	119	12687.3	440.7	151.3	106.7	1.42
STQ10_8	106	11693.9	432	158.7	93.8	1.69
STQ10_9	68	8106.5	359.4	117.2	88.1	1.33
STQ10_10	91	6908.5	343.4	106.4	82.7	1.29

A

Figure D-7. Grain map generated for sample Si-TQ. Upper image (A) and lower image (B) are shown. The joining area of images A-B contain overlapping grains.
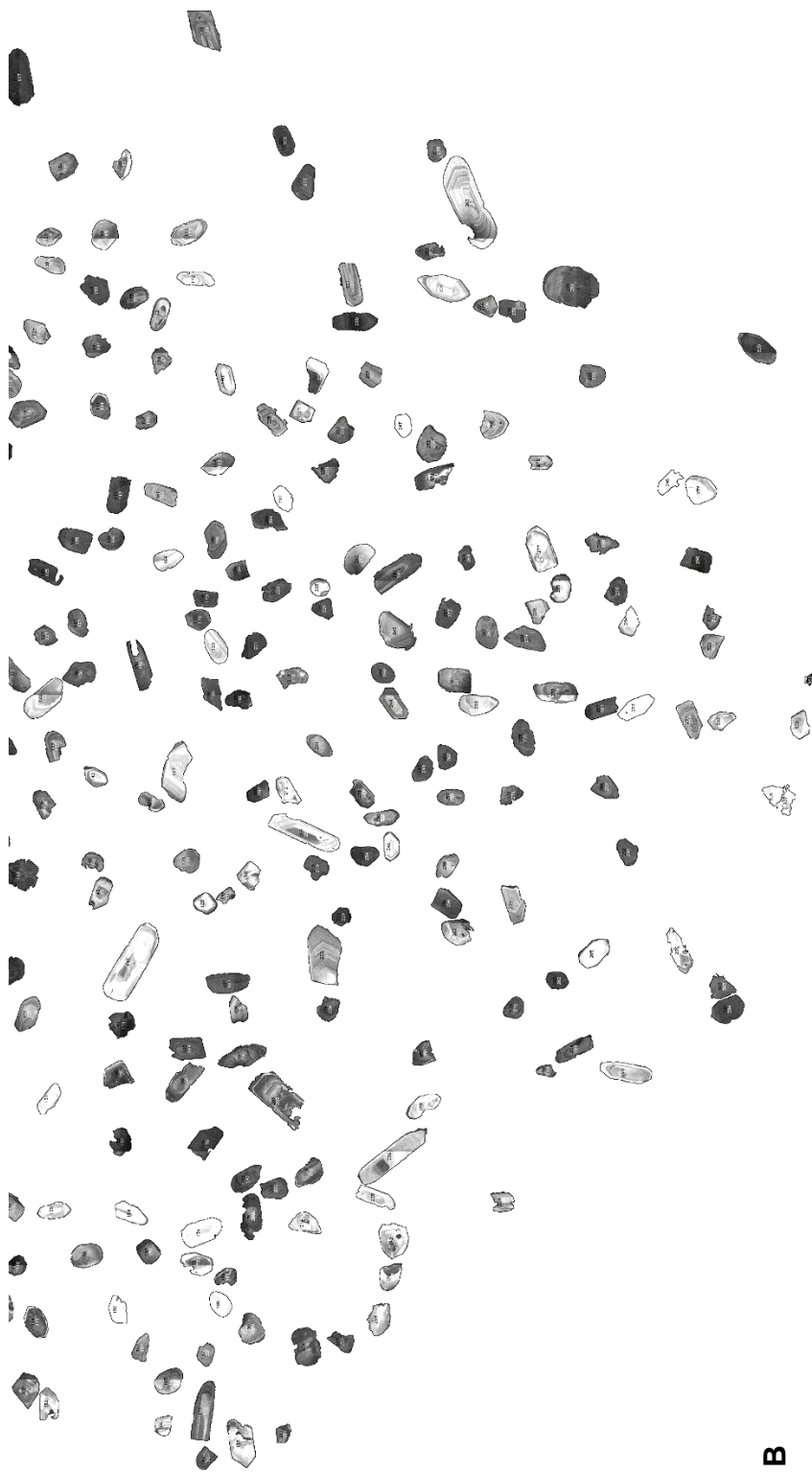
B

Figure D-7 Continued

Table D-8. Detrital zircon shape data for sample Si-KM. Grain map numbers correspond with Figure D-8.

Sample Name	Grain Map #	Area (µm^2)	Perimeter Length (µm)	Major Axis (µm)	Minor Axis (µm)	Aspect Ratio
			<10% Discordant Samples			
K1_2	102	8679.4	419.8	138.5	79.8	1.74
K1_3	130	17238.7	609.1	232.3	94.5	2.46
K1_4	121	8131	374.3	134	77.2	1.74
K1_5	177	8101.8	374.3	144.1	71.6	2.01
K1_6	186	6940.2	328.6	111.1	79.5	1.40
K1_7	215	19652.7	596.8	229.7	108.9	2.11
K1_9	208	5214.1	282.5	95.5	69.5	1.37
K1_10	199	8153.7	379.7	121.5	85.4	1.42
K1_11	190	5548.3	288.5	94.7	74.6	1.27
K1_12	105	7102.5	342.4	117.4	77	1.52
K1_13	120	7959.1	349.6	116.9	86.7	1.35
K1_14	88	8400.3	352.7	120.2	89	1.35
K1_15	67	9811.7	469.3	171	73.1	2.34
K1_16	38	11327	449	158.8	90.8	1.75
K2_1	40	9954.5	479.6	152.9	82.9	1.84
K2_2	39	7407.5	347.3	108.5	86.9	1.25
K2_3	24	16761.7	617	163	131	1.24
K2_4	12	7063.5	321.4	105.6	85.1	1.24
K2_6	17	9464.6	404.5	148.9	80.9	1.84
K2_7	26	10742.9	458.9	136.5	100.2	1.36
K2_8	36	11161.5	423.4	154.1	92.2	1.67
K2_9	48	15253	515.7	184.8	105.1	1.76
K2_10	70	14334.7	476.8	153.8	118.7	1.30
K2_11	87	10996	466.1	133.3	105	1.27
K2_12	94	8517.1	367.8	129.2	83.9	1.54
K2_13	84	9636.5	467	169	72.6	2.33
K2_14	139	8027.2	357.2	119.8	85.3	1.40
K2_15	135	6654.7	368.3	112.3	75.5	1.49
K2_16	34	8215.4	366.3	114.2	91.6	1.25
K3_2	14	11924	416	136.4	111.3	1.23
K3_3	25	7667	333.4	109.3	89.3	1.22
K3_4	32	8530.1	370.1	136.4	79.6	1.71
K3_5	37	8728	383.1	128.5	86.5	1.49
K3_6	35	15700.7	717.7	158.1	126.4	1.25
K3_7	29	6216.7	326	99.4	79.6	1.25
K3_8	18	11213.4	482.6	180.8	79	2.29
K3_9	47	5885.7	336.9	99.3	75.4	1.32
K3_10	89	7709.2	379.3	100.8	97.4	1.03
K3_11	111	7329.6	333.5	119.7	78	1.53
K3_12	128	9594.4	442.8	122	100.2	1.22
K3_13	109	5292	290.4	107.8	62.5	1.72
K3_14	136	8724.8	419	158.6	70.1	2.26
K3_15	157	9798.8	436.7	144.6	86.3	1.68
K3_16	152	8098.6	403.9	142.9	72.2	1.98
K4_1	144	6969.5	348.2	95.1	93.3	1.02
K4_3	180	8092.1	371.4	142.4	72.4	1.97
K4_4	153	6512	329.8	114.9	72.2	1.59
K4_5	167	9266.6	411.8	130.3	90.5	1.44

Table D-8 Continued

Sample Name	Grain Map #	Area (µm²)	Perimeter Length (µm)	Major Axis (µm)	Minor Axis (µm)	Aspect Ratio
			<10% Discordant Samples			
K4_6	197	6625.5	319.9	103.1	81.8	1.26
K4_7	212	7196.6	336.2	111.1	82.4	1.35
K4_10	246	9500.3	391.6	144.1	83.9	1.72
K4_11	237	9250.4	393.1	119.8	98.3	1.22
K4_12	231	5635.9	304.6	95.3	75.3	1.27
K4_13	226	5486.7	291	88.6	78.8	1.12
K4_14	227	7105.7	322.2	107.5	84.1	1.28
K4_16	234	6570.4	316.3	106.6	78.5	1.36
K5_1	216	5317.9	281.5	94.1	71.9	1.31
K5_3	170	6878.6	356	94.6	92.6	1.02
K5_4	173	6129.1	317	95.3	81.9	1.16
K5_5	182	8549.6	372.5	127.1	85.6	1.48
K5_7	220	4649.5	280.1	108	54.8	1.97
K5_8	101	6197.2	333.8	129.8	60.8	2.13
K5_9	97	6576.9	326.5	121	69.2	1.75
K5_10	98	6820.2	322.7	103.6	83.8	1.24
K5_12	86	6975.9	360.2	101.8	87.2	1.17
K5_13	45	5068.1	278.9	95.4	67.6	1.41
K5_14	30	10379.6	424.9	145.2	91	1.60
K5_15	22	4341.3	249.7	84.8	65.2	1.30
K5_16	19	7884.4	364.1	112.3	89.4	1.26
K6_3	189	4269.9	272.2	99	54.9	1.80
K6_4	179	5311.4	291.9	88.9	76.1	1.17
K6_6	134	9935	561.1	153.3	82.5	1.86
K6_7	164	7712.5	358.2	115.2	85.3	1.35
K6_8	187	10879.2	422.7	141.6	97.8	1.45
K6_9	211	8286.8	345.5	103.9	101.5	1.02
K6_10	184	13251	541.2	177.6	95	1.87
K6_11	224	6417.9	325.3	119.2	68.5	1.74
K6_12	244	9351	417.3	153	77.8	1.97
K6_13	243	8546.3	427.2	138.7	78.4	1.77
K6_14	259	6768.3	330.5	126.6	68.1	1.86
K6_16	272	6116.1	322	102.4	76	1.35
K7_3	255	8990.9	378.7	122.8	93.2	1.32
K7_4	285	9338	373.5	133	89.4	1.49
K7_5	200	3887.1	294.2	96.5	51.3	1.88
K7_6	291	9600.8	402.7	149.6	81.7	1.83
K7_7	310	7547	344	106.6	90.1	1.18
K7_8	319	10652.1	450.8	161.9	83.8	1.93
K7_9	342	13478.2	479.3	176	97.5	1.81
K7_10	366	7790.3	349.9	117.2	84.6	1.39
K7_11	339	5697.6	296	96.4	75.2	1.28
K7_12	304	12102.4	482.3	158.6	97.2	1.63
K7_13	320	8257.6	449.6	130.3	80.7	1.61
K7_14	335	6969.5	331.9	112.4	79	1.42
K7_15	329	8179.7	378.1	147.2	70.8	2.08
K7_16	327	17501.5	533.1	195.7	113.9	1.72
K8_1	290	10765.7	461.9	153.3	89.4	1.71
K8_3	286	8475	435.3	166.5	64.8	2.57
K8_4	277	10914.9	435.2	154	90.2	1.71

Table D-8 Continued

| Sample Name	Grain Map #	Area (μm^2)	Perimeter Length (μm)	Major Axis (μm)	Minor Axis (μm)	Aspect Ratio
			<10% Discordant Samples			
K8_6	321	10600.2	430.4	116.3	116.1	1.00
K8_7	381	6560.6	324.4	121.5	68.7	1.77
K8_8	391	8348.4	394.9	143.4	74.1	1.94
K8_9	418	8685.9	396.8	130.5	84.7	1.54
K8_10	449	11651.4	423.4	135.7	109.3	1.24
K8_11	417	9458.1	396.6	120.6	99.8	1.21
K8_12	403	13228.3	536.7	227.3	74.1	3.07
K8_13	463	13105	467.2	161.9	103.1	1.57
K8_14	470	8046.7	364.2	118.6	86.4	1.37
K8_15	485	12349	468	134.7	116.7	1.15
K8_16	478	15058.3	511.2	176.2	108.8	1.62
K9_1	501	10074.6	442.4	156.3	82	1.91
K9_3	498	7284.2	362.9	138.8	66.8	2.08
K9_4	502	8517.1	373.8	120	90.4	1.33
K9_6	461	16352.9	551.9	205.6	101.3	2.03
K9_7	414	6875.4	333.4	119.9	73	1.64
K9_9	360	14104.4	576.4	138.9	129.3	1.07
K9_12	440	6898.1	339.5	99.6	88.2	1.13
K9_13	423	8809.2	437.5	141.4	79.3	1.78
K9_14	479	9020.1	417.4	152	75.5	2.01
K9_15	467	8380.9	413.1	175.5	60.8	2.89
K9_16	437	9354.2	457.5	156.8	75.9	2.07
K10_1	430	10337.4	446.6	130.9	100.5	1.30
K10_2	404	8390.6	398.5	136.4	78.3	1.74
K10_3	346	11511.9	432.2	148	99.1	1.49
K10_4	357	8449	386.2	132.4	81.2	1.63
K10_5	354	5528.8	293.3	106.3	66.2	1.61
K10_6	316	6378.9	336.5	123.7	65.6	1.89
K10_8	369	10210.8	401.3	142.5	91.2	1.56
K10_9	273	5892.2	302.7	93.4	80.3	1.16
K10_10	282	18679.3	539.4	183.1	129.9	1.41
K10_11	314	10924.6	487.9	129.3	107.6	1.20
K10_12	305	8325.7	364.1	118.4	89.5	1.32
K10_13	301	6320.5	424.3	100.8	79.8	1.26
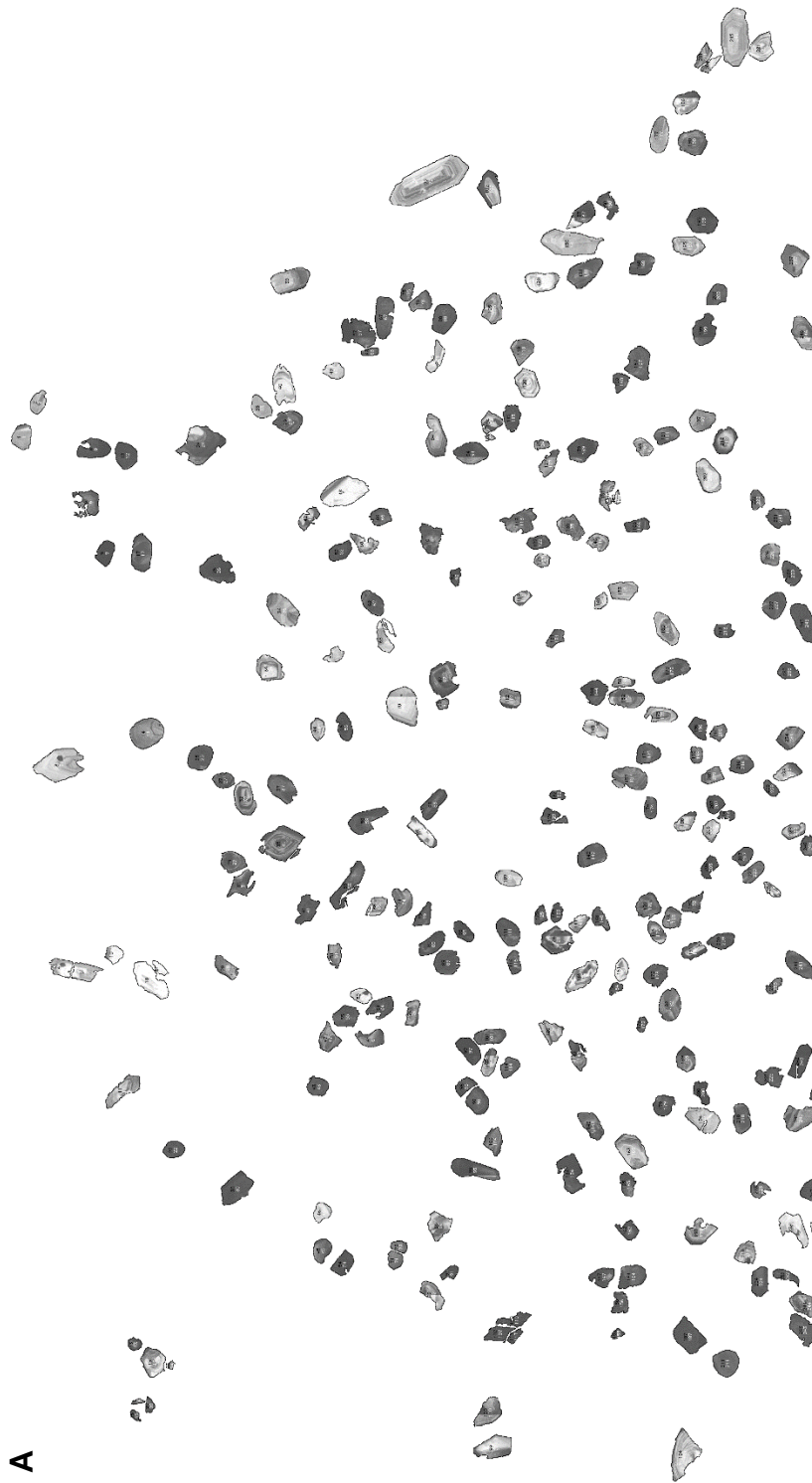
Figure D-8. Grain map generated for sample Si-KM. Upper image (A) and lower image (B) are shown. The joining area of images A-B contain overlapping grains.
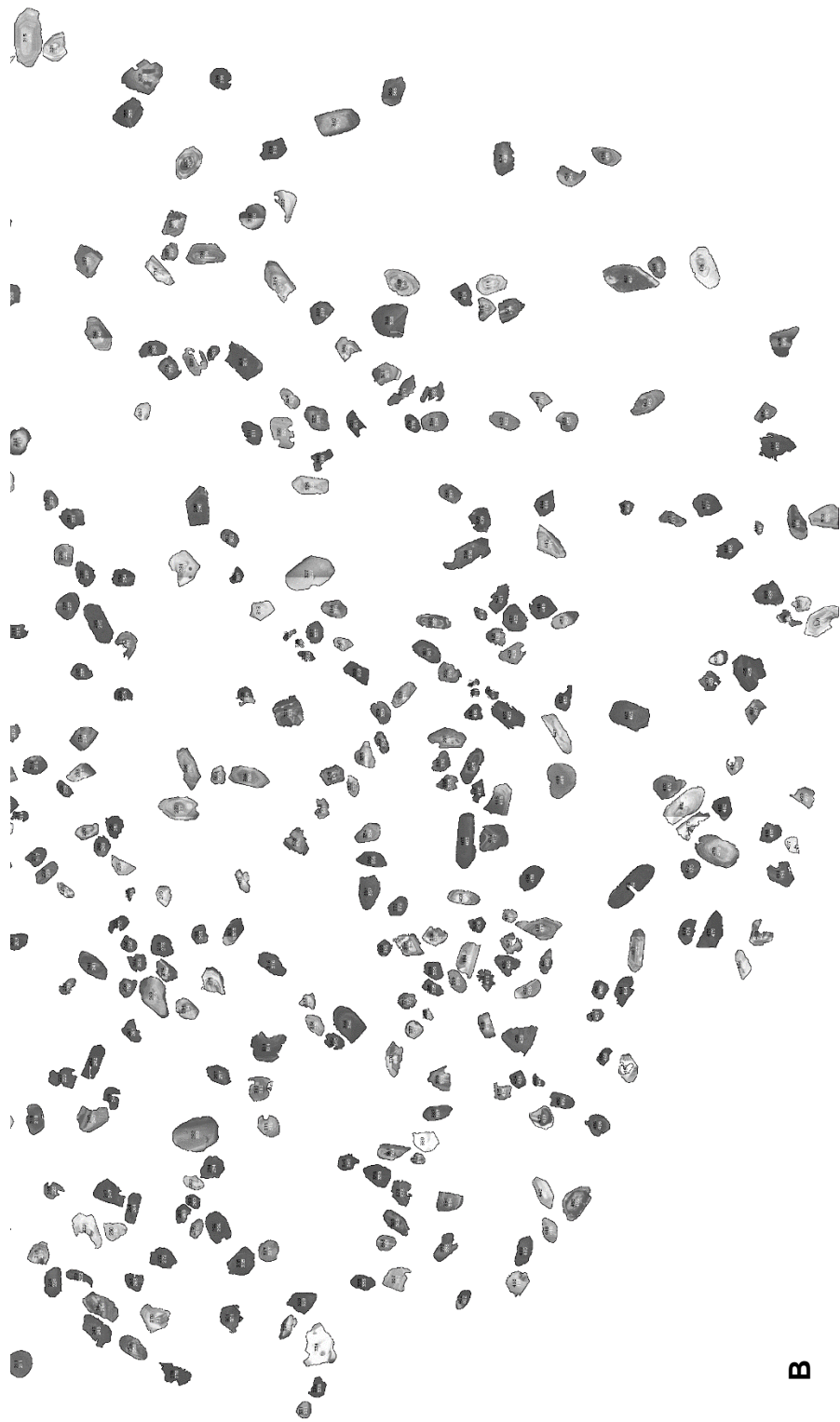
B

Figure D-8 Continued

Table D-9. Detrital zircon shape data for sample CB-BS. Grain map numbers correspond with Figure D-9.

Sample Name	Grain Map #	Area (µm²)	Perimeter Length (µm)	Major Axis (µm)	Minor Axis (µm)	Aspect Ratio
<10% Discordant Samples						
CBBS1_1	1	5885.9	308.9	97.2	77.1	1.26
CBBS1_3	10	4691.2	326.8	126.3	47.3	2.67
CBBS1_5	25	3058.2	210	67.7	57.5	1.18
CBBS1_7	31	4220.4	277.7	88.3	60.9	1.45
CBBS1_8	20	7061.1	357.9	140.6	63.9	2.20
CBBS1_10	43	4502.9	265.8	78.7	72.8	1.08
CBBS1_11	54	5616.4	290.5	92	77.8	1.18
CBBS1_12	70	6626.1	334.1	99.5	84.8	1.17
CBBS1_16	16	7590.3	398.1	172.2	56.1	3.07
CBBS2_1	11	5937.8	296.4	101.3	74.6	1.36
CBBS2_2	7	7720.2	397.6	144.6	68	2.13
CBBS2_3	4	7246.2	356.3	134.1	68.8	1.95
CBBS2_8	42	6512.5	317.4	116.8	71	1.65
CBBS2_9	68	4963.9	267.8	86.3	73.2	1.18
CBBS2_10	78	6320.9	334.4	93	86.5	1.08
CBBS2_11	94	4989.9	289	95.2	66.7	1.43
CBBS2_12	115	5960.6	314.4	110.4	68.7	1.61
CBBS2_13	130	4223.7	253.5	87.5	61.4	1.43
CBBS2_15	134	4175	252.9	78.2	68	1.15
CBBS2_16	121	7028.7	342.5	126.8	70.6	1.80
CBBS3_1	113	11099.7	397.4	127.6	110.7	1.15
CBBS3_2	100	6525.4	328.7	103.2	80.5	1.28
CBBS3_3	106	4928.2	277.9	99.7	62.9	1.59
CBBS3_4	96	8018.8	403.4	169.4	60.3	2.81
CBBS3_6	64	4671.7	289.4	86.7	68.6	1.26
CBBS3_7	29	5366.4	284.4	103.3	66.2	1.56
CBBS3_9	65	4041.9	255.3	78.4	65.6	1.20
CBBS3_10	67	2730.3	214.3	68.5	50.7	1.35
CBBS3_12	79	4895.7	273.9	84.6	73.7	1.15
CBBS3_13	99	5171.7	301.8	91.2	72.2	1.26
CBBS3_16	103	6924.8	357.6	127.1	69.3	1.83
CBBS4_1	97	4022.4	247.6	87.7	58.4	1.50
CBBS4_3	114	6882.6	320.4	101.1	86.7	1.17
CBBS4_4	112	5944.3	309.6	109.1	69.4	1.57
CBBS4_5	127	3707.5	252	72.8	64.8	1.12
CBBS4_7	140	4798.3	286.1	90.9	67.2	1.35
CBBS4_8	133	7846.8	376.1	137.5	72.6	1.89
CBBS4_9	125	7885.7	348.2	126	79.7	1.58
CBBS4_12	88	4382.8	274.8	96.1	58.1	1.65
CBBS4_16	117	5210.6	337.9	114.7	57.8	1.98
CBBS5_1	124	4830.8	280.3	104	59.2	1.76
CBBS5_2	131	4639.2	273.7	86.5	68.3	1.27
CBBS5_3	143	5463.8	302.7	105.6	65.9	1.60
CBBS5_6	173	9158.3	371.9	121.4	96	1.26
CBBS5_7	184	5937.8	301.3	104	72.7	1.43
CBBS5_8	171	5558	288.8	106.1	66.7	1.59
CBBS5_10	212	9739.5	402.2	127.8	97.1	1.32
CBBS5_11	198	2843.9	201.6	61.7	58.7	1.05

Table D-9 Continued

| Sample Name	Grain Map #	Area (μm^2)	Perimeter Length (μm)	Major Axis (μm)	Minor Axis (μm)	Aspect Ratio
			<10% Discordant Samples			
CBBS5_12	172	6476.7	320.7	121.4	67.9	1.79
CBBS5_14	189	7210.5	348	134.4	68.3	1.97
CBBS5_16	227	5590.5	295.6	104.4	68.2	1.53
CBBS6_1	228	6811.1	313.2	104.3	83.2	1.25
CBBS6_4	246	4853.5	335.9	94.8	65.2	1.45
CBBS6_6	257	4782.1	265.2	83.2	73.2	1.14
CBBS6_8	279	5963.8	314.3	110.1	68.9	1.60
CBBS6_9	251	5330.7	289.5	92.6	73.3	1.26
CBBS6_10	244	6405.3	353.6	135.6	60.1	2.26
CBBS6_12	264	4785.3	276.3	91.4	66.6	1.37
CBBS6_13	266	6249.5	312.1	104	76.5	1.36
CBBS6_14	268	6596.9	309.3	98.7	85.1	1.16
CBBS7_1	293	5194.4	303.6	98.4	67.2	1.46
CBBS7_2	292	5132.7	295.6	105.4	62	1.70
CBBS7_3	298	4798.3	305.2	98.7	61.9	1.59
CBBS7_5	296	5022.3	355	89	71.9	1.24
CBBS7_6	297	5236.6	329.4	94.8	70.3	1.35
CBBS7_8	302	6895.5	348.4	111.5	78.8	1.41
CBBS7_10	283	9638.8	400.6	121.3	101.2	1.20
CBBS7_12	290	5454.1	296.6	107.7	64.5	1.67
CBBS7_16	240	5915.1	323.7	110.7	68	1.63
CBBS8_2	243	11963.3	454.3	141.9	107.3	1.32
CBBS8_3	234	5174.9	282.4	102	64.6	1.58
CBBS8_4	224	9093.4	367.1	129.8	89.2	1.46
CBBS8_6	201	6674.8	320.2	105.8	80.3	1.32
CBBS8_8	210	6379.4	312.8	98.9	82.1	1.20
CBBS8_10	225	7158.5	370.1	109.7	83.1	1.32
CBBS8_11	221	6730	353.1	122.4	70	1.75
CBBS8_13	158	4301.6	257.6	88.3	62	1.42
CBBS9_1	233	6619.6	325.9	107.5	78.4	1.37
CBBS9_3	197	10132.3	411.6	153.9	83.8	1.84
CBBS9_5	167	5243.1	289.6	108.5	61.6	1.76
CBBS9_8	159	3434.8	242.1	72	60.7	1.19
CBBS9_10	223	4126.3	258.8	83.7	62.8	1.33
CBBS9_11	207	3610.1	248.8	73.9	62.2	1.19
CBBS9_12	195	5843.7	310.8	97.8	76.1	1.29
CBBS9_14	181	2649.1	203.4	67.9	49.7	1.37
CBBS9_15	177	3262.7	222.2	72.5	57.3	1.27
CBBS9_16	179	4876.2	260.5	81.1	76.5	1.06
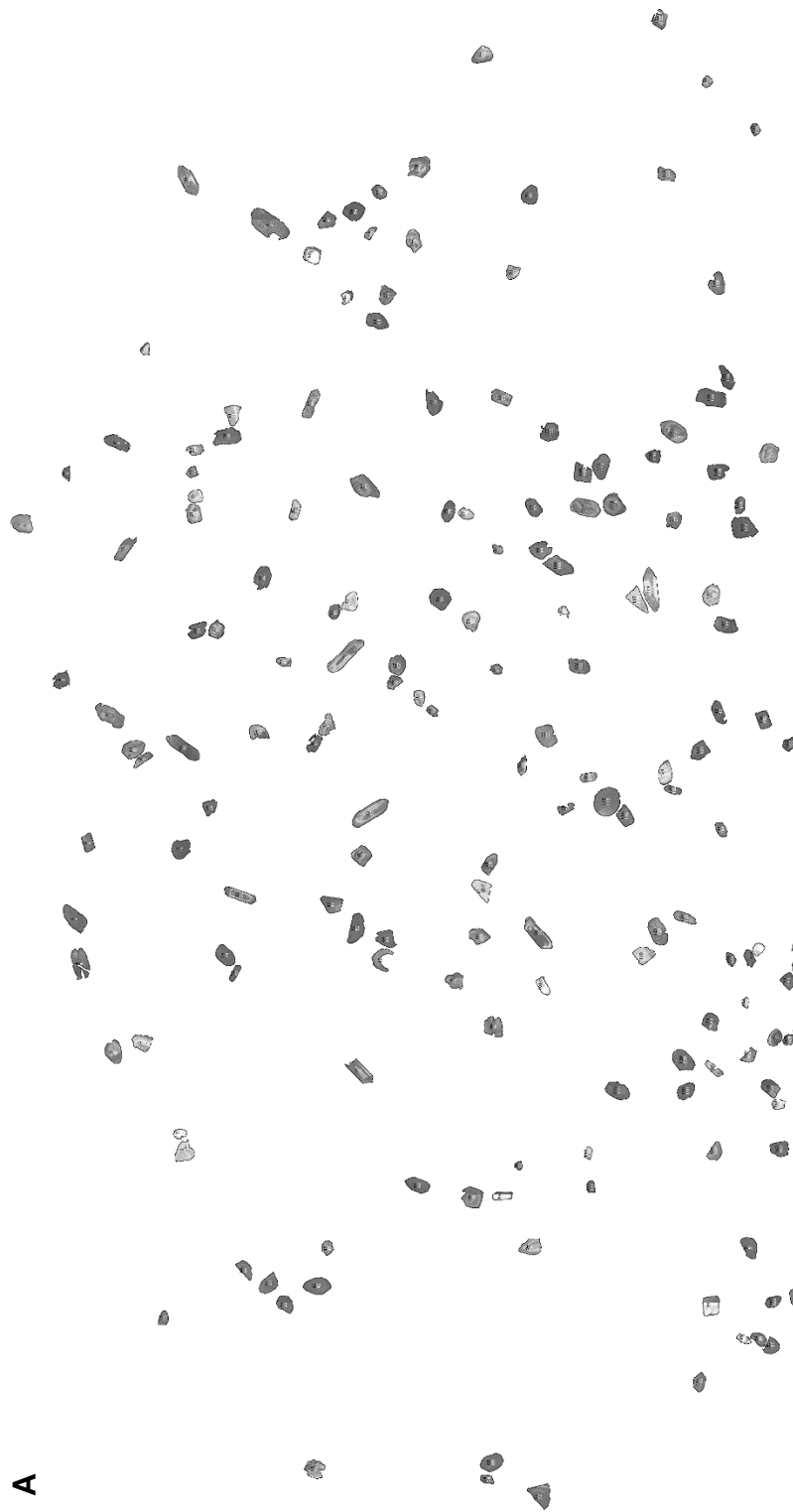
Figure D-9. Grain map generated for sample CB-BS. Upper image (A) and lower image (B) are shown. The joining area of images A-B contain overlapping grains.
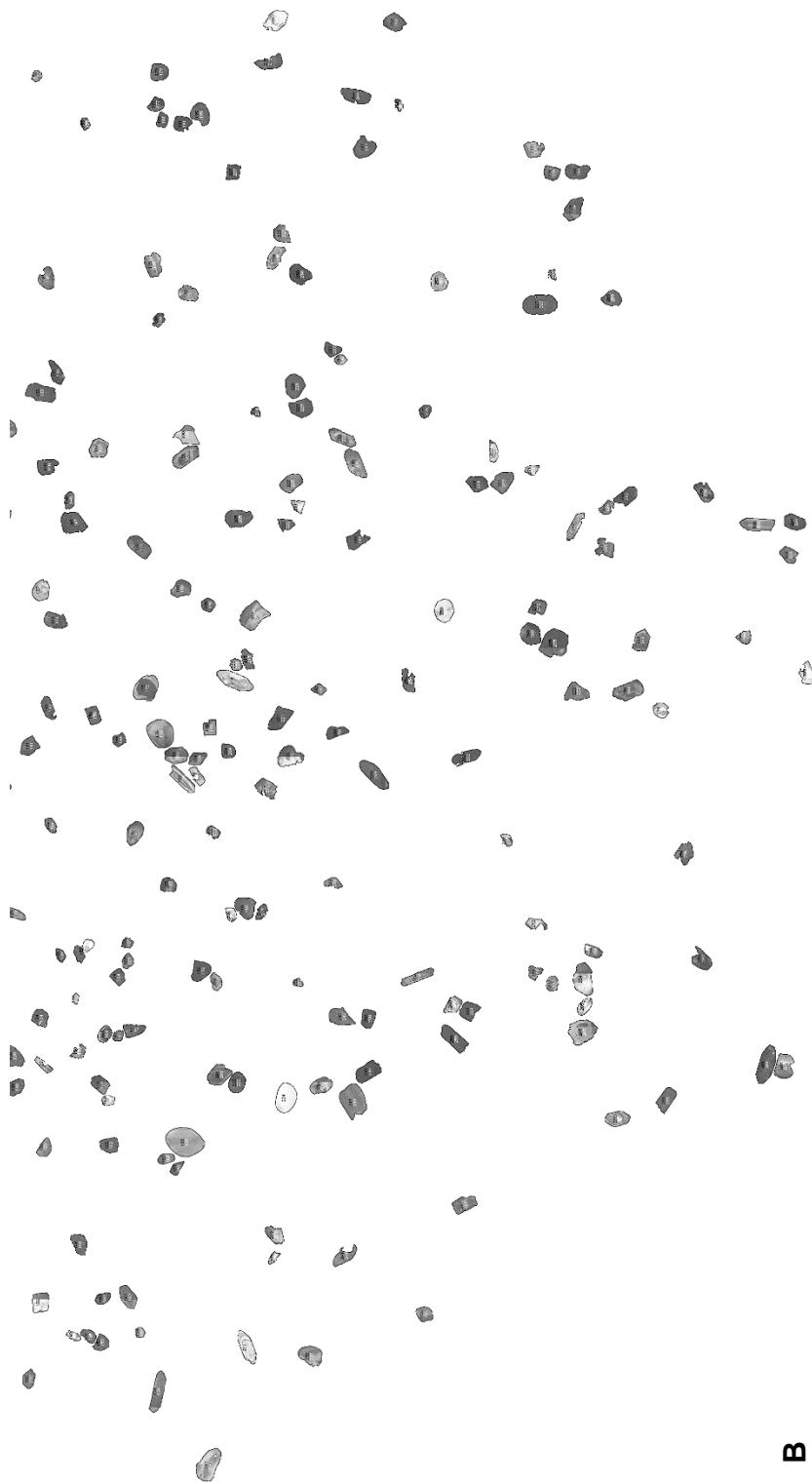
B

Figure D-9 Continued

Table D-10. Detrital zircon shape data for sample QC. Grain map numbers correspond with Figure D-10.

Sample Name	Grain Map #	Area (μm^2)	Perimeter Length (μm)	Major Axis (μm)	Minor Axis (μm)	Aspect Ratio
		<10% Discordant Samples				
Q1_1	17	9184.3	427.2	140.7	83.1	1.69
Q1_2	14	14804	645.4	282.6	66.7	4.24
Q1_3	10	6389.1	307.2	106.2	76.6	1.39
Q1_4	35	12852.9	481.1	188.2	86.9	2.17
Q1_5	48	10155	411.4	135.7	95.2	1.43
Q1_6	56	10758.9	454.1	180.5	75.9	2.38
Q1_7	38	8606.4	366.4	115.3	95.1	1.21
Q1_8	13	8522	371.6	135.2	80.2	1.69
Q1_10	43	8359.7	365.1	124.9	85.2	1.47
Q1_11	16	8999.3	422.1	154.1	74.4	2.07
Q1_12	4	7148.8	314.9	100.8	90.3	1.12
Q1_13	59	11161.4	436.7	152.9	93	1.64
Q1_14	50	11219.9	434.4	156.9	91.1	1.72
Q1_15	70	6609.9	323.7	121.4	69.3	1.75
Q1_16	52	4587.3	260.7	86.9	67.2	1.29
Q2_1	46	11917.9	429	150.4	100.9	1.49
Q2_2	36	8836.9	443.1	192.8	58.3	3.31
Q2_3	58	8450.6	377.8	146.2	73.6	1.99
Q2_4	62	8194.1	370.2	112.1	93.1	1.20
Q2_5	34	8229.9	430.2	119.8	87.4	1.37
Q2_6	41	8324	383	136.6	77.6	1.76
Q2_7	101	9583.6	397	133.1	91.7	1.45
Q2_8	109	12479.5	475.2	167.1	95.1	1.76
Q2_9	111	4441.2	252.7	79	71.5	1.10
Q2_11	126	7966.9	431.9	126.7	80	1.58
Q2_12	151	10531.6	504.3	204.2	65.7	3.11
Q2_13	182	3642.6	231.3	76.5	60.7	1.26
Q2_14	200	9629.1	403.4	140.3	87.4	1.61
Q2_15	220	4918.4	276.3	88.6	70.7	1.25
Q2_16	250	4989.9	282.5	106.8	59.5	1.79
Q3_1	81	6781.9	349.6	131	65.9	1.99
Q3_2	110	15748.7	663.4	276.1	72.6	3.80
Q3_4	201	8158.4	408.2	157.5	65.9	2.39
Q3_5	192	9122.6	452	198.1	58.6	3.38
Q3_6	208	9453.8	406.9	139	86.6	1.61
Q3_8	147	7665	377.9	121.5	80.3	1.51
Q3_9	129	10090.1	449.8	186.3	69	2.70
Q3_10	120	7996.1	360.8	128.2	79.4	1.61
Q3_12	146	9099.9	399.8	121.9	95.1	1.28
Q3_13	99	9784.9	398.3	134	93	1.44
Q3_14	88	10239.4	482.3	189.5	68.8	2.75
Q3_15	104	5632.7	315.1	118.7	60.4	1.97
Q4_1	63	7898.7	349.2	124.5	80.8	1.54
Q4_2	39	6152.1	308.5	102.4	76.5	1.34
Q4_3	82	5152.2	295.9	99.9	65.6	1.52
Q4_4	112	7927.9	372.8	140	72.1	1.94
Q4_7	121	8103.2	494.1	124.4	82.9	1.50
Q4_9	100	7184.5	348.4	110.3	82.9	1.33

Table D-10 Continued

Sample Name	Grain Map #	Area (µm^2)	Perimeter Length (µm)	Major Axis (µm)	Minor Axis (µm)	Aspect Ratio
			<10% Discordant Samples			
Q4_10	122	7197.5	355.8	113.3	80.9	1.40
Q5_1	358	6324.2	322.8	100.2	80.4	1.25
Q5_2	354	10343.3	407.6	146.3	90	1.63
Q5_4	307	11638.7	487	197.3	75.1	2.63
Q5_5	353	4892.5	304.3	90.2	69.1	1.31
Q5_6	280	7892.2	387.4	158.2	63.5	2.49
Q5_7	341	5054.8	286	107.7	59.8	1.80
Q5_8	413	7002.7	353.3	113.8	78.3	1.45
Q5_9	421	4288.6	251.2	81.7	66.9	1.22
Q5_11	378	5360	287.5	91.6	74.5	1.23
Q5_12	356	6947.5	349.2	121.9	72.6	1.68
Q5_14	525	4188	258.2	88.8	60.1	1.48
Q5_16	606	6531.9	353.1	114.3	72.8	1.57
Q6_1	602	3649.1	247.4	83	56	1.48
Q6_2	614	4525.6	268.2	95.7	60.2	1.59
Q6_3	644	8905.1	399.3	148.7	76.3	1.95
Q6_4	661	5100.2	291.8	94.3	68.8	1.37
Q6_5	675	6704	337	99.4	85.9	1.16
Q6_6	688	5561.2	297.9	111	63.8	1.74
Q6_7	657	6882.6	354.6	122.6	71.5	1.71
Q6_8	698	6681.3	334.4	125.4	67.8	1.85
Q6_9	716	5872.9	305.5	110.7	67.5	1.64
Q6_10	700	6541.7	361.5	151.4	55	2.75
Q6_13	742	6830.6	349.2	139.2	62.5	2.23
Q6_14	730	7859.8	377.6	105.5	94.8	1.11
Q6_15	736	5931.3	332.4	116.8	64.6	1.81
Q6_16	766	5866.4	289.2	90	82.9	1.09
Q7_1	767	8064.3	345.9	116	88.5	1.31
Q7_2	757	6207.3	309.8	102.3	77.2	1.33
Q7_3	739	10693.9	478.9	136	100.1	1.36
Q7_4	728	9158.3	374.7	127.9	91.1	1.40
Q7_6	695	5204.1	296.2	112.1	59.1	1.90
Q7_8	713	10223.2	456.8	146.8	88.7	1.66
Q7_9	705	5187.9	290.7	96.8	68.3	1.42
Q7_10	723	5460.6	313	101	68.9	1.47
Q7_11	707	4850.3	295.6	103.7	59.6	1.74
Q7_12	751	11245.8	561.3	245.3	58.4	4.20
Q7_13	729	6726.7	333.8	127.5	67.2	1.90
Q7_14	694	10979.6	420.8	154.8	90.3	1.71
Q7_15	673	6035.2	300.6	94	81.8	1.15
Q7_16	687	10216.7	439.2	132.5	98.2	1.35
Q8_1	643	5321	312.1	115.9	58.5	1.98
Q8_2	618	10771.9	422.8	129	106.3	1.21
Q8_3	623	10356.3	457.9	187.6	70.3	2.67
Q8_4	632	4746.4	273.7	83.8	72.1	1.16
Q8_6	568	6294.9	320	111.2	72.1	1.54
Q8_7	551	17878.4	611.3	239.6	95	2.52
Q8_8	472	8768.8	363.7	125	89.4	1.40
Q8_9	523	11288	443.7	146.3	98.2	1.49
Q8_10	429	10521.9	464	178.5	75	2.38

Table D-10 Continued

| Sample Name	Grain Map #	Area (μm^2)	Perimeter Length (μm)	Major Axis (μm)	Minor Axis (μm)	Aspect Ratio
			<10% Discordant Samples			
Q8_11	367	6074.2	313.6	114	67.9	1.68
Q8_12	368	18414.1	582.7	210.8	111.2	1.90
Q8_13	401	10255.7	393.6	126.1	103.5	1.22
Q8_14	359	7483.2	381.4	120.5	79.1	1.52
Q8_15	376	6561.2	347.3	128.7	64.9	1.98
Q8_16	398	8983	395.5	114.5	99.9	1.15
Q9_1	375	9496	489.3	190.1	63.6	2.99
Q9_2	349	11012.1	447.1	181.9	77.1	2.36
Q9_3	350	8161.7	373.7	135.6	76.6	1.77
Q9_4	363	8963.6	375.6	133.2	85.7	1.55
Q9_5	402	5525.5	311.9	93.2	75.5	1.23
Q9_6	427	11307.5	458.4	167	86.2	1.94
Q9_7	461	8632.4	459.3	138.9	79.1	1.76
Q9_8	507	7723.4	348.6	124.3	79.1	1.57
Q9_9	559	14898.1	551.9	209.4	90.6	2.31
Q9_10	530	7817.5	374.9	120.8	82.4	1.47
Q9_11	408	8385.7	447.7	171.7	62.2	2.76
Q9_12	389	10489.4	626.9	183.4	72.8	2.52
Q9_13	285	7963.6	381.3	125.2	81	1.55
Q10_1	340	11960.1	424.5	150.2	101.4	1.48
Q10_2	384	10989.4	454.9	146.3	95.7	1.53
Q10_4	560	9564.2	393.6	133.7	91.1	1.47
Q10_6	605	10859.5	468.8	176.6	78.3	2.26
Q10_7	579	12969.7	492.5	190.3	86.8	2.19
Q10_8	564	11486.1	452.5	177	82.6	2.14
Q10_11	653	7785.1	388.8	132.7	74.7	1.78
Q10_13	672	8385.7	420.2	110.3	96.8	1.14
Q10_15	597	6648.8	317.1	101.2	83.7	1.21
Q10_16	562	7807.8	349.5	115.4	86.1	1.34
Q10_17	535	15278	521	178.4	109.1	1.64
Q10_18	442	8635.7	374.5	137.9	79.7	1.73
Q10_19	387	7846.8	351.6	112.3	88.9	1.26
Q10_21	275	10008.9	432.7	149.5	85.2	1.75
Q10_22	260	9538.2	445.8	161.5	75.2	2.15
Q10_23	303	6879.3	358.2	103.5	84.6	1.22
Q10_24	288	10333.6	429	134.1	98.1	1.37
Q10_25	144	11664.6	458.1	175.2	84.8	2.07
Q10_26	130	10758.9	443.7	155.3	88.2	1.76

A
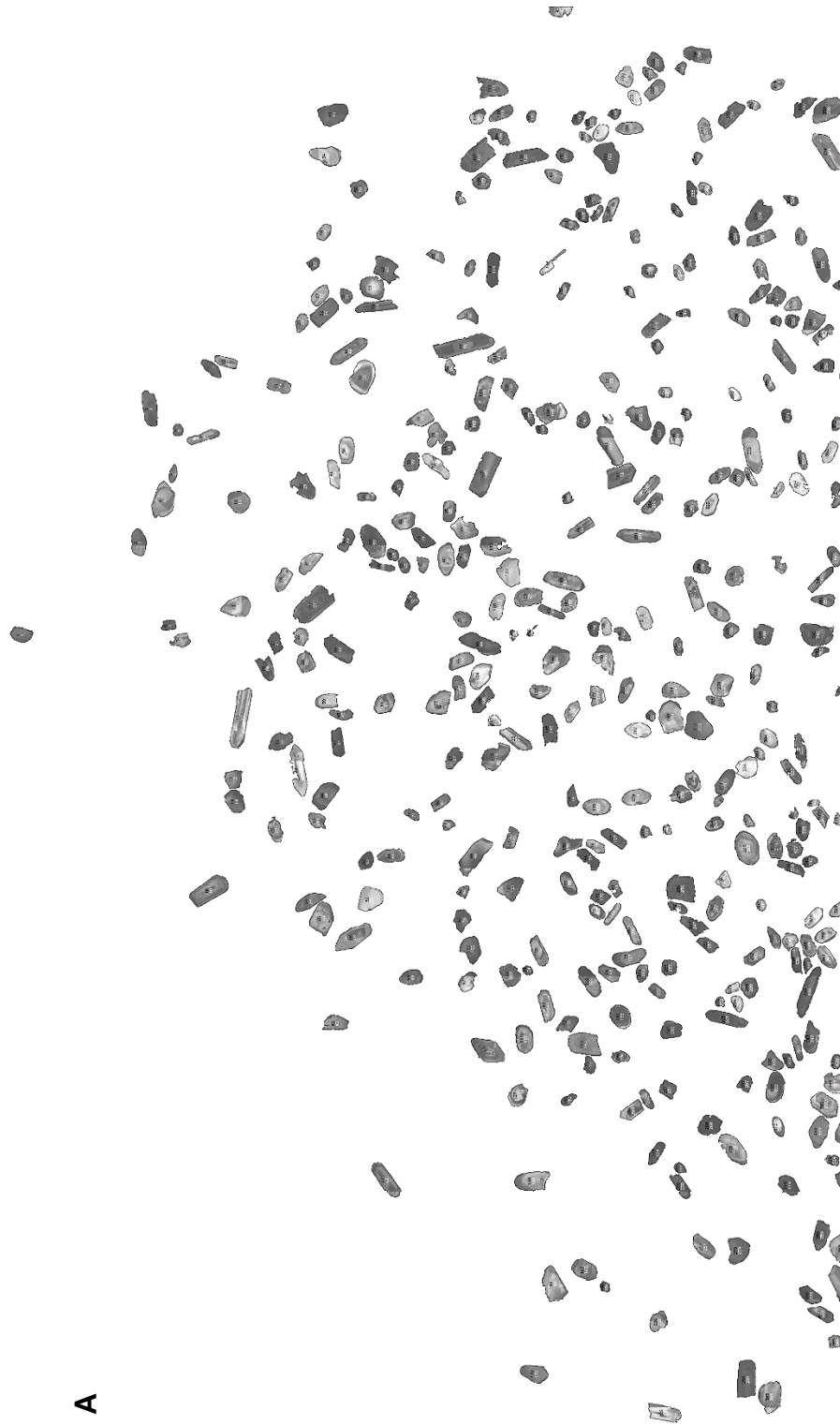
Figure D-10. Grain map generated for sample QC. Upper image (A) and lower image (B) are shown. The joining area of images A-B contain overlapping grains.
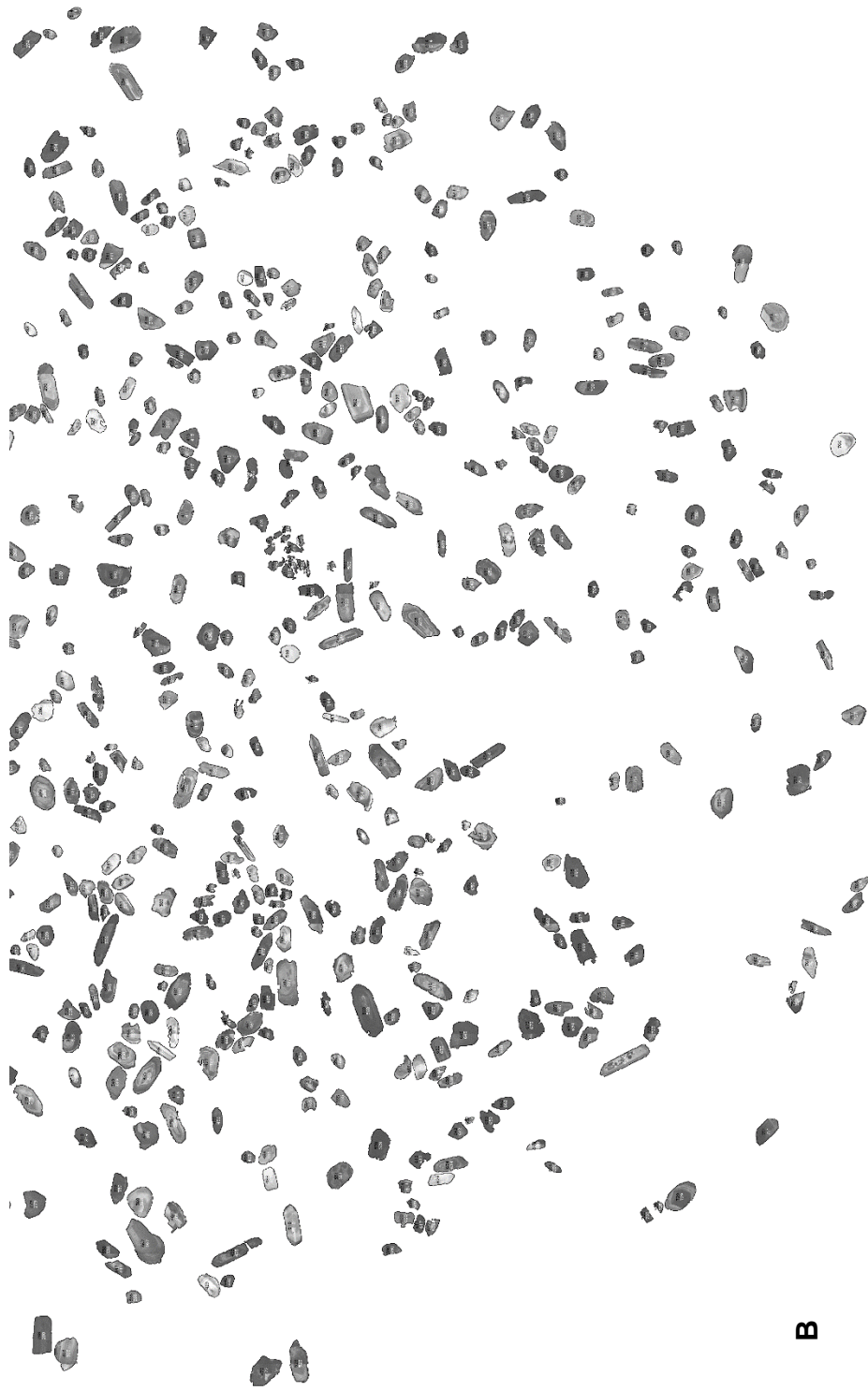
B

Figure D-10 Continued

184
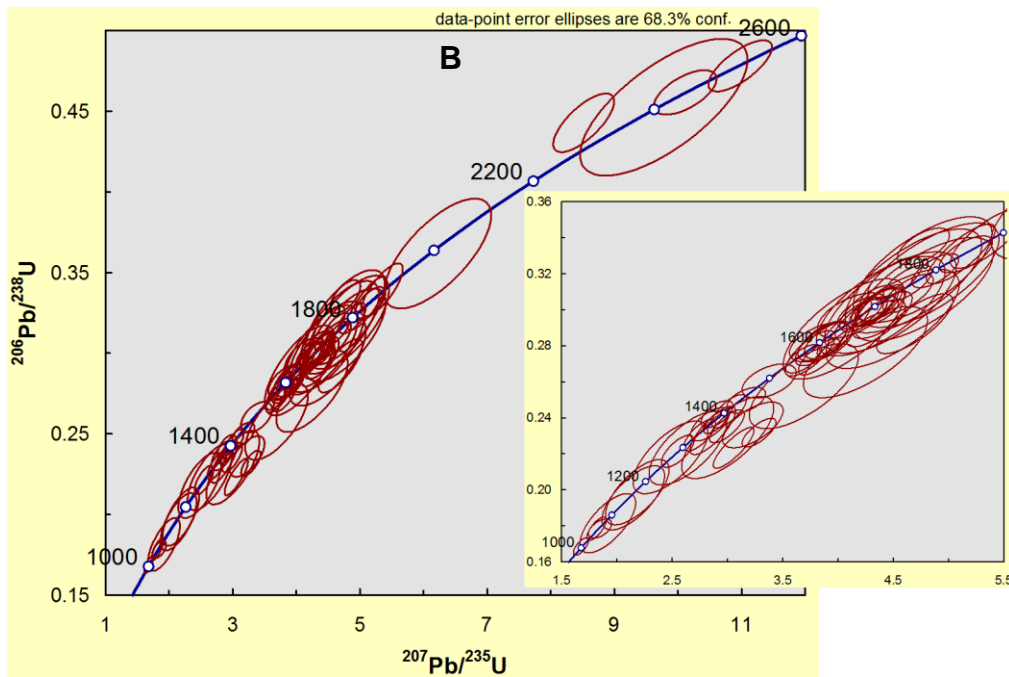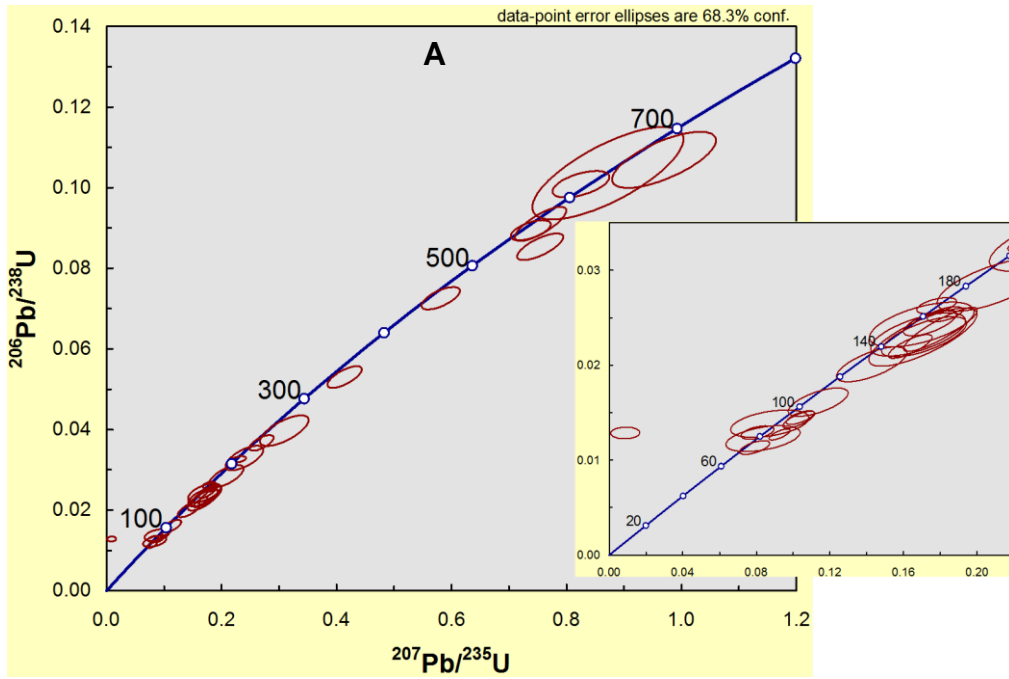
APPENDIX E

CONCORDIA DIAGRAMS

Figure E-1. Concordia diagram for sample Teh from A) 0-800 Ma with a 0-200 Ma subplot, and B) 1000-2600 Ma with a 1000-1900 Ma subplot.
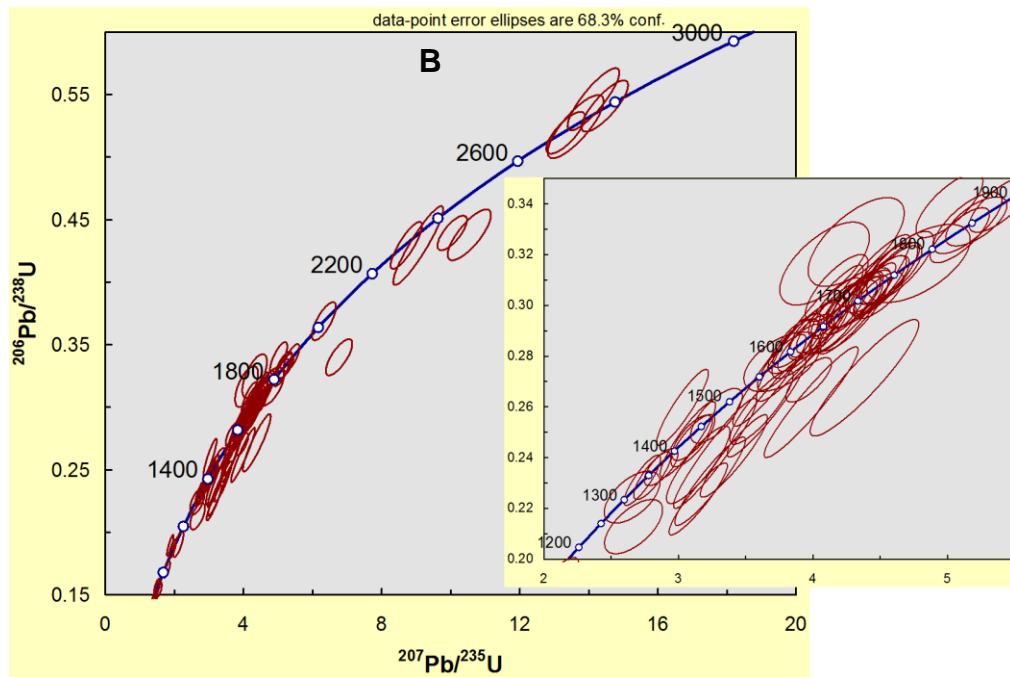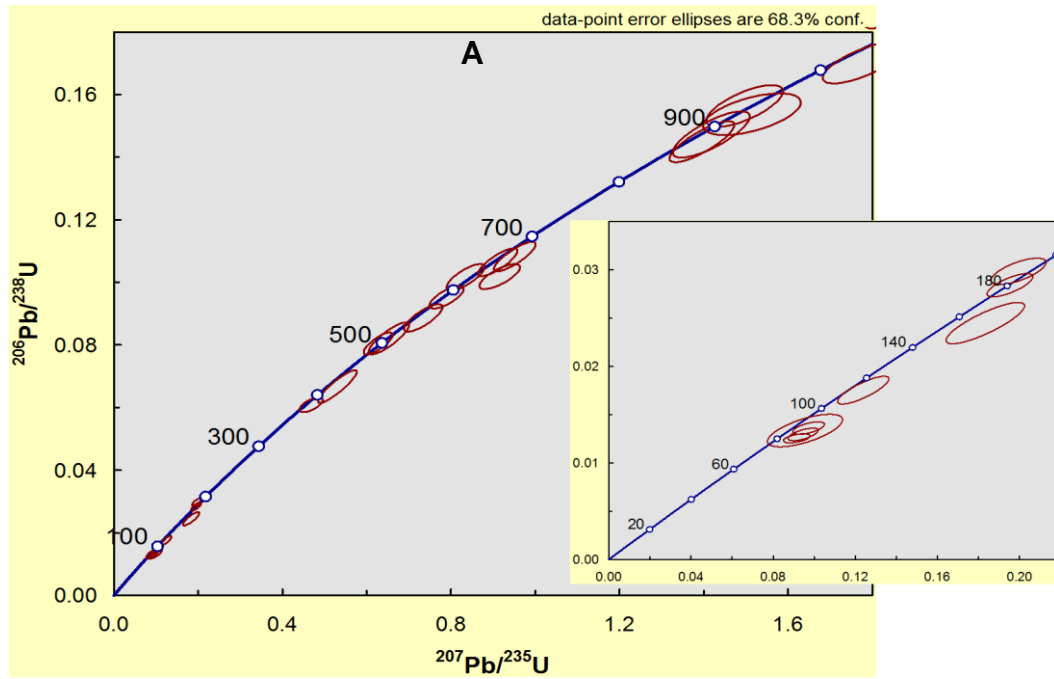
Figure E-2. Concordia diagram for sample Se-E from A) 0-1000 Ma with a 0-200 Ma subplot, and B) 1000-3000 Ma with a 1200-1900 Ma subplot.
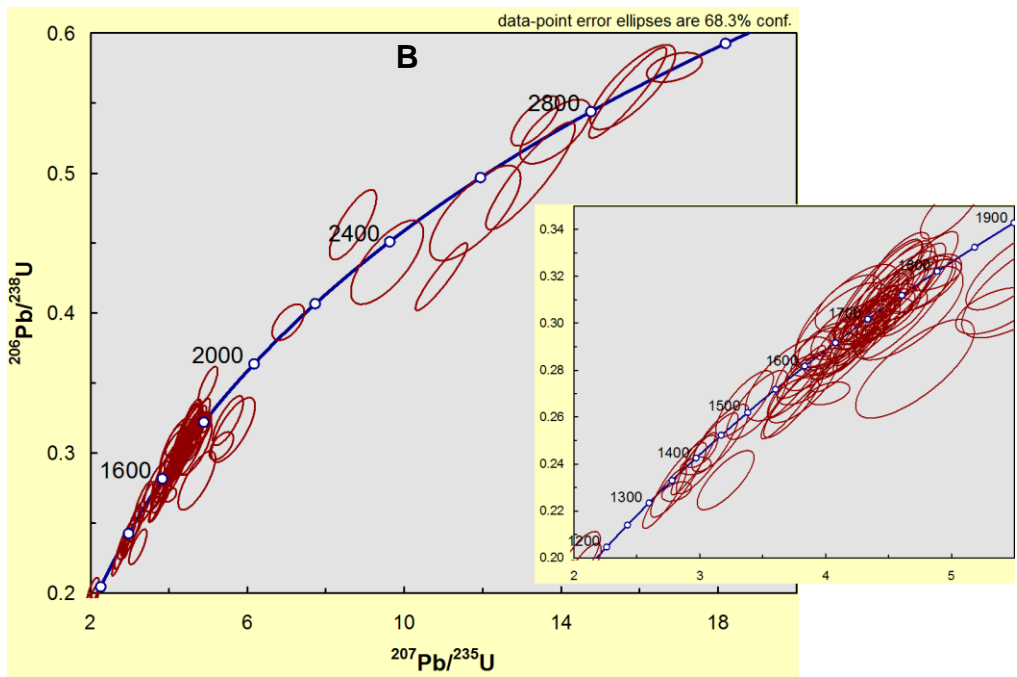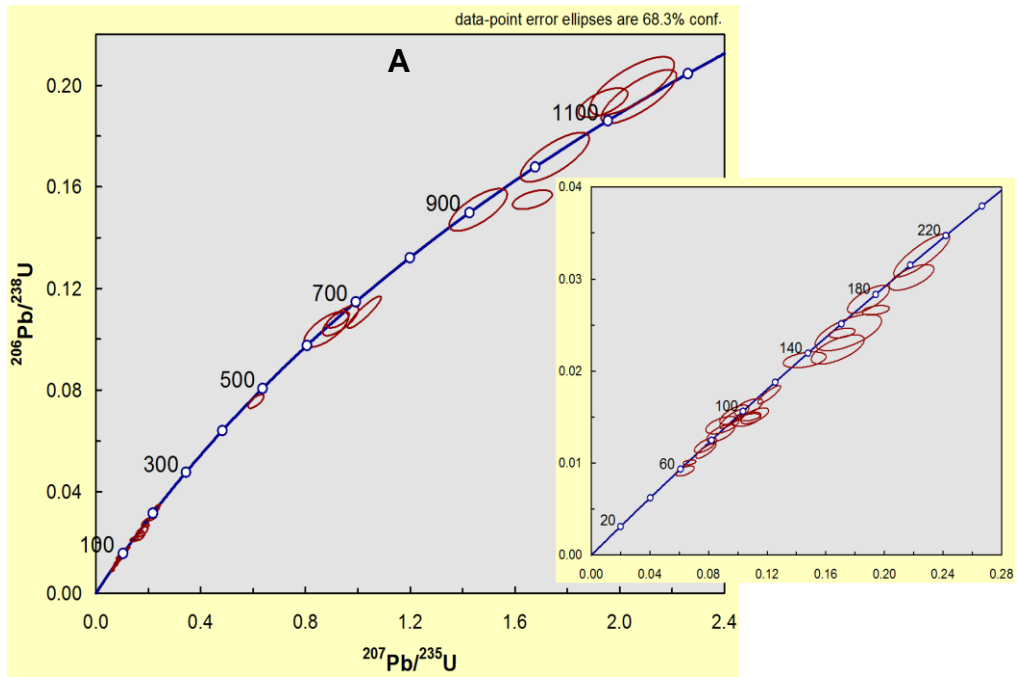
Figure E-3. Concordia diagram for sample HP-PC from A) 0-1200 Ma with a 0-250 Ma subplot, and B) 1200-3000 Ma with a 1200-1900 Ma subplot.
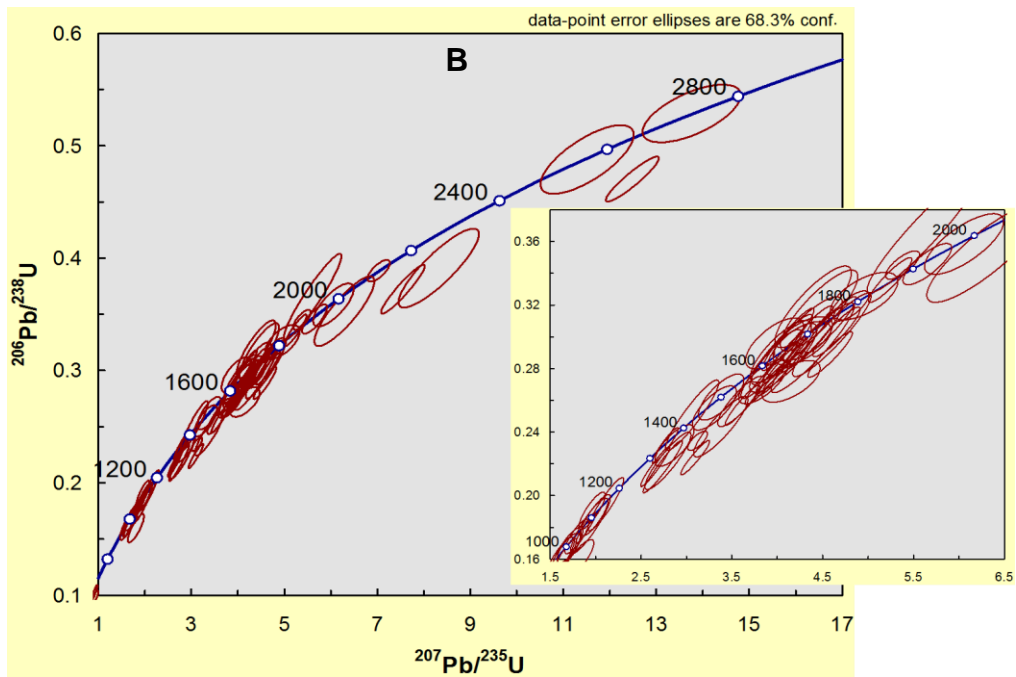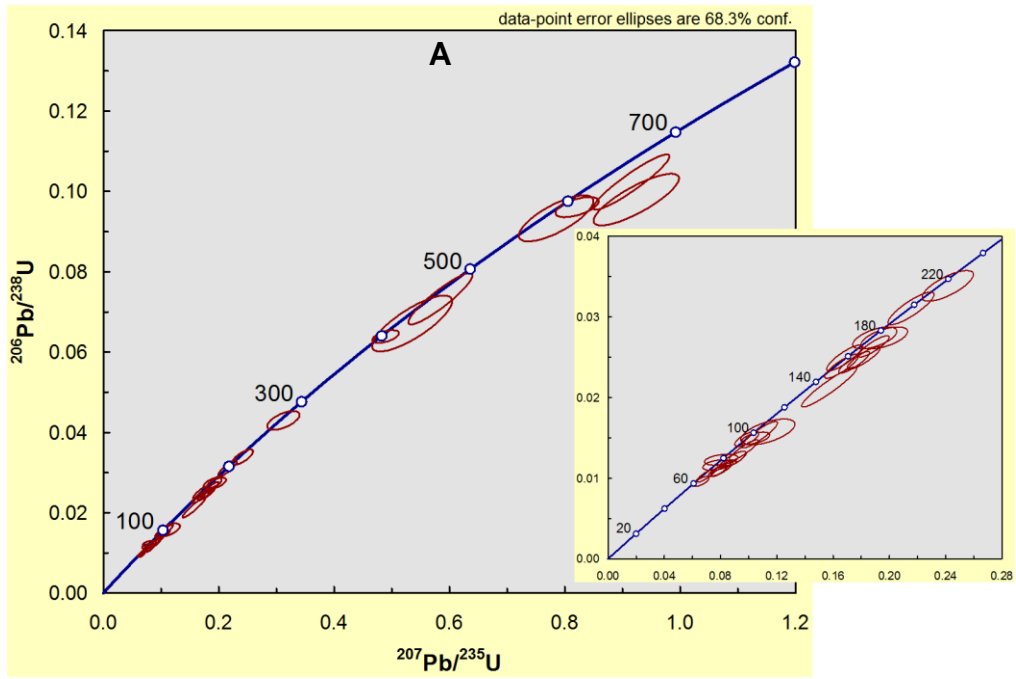
Figure E-4. Concordia diagram for sample HP-DR from A) 0-800 Ma with a 0-250 Ma subplot, and B) 1000-2900 Ma with a 1000-2000 Ma subplot.

Figure E-5. Concordia diagram for sample Si-B from A) 0-1200 Ma with a 0-300 Ma subplot, and B) 1200-3500 Ma with a 1200-1900 Ma subplot.
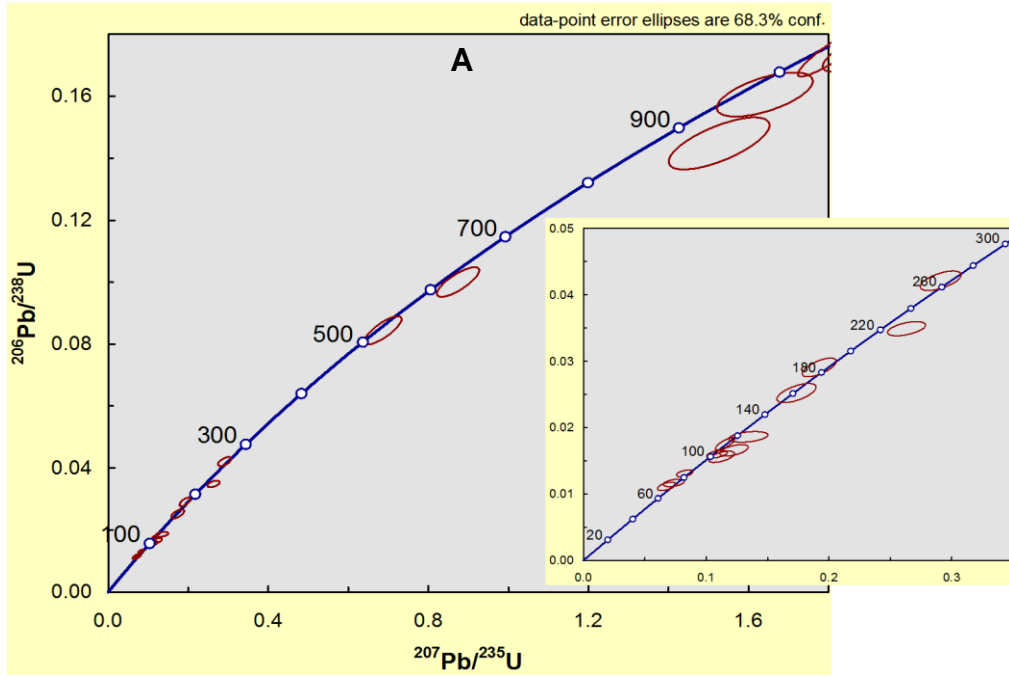
Figure E-6. Concordia diagram for sample Si-LP from A) 0-1000 Ma with a 0-300 Ma subplot, and B) 1000-2800 Ma with a 1000-2000 Ma subplot.
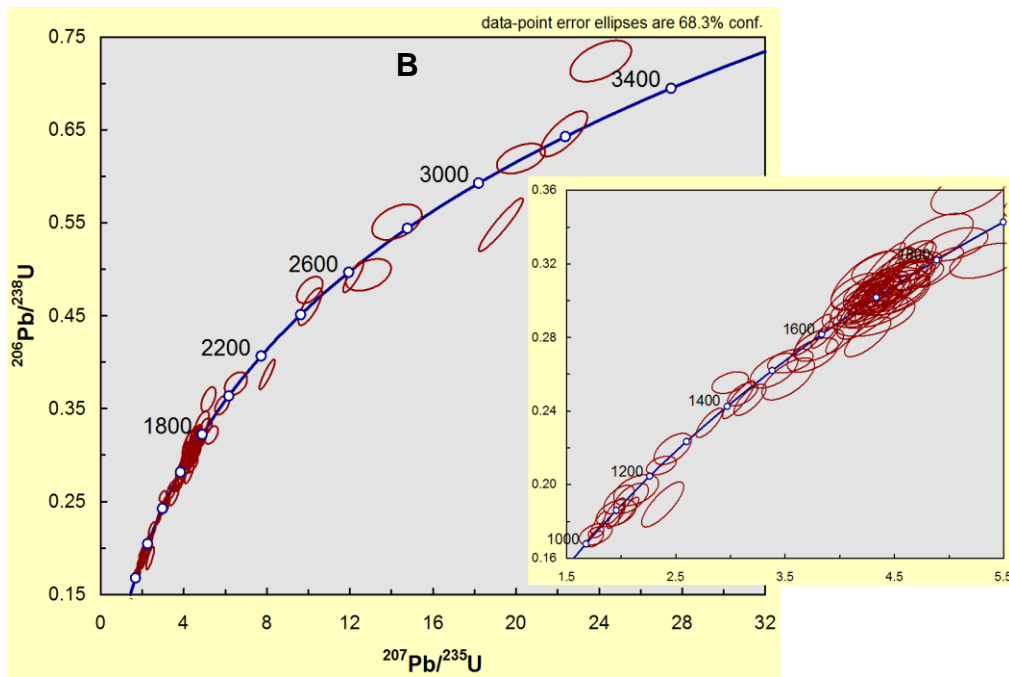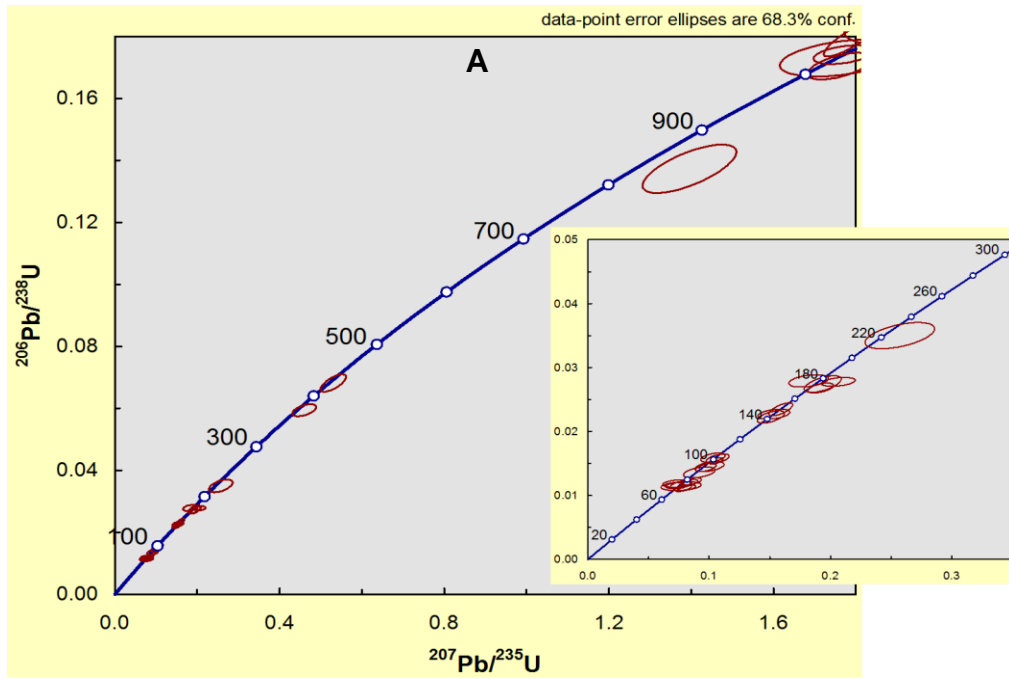
Figure E-7. Concordia diagram for sample Si-TQ from A) 0-1000 Ma with a 0-300 Ma subplot, and B) 1000-3500 Ma with a 1000-1900 Ma subplot.
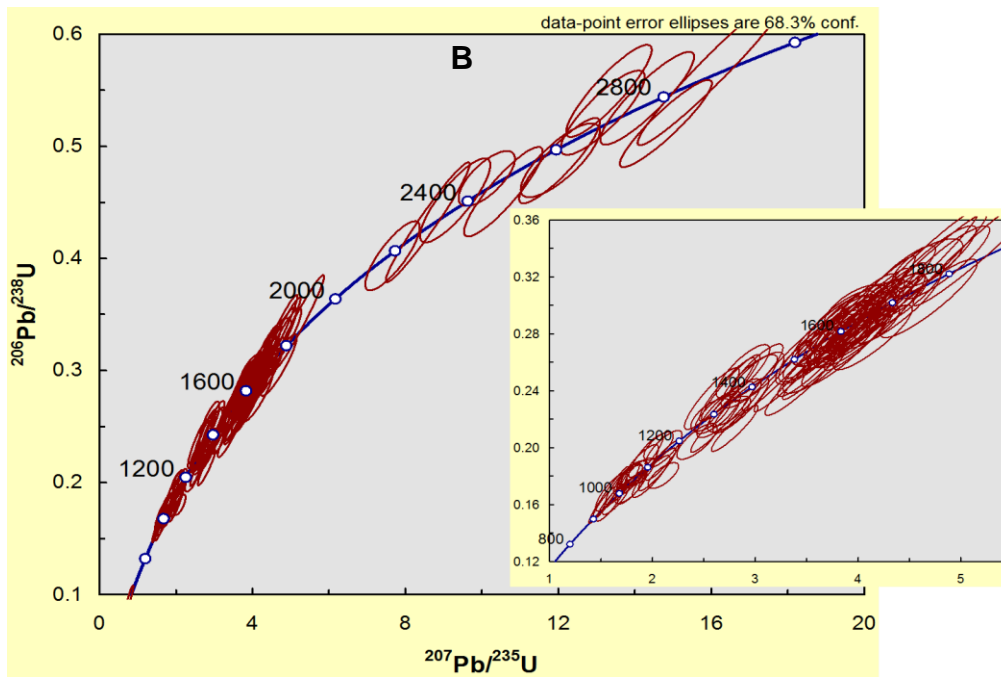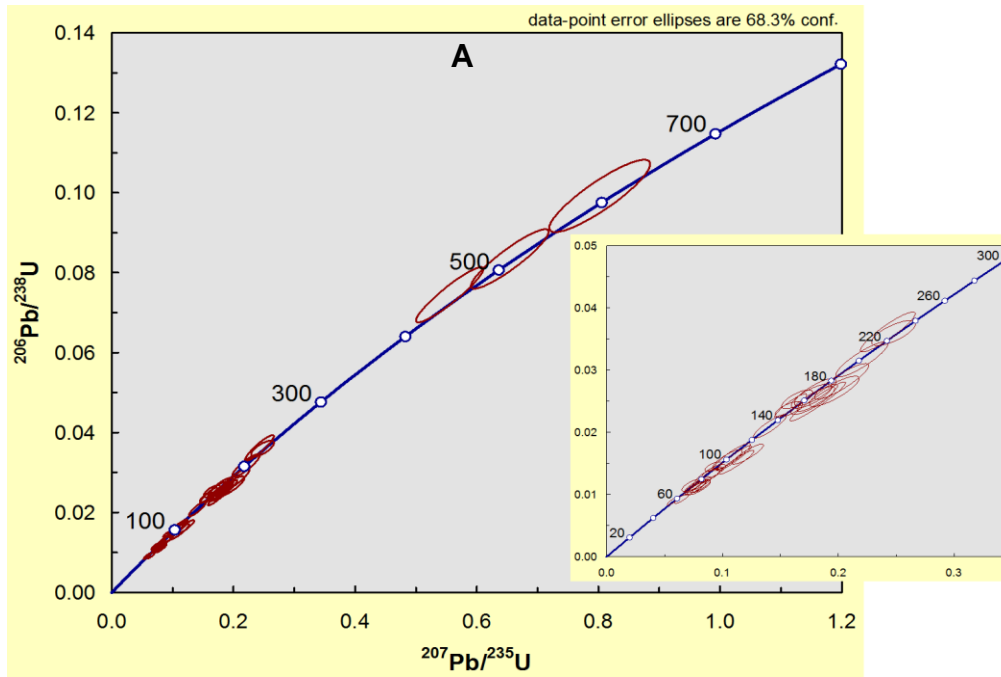
Figure E-8. Concordia diagram for sample Si-KM from A) 0-800 Ma with a 0-300 Ma subplot, and B) 800-3000 Ma with a 800-1900 Ma subplot.
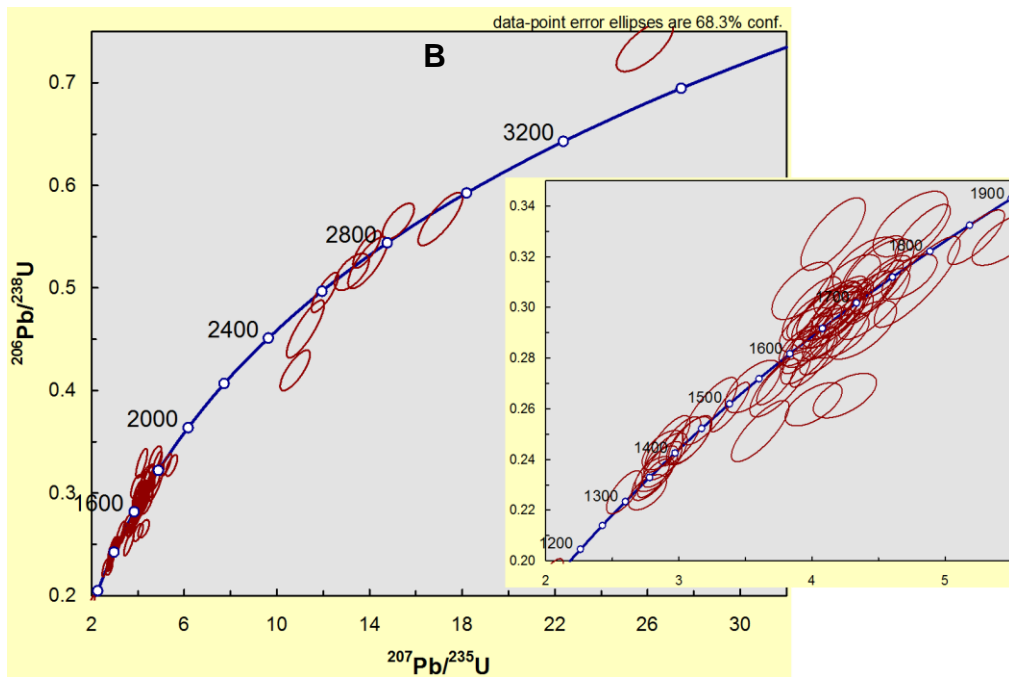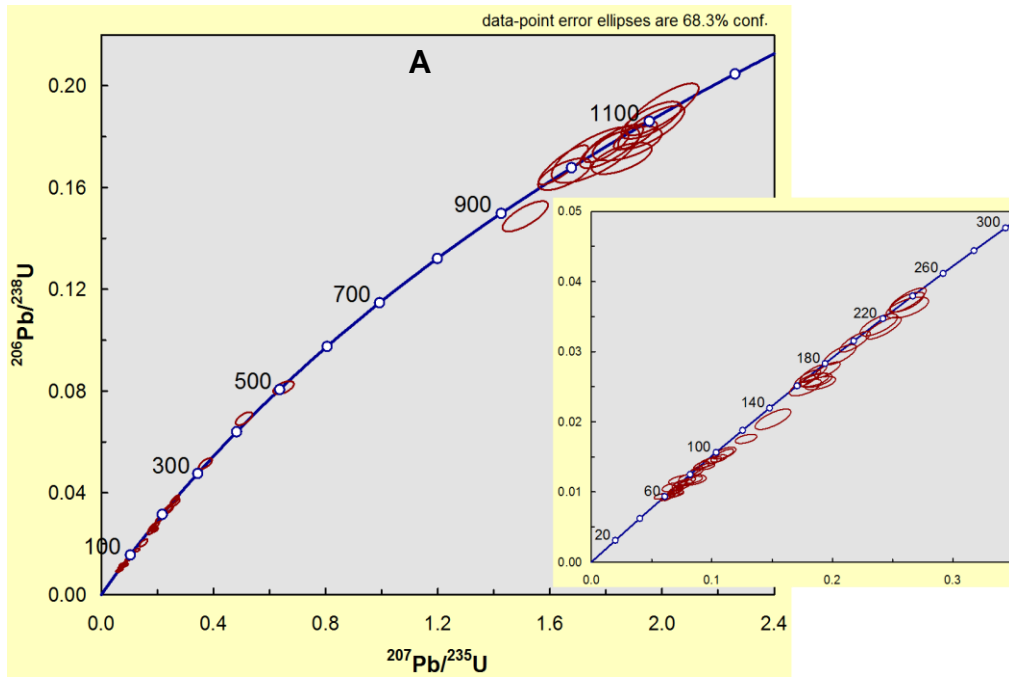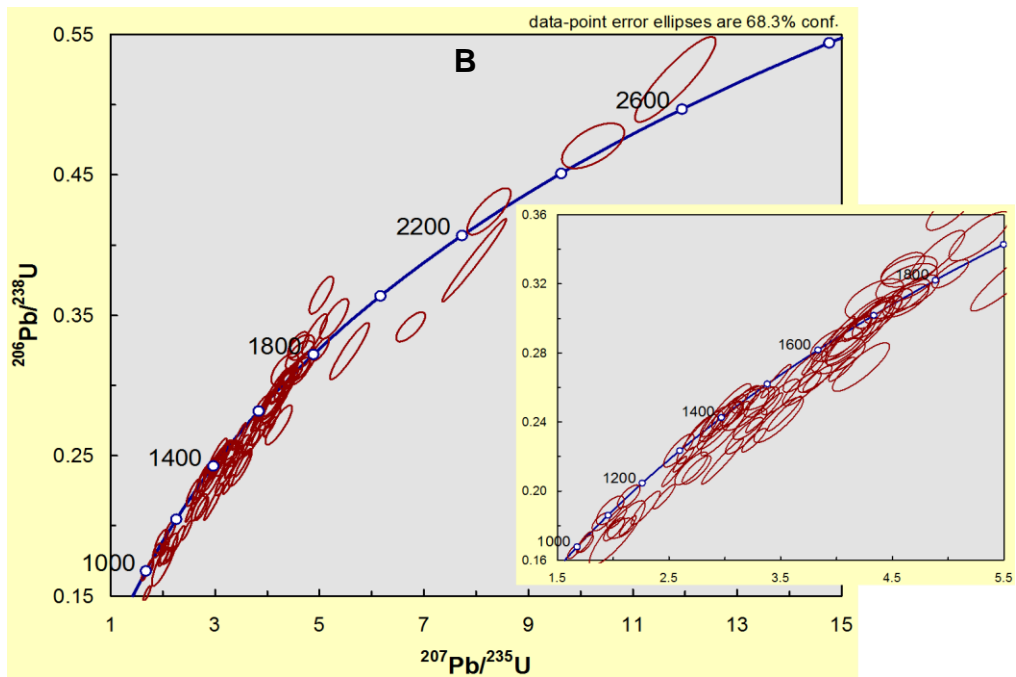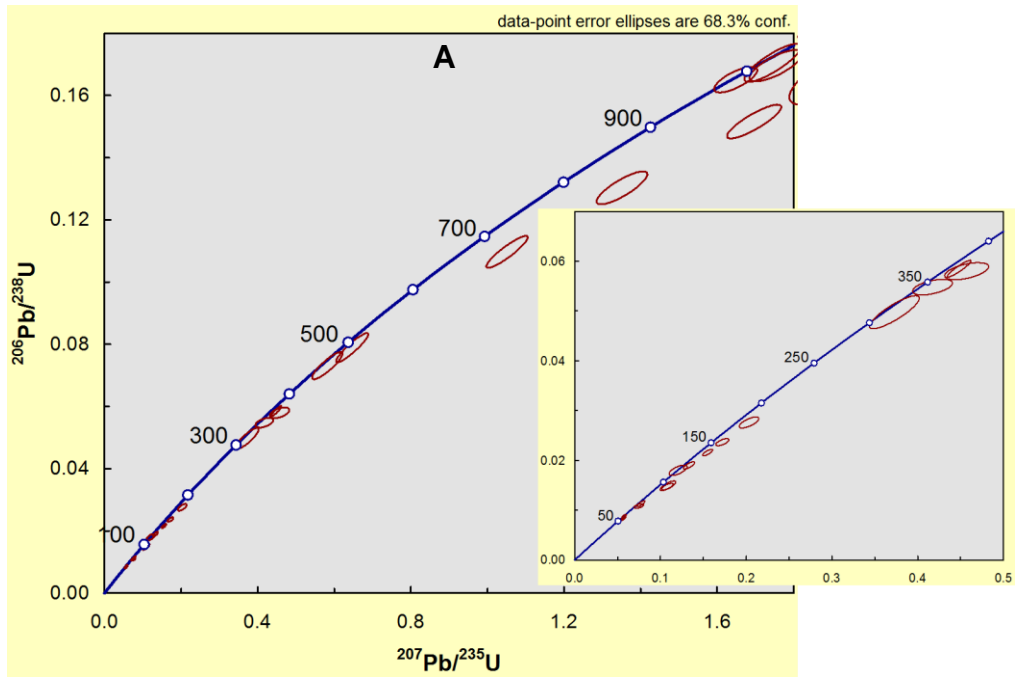
Figure E-9. Concordia diagram for sample CB-BS from A) 0-1000 Ma with a 0-400 Ma subplot, and B) 1000-2800 Ma with a 1000-1900 Ma subplot.
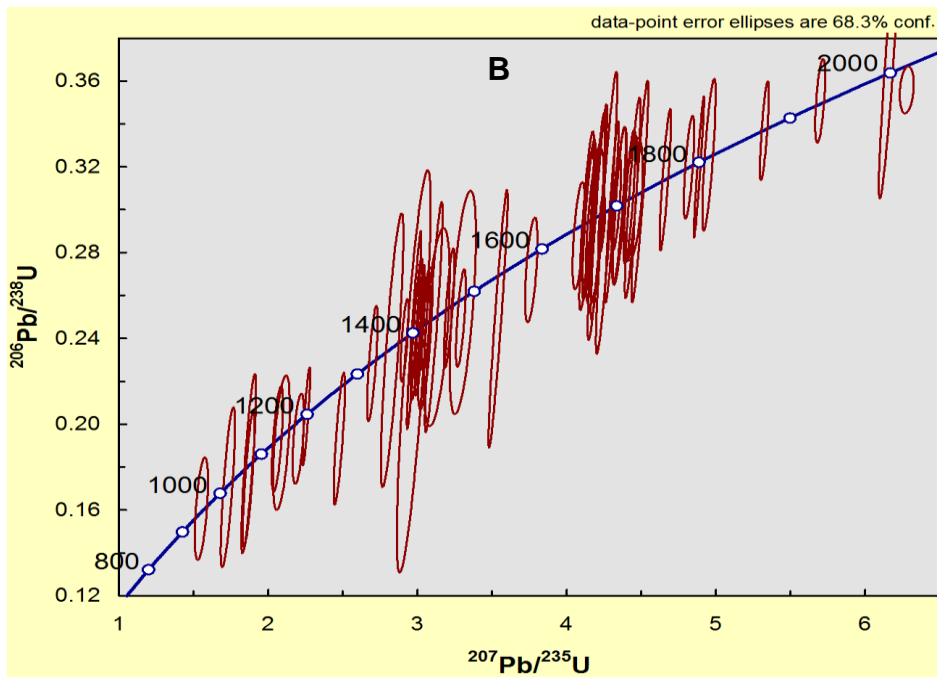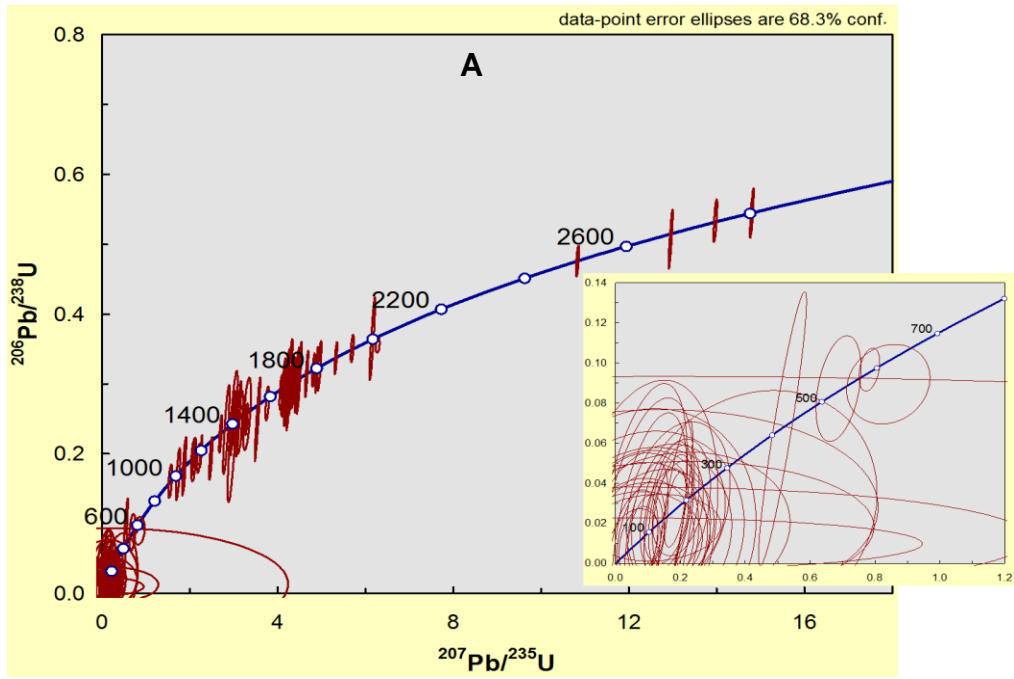
Figure E-10. Concordia diagram for sample CB-BBM from A) 0-2800 Ma with a 0-800 Ma subplot, and B) 800-2000 Ma.
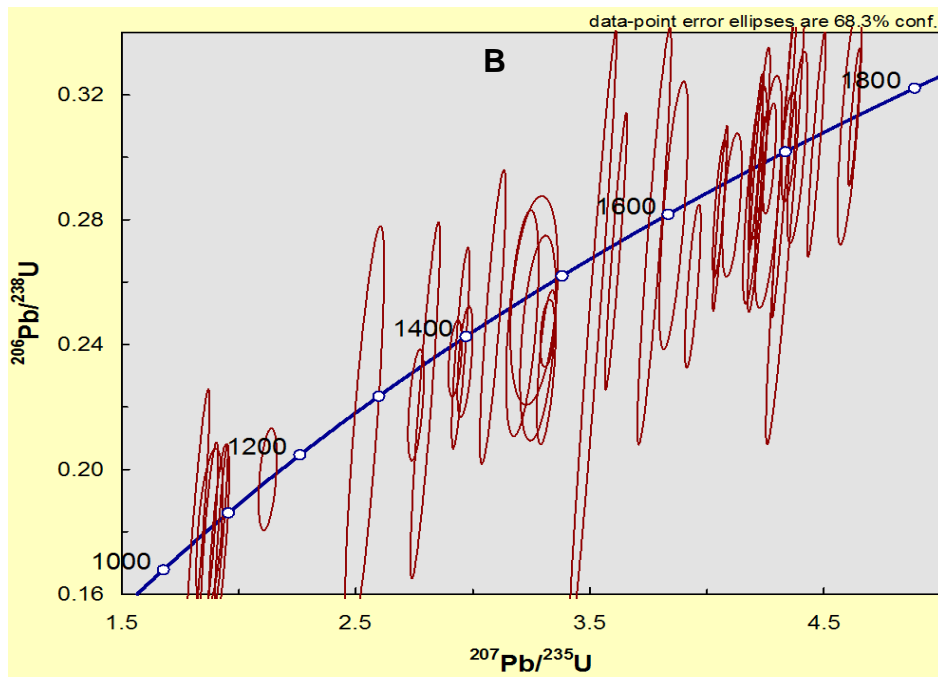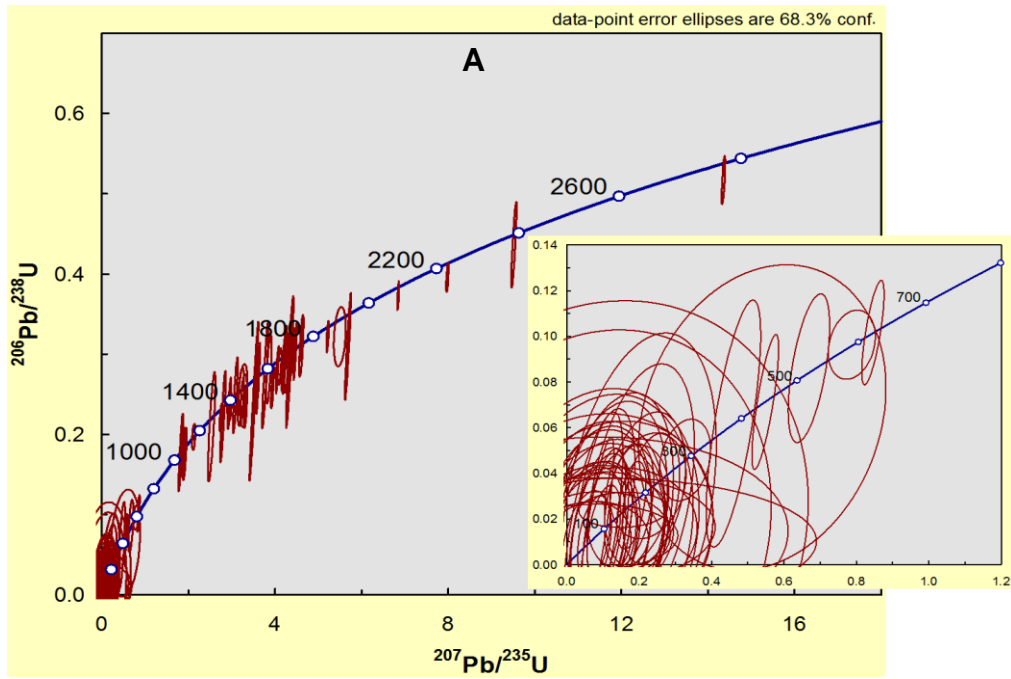
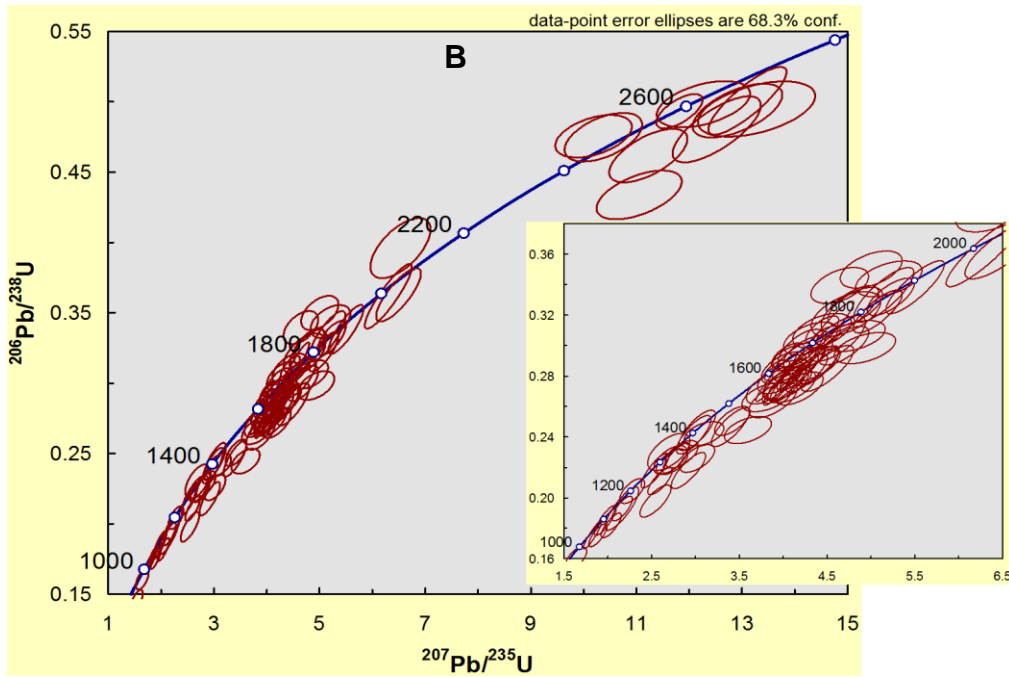**Figure E-11.** Concordia diagram for sample CZ from A) 0-2800 Ma with a 0-800 Ma subplot, and B) 1000-1800 Ma.
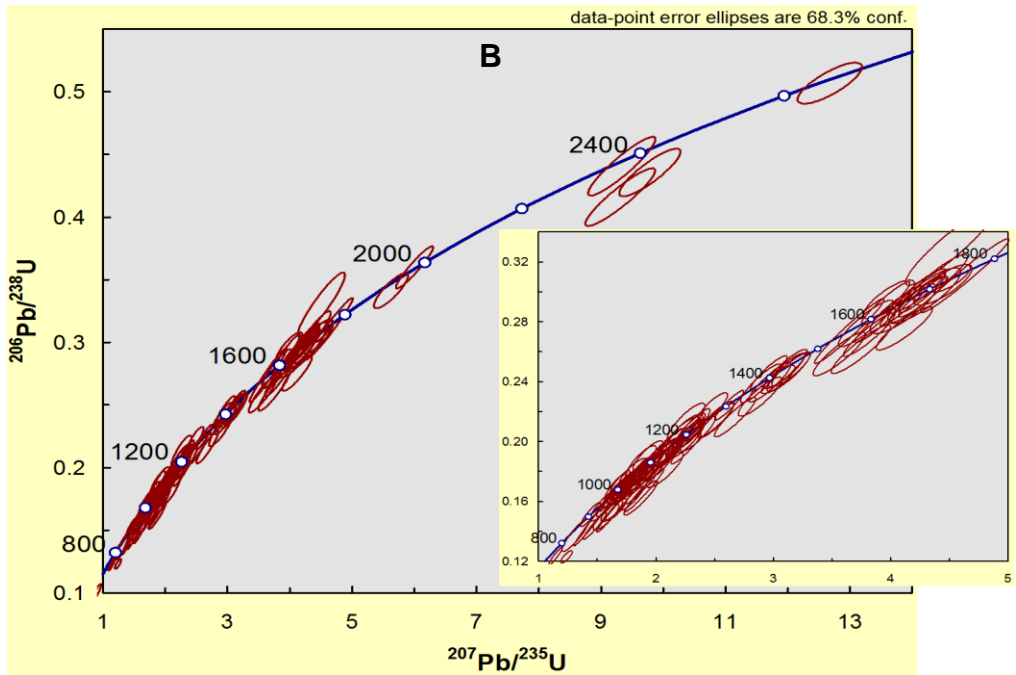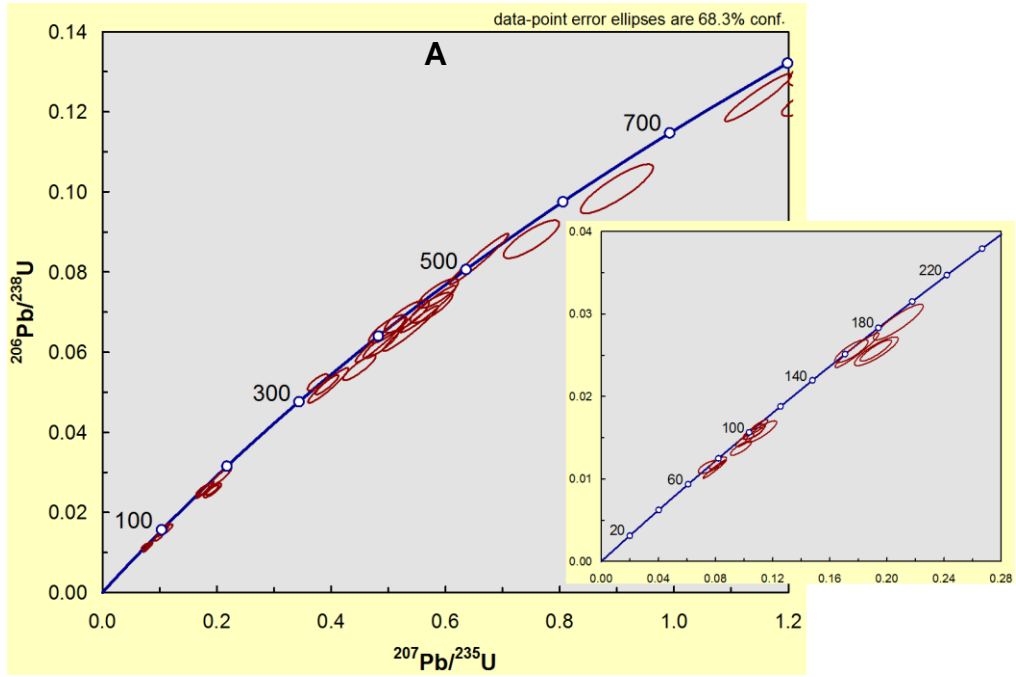
Figure E-12. Concordia diagram for sample QC from A) 0-800 Ma with a 0-250 Ma subplot, and B) 800-2700 Ma with a 800-1800 Ma subplot.

APPENDIX F

FRACTIONATION FACTORS FROM 91500 AND PEIXE ZIRCON STANDARDS

USED TO CORRECT DETRITAL ZIRCON SAMPLE DATA AND ZIRCON STANDARD

DATA

Table F. Daily fractionation factors calculated from Peixe and 91500 zircon standards.

Sample Name	Fractionation Factors		
	$^{207}Pb/^{206}Pb$	$^{206}Pb/^{238}U$	$^{207}Pb/^{235}U$
4/9/2014			
Px_a	0.9753	0.7748	0.7557
Px_b	0.9967	0.7776	0.7751
Px_c	1.0161	0.7722	0.7847
Px_d	0.9710	0.8098	0.7864
Px_e	0.9884	0.8184	0.8089
Px_f	1.0040	0.8494	0.8529
Px_g	0.9963	0.8124	0.8094
Px_h	1.0096	0.8218	0.8298
Px_i	1.0005	0.7826	0.7830
Px_J	1.0303	0.8061	0.8305
Px_k	0.9998	0.8071	0.8070
Px_L	0.9766	0.7671	0.7492
Px_m	1.0273	0.7984	0.8202
Px_n	1.0254	0.8222	0.8431
Px_o	0.9607	0.7755	0.7451
Px_p	1.0130	0.7757	0.7859
Px_q	0.9924	0.7731	0.7673
Px_r	1.0758	0.7830	0.8424
Px_s	1.0194	0.7519	0.7665
Px_t	1.0356	0.7570	0.7840
Px_u	0.9638	0.7664	0.7386
Px_v	1.0311	0.7236	0.7461
Px_w	1.0743	0.7861	0.8446
Px_x	0.9849	0.7832	0.7714
Px_y	1.0106	0.7605	0.7686
Px_z	0.9905	0.7708	0.7635
4/10/2014			
PX_a	1.0026	0.9151	0.9176
PX_b	1.0544	0.8710	0.9185
PX_c	1.1375	0.9023	1.0265
PX_d	1.0292	0.8364	0.8609
Px_e	0.9930	0.8549	0.8490
Px_f	1.0019	0.8342	0.8358
Px_g	0.9916	0.8694	0.8622
Px_h	0.9840	0.8228	0.8096
Px_i	1.0027	0.8207	0.8230

Table F Continued

Sample Name	Fractionation Factors		
	$^{207}Pb/^{206}Pb$	$^{206}Pb/^{238}U$	$^{207}Pb/^{235}U$
4/10/2014			
Px_J	0.9611	0.8238	0.7918
Px_k	1.0298	0.7933	0.8169
Px_l	0.9829	0.8398	0.8255
Px_m	1.0074	0.8473	0.8536
Px_n	1.0252	0.8165	0.8371
Px_o	1.0650	0.8507	0.9060
Px_p	0.9779	0.7954	0.7778
Px_q	0.9868	0.8330	0.8221
Px_r	1.0627	0.8114	0.8623
Px_s	0.9792	0.8302	0.8130
Px_t	0.9801	0.8312	0.8146
Px_u	1.0126	0.8131	0.8234
Px_v	0.9731	0.8179	0.7959
Px_w	0.9686	0.8332	0.8071
Px_x	1.0074	0.8625	0.8690
Px_aa	1.0544	0.7949	0.8381
Px_ab	1.0680	0.7917	0.8456
Px_ac	1.0647	0.8354	0.8895
Px_ad	1.2611	0.8156	1.0285
4/11/2014			
Px_a	1.0038	0.8047	0.8078
Px_b	0.9377	0.7847	0.7359
Px_c	1.0000	0.7762	0.7763
Px_d	0.9855	0.8016	0.7901
Px_e	1.0249	0.7921	0.8118
Px_f	0.9894	0.8232	0.8145
Px_g	0.9819	0.8173	0.8026
Px_h	1.0102	0.7941	0.8023
Px_i	0.9731	0.7466	0.7265
Px_J	1.0246	0.7974	0.8171
Px_k	1.0286	0.8047	0.8278
Px_l	1.1365	0.7796	0.8861
Px_m	1.0831	0.7352	0.7964
Px_n	0.9890	0.7885	0.7799
Px_o	0.9871	0.7836	0.7735
Px_p	1.0003	0.7748	0.7750

Table F Continued

Sample Name	Fractionation Factors		
	$^{207}Pb/^{206}Pb$	$^{206}Pb/^{238}U$	$^{207}Pb/^{235}U$
4/11/2014			
Px_q	0.9851	0.7917	0.7800
Px_r	1.0256	0.7521	0.7714
Px_s	0.9587	0.7896	0.7570
Px_t	1.1047	0.7141	0.7890
Px_u	1.0361	0.7890	0.8175
Px_v	0.9993	0.8192	0.8187
Px_w	1.0231	0.7626	0.7803
Px_x	0.9887	0.7941	0.7852
Px_y	1.0463	0.8133	0.8509
Px_z	1.0088	0.8103	0.8176
Px_aa	1.0061	0.8066	0.8115
Px_ab	0.9824	0.8072	0.7931
Px_ac	1.0160	0.7377	0.7496
Px_ad	0.9833	0.7970	0.7837
Px_ae	1.0149	0.7785	0.7902
Px_af	1.0676	0.8003	0.8545
Px_ag	0.9825	0.7694	0.7559
Px_ah	0.9852	0.7543	0.7432
Px_ai	0.9923	0.7821	0.7761
Px_aJ	1.0270	0.7797	0.8008
Px_ak	1.0093	0.8120	0.8196
Px_al	0.9918	0.7806	0.7743
Px_am	1.0257	0.7875	0.8077
Px_an	1.0065	0.7977	0.8029
Px_ao	0.9970	0.7737	0.7714
Px_ap	1.0377	0.7758	0.8051
Px_aq	1.0965	0.7652	0.8392
Px_ar	0.9746	0.7576	0.7384
Px_as	1.0030	0.7703	0.7727
9/9/2014			
91500_a	1.0095	0.9930	1.0025
91500_b	1.0027	1.0315	1.0343
91500_c	1.0076	0.9613	0.9687
91500_d	1.0058	1.0221	1.0280
91500_e	0.9993	0.9594	0.9588
91500_f	1.0017	0.9551	0.9567
91500_g	0.9877	0.9579	0.9462

Table F Continued

Sample Name	Fractionation Factors		
	$^{207}Pb/^{206}Pb$	$^{206}Pb/^{238}U$	$^{207}Pb/^{235}U$
9/9/2014			
91500_h	0.9807	0.9504	0.9320
91500_i	0.9780	0.9148	0.8947
91500_j	1.0294	0.8963	0.9227
91500_k	1.0187	0.9483	0.9660
91500_l	0.9683	0.9762	0.9452
9/11/2014			
91500_a	0.9691	0.8145	0.7893
91500_b	1.0023	0.9067	0.9088
91500_c	1.0029	0.8256	0.8281
91500_d	1.0032	0.8206	0.8232
91500_e	1.0196	0.8128	0.8287
91500_f	0.9882	0.8345	0.8246
91500_g	1.0538	0.7999	0.8429
91500_h	1.0123	0.8234	0.8335
91500_i	0.9681	0.8570	0.8296
91500_j	0.9875	0.8336	0.8232
91500_k	0.9739	0.7931	0.7724
91500_l	1.0155	0.8184	0.8311
9/12/2014			
91500_a	0.9965	0.8254	0.8225
91500_b	0.9869	0.8532	0.8420
91500_c	1.0125	0.8344	0.8449
91500_d	0.9896	0.8635	0.8545
91500_e	0.9841	0.8355	0.8222
91500_f	1.0080	0.8281	0.8346
91500_g	1.0236	0.8061	0.8251
91500_h	1.1058	0.8376	0.9263
91500_j	1.0181	0.7960	0.8104
91500_k	0.9847	0.8012	0.7890
91500_l	0.9978	0.7951	0.7934
9/13/2014			
91500_a	0.9862	1.0046	0.9907
91500_b	0.9693	0.9779	0.9478
91500_c	0.9875	1.0232	1.0104
91500_d	1.0835	0.9317	1.0096
91500_e	0.9512	0.9442	0.8981

Table F Continued

Sample Name	Fractionation Factors		
	$^{207}Pb/^{206}Pb$	$^{206}Pb/^{238}U$	$^{207}Pb/^{235}U$
9/13/2014			
91500_f	0.9828	0.9210	0.9052
91500_g	1.0112	0.9414	0.9519
91500_h	0.9511	0.5721	0.5441
91500_i	0.3613	0.7758	0.2803
91500_j	0.9844	0.8648	0.8512
91500_k	0.9646	0.8593	0.8289
91500_l	1.0062	0.8542	0.8595
91500_m	1.0068	0.8549	0.8607
91500_n	0.9678	0.8516	0.8242
91500_o	0.9872	0.8364	0.8257
91500_p	1.0044	0.8383	0.8420
91500_q	0.9975	0.8539	0.8518
91500_r	1.0070	0.8684	0.8745
91500_s	0.9933	0.8337	0.8281
91500_t	1.0721	0.8702	0.9329
9/15/2014			
91500_a	1.0739	0.8978	0.9642
91500_b	1.0345	0.8589	0.8885
91500_c	1.0543	0.8767	0.9243
91500_d	0.9936	0.8987	0.8929
91500_e	1.0040	0.9082	0.9118
91500_f	1.0856	0.8852	0.9609
91500_g	0.9705	0.8267	0.8023
91500_h	0.9947	0.8634	0.8588
91500_i	0.9866	0.8621	0.8505
91500_j	0.9755	0.8452	0.8245
91500_l	1.0936	0.7440	0.8137
91500_m	1.2607	0.7549	0.9516
91500_n	1.0007	0.8076	0.8082
11/7/2014			
91500_a	0.9411	0.7878	0.7414
91500_b	1.1027	0.7810	0.8612
91500_c	1.0144	0.8234	0.8352
91500_d	1.0127	0.8202	0.8306
91500_e	0.9561	0.8293	0.7929
91500_f	1.0007	0.8218	0.8224

Table F Continued

Sample Name	Fractionation Factors		
	$^{207}Pb/^{206}Pb$	$^{206}Pb/^{238}U$	$^{207}Pb/^{235}U$
11/7/2014			
91500_g	0.9747	0.7918	0.7718
91500_h	0.9779	0.8207	0.8026
91500_i	0.9601	0.7919	0.7603
91500_j	0.9767	0.7946	0.7761
91500_k	1.0091	0.7888	0.7959
91500_l	0.9907	0.7839	0.7766
91500_m	0.9379	0.7856	0.7368
91500_n	1.0060	0.8013	0.8061
91500_o	0.9784	0.7866	0.7696
91500_p	0.9907	0.7857	0.7783
91500_q	0.9932	0.8040	0.7985
91500_r	0.9529	0.7693	0.7330
91500_s	0.9891	0.8053	0.7965
91500_t	0.9818	0.7980	0.7835
91500_u	0.9888	0.8175	0.8084
91500_v	1.0046	0.8017	0.8054
91500_w	0.9955	0.7733	0.7698
91500_x	0.9849	0.7753	0.7636
11/8/2014			
91500_a	1.0034	0.8000	0.8027
91500_b	0.9857	0.8022	0.7907
91500_c	0.9899	0.8274	0.8190
91500_d	1.0002	0.7639	0.7641
91500_e	0.9808	0.7779	0.7630
91500_f	0.9851	0.7794	0.7678
91500_g	1.0167	0.8233	0.8371
91500_h	0.9865	0.8169	0.8059
91500_i	0.9899	0.7725	0.7647
91500_j	0.9672	0.7651	0.7400
91500_k	0.9414	0.8042	0.7571
91500_l	1.0251	0.8796	0.9017
91500_m	0.9533	0.7528	0.7177
91500_n	1.1486	0.7831	0.8995
91500_p	1.0340	0.7596	0.7855
91500_q	1.1260	0.7490	0.8434
91500_r	1.0007	0.7814	0.7819

Table F Continued

Sample Name	Fractionation Factors		
	$^{207}Pb/^{206}Pb$	$^{206}Pb/^{238}U$	$^{207}Pb/^{235}U$
11/8/2014			
91500_t	0.9977	0.7712	0.7694
91500_u	1.0464	0.8245	0.8627
91500_w	1.0558	0.7828	0.8265
91500_y	1.0513	0.7993	0.8404
91500_z	0.9777	0.7328	0.7165
91500_ab	1.0034	0.7796	0.7822
91500_aa	1.0062	0.7559	0.7606
11/9/2014			
91500_a	1.0143	0.7765	0.7876
91500_b	0.9684	0.7674	0.7432
91500_c	1.0283	0.7767	0.7987
91500_d	0.9825	0.8258	0.8114
91500_e	1.0026	0.7970	0.7990
91500_f	0.9706	0.7723	0.7496
91500_g	1.0298	0.8110	0.8351
91500_h	1.0093	0.8141	0.8217
91500_i	0.9845	0.7546	0.7429
91500_j	0.9915	0.7711	0.7646
91500_k	0.9613	0.7853	0.7549
91500_l	0.9882	0.7746	0.7655
91500_m	0.9769	0.6952	0.6791
91500_n	1.0065	0.7753	0.7803
91500_o	0.9807	0.7968	0.7815
91500_p	0.9795	0.8078	0.7913
91500_q	0.9758	0.7920	0.7728
91500_r	1.0029	0.7929	0.7952
91500_s	1.0343	0.7651	0.7914
91500_t	1.0002	0.8040	0.8041
91500_u	0.9619	0.7885	0.7584
91500_v	0.9613	0.7920	0.7613
91500_w	1.0191	0.7588	0.7733
91500_x	0.9964	0.7624	0.7597
91500_y	0.9664	0.7348	0.7101
91500_z	0.9630	0.7087	0.6825
91500_aa	1.0112	0.7402	0.7485
91500_ab	0.9761	0.7697	0.7513

Table F Continued

Sample Name	Fractionation Factors		
	$^{207}Pb/^{206}Pb$	$^{206}Pb/^{238}U$	$^{207}Pb/^{235}U$
11/9/2014			
91500_ac	0.9929	0.7617	0.7563
91500_ad	1.0168	0.7326	0.7448
91500_ae	0.9669	0.7499	0.7251
91500_af	0.9786	0.7774	0.7608
91500_ag	0.9776	0.6910	0.6755
91500_ah	1.0028	0.7556	0.7577
91500_ai	0.9792	0.7323	0.7171
91500_aj	0.9998	0.7077	0.7075
11/10/2014			
91500_a	0.9861	0.7918	0.7808
91500_b	0.9692	0.8613	0.8348
91500_c	0.9974	0.8453	0.8431
91500_d	1.0161	0.8472	0.8609
91500_e	0.9954	0.8474	0.8435
91500_f	0.9738	0.8790	0.8560
91500_g	0.9793	0.8102	0.7934
91500_h	0.9721	0.8058	0.7833
91500_i	0.9714	0.7991	0.7762
91500_j	1.0173	0.7814	0.7949
91500_k	1.0104	0.7930	0.8013
91500_l	0.9783	0.7931	0.7758
91500_m	0.9957	0.8087	0.8052
91500_n	0.9916	0.8091	0.8023
91500_o	0.9591	0.8327	0.7986
91500_p	0.9981	0.8018	0.8003
91500_q	0.9997	0.8042	0.8040
91500_r	0.9626	0.7780	0.7489
91500_s	0.9724	0.7894	0.7676
91500_t	0.9778	0.7636	0.7466
91500_u	1.0082	0.8143	0.8210
91500_v	0.9835	0.8326	0.8189
91500_w	0.9848	0.8273	0.8148
91500_x	0.9990	0.7915	0.7907
91500_y	0.9874	0.8078	0.7977
91500_z	0.9684	0.8065	0.7810
91500_aa	0.9865	0.7884	0.7778

Table F Continued

Sample Name	Fractionation Factors		
	$^{207}Pb/^{206}Pb$	$^{206}Pb/^{238}U$	$^{207}Pb/^{235}U$
11/10/2014			
91500_ab	1.0204	0.7865	0.8025
91500_ac	0.9863	0.7862	0.7754
91500_ad	0.9802	0.7902	0.7745
91500_ae	0.9824	0.7801	0.7664
91500_af	0.9819	0.7844	0.7702
91500_ah	0.9659	0.7972	0.7700
91500_ai	0.9950	0.7892	0.7852
91500_aj	0.9917	0.7918	0.7852
91500_ak	0.9810	0.7717	0.7571
91500_al	1.0057	0.7709	0.7753
91500_am	0.9837	0.8063	0.7931
91500_an	0.9107	0.7998	0.7283
91500_ao	0.9629	0.8077	0.7777
11/11/2014			
91500_p	0.9911	0.7778	0.7709
91500_o	0.9906	0.8118	0.8042
91500_n	1.0088	0.7390	0.7455
91500_m	0.9874	0.7934	0.7834
91500_l	1.1974	0.7825	0.9369
91500_k	0.9957	0.7943	0.7909
91500_j	0.9972	0.7712	0.7690
91500_i	0.9856	0.8186	0.8068
91500_h	1.0267	0.7774	0.7981
91500_g	0.9836	0.7864	0.7735
91500_f	1.2877	0.8414	1.0835
91500_e	1.0006	0.8595	0.8600
91500_d	1.0040	0.8483	0.8517
91500_c	1.0017	0.8289	0.8303
91500_b	0.9975	0.8039	0.8019
91500_a	1.1122	0.8021	0.8920
12/10/2014			
91500_a	0.9844	1.8423	1.8134
91500_b	0.9887	1.8709	1.8497
91500_c	0.9928	1.8332	1.8200
91500_d	0.9893	1.8511	1.8312
91500_e	0.9887	1.7380	1.7184

Table F Continued

Sample Name	Fractionation Factors		
	$^{207}Pb/^{206}Pb$	$^{206}Pb/^{238}U$	$^{207}Pb/^{235}U$
12/10/2014			
91500_f	0.9889	1.7845	1.7646
91500_g	1.0104	1.7657	1.7842
91500_h	1.0095	1.7767	1.7937
91500_i	0.9929	1.7213	1.7090
91500_j	1.0064	1.7278	1.7389
91500_k	0.9934	1.7373	1.7258
91500_l	1.0032	1.7333	1.7389
91500_m	0.9934	1.7531	1.7416
91500_n	1.0288	1.7495	1.7999
91500_o	0.9930	1.7311	1.7189
91500_p	0.9741	1.7284	1.6836
91500_q	1.0059	1.7147	1.7249
91500_r	0.9500	1.6982	1.6133
91500_s	0.9864	1.6897	1.6666
91500_t	1.0064	1.6725	1.6833
91500_u	0.9839	1.7147	1.6871
91500_v	0.9575	1.6584	1.5880
91500_w	0.9817	1.7161	1.6846
91500_x	0.9903	1.6900	1.6736
91500_y	0.9983	1.7090	1.7061
91500_z	0.9932	1.7355	1.7236
91500_aa	0.9702	1.7116	1.6607
91500_ab	0.9891	1.6960	1.6775
12/11/2014			
91500_a	0.9896	1.6855	1.6679
91500_b	1.0116	1.6860	1.7056
91500_c	0.9394	1.7733	1.6658
91500_d	0.9718	1.7570	1.7075
91500_e	1.0010	1.6131	1.6148
91500_f	1.0339	1.6945	1.7520
91500_g	0.9929	1.7181	1.7058
91500_h	0.9851	1.7081	1.6827
91500_i	1.3378	1.5456	2.0678
91500_j	1.8659	1.6734	3.1224
91500_k	1.7562	1.6220	2.8485
91500_l	1.0127	1.6582	1.6792

Table F Continued

Sample Name	Fractionation Factors		
	$^{207}Pb/^{206}Pb$	$^{206}Pb/^{238}U$	$^{207}Pb/^{235}U$
12/11/2014			
91500_o	1.0415	1.4924	1.5544
91500_p	1.0181	1.5306	1.5584
91500_pp	1.0537	1.6216	1.7086
91500_q	0.9902	1.5339	1.5189
91500_r	1.0475	1.5855	1.6608
91500_s	1.0097	1.5787	1.5940
91500_t	1.0443	1.6547	1.7280
91500_u	1.0514	1.5398	1.6191
91500_v	0.9995	1.5553	1.5545
91500_w	0.9894	1.6080	1.5910
91500_x	0.9581	1.6129	1.5453
91500_y	0.9725	1.6005	1.5564
91500_z	1.0530	1.6486	1.7360
91500_aa	1.0281	1.6321	1.6779
91500_ab	1.0099	1.6279	1.6439
91500_ac	1.6156	1.8009	2.9096
91500_ad	1.2978	1.7558	2.2787
91500_ae	1.4774	1.6878	2.4935
91500_af	1.0832	1.6831	1.8231
91500_ag	1.0477	1.5014	1.5731
91500_ah	1.0066	1.6596	1.6706
91500_ai	1.0613	1.6482	1.7493
91500_aj	1.0305	1.5844	1.6328
91500_ak	1.0061	1.7091	1.7196
91500_al	0.9906	1.6477	1.6322
91500_am	1.0478	1.6421	1.7205
91500_an	0.9178	1.6416	1.5067
91500_ao	1.0193	1.5420	1.5717
91500_ap	1.0471	1.6545	1.7324
91500_aq	1.0130	1.6348	1.6560
91500_ar	1.0175	1.8420	1.8743
12/12/2014			
91500_a	0.9901	1.7666	1.7492
91500_b	1.0198	1.7683	1.8034
91500_c	1.0227	1.7132	1.7521
91500_d	1.0417	1.7608	1.8342

Table F Continued

	Fractionation Factors		
Sample Name	$^{207}Pb/^{206}Pb$	$^{206}Pb/^{238}U$	$^{207}Pb/^{235}U$
12/12/2014			
91500_e	1.0629	1.7859	1.8983
91500_f	0.9948	1.8049	1.7956
91500_g	0.9666	1.8071	1.7467
91500_h	0.9890	1.7831	1.7635
91500_i	1.0294	1.7550	1.8065
91500_j	1.0043	1.7926	1.8004
91500_k	0.9957	1.7992	1.7915
91500_l	0.9721	1.7328	1.6845
91500_m	0.9896	1.7184	1.7006
91500_n	0.9727	1.7251	1.6779
91500_q	0.9723	1.6777	1.6311
91500_r	0.9952	1.7021	1.6939
91500_s	0.9787	1.7117	1.6753
91500_t	0.9747	1.7137	1.6703
91500_u	0.9972	1.7450	1.7402
91500_v	1.0109	1.6794	1.6976
91500_w	0.9815	1.6952	1.6638
91500_x	0.9928	1.7568	1.7442
91500_y	0.9979	1.7184	1.7149
91500_z	0.9974	1.7153	1.7108
91500_aa	0.9842	1.7252	1.6980
91500_ab	1.0735	1.6736	1.7966
91500_ac	1.0113	1.6978	1.7170
91500_ad	1.0183	1.7530	1.7851
91500_ae	1.1130	1.6598	1.8474
91500_af	0.9956	1.7570	1.7494
91500_ag	0.9873	1.7013	1.6796
91500_ah	0.9637	1.7830	1.7182
91500_ai	0.9686	1.6363	1.5849
91500_ak	1.0019	1.6720	1.6751
91500_al	1.0097	1.6544	1.6705
91500_am	0.9963	1.7080	1.7017
91500_an	1.0640	1.6781	1.7855
91500_ao	0.9787	1.7691	1.7315
91500_ap	0.9859	1.7238	1.6995
91500_aq	1.0114	1.7281	1.7478
91500_ar	1.0121	1.6757	1.6960

Table F Continued

Sample Name	Fractionation Factors		
	^{207}Pb/^{206}Pb	^{206}Pb/^{238}U	^{207}Pb/^{235}U
1/28/2015			
91500_a	0.9836	0.8062	0.7930
91500_b	0.9387	0.7821	0.7341
91500_c	0.9782	0.7778	0.7609
91500_d	0.9780	0.7939	0.7764
91500_e	0.9626	0.7083	0.6818
91500_f	0.9870	0.7077	0.6985
91500_g	1.0071	0.6982	0.7032
91500_h	0.9542	0.7111	0.6786
91500_i	0.9859	0.6797	0.6701
91500_j	0.9749	0.6811	0.6640
91500_k	0.9363	0.6740	0.6311
91500_l	0.9727	0.6896	0.6708
91500_q	0.9849	0.6868	0.6764
91500_r	0.9777	0.6599	0.6452
91500_s	0.9495	0.6588	0.6255
91500_t	0.9797	0.6541	0.6408
91500_u	0.9557	0.6612	0.6319
91500_v	0.8824	0.6800	0.6000
91500_w	0.9214	0.6820	0.6285
91500_x	0.9587	0.6542	0.6272
91500_y	0.9405	0.6059	0.5698
91500_z	0.9635	0.6238	0.6011
91500_aa	0.9821	0.6179	0.6068
91500_ab	0.9540	0.6101	0.5821
91500_ac	0.9750	0.5999	0.5849
91500_ad	0.9897	0.6108	0.6045
91500_ae	0.9711	0.5858	0.5689
91500_af	0.9866	0.6117	0.6035
1/29/2015			
PX_a	0.9626	0.8159	0.7854
PX_b	0.9120	0.7801	0.7115
PX_c	0.8616	0.7485	0.6449
PX_d	0.9786	0.7913	0.7744
PX_e	0.9123	0.6417	0.5854
PX_f	0.9445	0.6496	0.6136
PX_g	0.9839	0.6419	0.6316

Table F Continued

	Fractionation Factors		
Sample Name	$^{207}Pb/^{206}Pb$	$^{206}Pb/^{238}U$	$^{207}Pb/^{235}U$
1/29/2015			
PX_h	1.0267	0.6590	0.6766
PX_i	0.9962	0.6180	0.6157
PX_j	0.9493	0.6259	0.5942
PX_k	0.9833	0.6043	0.5942
PX_l	1.0031	0.6077	0.6096

APPENDIX G

DETRITAL ZIRCON SAMPLE LOCATION INFORMATION

Table G. Stratigraphic sampling level and location details for respective detrital zircon samples.

Sample Name	Strat. Level	Location	Lat/Long	River System
Queen City Fm.	base	Buffalo South, Rt. 79 roadcut near pond, 6 km SW of I-45 at Buffalo, Leon Co., TX	31.405461°N; 96.111382°W	Navasota
Carrizo Fm.	fluvial base	Cart Path on Pine Forest golf course, 90 m north of Colorado River, 4.5 km from Rts.21-71 intersection, Tahitian Village, Bastrop Co., TX	30.073912°N; 97.281754°W	Colorado
Calvert Bluff Fm.	mid	Big Brown mine, NE end, N side Rt. 2570, west side Trinity River, 16 km NE of Fairfield, Freestone Co., TX	31.838566°N; 96.050466°W	Trinity
Calvert Bluff Fm.	base	Black Shoals, Brazos River, 0.4 km SW of Rt. 979 bridge, east side of river, 8.4 km due west of Calvert, Robertson Co., TX	30.976752°N; 96.760524°W	Brazos
Simsboro Fm.	high	Thornton quarry, south side Rt. 1246, 6 km SE of Thornton, Limestone Co., TX	31.386536°N; 96.509098°W	Navasota
Simsboro Fm.	top	Kosse mine (U. S. Silica), east side of Rt. 2749, 1.3 km north of Rts.7 and 2749 intersection, 11.6 km ESE of Kosse, Limestone Co., TX	31.295041°N; 96.508852°W	Navasota
Simsboro Fm.	mid	Luminant pit, 0.6 km west of Rt. 2749, 1.1 km NW of Kosse U.S. Silica mine plant, 10.8 km due east of Kosse, Limestone Co., TX	31.314138°N; 96.516782°W	Navasota
Simsboro Fm.	low	Rt. 14 roadcut, east side of road, 160 m SW of Rt. 276 intersection to the east, 9.5 km SW of Kosse, Limestone Co., TX	31.223429°N.; 96.649808°W	Brazos
Hooper Fm.	high	Denison ranch, 0.25 km east of Rt. 2027, 2.4 km NW of Rts. 979 and 2027 intersection (Crossroads) and 12 km west of Calvery, in Milam Co., TX	30.984650°N; 96.801772°W	Brazos
Hooper Fm.	low	Polecat Creek, west roadcut of Rt. 268 on south side of creek, 100 m north of Rt. 268-270 intersection. 5.8 km SW of Kosse, Limestone Co., TX	31.258617°N; 96.654352°W	Brazos
Seguin Fm.	low	Elysium, east bank of Dry Creek 500 m upstream of mouth, south bank of Colorado River, 28 km east of downtown Austin, in Bastrop Co., TX	30.1797.35°N; 97.470073°W	Colorado
Tehuacana Mbr.	base	Steele quarry of Frost quarries complex, south side of north pit, 1 km north of Rt. 1771, 12.2 km WSW of Thornton, on east side of Falls-Limestone county line, in Limestone Co., TX	31.380947°N; 96.703990°W	Brazos

APPENDIX H

DETRITAL ZIRCON AGE GROUP PROPORTION DATA

Table H-1. Age range, number of grains, and respective group proportions for all samples.

All Samples

Group	Age Range	# of grains	Overall Proportion (%)
A	3217-1970	107	8.25
B	1958-1530	488	37.63
C	1518-1303	139	10.72
D	1293-843	195	15.03
E	799-676	9	0.69
F	652-265	63	4.86
G	251-134	102	7.86
H	130-52	194	14.96
HL	64-52	34	2.62

Table H-2. Age range, number of grains, and respective group proportions for sample Teh.

Teh

Group	Age Range	# of grains	Overall Proportion (%)	Group Proportion (%)	Sample Proportion (%)
A	3217-1970	5	0.39	0.36	5.15
B	1958-1530	41	3.16	8.40	42.27
C	1518-1303	10	0.77	7.19	10.31
D	1293-843	8	0.62	4.10	8.25
E	799-676	1	0.08	11.11	1.03
F	652-265	7	0.54	11.11	7.22
G	251-134	14	1.08	13.73	14.43
H	130-52	10	0.77	5.15	10.31
HL	64-52	0	0.00	0.00	0.00

Table H-3. Age range, number of grains, and respective group proportions for sample Se-E

Se-E

Group	Age Range	# of grains	Overall Proportion (%)	Group Proportion (%)	Sample Proportion (%)
A	3217-1970	10	0.77	0.72	10.53
B	1958-1530	48	3.70	9.84	50.53
C	1518-1303	11	0.85	7.91	11.58
D	1293-843	8	0.62	4.10	8.42
E	799-676	3	0.23	33.33	3.16
F	652-265	7	0.54	11.11	7.37
G	251-134	3	0.23	2.94	3.16
H	130-52	5	0.39	2.58	5.26
HL	64-52	0	0.00	0.00	0.00

Table H-4. Age range, number of grains, and respective group proportions for sample H-PC

H-PC

Group	Age Range	# of grains	Overall Proportion (%)	Group Proportion (%)	Sample Proportion (%)
A	3217-1970	15	1.16	1.08	13.89
B	1958-1530	51	3.93	10.45	47.22
C	1518-1303	10	0.77	7.19	9.26
D	1293-843	7	0.54	3.59	6.48
			0.00		
E	799-676	2	0.15	22.22	1.85
F	652-265	2	0.15	3.17	1.85
G	251-134	8	0.62	7.84	7.41
H	130-52	13	1.00	6.70	12.04
HL	64-52	2	0.15	1.03	1.85

Table H-5. Age range, number of grains, and respective group proportions for sample H-DR.

H-DR

Group	Age Range	# of grains	Overall Proportion (%)	Group Proportion (%)	Sample Proportion (%)
A	3217-1970	8	0.62	0.58	8.51
			0.00		
B	1958-1530	35	2.70	7.17	37.23
C	1518-1303	8	0.62	5.76	8.51
D	1293-843	12	0.93	6.15	12.77
E	799-676	1	0.08	11.11	1.06
F	652-265	6	0.46	9.52	6.38
G	251-134	10	0.77	9.80	10.64
H	130-52	14	1.08	7.22	14.89
HL	64-52	1	0.08	0.52	1.06

Table H-6. Age range, number of grains, and respective group proportions for sample Si-B

Si-B

Group	Age Range	# of grains	Overall Proportion (%)	Group Proportion (%)	Sample Proportion (%)
A	3217-1970	10	0.77	0.72	7.94
			0.00		
B	1958-1530	40	3.08	8.20	31.75
C	1518-1303	15	1.16	10.79	11.90
D	1293-843	13	1.00	6.67	10.32
					0.00
E	799-676	0	0.00	0.00	0.00
F	652-265	3	0.23	4.76	2.38
G	251-134	14	1.08	13.73	11.11
H	130-52	31	2.39	15.98	24.60
HL	64-52	8	0.62	4.12	6.35

Table H-7. Age range, number of grains, and respective group proportions for sample Si-LP.

Si-LP

Group	Age Range	# of grains	Overall Proportion (%)	Group Proportion (%)	Sample Proportion (%)
A	3217-1970	12	0.93	0.86	12.37
			0.00		
B	1958-1530	51	3.93	10.45	52.58
C	1518-1303	11	0.85	7.91	11.34
D	1293-843	9	0.69	4.62	9.28
E	799-676	1	0.08	11.11	1.03
F	652-265	2	0.15	3.17	2.06
G	251-134	3	0.23	2.94	3.09
H	130-52	8	0.62	4.12	8.25
HL	64-52	0	0.00	0.00	0.00

Table H-8. Age range, number of grains, and respective group proportions for sample SI-TQ.

Si-TQ

Group	Age Range	# of grains	Overall Proportion (%)	Group Proportion (%)	Sample Proportion (%)
A	3217-1970	11	0.85	0.79	10.00
			0.00		
B	1958-1530	54	4.16	11.07	49.09
C	1518-1303	7	0.54	5.04	6.36
D	1293-843	14	1.08	7.18	12.73
E	799-676	0	0.00	0.00	0.00
F	652-265	2	0.15	3.17	1.82
G	251-134	8	0.62	7.84	7.27
H	130-52	14	1.08	7.22	12.73
HL	64-52	0	0.00	0.00	0.00

Table H-9. Age range, number of grains, and respective group proportions for sample Si-KM.

Si-KM

Group	Age Range	# of grains	Overall Proportion (%)	Group Proportion (%)	Sample Proportion (%)
A	3217-1970	12	0.93	0.86	8.89
			0.00		
B	1958-1530	50	3.86	10.25	37.04
C	1518-1303	12	0.93	8.63	8.89
D	1293-843	25	1.93	12.82	18.52
E	799-676	0	0.00	0.00	0.00
F	652-265	3	0.23	4.76	2.22
G	251-134	13	1.00	12.75	9.63
H	130-52	19	1.46	9.79	14.07
HL	64-52	2	0.15	1.03	1.48

Table H-10. Age range, number of grains, and respective group proportions for sample CB-BBS.

CB-BBS

Group	Age Range	# of grains	Overall Proportion (%)	Group Proportion (%)	Sample Proportion (%)
A	3217-1970	6	0.46	0.43	6.12
			0.00		
B	1958-1530	41	3.16	8.40	41.84
C	1518-1303	19	1.46	13.67	19.39
D	1293-843	14	1.08	7.18	14.29
E	799-676	0	0.00	0.00	0.00
F	652-265	6	0.46	9.52	6.12
G	251-134	3	0.23	2.94	3.06
H	130-52	9	0.69	4.64	9.18
HL	64-52	3	0.23	1.55	3.06

Table H-11. Age range, number of grains, and respective group proportions for sample CB-BBM.

CB-BBM

Group	Age Range	# of grains	Overall Proportion (%)	Group Proportion (%)	Sample Proportion (%)
A	3217-1970	7	0.54	0.50	7.07
			0.00		
B	1958-1530	29	2.24	5.94	29.29
C	1518-1303	14	1.08	10.07	14.14
D	1293-843	8	0.62	4.10	8.08
E	799-676	0	0.00	0.00	0.00
F	652-265	4	0.31	6.35	4.04
G	251-134	11	0.85	10.78	11.11
H	130-52	26	2.00	13.40	26.26
HL	64-52	8	0.62	4.12	8.08

Table H-12. Age range, number of grains, and respective group proportions for sample CZ.

CZ

Group	Age Range	# of grains	Overall Proportion (%)	Group Proportion (%)	Sample Proportion (%)
A	3217-1970	6	0.46	0.43	6.12
			0.00		
B	1958-1530	25	1.93	5.12	25.51
C	1518-1303	9	0.69	6.47	9.18
D	1293-843	6	0.46	3.08	6.12
E	799-676	0	0.00	0.00	0.00
F	652-265	7	0.54	11.11	7.14
G	251-134	9	0.69	8.82	9.18
H	130-52	36	2.78	18.56	36.73
HL	64-52	10	0.77	5.15	10.20

Table H-13. Age range, number of grains, and respective group proportions for sample QC.

QC

Group	Age Range	# of grains	Overall Proportion (%)	Group Proportion (%)	Sample Proportion (%)
A	3217-1970	5	0.39	0.36	3.57
B	1958-1530	22	1.70	4.51	15.71
C	1518-1303	13	1.00	9.35	9.29
D	1293-843	71	5.47	36.41	50.71
E	799-676	1	0.08	11.11	0.71
F	652-265	14	1.08	22.22	10.00
G	251-134	5	0.39	4.90	3.57
H	130-52	9	0.69	4.64	6.43
HL	64-52	0	0.00	0.00	0.00